Development of Immunotherapy for Classical Hodgkin Lymphoma and Anaplastic Large Cell Lymphoma Using CSF1R Re-targeted Human T-lymphocytes.

Achkova, Daniela Yordanova

Awarding institution:
King's College London

DEVELOPMENT OF IMMUNOTHERAPY FOR CLASSICAL HODGKIN'S LYMPHOMA AND ANAPLASTIC LARGE CELL LYMPHOMA USING COLONY-STIMULATING FACTOR-1 RECEPTOR RE-TARGETED T-LYMPHOCYTES

Daniela Yordanova Achkova (1261437)

Submitted to King's College London for the award of

Doctor of Philosophy

CAR Mechanics Group, Research Oncology,

Division of Cancer Studies, King's College London

September 2016

На моите родители

Abstract

Classical Hodgkin's lymphoma (cHL) represents the most common subtype of malignant lymphoma in young people in the Western world. Despite modern treatment strategies, about 20% of patients still die due to relapse or progressive disease. Anaplastic large cell lymphoma (ALCL) is a type of T/null-cell lymphoma that represents about 20-30% of paediatric lymphomas and has an aggressive clinical course with frequent relapse. Recently, high-level expression of CSF-1R on malignant cells in cHL and ALCL has been linked to shorter progression free survival, providing a rationale to test adoptive CSF-1R-targeting chimeric antigen receptor (CAR) T-cell therapy. This approach encompasses the genetic modification of T-cells to express a CAR, a fusion receptor coupling the recognition of CSF-1R on the tumour cell surface to the delivery of tailored T-cell activation signal. To optimize this approach for human translation, a panel of CSF-1R-targeting CARs were designed and co-expressed with the chimeric cytokine receptor 4αβ, which allows for selective expansion and enrichment of CAR-transduced T-cells using IL-4.

Successful re-direction of CAR-grafted T-cells against a panel of cHL and ALCL tumour cell lines was confirmed by monitoring target cell destruction, cytokine release and T-cell proliferation. An innovative approach was developed and optimised in which target engagement results in provision of CAR-derived dual co-stimulation *in trans* ("double targeting"). Data outlined in this thesis suggest that the "double targeting" approach elicits more robust and sustained anti-tumour activity both *in vitro* and *in vivo* in comparison to second and third generation CARs. This is accompanied by superior antigen-specific proliferation, cytokine secretion (IL-2 and IFN-γ) and cytotoxicity upon consecutive rounds of antigen stimulation. These results warrant further investigation into the translational potential of "the double targeting" approach. Furthermore, the data detailed in this thesis provide for the first time the basis for successful application of CAR-based immunotherapy against CSF-1R-expressing malignancies.

Table of Contents

Table of Figures

Table of Tables

Acknowledgements

First and foremost I would like to thank my supervisor, Dr John Maher, for giving me the opportunity to undertake this PhD in his lab. Working with you has been truly inspirational. Thank you for the continuous support, encouragement and scientific advice throughout this project.

To all past and present members of the CAR Mechanics group (Dr Astero Klabatsa, Dr Vincent Kao, Dr Ana Parente Pereira, Dr Lynsey Whilding, Dr David Davies, Thivyan Thayaparan, Roseanna Petrovic, Tomasz Zabinski, Michael Metoudi) Immunoengineering (Dr Sophie Papa, Dr Nia Emami-Shahri, Erin Runbeck) and BCBG (Prof Joy Burchell, Prof Joyce Taylor-Papadimitriou, Dr Richard Beatson, Dr Virginia Tajadura-Ortega, Dr Steven Catchpole, Dr Gianfranco Picco), thank you for your friendships, and useful scientific and non-scientific communications. I would like to especially thank my friends Antonella Adami, Artemis Gavriil and Fiona Kogera for their continuous support and invaluable advice in time of need.

I extend my sincere gratitude to Kristina Ilieva for her encouragement, love and firm belief in my success, to Dr Thomas Adie, Dr Jonathan Smith and Dr Ke Yan Wen for helping me maintain perspective and to my life long friends Serafima Slavcheva and Liliana Vasileva for always standing by my side.

Last but not least, I'd like to express my profound love and appreciation for my parents, my brother and his wife Paige. Thank you for all that you have done for me. Above all else, I want to thank my Mum and Dad who have supported me in all my endeavours and provided me with the opportunities that have taken me to where I am today. Without you I would have never gotten this far. This thesis is dedicated to you.

Abbreviations

AA	Amino acid
Ag	Antigen
aGvHD	Acute graft versus host disease;
ALCL	Anaplastic large cell lymphoma
ALK	Anaplastic lymphoma kinase
ALL	Acute lymphoblastic leukaemia
ALL Ph^-	Philadelphia chromosome negative acute lymphoblastic leukemia
ALL Ph^+	Philadelphia chromosome positive acute lymphoblastic leukaemia
allo SCT	Allogeneic stem cell transplant;
AML	Acute myeloid leukaemia;
APC	Allophycocyanin
APC-Cy7	Allophycocyanin-Cyanine 7
ATC	Activated T-cells
ATP	Adenosine Triphosphate
auto HCT	Autologous stem cell transplant;
B	Bendamustine
B-NHL	B-cell non-Hodgkin’s lymphoma
BCR	B-cell receptor
BLI	Bioluminescence imaging
bp	Base pair
BR	Bendamustine + rituximab
BSA	Bovine Serum Albumin
C	Cyclophosphamide
c-ALCL	Cutaneous anaplastic large cell lymphoma
CA	Capsid (virus protein)
CAIX	Carbonic anhydrase IX
CAR	Chimeric antigen receptor

CBD	Cell-binding domain
Cbl	Casitas B lineage
CCD	Charged-coupled device
CCR7	C-C Chemokine Receptor 7
CD	Cluster of differentiation
CD3ζ	CD3 zeta chain
CD8α	CD8 alpha chain
cDNA	Copy DNA
CEA	Carcinoembryonic antigen
CF	Cyclophosphamide and fludarabine-based lymphodepletion
CFSE	Carboxyfluorescein succinimidyl ester
cHL	Classical Hodgkin's lymphoma
CLL	Chronic lymphocytic leukaemia
CLTC1	Clathrin heavy chain-like 1
CMV	Cytomegalovirus
Cond	Conditioning therapy prior to T-cell infusion
CP	Cyclophosphamide and pentostatin
CR	Complete remission
CRS	Cytokine release syndrome
CSF-1	Colony-stimulating factor-1
CSF-1R	Colony-stimulating factor-1 receptor
CTX	Cytoreductive chemotherapy
DAPI	4',6-diamidino-2-phenylindole
DEAE	Diethylaminoethyl
DLBCL	Diffuse large B-cell lymphoma
DLI	Donor leukocyte infusion
DMEM	Dulbecco`s Modified Eagle Medium
DMSO	Dimethyl Sulfoxide

dNTP	Deoxynucleotide triphosphate
dsDNA	Double stranded DNA
DUSP22	Dual specificity phosphatase 22
E.coli	Escherichia coli
EBV	Epstein-Barr virus
EBV-CTL	Epstein Barr virus specific cytotoxic T-lymphocytes
EC	Etoposide + cyclophosphamide
ECL	Enhanced Chemiluminescence
EDTA	Ethylenediaminetetraacetic acid
EGF	Epidermal growth factor
EGFP	Enhanced green fluorescent protein
ELISA	Enzyme-linked Immunosorbent Assay
F	Fludarabine;
F-NHL	Follicular NHL
FCS	Foetal Calf Serum
ffLuc	Firefly luciferase
FIRE	FMS intronic regulatory element
FR-α	Folate receptor-α
g	Gram
GaLV	Gibbon Ape Leukaemia Virus
gamma c	Common amma
GC	Germinal centres
GC	Gluccorticoids
GD2	Ganglioside D2
GM-CSF	Granulocyte-macrophage colony-stimulating factor
GR	Glucocorticoid receptors
GR1	Protein Gamma Response 1
GRE	Glucocorticoid response elements

GvHD	Graft versus host disease
HEK 293	Human Embryonic Kidney 293
HL	Hodgkin's lymphoma
HLA	Human leukocyte antigen
HRP	Horseradish peroxidase
HRS cells	Hodgkin and Reed-Sternberg cells
HZ-5	Hardy-Zuckerman five strain
IFN-γ	Interferon-gamma
IFRT	Involved field radiotherapy
Ig	Immunoglobulin
IL	Interleukin
IL-2Rβ	Interleukin-2 receptor beta subunit
IL-4Rα	Interleukin-4 receptor alpha subunit
IN	Viral integrase
IκBα	Inhibitor of -κB
JAK-STAT	Janus kinase/ signal transducers and activators of transcription
kb	kilobase
L&H cells	Lymphocytic and histocytic cells
LAG3	Lymphocyte-activation gene 3
LB	Luria Broth
LD	Lymphodepletion
LDHL	Lymphocyte-depleted Hodgkin's lymphoma
LeY	Lewis Y antigen
LGNHL	Low grade NHL
LRHL	Lymphocyte-rich Hodgkin's lymphoma
LTR	Long Terminal Repeat
M-CSF	Macrophage colony-stimulating factor
M-CSFR	Macrophage colony-stimulating factor receptor

MA	Matrix (virus protein)
mA	Miliamper
Mab	Monoclonal antibody
MCHL	Mixed cellularity Hodgkin's lymphoma
MCL	Mantle cell lymphoma
MEK	Mitogen-activated protein kinase kinase
mL	Mililiter
mM	Milimolar
MMPs	Matrix metalloproteases
MoMLV	Moloney murine leukaemia virus
Mona	Monocyte adaptor
MOPS	3-(N-Morpholino)-propanesulfonic acid
MPM	Malignant pleural mesothelioma
MR	Minor responses
mRNA	Messenger RNA
MTT	3-[4,5-dimethylthiazol-2-yl]-2,5- diphenyltetrazolium bromide
NC	Nucleocapsid (virus protein)
NE	Not evaluable for disease status
NEB	New England Biolabs
NHL	Non-Hodgkin's lymphoma
NK	Natural killer cells
NLPHL	Nodular lymphocyte-predominant Hodgkin's lymphoma
nm	Nanometer
NOD	Non-obese Diabetic
NPM	Nucleophosmin
NSCLC	Non-small cell lung carcinoma
NSHL	Nodular sclerosis Hodgkin's lymphoma
OS	Overall survival

PAI-1	Plasminogen activator inhibitor-1
PBMCs	Peripheral blood mononuclear cells
PBS	Phosphate Buffered Saline
PCR	Polymerase Chain Reaction
PD1	Programmed cell Death protein 1
PDAC	Pancreatic ductal adenocarcinoma
PDGFR	Platelet-derived growth factor receptor
PE	Phycoerythrin
PE-Cy7	Phycoerythrin-Cyanine 7
PEI	Polyethylenimine
PerCP-Cy5.5	Peridinin-chlorophyll-protein complex-Cyianine 5.5
PET/CT	Positron-emission tomography/computerized tomography
PI3K	Phosphatidylinositol 3-kinase
PIPE	Polymerase Incomplete Primer Extension
Poly(A) site	Polyadenilaton site
PPT	Polypurine tract
PR	Partial response
PR	Protease (viral)
PTPζ	Protein Tyrosine Phosphatase Zeta
REAL	Revised European-American Lymphoma
rhIL	Recombinant Human Interleukin
RIPA	Radioimmunoprecipitation Assay
RNA	Ribonucleic Acid
rpm	Rotations per minute
RPMI	Roswell Park Memorial Institute
RT	Reverse transcriptase
RTK	Receptor tyrosine kinase
SC	Subcutaneous

scFv	Single chain antibody fragment
SCID	Severe Combined Immunodeficiency
SD	Stable disease
SDS	Sodium dodecyl sulphate
SHM	Somatic hypermutation
siRNA	Small interfering RNA
SLL	Small lymphocytic lymphoma
SM	Susan McDonough strain
SMZL	Splenic marginal zone lymphoma
SOC	Super Optimal Broth
SOCS1	Suppressor of cytokine signalling 1
SP	Surface proteins
SUSAR	Suspected unexpected severe adverse reaction
T2A	*Thosea asigna* derived sequence
TAG-72	Tumour-associated glycoprotein 72
TAM	Tumour-associated macrophages
TBE	Tris/Borate/EDTA
TBM	Tetramethylbenzadine
TBST	Tris Buffered Saline and Tween 20
TCR	T cell receptor
TE	Tris/EDTA
TFG	TRK-fused gene
TIM3	T-cell immunoglobulin and mucin-domain containing-3
TKI	Tyrosine kinase inhibitor
TM	Transmembrane
TNFR	Tumor necrosis family receptor
TP63	Tumour protein p63
Treg	Regulatory T-cells

tRNA	Transfer RNA
T_{SCM}	Memory stem T-cells
tTa	Transactivator
uPA	Urokinase plasminogen activator
URD	Unrelated donor
UV	Ultraviolet
V/cm	Volt/centimeter
VEGF	Vascular endothelial growth factor
VH	Variable heavy chain
VL	Variable light chain
VSV-G	Vesicular stomatitis virus - G
WHO	World Health Organization
β_C	Common beta subunit
γ_C	Common gamma chain
µl	Microliter

Chapter 1 Introduction

The adoptive transfer of chimeric antigen receptor (CAR)-expressing T-cells is a relatively new but promising approach in the field of cancer immunotherapy. It relies on genetic reprogramming of T-cells with an artificial immune receptor that redirects their specificity against a target of choice expressed by cancer cells. The goal of this PhD was to develop a CAR based immunotherapeutic approach for classical Hodgkin's lymphoma (cHL) and anaplastic large cell lymphoma (ALCL). To achieve this goal, I set out to engineer an optimised CAR directed against the colony-stimulating factor-1 receptor (CSF-1R), a molecule that is aberrantly up-regulated in these malignant disorders.

1.1 Hodgkin's Lymphoma

Hodgkin's lymphoma (HL) is a B-cell derived haematological malignancy that was first described in 1832 by Thomas Hodgkin, working at Guy's hospital [1]. It usually presents with lymphadenopathy, typically affecting the supraclavicular or lower cervical region, often coupled with symptoms that include fever (>38^{o}C), night sweats, fatigue and/or weight loss (systemic B symptoms).

Hodgkin's lymphoma is one of the most common lymphoid malignancies in the Western world, occurring at an annual frequency of 3 new cases per 100 000 people [2]. Each year roughly 2000 new cases are diagnosed in the UK [3]. The disease presents with two age-related peaks of incidence – the first peak occurs in young adults (20-30 years old) while the second smaller peak affects adults aged over 65 years. Despite the introduction of multi-agent chemotherapy and improved radiation techniques in recent years, 20-30% of patients experience relapse or progressive disease after initial treatment [4]. In 2012, over 25,000 people died of this cancer worldwide (http://www.cancerresearchuk.org/health-professional/hodgkin-lymphoma-mortality-statistics#heading-Three; accessed February 15th, 2016). Therefore, a more

effective targeted therapy is urgently needed for those patients in whom standard management approaches fail.

1.1.1 Classification of Hodgkin's Lymphoma

Hodgkin's lymphoma is a germinal centre B-cell derived lymphoma. According to the World Health Organization (WHO)/Revised European-American Lymphoma (REAL) classification [5], Hodgkin's lymphoma is divided into two clinico-pathologically distinctive disease entities, based on biology, clinical features, morphology, immunophenotype and composition of associated leukocytic infiltrate. Classical Hodgkin's lymphoma (cHL) accounts for approximately 95% of cases while nodular lymphocyte-predominant Hodgkin's lymphoma (NLPHL) comprises the remaining 5% [6].

1.1.1.1 Nodular lymphocyte-predominant Hodgkin's lymphoma (NLPHL)

In nodular lymphocyte-predominant HL, the malignant cell population consists of lymphocytic and histocytic (L&H) cells. These abnormal cells have a different origin and immunophenotype to those found in cHL, which are termed Hodgkin and Reed-Sternberg cells (HRS) [7]. In cHL, HRS cells have the following phenotype: $CD30^{+}CD15^{+}CD20^{-}CD45^{-}$ while L&H cells in NLPHL display the phenotype: $CD30^{-}CD15^{-}CD20^{+}CD45^{+}$. The NLPHL sub-type of Hodgkin's lymphoma will not be discussed any further in this thesis since the focus of my study has been cHL and anaplastic large cell lymphoma (ALCL).

Classical Hodgkin's lymphoma is further subdivided into 4 groups:

- Nodular sclerosis Hodgkin's lymphoma (NSHL)
- Mixed cellularity Hodgkin's lymphoma (MCHL)
- Lymphocyte-depleted Hodgkin's lymphoma (LDHL)
- Lymphocyte-rich Hodgkin's lymphoma (LRHL)

1.1.1.2 Nodular sclerosis Hodgkin's lymphoma (NSHL)

Nodular sclerosis HL is the most frequent type of cHL, accounting for about 70% of cases [6]. This disease subtype is characterized by the presence of collagen bands that divide the node into nodular clusters and by the presence of HRS variants called Lacunar cells. In general, nodular sclerosis HL has a good prognosis. This variant can be subdivided into nodular sclerosis grade 1 (NS1) and nodular sclerosis grade 2 (NS2) depending on the number of RS cells and the degree of fibrosis. These sub-types have relatively better and poorer prognosis respectively.

1.1.1.3 Mixed cellularity Hodgkin's lymphoma (MCHL)

Mixed cellularity HL accounts for about 20% of cHL cases [6]. This variant is characterized by scattered HRS cells in a diffuse inflammatory background. Prognosis of MCHL is not as good as in NSHL.

1.1.1.4 Lymphocyte-depleted Hodgkin's lymphoma (LDHL)

Lymphocyte-depleted HL is very rare, accounting for less than 1% of cHL cases. However, it is the most aggressive subtype of this disease. Patients often present with advanced stage disease (eg stage III-IV; see Table 1.1) and have the poorest prognosis. Lymphocyte-depleted HL is characterized by high number of malignant (HRS) cells and relatively few non-neoplastic lymphocytes.

1.1.1.5 Lymphocyte-rich Hodgkin's lymphoma (LRHL)

Lymphocyte-rich HL accounts for about 3% of cases [6]. It is characterized by small numbers of HRS cells associated with an immune infiltrate similar to that observed in NLPHL. Prognosis of this subtype of cHL is generally excellent.

1.1.2 Clinical presentation, diagnosis and stages

Most patients with cHL present with enlarged lymph nodes in one or more supra-diaphragmatic areas, mainly in the neck. Diagnosis and disease staging is based upon physical examination, tumour biopsy, positron-emission tomography/computerized tomography (PET/CT) from the neck to the pelvis and bone marrow biopsy [8]. The disease is staged according to the Ann Arbor staging system (Table 1.1), which was developed in 1971 [9] and later modified in 1989 (Cotswold modification) [10]. This staging system defines the extent of disease progression, which facilitates the selection of initial treatment options. Patients are classified into four stages followed by a letter A or B indicating respectively the lack or presence of B symptoms (fatigue, weight loss, fever, night sweats, itchy skin etc.)

Table 1.1 Staging of Hodgkin's Lymphoma according to the Ann Arbor system.

STAGE	SYMPTOMS
I	Involvement of one lymph node or lymphoid structure
II	Involvement of two or more lymph nodes on the same side of the diaphragm
III	Involvement of lymph nodes on both sides of the diaphragm
IV	Involvement of extranodal site(s) with or without associated node involvement

1.1.3 Origin of Hodgkin and Reed-Sternberg (HRS) cells

The malignant cells in cHL, referred to as Hodgkin and Reed-Sternberg cells (HRS), account for only about 2% of the tumour mass, whereas the majority of the malignancy

is composed of a mixed inflammatory infiltrate comprised of T-cells, neutrophils, eosinophils, mast cells, plasma cells, fibroblasts and macrophages. The vast variety of cell types surrounding HRS cells underlines the importance of the tumour micro-milieu in cHL [11]. Hodgkin and Reed-Sternberg cells are large (20-60μm in diameter) and are either mono-nucleated (Hodgkin cells) or bi- and multinucleated cells (Reed-Sternberg cells) [12].

1.1.3.1 Phenotype of HRS cells

Hodgkin and Reed-Sternberg cells have largely down-regulated their B-cell specific gene expression program and have gained expression of markers associated with other haematopoietic lineages [13]. They lack several classical B-cell markers, including B-cell receptor, CD79A, CD79B, CD19, CD20, PU.1, OCT2 and BOB1 expression [14]. By contrast, those cells typically demonstrate constitutive activation of NF-κB and JAK-STAT pathways and aberrantly express T-cell markers (CD3, NOTCH1, GATA3), cytotoxic cell markers (granzyme B, perforin), dendritic cell markers (CCL17), NK cell markers (ID2), granulocyte markers (CD15) and myeloid cell markers (CSF-1R) [2, 15].

1.1.3.2 Anti-apoptotic evasion strategies employed by HRS cells

Classical HL is considered to have a germinal centre B-cell origin since immunoglobulin (Ig) gene rearrangements have been identified in HRS cells, excised by micro-manipulation from cHL cases [16, 17]. Germinal centres (GC) are micro-anatomical structures arising within lymphoid follicles, which develop as a result of the clonal expansion of antigen-specific B-cells. During germinal centre development, antigen-stimulated B-cells undergo several rounds of proliferation and somatic hypermutation (SHM) of Ig V genes. Only those cells with a B-cell receptor (BCR) that displays high affinity for antigen and is non self-reactive are rescued from apoptosis. Hodgkin and RS cells exhibit evidence of SHM and lack of BCR expression, which suggests that they are pre-apoptotic B-cells that have escaped antigen selection by

acquiring transforming mutations [17]. In the sections that follow, three of the anti-apoptotic evasion strategies implicated in HRS survival within the GC are described briefly.

1.1.3.2.1 NF-κB signalling pathway

The NF-κB signalling pathway plays a key role in the regulation of cell proliferation and apoptosis. This pathway has repeatedly been shown to be constitutively activated in cHL [18, 19]. Subsequently, this phenomenon was explained by the presence of mutations that render IκBα defective [18]. Those observations suggest that the NF-κB signalling pathway contributes to the survival of malignant B-cells in cHL.

1.1.3.2.2 JAK-STAT signalling

Signalling by the Janus kinase/ signal transducers and activators of transcription (JAK-STAT) system has also been implicated in proliferation and apoptosis resistance in HRS cells. Cytokine-mediated activation of the JAK-STAT pathway in response to interleukin (IL)-6, IL-9 and IL-13 is well documented in cHL and involves downstream activation of STAT3, STAT5 and STAT6 [20, 21]. Additionally, frequent genomic gains of JAK2 [22] and inactivating mutations of suppressor of cytokine signalling 1 (SOCS1 - a negative regulator of JAK-STAT signalling) [23], have been described.

1.1.3.2.3 Fas death receptor pathway escape

The Fas receptor is a member of the tumor necrosis family receptor superfamily (TNFR). Fas is a death receptor and is directly involved in B-cell apoptosis during antigen selection in the GC. Several studies have reported that HRS cells are resistant to Fas-mediated apoptosis due to high levels of expression of the inhibitory molecule c-FLIP [24].

1.1.4 Role of Epstein-Barr virus in Hodgkin's lymphoma pathogenesis

Epstein-Barr virus (EBV) is a ubiquitous human gamma-herpesvirus that has infected over 90% of adults infected worldwide, leading to life-long latent infection [25]. Although EBV is found in about 40% of cHL cases [26], its contribution to the pathogenesis of the disease is unknown. In EBV^+ tumours, all of the HRS cells are infected [27]. This is extremely unlikely to happen by chance bearing in mind that infected cells form a tiny fraction (1-100 cells per million) of the B-cell population. Furthermore, the monoclonality of EBV DNA in HRS cells has been demonstrated which indicates that the EBV infection precedes the clonal expansion of tumour cells [28].

Although the role of EBV infection in the pathogenesis of cHL is unclear, it has been established that two EBV proteins (LMP1 and LMP2A) provide signals that mimic those derived from CD40 and BCR. By this means, EBV infection could theoretically provide an apoptotic escape mechanism for HRS cells within the GC [29].

1.1.5 Signalling by Receptor Tyrosine Kinases (RTK) in cHL

Receptor tyrosine kinases (RTK) are commonly involved in cancer pathogenesis and usually signal through the phosphatidylinositol 3'kinase (PI3K)/AKT, mitogen-activated protein kinase (MEK1/2/ERK1/2) and JAK-STAT pathways [30, 31]. Several RTKs showing autocrine activation in HRS cells have been implicated in the pathogenesis of cHL, including platelet-derived growth factor receptor A (PDGFRA), DDR2, tropomyosine related kinase A (TRKA), tropomyosine related kinase B (TRKB), tyrosine kinase with Ig and EGF homology domain (TIE1), ephrin type B receptor 1 (EPHB1) and RON [32, 33]. These findings indicate that aberrant RTK signalling is an important factor in cHL pathogenesis and that it may be a novel therapeutic target.

Recently, Lamprecht *et al*. have reported that CSF-1R is constitutively activated in most cHL-derived cell lines and that primary cHL cells are characterized by aberrant

CSF-1 and CSF-1R co-expression [34, 35]. Additionally, a separate study has outlined a correlation between CSF-1R expression on HRS cells and first line treatment failure in a cohort of 29 cHL patients [4]. It has been demonstrated that the number of tumour-associated macrophages (TAM) and CSF-1R expression on HRS cells, taken as individual markers, are both linked with inferior treatment outcome. The combined use of those 2 gene expression features has been suggested as a prognostic factor for identification of high-risk patients for primary treatment failure and death after ABVD-type combination chemotherapy (see Table 1.2 for acronym). Although the nature of interactions between HRS cells and TAMs is not clear, it is possible that tumour cell growth is supported by autocrine (HRS cells) or paracrine (TAM) CSF-1 secretion, acting to stimulate CSF-1R on HRS cells. In the light of these findings, CSF-1R emerges as a promising target for at-risk and refractory cHL patients.

1.1.6 Management of cHL: from standard care to novel agents

Treatment recommendations for cHL vary in different countries but, in general, patients with early stage disease (e.g. stage I and II) receive a combination of 2-4 cycles of chemotherapy (ABVD or BEACOPP) (Table 1.2) and radiotherapy (20 Gy involved field radiotherapy (IFRT)) [36, 37]. Patients with advanced stage disease (e.g. stage III and IV) are treated with 6-8 cycles of chemotherapy [36, 37].

1.1.6.1 Radiotherapy

Radiotherapy was the first curative treatment for cHL, as described by Peters in 1958 and Kaplan in 1966 [38, 39]. Owing to the contiguous manner by which cHL usually spreads, radiation therapy was initially administered to large fields (e.g. mantle fields, “inverted Y fields” or both). This approach provides effective treatment both to tumours and to clinically unaffected neighbouring tissues, but resulted in significant toxicity in some cases. Owing to the effectiveness of modern chemotherapy, wide field radiotherapy is now rarely practiced although IFRT may be used in some cases.

1.1.6.2 Chemotherapy

In the mid 1960s the treatment of cHL was revolutionized by the introduction of the first multidrug chemotherapy regimen, MOPP, which consisted of mechlorethamine, vincristine, procarbazine and prednisone [40]. Next, the ABVD regimen was developed (Table 1.2) and owing to its superior efficacy and lower toxicity, it replaced MOPP as a standard treatment [41]. More recently, the "escalated BEACOPP" regimen (Table 1.2) was developed and has achieved improved complete remission rates compared to ABVD in a number of clinical trials, although toxicity appears to be increased [42]. Alternatively, patients who fail to achieve complete response to ABVD may be treated with more intensive regimens such as escalated BEACOPP followed by autologous stem cell transplantation (ASCT).

Table 1.2 Chemotherapy regimens

	Drug	**Group of Drug**
ABVD	Doxorubicin (Adriamycin) (A)*	Anthracycline
	Bleomycin (B)	Glycopeptide antibiotic complex
	Vinblastine (V)	Vinca-alkaloid
	Dacarbazine (D)	Alkylating
BEACOPP	Bleomycin (B)	Glycopeptide antibiotic complex
	Etoposide (E)	Topoisomerase II inhibitor
	Doxorubicin (Adriamycin) (A)	Anthracycline
	Cyclophosphamide (C)	Alkylating
	Vincristine (Oncovin) (O)	Vinca-alkaloid
	Procarbazine (P)	Alkylating
	Prednisone (P)	Corticosteroid

1.1.6.3 Targeted therapies

Classical HL is largely associated with good prognosis and is characterized by 70-80% overall survival (OS) of advanced stage patients treated with standard chemotherapy regimens [43]. The main risk of death in those patients comes from the development of late complications including secondary malignancies (leukaemia and solid tumours) and cardiac disease, such that 15 years after the end of treatment, mortality related to late effects exceeds that of the original disease [44]. Furthermore 20-30% of patients present with relapse or progressing disease after initial treatment [4]. Those patients receive salvage chemotherapy plus potentially further treatment including ASCT with or without involved field radiotherapy. Each of those additional treatments entails significant risk for the patient, with ASCT having a non-relapse mortality rate of 2-3% [45-47]. In order to improve disease outcome further, there has been considerable interest in the development of targeted therapies. So far, the anti-CD20 monoclonal antibody rituximab has been the only targeted therapy introduced into primary treatment for NLPHL and is now under investigation for cHL (e.g. HD18 study, exploring the combination of this agent with escalated BEACOPP) [48-50]. A blocking anti-CD40 antibody (lucatumumab) and a chimeric anti-CD80 antibody (galixumab) have also been tested in early phase clinical trials but have shown limited efficacy (13.5% and 10.3% overall response rate, respectively) [51, 52]. Similarly, early phase studies with anti-CD25 antibodies, either conjugated with recombinant diphtheria toxin or with ^{131}Iodine, showed discouraging results [53, 54]. Monoclonal antibodies against CD30 are also under investigation. Despite initial low response rate with the anti-CD30 monoclonal antibodies SGN-30 [55] and MDX-060 [56], antibody engineering has allowed for enhanced antibody-directed cell mediated cytotoxicity (ADCC) bringing a second line of CD30-targeting antibodies in early phase clinical trials (MDX-1401 (trial reference: NCT00634452) and XmAb2513 (NCT00606645) (clinicatrials.gov website, accessed on 15/02/2016) [57].

By far the most exciting advancement in the therapy of cHL has been brentuximab vedotin, a CD30-specific antibody-drug conjugate. In 2011, the U.S. Food and Drug Administration (FDA) approved brentuximab vedotin for the treatment of cHL after failure of ASCT or after failure of at least two prior multi-agent chemotherapy regimens in patients who are not ASCT candidates. In a phase II clinical trial of patients with relapsed/refractory Hodgkin's lymphoma, treatment with single-agent brentuximab vedotin resulted in overall response rates of 75% with 34% complete remissions [58]. Median duration of response was 20.5 months for those in complete remission and 6.7 months for all responding patients. More recently, brentuximab has been evaluated in combination with a number of chemotherapy regimens including DHAP (dexamethasone, cytarabine, cisplatin – NCT02280993), ICE (ifosfamide, carboplatin, etoposide – NCT02227199), gemcitabine (NCT01780662) and ABVD, the latter resulting in unacceptable lung toxicity [59]. Consequently, the ABVD chemotherapy regimen was modified to omit bleomycin and include brentuximab, resulting in 96% complete response with no significant pulmonary toxicities registered [59]. Following these encouraging results a phase 3 clinical trail comparing standard ABVD treatment to AVD plus brentuximab vedotin is currently underway (NCT01712490).

Recently, combination therapy with brentuximab and checkpoint inhibition has become an area of extensive interest. The combination of brentuximab and ipilimumab (CTLA-4 checkpoint inhibitor) is already under investigation (NCT01896999). Furthermore, a striking response to PD1 blockade as a single agent has been reported in two clinical trials using nivolumab (74% overall response and 17% complete response) [60] and pembrolizumab (66% overall response and 21% complete response) [61]. Given these promising results, a combination therapy of PD1 checkpoint blockade with brentuximab can be envisaged in the near future [57].

Other targeted therapies, currently in early phase clinical trials, include novel agents like the mTOR inhibitor everolimus, the histone deacetylase inhibitor panobinostat,

JAK/STAT (INCB039110) and PI3 kinase (INCB040093) inhibitors [42]. High response rates have been seen with the use of everolimus (47% overall response, 1 complete response) [62] and panobinostat (27% overall response) [63] as single agents. Additionally, in a phase 1 study patients who received a combination of the JAK1 inhibitor and the PI3 kinase inhibitor had an overall response rate of 67% [64]. Further studies will be needed to confirm these results, but combined modulation of several pathways may be a promising approach in this disease.

1.1.6.4 Clinical evaluation of CAR T-cell immunotherapy for cHL

Currently, there are several ongoing early phase clinical trials using CD30-targeting CAR T-cells in cHL. Baylor College has 2 open clinical trials using a CAR targeting CD30 in cHL (NCT01192464 and NCT01316146) while the University of Cologne has one (NCT01645293) and the Chinese PLA General Hospital has one such trial (NCT02259556) [65]. Reported preliminary results from Baylor College are encouraging in that no treatment attributable adverse events have been observed in the 9 enrolled patients (7 cHL and 2 ALCL). However, one patient has achieved complete response with 1 partial response and 4 patients with stable diseases at 6 weeks post treatment [66].

Classical Hodgkin's lymphoma has become a highly curable disease over the last few decades due to the introduction of multidrug chemotherapy. However late complications (including secondary malignancies) and long term toxic effects are still a major concern in cured patients. Furthermore novel more effective targeted therapies are needed for cHL patients who have relapsed after ASCT and patients who have failed two multidrug regimens and are not candidates for ASCT.

1.2 Anaplastic Large Cell Lymphoma

Anaplastic large cell lymphoma (ALCL) is a type of Non-Hodgkin's lymphoma (NHL) first described by Stein *et al*. in 1985 [67]. It represents a diverse group of tumours with common morphological and immunophenotypic characteristics, but with varying clinical and genetic features. Anaplastic large cell lymphoma is a T-cell or null-cell lymphoma, named after the frequent anaplastic features evident in histological analysis [67].

1.2.1 Classification of anaplastic large cell lymphoma

Anaplastic large cell lymphoma can present in two forms: cutaneous (c-ALCL) and systemic. Cutaneous ALCL is limited to the skin whereas systemic ALCL can involve lymph nodes, bone, soft tissue, liver and lung. Distinction between cutaneous ALCL and systemic ALCL with cutaneous involvement is clinically important, as these disorders require different forms of treatment. Cutaneous ALCL generally has a less aggressive disease course than systemic ALCL. The following paragraphs refer to systemic ALCL unless mentioned otherwise.

According to the World Health Organization (WHO) tumour classification, ALCL is sub-divided into two types depending on the anaplastic lymphoma kinase expression (ALK), giving ALK positive (ALK^+) and ALK negative (ALK^-) ALCL [68]. Both types of ALCL are characterized by uniform expression of the CD30 antigen on the cell surface.

Anaplastic lymphoma kinase (ALK) is a receptor tyrosine kinase, whose expression is generally limited to perinatal neural tissue. The *ALK* gene has a recognized pathogenic role as it is frequently involved in chromosomal translocations, mutations and amplifications that are often seen in a variety of neoplasms [69].

1.2.2 Clinical presentation, epidemiology and diagnosis

Anaplastic large cell lymphoma represents about 5% of NHL cases in adults and 20-30% of all paediatric lymphomas [70, 71]. Expression of ALK is typically found in about 60-80% of cases of ALCL. The ALK^+ subtype of ALCL is mainly observed in children and young adults with a male predominance (6.5:1 male to female ratio). By contrast, ALK^- ALCL primarily occurs in older individuals and presents with no gender predominance [5].

Anaplastic lymphoma kinase positive ALCL often presents as an aggressive disease with systemic symptoms. By contrast, a less aggressive presentation is typical for ALK negative ALCL cases, although these lymphomas are associated with worse prognosis. Diagnosis is based upon physical examination and tumour biopsy. The disease is then staged according to the Ann Arbor staging system (Table 1.1), which was developed in 1971 [9] and later modified in 1989 [10]. About 70% of patients present with advanced (stage III or IV) disease with abdominal and/or peripheral lymphadenopathy, often associated with extra-nodal infiltrates and involvement of the bone marrow [72]. In adults, breast involvement most frequently associated with breast implants has also been described [73-75].

Anaplastic lymphoma kinase expression is an important prognostic factor in ALCL. The overall 5-year survival rate is approximately 70-80% for ALK^+ ALCL and substantially less (30-40%) for ALK^- ALCL. [76]

1.2.3 Chromosomal translocations

The expression of ALK in ALCL is a consequence of chromosomal translocations involving the ALK gene locus. In 80% of ALK^+ ALCL cases, translocation occurs between the ALK gene on chromosome 2 and the nucleophosmin (NPM) gene on chromosome 5, giving rise to the fusion protein, NPM-ALK [77]. Since the initial

discovery of NPM-ALK, numerous other fusion partners of ALK have been discovered, including tropomyosin 3 and 4, clathrin heavy chain-like 1 (CLTC1), TRK-fused gene (TFG) and many more [78, 79]. Fusion proteins derived from translocations involving the ALK gene have oncogenic potential due to aberrant constitutive tyrosine kinase activation, resulting in the continuous transmission of growth-promoting cellular signals [80]. The ALK kinase activates different downstream signalling cascades. In particular, Ras-ERK activation is essential for ALCL cell proliferation while the JAK3-STAT3 and PI3K-AKT pathways are central for cell survival [81].

Despite ALK^- ALCL being characterized by the absence of chromosomal translocations involving the ALK gene, two different translocations have recently been reported. These involve dual specificity phosphatase 22 (DUSP22), located on chromosome 6p25.3 and tumour protein p63 (TP63), found on chromosome 3q28. Importantly, chromosomal rearrangements involving these loci have been implicated in the further stratification of disease prognosis [82]. While DUSP22 rearranged ALK^- disease has similar overall survival rates compared to ALK^+ disease (5-year overall survival (OS) of 70-80%), TP63 rearrangements convey a worsened prognosis (5-year OS of 15%) and poor response to initial treatment [82]. The mechanistic implications of these rearrangements for disease pathogenesis are currently unknown and remain under investigation.

1.2.4 Morphologic features and subtypes

Systemic ALCL can be subdivided morphologically into 3 types – common variant, lymphohistiocytic variant and the small cell variant [83].

- In the common variant, large lymphoid cells are found in which nuclei have been described as horseshoe shaped and chromatin poor [84], with multiple nucleoli. These cells, called “hallmark” cells, form large sheet-like structures within the tumour. Multinucleated cells with Reed-Sternberg–like appearance may also occur.

- The lymphohistiocytic variant is characterized by a large number of histiocytes, which may mask the anaplastic tumour cell population. The neoplastic cells are $CD30^+$ and often cluster around blood vessels [85].
- The small cell variant is characterized by a mixture of small, medium-sized and large lymphoid cells with irregular shaped nuclei. A typical feature of this variant is large cells surrounding small vessels [86].

1.2.5 Immunophenotype

Anaplastic large cell lymphoma is a T-cell derived malignancy but in some cases it may have an apparent “null cell” phenotype due to loss of several pan T-cell antigens. Regardless, all ALCL cases show evidence for a T-cell lineage of origin at the genetic level. In more than 75% of cases, tumour cells are CD3 negative. They are mostly CD4 positive, variably positive for CD45 and strongly positive for CD25. Most typically, all tumour cells are CD30 positive [87]. Some cases express markers typically associated with other lineages including CD15, PAX5, CD13, CD33 and CSF-1R [34, 88-90].

1.2.6 Management of ALCL: from standard care to novel agents

Currently first line of treatment for ALCL consists of chemotherapy regimens such as CHOP (**c**yclophosphamide, doxorubicin (**h**ydroxydaunorubicin), vincristine (**o**ncovin), and **p**redniso(lo)ne) but long-term disease outcome varies depending on the subtype [79]. While about 80% of patients respond to treatment, 40-65% of patients develop recurrent disease [91]. The overall 5-year survival rate is approximately 70-80% for ALK^+ ALCL and 30-40% for ALK^- ALCL [76]. The standard management of patients who fail a multidrug chemotherapy regimen includes the use of salvage chemotherapy such as romidepsin (Istodax) [92] and pralatrexate (Folotyn) [93], followed by ASCT [94, 95]. For patients who are not suitable or who fail ASCT, the prognosis is extremely poor. This underlines the need for development of targeted therapies.

1.2.6.1 Targeted therapies

Targeted therapies for ALCL largely overlap with those for cHL because of the ubiquitous expression of CD30 in both malignancies. In a phase I study by Younes *et al*., 2 patients with refractory ALCL (unknown ALK status) were enrolled and treated with brentuximab, leading to complete response in both cases [96]. In a similar phase I study involving 5 patients with refractory/relapsed ALCL (also unknown ALK status), 80% achieved a complete response following treatment with this agent [97]. Notably, the first study to show no difference in outcomes between brentuximab-treated ALK^- and ALK^+ subgroups was a phase II clinical trial, which enrolled 53 patients with refractory/relapsed ALCL (72% of which were ALK^-). In that study, 52% of patients achieved a complete response regardless of the ALK status, thereby eliminating the historical survival difference observed between the two subtypes of ALCL. Based on that pivotal trial in 2011, FDA approved brentuximab vedotin for the treatment of ALCL in the second line setting, after failure of at least one prior multi-agent chemotherapy regimen. Currently, patients with $CD30^+$ newly diagnosed mature T-cell lymphomas are being enrolled in a phase III clinical trial (ECHELON-2, NCT01777152), which aims at comparing brentuximab vedotin in combination with CHP with the standard-of-care CHOP in first-line setting [98].

Another approach to the treatment of ALK^+ ALCL involves the use of ALK inhibitors. The current leading compound is crizotinib. This agent has shown clinical success and is currently FDA approved for the treatment of non-small cell lung carcinoma (NSCLC) harbouring ALK translocations [99]. While initial treatment with crizotinib is frequently successful against ALCL, tumours acquire resistance to this therapy. Initial response to therapy lasts on average 10.5 months [100].

The limited successes of current therapeutic approaches for advanced-stage risk group patients who have failed several multidrug regimens and have relapsed after ASCT or

are not eligible for ASCT underlines the need for the development of more effective targeted therapy that will improve the success of sustained remission of this disease.

1.3 Colony-Stimulating Factor-1 Receptor and its Ligands

Historically, members of the receptor tyrosine kinase (RTK) family have been the subject of intense investigation owing to their fundamental role in signal transduction and cellular communication. Several RTKs are central players in determining whether cells proliferate, differentiate, migrate or die. In addition to their role in normal cellular processes, RTKs are also widely known for their role in the initiation and progression of a number of cancer types.

The colony-stimulating factor-1 receptor (CSF-1R) is also known as macrophage colony-stimulating factor receptor (M-CSFR) or CD115. This integral transmembrane glycoprotein exerts its biological functions in response to two competing ligands, namely colony-stimulating factor-1 (CSF-1) or interleukin (IL)-34. Binding of either ligand promotes oligomerisation and transphosphorylation of the receptor, leading to the activation of signal transduction [101, 102].

1.3.1 Structure and function of CSF-1R

Colony-stimulating factor-1 receptor is a member of the type III RTK family, which also includes c-*kit* [103], Flt-3 [104], platelet-derived growth factor receptor (PDGFR)α [105] and PDGFRβ [106]. Similar to the other members of its family, CSF-1R is composed of an extracellular glycosylated ligand-binding segment with 5 immunoglobulin (Ig)-like domains, a transmembrane domain and a kinase insert, dividing the intracellular kinase domain into 2 lobes [107]. Within the cytoplasmic kinase domain, 8 tyrosine phosphorylation sites have been described, distributed between the juxtamembrane section (Y546 and Y561), the kinase insert (Y699, Y708 and Y723) and the distal kinase domain (Y809, Y923 and Y969) [108-111].

Signalling through CSF-1R has been primarily studied in macrophages [112]. In the inactive form of CSF-1R, the juxtamembrane domain mediates a critical auto-inhibitory role by preventing the activation loop from adopting an active conformation [113]. Ligand binding induces non-covalent dimerization of the receptor chains, thus relieving inhibition by phosphorylation of Y561 (Y559 in mouse) [114]. This tyrosine is the first residue to be phosphorylated in response to ligand binding and is crucial for full receptor activation and subsequent tyrosine phosphorylation [112, 114, 115]. The phosphorylated sites function as docking sites for a variety of proteins that include several Src family kinases, the p85 subunit of PI3K, phospholipase Cγ2, suppressor of cytokine signalling-1, Grb2, and c-Cbl [110, 116]. In turn, this leads to signalling waves involving ERK1/2, PI3K, Raf and MAP kinase and Akt (Figure 1.1) [117]. The resultant gene expression program promotes proliferation, differentiation and survival of the cell.

Binding of IL-34 to CSF-1R triggers phosphorylation of ERK1/2, indicating that CSF-1 and IL-34 generate signals that at least in part overlap [102]. However, the kinetics of CSF-1R signalling in response to IL-34 as well as the rate of receptor internalization, are still to be described.

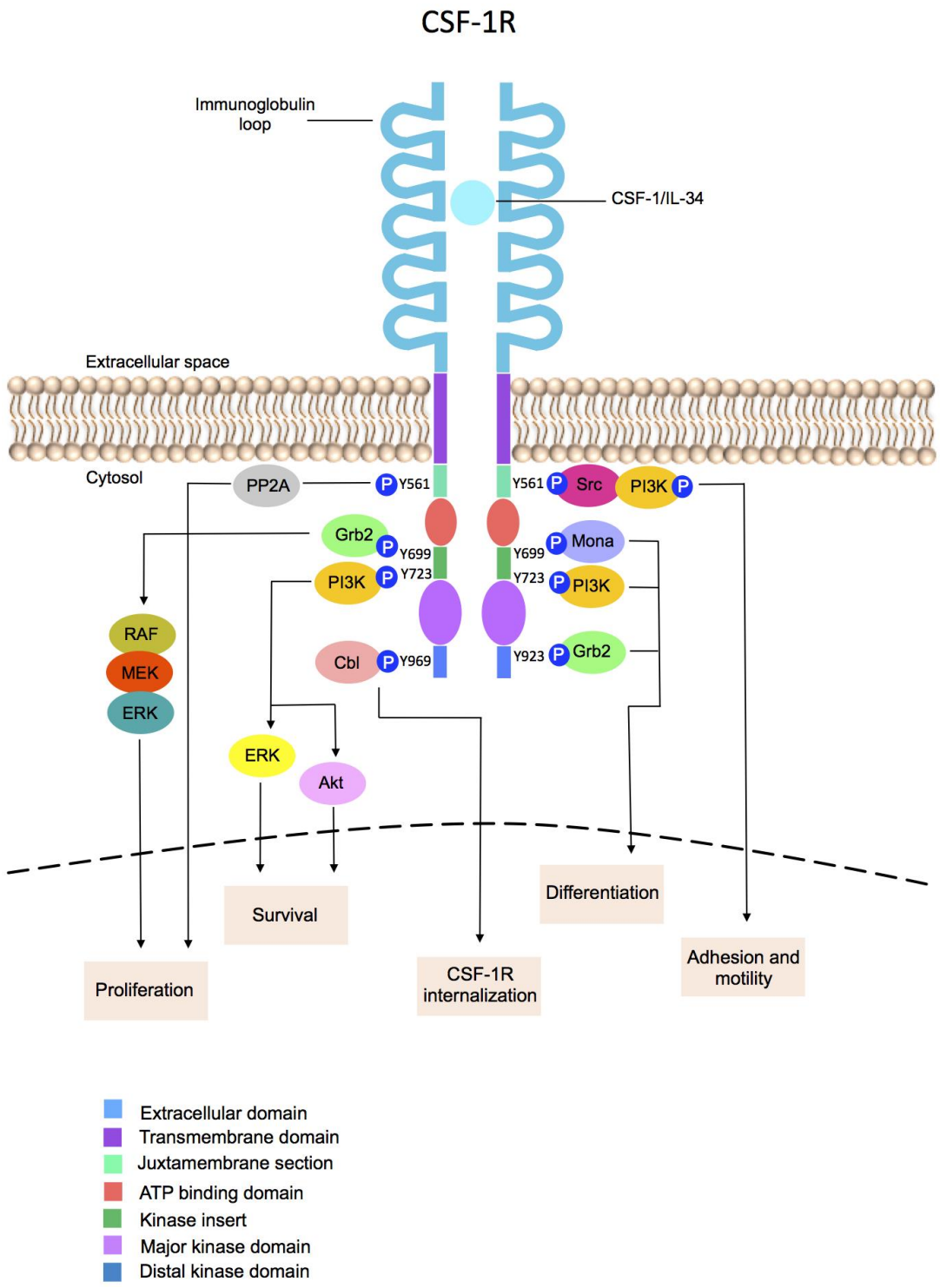

Figure 1.1 CSF-1R signalling in myeloid cells.

Binding of CSF-1 or IL-34 induces CSF-1R chain dimerization, leading to cross-tyrosine phosphorylation, and the direct association of signalling molecules with the receptor through their phosphotyrosine-binding domains. The resultant gene expression program promotes proliferation, differentiation and survival of the cell. Abbreviations: Cbl, Casitas B lineage; MEK, mitogen-activated protein kinase kinase; Mona, monocyte adaptor; PI3K, phosphatidylinositol 3-kinase.

1.3.2 CSF-1R and its ligands

Colony-stimulating factor-1 receptor is encoded by the *c-fms* proto-oncogene. This was first discovered as the cellular homologue of the active viral oncogene *v-fms*, encoded by the Susan McDonough (SM) and Hardy-Zuckerman five (HZ-5) strains of the feline sarcoma virus [101]. The human *c-fms* gene, located on chromosome 5q33.3, is 75 kb in length and is under the tight regulation of a promoter and an intronic enhancer element (FMS intronic regulatory element or FIRE), both of which are evolutionarily highly conserved [118]. Two naturally occurring isoforms of CSF-1R have been reported, as a result of different processing pathways, but no significant ligand affinity differences have been established between both CSF-1R isoforms. [119].

Colony-stimulating factor-1 receptor has two known ligands – it is the unique receptor for CSF-1 and recently it has been shown to also bind IL-34 [102].

1.3.2.1 Colony-stimulating factor-1

Colony-stimulating factor-1, also known as macrophage colony stimulating factor (M-CSF), is a homodimeric glycoprotein. Owing to alternative mRNA splicing and post-translational modification, CSF-1 exists in three isoforms: secreted glycoprotein, secreted proteoglycan and cell surface glycoprotein [120]. Under physiological conditions, CSF-1 is produced by fibroblasts, endothelial cells, monocytes, macrophages, osteoblasts, microglia, keratinocytes, bone marrow stromal cells, natural killer cells, B-cells and T-cells [118, 121-124]. The main physiological role of CSF-1 is as a haematopoietic growth factor responsible for the survival, proliferation, differentiation and motility of cells of the monocyte lineage [125]. In addition, CSF-1 plays a major role in bone remodelling by osteoclasts. [120].

Inactivating mutation of the *Csf1* locus in the op/op mouse ($Csf1^{op}$/ $Csf1^{op}$) leads to a decrease in tissue macrophages and severe deficiency in osteoclasts [126]. Gene targeting of the c-*fms* locus essentially results in the same phenotype, the most striking

manifestation of which is osteopetrosis. Notably, osteopetrotic mice exhibit CSF-1-independent recovery of macrophages and osteoclasts, reaching normal numbers by 7-9 months of age [127]. The mechanism of this process is yet not clear, but most probably it is mediated by vascular endothelial growth factor (VEGF) [128] and/or IL-3 and granulocyte-macrophage colony-stimulating factor (GM-CSF) [129], although the contribution of other growth factors cannot be ruled out.

1.3.2.2 Interleukin 34

The existence of an additional CSF-1R ligand was suspected for a long time due to the greater severity of the osteopetrotic phenotype of CSF-1R$^{-/-}$ mice compared to the op/op mice, but the actual ligand, termed IL-34, was discovered only recently [102]. Interleukin 34 binds CSF-1R in a specific and CSF-1-independent manner and surprisingly shows no sequence similarity to CSF-1 or to any other known protein [102]. Interleukin 34 overlaps functionally with CSF-1 by promoting survival, proliferation and macrophage colony formation. Yet, these two cytokines exhibit significant tissue-specific and developmental differences in their expression patterns. For example, both IL-34 and CSF-1 are indispensable for brain development but are expressed within different regions [130]. This implies that IL-34 is functionally redundant with CSF-1 but their differential spatial expression points towards complementary functioning.

Despite the functional similarities between IL-34 and CSF-1, they exhibit several significant differences:

- IL-34 and CSF-1 have overlapping, but yet distinct binding sites on CSF-1R [102].
- IL-34 binds with considerably higher affinity to CSF-1R than does CSF-1 (Kd of 1pM versus 34 pM respectively) [102].

Recently, a novel IL-34 receptor was identified termed PTP-ζ [131]. It is primarily expressed on neural progenitors and glial cells and is highly expressed in human

glioblastomas [132]. Unsurprisingly, IL-34 is highly expressed in the brain and has an important role in microglial development. In agreement with this, IL-34-deficient (IL-$34^{-/-}$) mice exhibit severe deficits in microglia formation [133].

1.3.3 CSF-1R in normal physiology and pathology

In normal physiology, CSF-1R expression is limited to the mononuclear phagocyte lineage. It is primarily expressed on macrophages, non-classical monocytes ($CD14^{+}CD16^{+}$) and osteoclasts. During inflammation, signalling through CSF-1R promotes cytotoxicity, phagocytosis, chemotaxis and cytokine production by these cell types and furthermore modulates the development and function of dendritic and Langerhans cells [134]. In addition, the CSF-1/CSF-1R axis plays a key role in bone metabolism [135], brain inflammation mediated by microglia [136] and in female reproduction [137]. Abnormal signalling through CSF-1R has been reported to be implicated in a number of inflammatory disorders such as arthritis [138], atherosclerosis [139], obesity, tumour growth and metastasis [140].

Expression of CSF-1R has been reported in diverse cancer types. Lamprecht *et al*. have demonstrated that CSF-1R is constitutively activated in most cHL-derived cell lines and that primary cHL cells express both CSF-1 and CSF-1R [141, 142]. In cHL and ALCL, CSF-1R expression has been shown to originate from an aberrantly activated endogenous long terminal repeat (LTR), suggesting that the origin of the unnatural CSF-1R expression found on HRS and ALCL cells is loss of epigenetic control. Aberrant CSF-1R expression is also commonly documented in tumours of epithelial origin such as breast [143, 144] and ovarian cancer [145]. Furthermore CSF-1R expression has been strongly associated with poor prognosis in those cancers, which makes it an attractive target for drug discovery [146-148]. A more detailed discussion of the role of CSF-1/ CSF-1R in cancer is provided in section 3.1.1 (page 127).

1.4 Chimeric Antigen Receptors

Chimeric antigen receptors are also known as “T-bodies” or chimeric immune receptors. These molecules were first developed by Eshhar *et al*. [149, 150] and are engineered as bespoke cDNA fusions. Efficient host cell delivery may be achieved using viral or non-viral expression systems, leading to transient or stable transgene expression. In general, CARs are expressed within host cells as membrane-spanning homodimers at the cell surface. Most commonly, T-cells are used as host cells although other populations such as natural killer (NK) cells may also be used. Upon target engagement, CARs undergo cross-linking at a synaptic interface formed with the target cell [151], leading in turn to activation of one or more immune effector functions.

1.4.1 Structure and evolution of chimeric antigen receptors

Structurally, CARs consist of an extracellular targeting domain and variable spacer domain (hinge), followed by a transmembrane region and an endodomain with signalling function (please refer to Figure 4.1, A on page 150).

1.4.1.1 Targeting domain

The targeting or antigen-recognition domain most commonly consists of a single-chain antibody fragment (scFv) that has been assembled from an antibody variable heavy (VH) and light (VL) chain, joined by a flexible linker. Alternatively, natural [152-155] or chimeric ligands [156] may serve in this role. A recent innovation entails the design of universal CARs that may be used in a “plug and play” manner with biotinylated [157] or fluorescein-conjugated monoclonal antibodies [158]. Similarly, FcγRIIIa (CD16)-based CARs have been developed in which the high affinity V158 Fc receptor variant is employed as a targeting adaptor. These CARs harness the ability to mediate antibody-directed cytotoxicity and other lymphocyte effector functions when engineered cells are co-infused with a suitable monoclonal antibody [159].

Chimeric antigen receptors bind directly to native cell surface polypeptides, glycoproteins, glycans or glycolipids. This means that the need for antigen processing or human leukocyte antigen (HLA)-restricted presentation is bypassed, in contrast to αβ T-cell receptors (TCRs). This is an important advantage since down-regulation of HLA antigen expression is a widespread immune escape mechanism employed by transformed cells [160]. Furthermore, this attribute eliminates the need for matching to the patient's HLA haplotype.

1.4.1.2 Hinge/ spacer domain

The targeting domain is generally separated from the T-cell membrane by a hinge/ spacer, which facilitates binding of the target epitope. Consequently, optimization of length [161] or flexibility [162] of this element may prove crucial to the attainment of enhanced function. Most commonly, hinge/spacers are derived from immunoglobulin Fc/ hinge regions or lymphocyte transmembrane receptors, such as $CD8^+$. The choice is important since immunoglobulin-derived modules may interact with Fc-receptor bearing myeloid cells, leading to off-target effects [163] or *in vivo* exhaustion and activation-induced T-cell death [164].

1.4.1.3 Transmembrane domain

The transmembrane domain also primarily serves a structural role and is commonly derived from membrane-spanning lymphocyte molecules such as CD28, CD4 or CD8 [165, 166]. In some cases, sequence selection may also influence CAR function. One such example is the ability of CARs containing the CD3ζ transmembrane domain to recruit other elements of the TCR/ CD3 complex, thereby potentiating signal delivery [167].

1.4.1.4 Signalling domain – defining the generations of chimeric antigen receptors

Refinement of the signalling domain has engendered the greatest interest in the optimization of CAR-mediated anti-tumour activity. Indeed, endodomain composition has given rise to the classification system used most commonly to describe these molecules. First generation CARs contain a single module that delivers a TCR-like "signal 1", most commonly the endodomain of CD3ζ or the closely related γ subunit of the high affinity receptor for IgE, FcεR1 (for a schematic please refer to Figure 4.1, A) [168]. Disappointingly however, clinical studies using T-cells that express first generation CARs have yielded unsatisfactory results (Tables 1.3 and 1.4) [169-171]. While safety was acceptable, sub-optimal anti-tumour responses associated with a lack of *in vivo* expansion and persistence of CAR T-cells were observed. These clinical observations provided a strong rationale for the development of systems whereby "signal 2" or co-stimulation could also be provided to CAR-engineered T-cells. This may be achieved by expression of the CAR in T-cells that undergo periodic stimulation by antigen-presenting T-cells (e.g. T-cells with specificity for latent viruses) [172] or alternatively through further CAR engineering.

The latter approach is best illustrated by the development of second generation CARs, in which a co-stimulatory signalling motif is also incorporated within the CAR endodomain (for a schematic please refer to Figure 4.1, A). [173] Several groups have demonstrated in both pre-clinical and clinical studies that CARs in which CD3ζ and a co-stimulatory motif are aligned *in-cis* are functionally superior to those containing CD3ζ alone. Commonly used co-stimulatory domains include those derived from CD28 [173, 174], 4-1BB [175, 176], OX40 [176, 177], ICOS [176, 178], CD27 [179], DAP10 [180], or 2B4(CD244) [181]. Importantly however, the order of these signalling motifs appears to be paramount for delivery of optimal co-stimulation [173, 174]. Furthermore, uncertainty persists as to what constitutes the optimal configuration of the CAR co-stimulatory domain(s). In general, IL-2 release is greatest using the CD28-CD3ζ

configuration [180]. However, the combination of ICOS-CD3ζ has been reported to elicit enhanced cytotoxicity [176], accompanied by Th17 differentiation [178]. Adding to complexity, contrasting results have also been obtained in distinct models. For example, in one model, the inclusion of CD28 sequences protected CAR-engineered cells from the inhibitory effects of regulatory T-cells (Treg) and cytokines such as IL-10 and transforming growth factor-β [182]. By contrast, the ability of CD28-containing CARs to mediate enhanced IL-2 production has also been reported to enhance Treg infiltration, ultimately compromising anti-tumour activity [183]. Chimeric antigen receptors containing 4-1BB have been reported in some [184] but not all studies [180] to promote multi-functionality of cytokine production, which is generally considered desirable. However, 4-1BB containing CARs may deliver constitutive signalling in the absence of target engagement, a property that may be advantageous or disadvantageous depending upon clinical indication [185].

More recently, third generation CARs have been described in which two or more co-stimulatory signalling domains are placed *in-cis* within the CAR endodomain (for a schematic please refer to Figure 4.1, A). Examples include CARs in which CD3ζ and CD28 have been co-expressed with p56lck [186] OX-40 [162, 177, 187] or 4-1BB [162, 184, 188, 189]. Simultaneous provision of co-stimulation through complementary signalling pathways may further improve *in vivo* survival and function of CAR T-cells. Nonetheless, careful comparison with appropriate matched second generation CARs is warranted to provide clear evidence of the superiority of these more complex endodomain configurations.

1.4.2 Toxicity induced by CAR T-cell immunotherapy

Whilst CAR T-cell immunotherapy has shown unprecedented success against otherwise untreatable haematological malignancies, it also holds the capacity to elicit a number of toxicities including cytokine release syndrome (CRS), tumour lysis syndrome (TLS), neurologic toxicity, “on-target/off-tumour” recognition and anaphylaxis.

1.4.2.1 Tumour lysis syndrome

Tumour lysis syndrome refers to a group of metabolic abnormalities caused by the rapid lysis of malignant cells and the subsequent release of intracellular metabolites. It is most commonly associated with haematological malignancies after the administration of cytotoxic therapy [190]. Tumour lysis syndrome is characterised by elevated serum levels of uric acid, potassium and phosphate, accompanied by hypocalcaemia and sometimes progressing to renal failure. It has been successfully managed with aggressive hydration and diuresis, allopurinol and rasburicase treatment [191] .

1.4.2.2 Cytokine release syndrome

Cytokine release syndrome is a potentially life-threatening toxicity that has been observed after administration of IL-2 [192], some monoclonal antibodies [193, 194] as well as following CAR T-cell administration [195-198]. Severe CRS is described as cytokine storm and can be fatal [195]. It usually occurs up to 20 days post CAR T-cell infusion and is currently managed with corticosteroids, cytokine antagonists and supportive therapy [199]. Cytokine storm is characterized by high fever, hypotension, tachycardia and seizures. Those symptoms are correlated with rise in serum IL-6 and C-reactive protein (CRP). The severity of CRS has been associated with disease burden, which implies that it is most probably caused by T-cell and macrophage activation. Cytokines most commonly up-regulated include IFNγ, TNFα, IL-6 and IL-10. To date, there has been no reported implication of IL-4 in a cytokine storm event induced by CAR T-cell administration.

1.4.2.3 Neurologic toxicity

Neurotoxicity is another serious toxicity observed in several patients treated with CD19-targeting CAR T-cells [200-202]. Symptoms of neurologic toxicity include visual hallucination, delirium, dysphasia and epilepsy or seizures. Whilst to date neurotoxicity

has been fully reversible, the underling mechanism as to how CAR T-cells induce neurotoxicity is unclear, particularly as it does not correlate with the severity of CRS. However, it is plausible that elevated cytokine levels are partially responsible for the neurological symptoms, since similar events have been reported with blinatumomab (a bispecific T-cell engager antibody against CD19/CD3) administration [203, 204].

1.4.2.4 Anaphylaxis

In addition to those toxicities, anaphylactic shock following CAR T-cell infusion has also been observed [205]. One patient developed anaphylaxis and cardiac arrest within minutes of completing a third infusion of CAR T-cells. The patient was treated with mRNA electroporated murine anti-human mesothelin CAR T-cells and the adverse effect was most probably due to the induction of IgE antibodies specific for the murine-based antibody sequences present in the CAR. Ultimately the IgE-mediated event developed as a result of the intermittent dosing schedule spanning over 49 days and allowing enough time for immunoglobulin class switching from IgG to IgE. Shortening the infusion scheduale to 20 days would greatly improve the safety of the therapy and switching in the future to fully humized antibodies will eliminate their antigenic potential as allergens.

1.4.2.5 “On-target/off-tumour” toxicity

Most CAR T-cell targets are not tumour restricted but have shared expression on normal tissue thereby causing some degree of “on-target/off-tumour” toxicity upon target engagement on nonpathogenic tissues. A typical example of “on-target/off-tumour” toxicity is B-cell aplasia with resultant hypogammaglobulinaemia caused by CD19-targeting CAR T-cells. Another example of “on-target/off-tumour” toxicity has been reported in patients with metastatic renal cell carcinoma following treatment with first generation CAR T-cells targeted against carbonic anhydrase-IX (CAIX) [206-208]. A number of the patients developed hepatotoxicity owing to recognition of target on biliary epithelium and which could be mitigated by prior treatment with a CAIX-specific

blocking antibody. Finally, in a fatal example of “on-target/off-tumor” toxicity, a patient treated with HER2-targeting CAR T-cells developed respiratory failure followed by multi-organ failure, associated with severe CRS [195]. This was believed to be due to on-target toxicity following recognition of HER2 in pulmonary parenchyma [195] or microvasculature [209].

Safety of CAR T-cell immunotherapy remains problematic. On-target toxicity has been linked to frequent occurrence of CRS (which has been lethal on occasions), in addition to other organ-based toxicities (e.g. B-cell aplasia with CD19-targeted CAR T-cells). These findings emphasize the need for identification of new and safer targets. In parallel, management of CRS is becoming more streamlined with recent descriptions of grading systems [201] and recommended management protocols for this adverse reaction [200]. In particular, the usefulness of the IL-6 receptor-α antagonist antibody tocilizumab has been emphasized in a number of recent studies [200-202, 210].

Table 1.3 Published clinical experience of CAR-based cancer immunotherapy of solid tumours.

Ref.	Target	No.	Responses	Dose	Disease	CAR gen.	Cond.	Toxicity	Notes
[211]	TAG-72	16	1SD	Up to 10^{10} cells	Colorectal cancer	1 (CD3ζ)	No	Hyperbilirubinaemia n=2	Intrahepatic delivery in n=6
[212]	CEA	7	2MR	Up to 10^{11} cells in multiple doses	Colorectal cancer (n=5) Breast cancer (n=2)	1 (CD3ζ)	No	Tolerance "adequate"	IL-2 administered to n=2
[169]	FR-α	14	Nil	3 - 169 x 10^9 in 1-3 doses	Epithelial ovarian cancer	1(FcRγ)	No	Grade 3-4 toxicity, attributed to IL-2	IL-2 administered in n=8 Allogeneic (alloreactive) cells used in n=6 No trafficking to tumor seen. Anti-CAR serum inhibitory factor in some patients. All T-cells cleared within 3 weeks
[170]	CD171/ L1 cell adhesion molecule	6	1PR	0.1 - 11 x $10^9/m^2$ in 1-3 doses	Neuroblastoma	1 (CD3ζ)	No	1-2 episodes of grade 3 lymphopenia, neutropenia, bacteraemia, anaemia, pneumonitis	$CD8^+$ T-cell clones electroporated to co-express CAR and hygromycin resistance gene, allowing selection. T-cell survival up to 7 days, shorter on subsequent infusions
[206-208]	CAIX	12	Nil	0.2 - 2.1 x 10^9 in up to 10 infusions	Renal cell carcinoma	1 (FcRγ)	No	Grade 3-4 hepatotoxicity (n=4). Subsequent patients received blocking anti-CAIX antibody prior to T-cell infusion.	Patients also received IL-2 Circulating T-cells peaked on day 6-21 and were detectable for up to 53 days. Antibody and cellular responses against CAR T-cells may have accelerated their clearance in some cases.
[172, 213]	GD2	19	3CR 1PR 1SD 8NE	Single dose of 2 - 20 x $10^7/m^2$	Neuroblastoma	1 (CD3ζ)	No	No severe or dose-limiting toxicity was observed following 44 infusions.	CAR-engineered ATCs and EBV-CTL administered together in equal numbers. Two patients had evidence of tumour necrosis. Low-level persistence of CAR cells for up to 96 weeks for CAR-engineered EBV-CTLs and 192

									weeks for CAR-ATCs. This was opposite to what was seen in the initial weeks and correlated with central memory $CD4^+$ T-cell number.
[195]	ErbB2	1	Nil	1×10^{10} (one dose)[§]	Colonic carcinoma	3 (CD28-4-1BB-CD3ζ)	CF	Fatal SUSAR	The cause of death was respiratory failure followed by multi-organ failure, associated with CRS. This was believed to be due to on-target toxicity following recognition of ErbB2 in pulmonary parenchyma (78) or microvasculature (79).
[214]	ErbB2	19	4SD	1×10^4 to 1×10^8 / m^2	Sarcoma	2 (CD28-CD3ζ)	No	No severe or dose-limiting toxicity	T-cells persisted for at least 6 weeks in 7 out of the 9 evaluable patients without evident toxicities,
[215]	Mesothelin	2	1PR	1×10^8 to 1×10^9 per dose	MPM and PDAC	2 (4-1BB-CD3ζ)	No	CRS	T-cells were engineered to express the CAR transiently using mRNA electroporation
[216, 217]	CEA	6	1SD	Up to 3×10^{10} over 3 doses	Liver metastases	2 (CD28-CD3ζ)	No	No severe or dose-limiting toxicity	IL-2 administered to n=3 at the maximum CAR T-cell dose
[218]	IL-13Rα2	3	Nil	Up to 12 infusions of 10^8 T-cells	Glioblastoma	2 (4-1BB-CD3ζ)	No	No severe or dose-limiting toxicity	Transient response was observed in 2 patients.

Abbreviations: ATCs – activated T-cells; CAIX – carbonic anhydrase IX; CEA – carcinoembryonic antigen; CF – cyclophosphamide and fludarabine-based lymphodepletion; Cond – conditioning therapy prior to T-cell infusion; CR – complete remission; CRS – cytokine release syndrome; EBV-CTL – Epstein Barr virus specific cytotoxic T-lymphocytes; FR-α – folate receptor-α□□GD2 – ganglioside D2; gen – generation; MPM – malignant pleural mesothelioma; MR – "minor responses"; NE – not evaluable for disease status; PDAC - pancreatic ductal adenocarcinoma; PR – partial response; SD – stable disease; SUSAR – suspected unexpected severe adverse reaction; TAG-72 – tumour-associated glycoprotein 72; [§]dose of CAR T-cells

Table 1.4 Published clinical experience of CAR-based cancer immunotherapy of haematological malignancies.

Ref.	Target (scFv)	No.	Responses	Dose	Disease	CAR gen.	Cond.	Toxicity	Notes
[219, 220]	CD19 (FMC63)	8	1CR 5PR	0.5 – 5.5 x 10^7 cells/kg	F-NHL x 3 CLL x 4 SMZL x 1	2 – CD28 + CD3ζ	CF	≥Grade 3 toxicity in all patients. CRS in ≥4 patients. One death due to influenza.	IL-2 (720 000 IU/kg) q 8 hourly (1-10 doses). Seven patients had evaluable disease. One patient treated twice and achieved PR x 2 B-cell depletion observed in 4 patients
[221]	CD19 (FMC63)	2	NE	4.1 - 6.1 x $10^9/m^2$ in 3 doses	F-NHL	1 (CD3ζ)	No	No T-cell related toxicity noted.	T-cell bulk cultures electroporated to co-express CAR and hygromycin resistance gene, allowing selection. T-cell dose no. 1 followed by administration of fludarabine (days 4-8).
[222]	CD19 (FMC63)	6	2SD	0.2 - 2 x $10^8/m^2$ per dose (1-2 doses)	SLL x 1 DLBCL x 5	1 (CD3ζ) 2 (CD28+ CD3ζ)	No	Infusions were well tolerated without any immediate adverse side effects.	*In vivo* proliferation of the second generation (but not first generation) CAR^+ T-cells occurred within the initial 1-2 weeks, followed by decline to a nadir at 4-6 weeks.
[196, 223]	CD19 (FMC63)	3	2CR 1PR	1.4 x 10^7 – 1.1 x 10^9 in 3-4 doses§	CLL	2 (4-1BB-CD3ζ)	B x 1 BR x 1 PC x 1	CRS in all patients. Tumour lysis syndrome in 1 patient.	
[224]	CD19 (SJ25C1)	9	1PR 2SD	1.8 x 10^8 – 2.5 x 10^9 (single dose, split in some cases)§	CLL x 8 ALL x 1	2 (CD28-CD3ζ)	Nil x 3 C x 6	1 fatal SUSAR. Fever and rigors in all patients B-cell aplasia in the ALL patient	The first cyclophosphamide treated patient died, perhaps due to occult sepsis The ALL patient was in remission following salvage chemotherapy and received CAR T-cells as a bridge to allo SCT.
[225]	CD19 (FMC63)	10	1CR 1PR 6SD	1 – 10 x 10^6 cells/kg	CLL x 4 DLBCL x 2 MCL x 4	2 (CD28-CD3ζ)	Nil	Fatigue, fever, hypotension. Reversible drop in ejection fraction from 66% to 25% x 1 Tumour lysis syndrome x 1, B-cell depletion x 3 Pneumonitis x 1	All patients had persistent malignancy following allo SCT and at least 1 DLI. Consequently, allogeneic (donor) T-cells were used as hosts for the CD19 CAR. Lymphodepletion was not administered in light of risk of GvHD. No GvHD was seen.

[226]	CD19 (FMC63)	8	1CR 1PR 1SD 2NE	3.15 x 10^7 to 1.13 x 10^8 cells over 1-3 infusions	ALL x 4 CLL – Richter x 2 CLL x 2	2 (CD28-CD3ζ)	Nil	Well tolerated No GvHD	Patients had relapsed following allo SCT Donor-derived virus-specific T-cells (reactive against EBV, CMV and adenovirus) engineered to express CAR
[198]	CD19 (FMC63)	2	2CR	1.4 – 12.0 x 10^6 cells/kg	ALL	2 (4-1BB-CD3ζ)	EC x 1 CTX x 1	CRS B-cell aplasia	Paediatric ALL One patient relapsed with CD19 null disease
[197]	CD19 (SJ25C1)	5	5CR	1.5 - 3 x 10^6 cells/kg	ALL	2 (CD28-CD3ζ)	C	CRS Neurotoxicity	Adult ALL. Four patients then proceeded to allo SCT CRS correlated to tumour burden
[202]	CD19 (FMC63)	30	27CR	0.76 – 20 x 10^6 cells/kg	ALL (1 T-ALL that expressed CD19)	2 (4-1BB-CD3ζ)	LD (various)	CRS (all) Neurotoxicity (n=13) B-cell aplasia (all responders)	25/30 patients aged ≤22 years Overall survival of 78% at 6 months Relapse with $CD19^+$ disease in 4 cases and CD19 null disease in 3 cases Tocilizumab ameliorated CRS 50% of patients had relapsed following previous allo-SCT
[200]	CD19 (SJ25C1)	16	14CR	0.48 - 3 x 10^6 cells/kg	ALL	2 (CD28-CD3ζ)	Salvage CTX; then C	CRS Neurotoxicity	Adult ALL – median age 50 years Defined clinical criteria for severe (s)CRS and identified C-reactive protein as a biomarker predictive of sCRS
[201]	CD19 (FMC63)	21	14CR 3SD	1-3 x 10^6 cells/kg	ALL x 20 DLBCL x 1	2 (CD28-CD3ζ)	CF	Grade 4 CRS in 3 patients at higher dose level Reversible neurotoxicity in 6 patients	Children and young adults Dose escalation phase I trial with intention to treat analysis Maximum tolerated dose 1 x 10^6 cells/kg Two patients relapsed with CD19 null disease T-cell mediated anti-CAR responses detected
[227]	CD19 (FMC63)	15	8CR 4PR 1SD 2NE	1-5 x 10^6 cells/kg	DLBCL x 9 CLL x 4 SMZL x 1 LGNHL x 1	2 (CD28-CD3ζ)	CF	One unexplained death 16 days after CAR T-cell infusion Hypotension, Neurotoxicity	Exogenous IL-2 not administered
[228]	CD19	20	6CR 2PR 3SD	0.4 – 8.2 x 10^6 cells	ALL Ph^- x 4 ALL Ph^+ x 1 CLL x 5	2 (CD28-CD3ζ)	Nil	Fever, Tachycardia, and Hypotension	Lack of new-onset of aGvHD post CAR T-cell infusion CAR T-cell persistence less than 4 weeks Separate dose escalations conducted for recipients of URD

			12PD		DLBCL x 4 FL x 1 MCL x 5				transplants and recipients of sibling transplants .
[229]	CD20	9	1PR 4SD 2NE	4.4 x 10^9 cells in 3 escalating doses, over 2-5 days	F-NHL x 8 MCL x 1	1 (CD3ζ)	CTX	No grade 3-4 toxicity	T-cell cultures/ $CD8^+$ clones electroporated to co-express CAR and G418 resistance gene, allowing selection. IL-2 in n=4, which prolonged T-cell survival. No anti-CAR inhibitory factor induced, perhaps owing to immunosuppressed status of patients.
[221]	CD20	2	NE	1.2 - 2.1 x $10^9/m^2$ in 3 doses	DLBCL	1 (CD3ζ)	28 days post auto HSCT	No T-cell related toxicity noted.	$CD8^+$ T-cell clones electroporated to co-express CAR and G418 resistance gene, allowing selection. Responses cannot be assessed owing to additional therapeutic agents.
[230]	CD20	4	1PR 2NE	Three doses: (i) 10^8 (ii) 10^9 (iii) 3 x $10^9/m^2$	Mantle cell lymphoma (n=3) F-NHL (n=1)	3 (CD28-4-1BB-CD3ζ)	C	Fever and hypotension post two infusions	T-cell bulk cultures electroporated to co-express CAR and G418 resistance gene, allowing selection. Low dose IL-2 administered for 14 days. Two patients with NE disease remained free of progression for 12 and 24 months. The duration of cell culture before infusion was ≥69 days. B-cell aplasia was not observed.
[231]	CD20	7	1CR 3PR	18-55 x 10^8 cells, infused over 5 days	DLBCL	2 (4-1BB-CD3ζ)	CTX	CRS 1 terminal gastrointestinal hemorrhage	
[232]	LeY	4	2SD	Up to 1.3 x 10^9	AML	2 (CD28-CD3ζ)	F	Neutropenia x 1 Fever, rigors. skin “flare” reaction x 1 No grade 3-4 toxicity	T-cells imaged by SPECT in some patients
[233]	CD33	1	Transient decrease in marrow blasts	1.12 x 10^9 cells, infused over 4 days	AML	2 (4-1BB-CD3ζ)	Nil	CRS	

Abbreviations: aGvHD – acute graft versus host disease; ALL – acute lymphoblastic leukaemia; ALL Ph^+ - Philadelphia chromosome positive acute lymphoblastic leukaemia; ALL Ph^- - Philadelphia chromosome negative acute lymphoblastic leukemia; allo SCT – allogeneic stem cell transplant; AML – acute myeloid leukaemia; auto HCT – autologous stem cell transplant; B – bendamustine; B-NHL – B-cell non-Hodgkin's lymphoma; BR – bendamustine + rituximab; C – cyclophosphamide; CF – cyclophosphamide and fludarabine-based lymphodepletion; CMV – cytomegalovirus; CLL – chronic lymphocytic leukaemia; Cond – conditioning therapy prior to T-cell infusion; CP – cyclophosphamide and pentostatin; CR – complete remission; CRS – cytokine release syndrome; CTX – cytoreductive chemotherapy; DLBCL – diffuse large B-cell lymphoma; DLI – donor leukocyte infusion; EBV-CTL – Epstein Barr virus specific cytotoxic T-lymphocytes; EC – etoposide + cyclophosphamide; F – fludarabine; F-NHL – follicular NHL; gen - generation; GvHD – graft versus host disease; LD – lymphodepletion; LGNHL – low grade NHL; LeY – Lewis Y antigen; MCL – mantle cell lymphoma; NE – non evaluable disease; PR – partial remission; SC – subcutaneous; scFv – single chain antibody fragment used to target CD19; SD – stable disease; SLL – small lymphocytic lymphoma; SMZL – splenic marginal zone lymphoma; SUSAR – suspected unexpected severe adverse reaction; URD – unrelated donor. [§]dose of CAR T-cells

1.4.3 Clinical evaluation of CAR T-cells

Over the past decade, there has been an exponential increase in the number of clinical studies undertaken to evaluate the safety and efficacy of CAR T-cell based immunotherapy in patients with diverse malignant disorders.

1.4.3.1 Clinical experience in patients with solid tumours

Solid tumours account overwhelmingly for the greatest unmet need in the modern management of cancer. It is unsurprising therefore that initial clinical trials of CAR T-cell immunotherapy were undertaken in this setting (Table 1.3). Although ultimately disappointing to date, this initial clinical experience provides a highly valuable insight into the challenges posed by the development of effective CAR T-cell immunotherapy for common cancer types.

The first study to be published in full was undertaken in patients with metastatic epithelial ovarian cancer [169]. T-cells were targeted against folate receptor-α using an scFv-based first generation CAR and were administered intravenously (IV), without prior lymphodepletion. Although no substantial toxicity was observed, an efficacy signal was not demonstrated in this study. Lack of anti-tumour activity was linked to failure of T-cell persistence and poor homing to the tumour.

In the context of solid tumour immunotherapy, greatest success has been achieved when CARs have been delivered to virus-specific T-cells. This approach has been pioneered by the group at Baylor College of Medicine who demonstrated moderate efficacy in children with neuroblastoma, treated with GD2 re-targeted first generation CAR T-cells [172, 213]. Efficacy was most apparent in patients in whom CAR T-cells persisted, justifying the move towards evaluation of second generation CARs. Nonetheless, a key challenge is presented by the frequency with which CAR T-cell targets are expressed in vital healthy organs, imposing a clear risk of induction of

unacceptable toxicity. Illustrating this, one patient with $HER2^+$ metastatic colon cancer unfortunately succumbed to a suspected unexpected serious adverse reaction (SUSAR) that occurred soon after the IV infusion of HER2 re-targeted T-cells [195]. The CAR contained an scFv derived from the trastuzumab (Herceptin) antibody which was coupled to a fused CD28 + 4-1BB + CD3ζ "third generation" endodomain. A total of 1 x 10^{10} cells (79% transduced) were infused, following conditioning with lymphodepleting chemotherapy. However, respiratory distress occurred rapidly and progressed to multi-organ failure, CRS and death. This SUSAR was believed to have resulted from recognition of low levels of HER2, which is present in both the pulmonary parenchyma [195] and microvasculature [209]. Imaging studies highlight the challenge imposed by IV delivery of CAR T-cells, which persist in the pulmonary circulation for several hours after administration [234]. Earlier imaging studies in man using indium-labelled CAR T-cells suggests that sustained pulmonary retention of these cells may not be target-dependent and is more prolonged and accompanied by dyspnea when highly activated T-cells are infused [169].

A second example of on-target toxicity has been reported in patients with metastatic renal cell carcinoma following treatment with first generation CAR T-cells targeted against carbonic anhydrase-IX (CAIX) [206-208]. A number of the patients developed hepatotoxicity owing to recognition of target on biliary epithelium and which could be mitigated by prior treatment with a CAIX-specific blocking antibody.

In summary, solid tumours have largely proven refractory to treatment with CAR T-cells to date. Nonetheless, several studies are currently ongoing involving second generation CAR T-cells in several solid tumour types (Table 1.5). There is a clear need to refine systems to achieve delivery, persistence, intra-tumoural penetration and sustained effector function of these cells within the often hostile tumor microenvironment. Solutions may require even greater levels of innovative CAR engineering and/ or the combined use of these cells with traditional and emerging

cancer therapeutic agents, including chemotherapy [235], radiotherapy [236] and/ or immune checkpoint blockers [237] respectively. Use of regional delivery systems in selected tumor types such as mesothelioma [238] and head and neck cancer [156, 239, 240] are also under evaluation. A further recently developed technology that may potentiate such loco-regional delivery systems entails the use of biodegradable implants to enhance the dispersal and persistence of CAR T-cells [241].

1.4.3.2 Clinical experience in patients with haematological malignancies

B-cell malignancy has been the focus of greatest interest and success in the clinical evaluation of CAR T-cell immunotherapy [242]. The approach builds upon the efficacy of monoclonal antibodies targeted against B-cell lineage antigens, notably the anti-CD20 antibody, rituximab. However, greatest impact has been achieved using CAR T-cells directed against CD19 rather than CD20 (Table 1.4) [242]. CD19 is a particularly attractive target since it is expressed by virtually all B-cell malignancies and throughout all stages of B-lineage differentiation but it is not found on haematopoietic stem cells or other tissues [243]. Consequently, it is predicted that effective targeting of CD19-expressing cells would be accompanied by B-cell depletion and impaired antibody-forming capacity, consequences that can be managed effectively by immunoglobulin replacement therapy.

The first study in which CAR^+ T-cells were redirected against a haematological malignancy yielded disappointing results [229]. In that study, T-cells were re-targeted against CD20 using an scFv-based first generation CAR and were administered to patients with relapsed or refractory B-cell non-Hodgkin's lymphoma (NHL). While no substantial toxicity was observed, no CAR-attributed clinical responses occurred.

Since this report, several other clinical trials have targeted B-cell malignancies using a diversity of CARs directed most commonly against CD19 or CD20 (Table 1.4). With the introduction of second generation CARs, dramatic responses have regularly been

observed in trials conducted at a number of independent centres. In a proof of principle study, the group at Baylor College of Medicine simultaneously infused T-cells transduced with either a first-generation (CD3ζ) or a 2nd generation (CD28-CD3ζ) CD19-targeted CAR to patients with relapsed or refractory NHL [222] The study conclusively demonstrated that T-cells modified with the 2nd generation CAR exhibited enhanced expansion and persistence *in vivo*, accompanied by an improved capacity to penetrate $CD19^+$ malignant lesions. However, the overall efficacy of the CAR T-cells in this study was limited, perhaps in part since preparatory lymphodepletion was not employed [222].

Strikingly compelling efficacy has been achieved when second generation CD19-targeted CAR T-cells have been administered after cytotoxic or lymphodepleting chemotherapy. Studies conducted at the University of Pennsylvania indicate that engraftment of engineered cells occurs optimally when they are infused 2 days after such conditioning therapy [244]. Arguably, results have been most impressive in patients with adult and childhood ALL, in whom complete remission (CR) rates of over 66% have been consistently achieved [197, 200-202, 210]. The data are all the more impressive given the fact that they have been attained in multiple centres using distinct CD19-targeted CAR formats and following conditioning using a variety of regimens (Table 1.4).

The University of Pennsylvania group has pioneered the clinical development of the FMC63/CD8/4-1BB/CD3ζ CAR, described originally by Campana [245]. In ALL patients, they have reported a 90% CR rate (27/30 patients). Sustained remission of up to 2 years was achieved in 19 patients [202]. The success of this study is perhaps best exemplified by the 50% rate of sustained long-term remission that is attributable to CAR T-cell immunotherapy in the absence of subsequent allogeneic stem cell transplantation. This finding has been linked to the long-term persistence of CAR-modified T-cells, which have been detected for up to 4 years in this cohort.

The Memorial Sloan Kettering Group reported an 88% CR rate with their CD19 CAR, which is configured as an SJ25C1/CD28/CD3ζ fusion [200]. The National Cancer Institute are employing a CAR in which the FMC63 scFv is coupled to CD28/CD3ζ and which has achieved a highly impressive 67% CR rate when analyzed on an intention to treat basis [201]. In both of the latter cases, T-cells appear to persist for a considerably shorter period (approximately 30 days) when compared to the 4-1BB-based CAR, meaning that the therapy is of particular utility as a device to attain molecular CR as a bridge to allogeneic stem cell transplantation.

CD19-targeted CAR T-cells have also resulted in an impressive CR rate in patients with diffuse large B-cell lymphoma, indolent lymphomas and chronic lymphocytic leukaemia (CLL) [227]. Of 15 patients treated, there were eight CRs (including four patients with DLBCL), four partial remissions, one patient with stable disease and two who were not evaluable [227]. Encouraging data have also been generated when donor-derived anti-CD19 CAR T-cells have been used to treat B-cell malignancies that have relapsed after allogeneic hematopoietic stem cell transplantation (Table 1.4). A small number of studies have been reported in patients with myeloid malignancies, although success has been much more limited to date. Several trials are ongoing at the time of writing in patients with B-cell and other haematological malignancies (Table 1.5).

While data generated using CD19 CAR T-cells are extremely impressive, several points warrant further exploration. Direct comparison of data generated by different centres is highly challenging since patients differ with respect to several key parameters, including disease nature and burden, prior treatment history and conditioning regimen employed (including the use of some agents with direct anti-tumour activity). Furthermore, studies have employed CARs that differ in scFv targeting moiety, hinge/ spacer, co-stimulatory module, T-cell activating stimulus used during

manufacture, gene transfer vector, T-cell expansion protocols and final composition of cell products used [242]. Nonetheless, these data collectively provide a great impetus to the field and encourage the development of analogous approaches for other lymphomas, including cHL and ALCL.

This thesis details the work that I have undertaken to investigate the feasibility of using CAR-grafted T-cells for the treatment of cHL and ALCL. To the best of my knowledge, this is the first time that CAR^+ T-cells have been used to target CSF-1R. The data contained within this thesis suggest that such a targeting strategy is justified and that the use of CSF-1R-targeted CAR^+ T-cells could represent a possible future treatment for patients with refractory/relapsed cHL and ALCL.

Table 1.5 Ongoing unpublished trials involving CAR-based cancer immunotherapy.

Target	Cancer	CAR	Sponsor	Phase	Identifier*
CD19	B-cell malignancies	CD28-CD3ζ	National Cancer Institute	I/II	NCT01087294
CD19	ALL	CD28-CD3ζ	Seattle Children's Hospital	I	NCT01683279
CD19	NHL	CD28-CD3ζ	MSKCC	I	NCT01840566
CD19	CLL	CD137-CD3ζ	University of Pennsylvania	II	NCT01747486
CD19	ALL	CD137-CD3ζ	University of Pennsylvania	I	NCT01551043
CD19	B-cell malignancies	CD137-CD3ζ	University of Pennsylvania	I	NCT01626495
CD19	B-cell malignancies	NI	National Cancer Institute	I	NCT02659943
CD19	NHL, CLL	CD28-CD3ζ and CD28-CD137-CD3ζ	Baylor College of Medicine	I	NCT01853631
CD19	B-cell malignancies	CD28-CD3ζ	National Cancer Institute	I/II	NCT00924326
CD19	B-cell malignancies	CD28-CD3ζ	Fred Hutchinson Cancer Research Center	I/II	NCT01475058
CD19	ALL, CLL, NHL	CD3ζ	Fred Hutchinson Cancer Research Center	I/II	NCT01865617
CD19	NHL	CD3ζ	City of Hope	I/II	NCT01318317
CD19	B-cell malignancies	CD28-CD137-CD3ζ	Affiliated Hospital to Academy of Military Medical Sciences	I	NCT02186860

CD19	B-cell malignancies	CD28-CD3ζ	MD Anderson Cancer Center	I	NCT00968760
CD19	B-cell malignancies	CD28-CD3ζ	MD Anderson Cancer Center	I	NCT01497184
CD19	Leukaemia, Lymphoma	CD28-CD3ζ	MD Anderson Cancer Center	I	NCT01362452
CD19	CLL	CD28-CD3ζ	MD Anderson Cancer Center	I	NCT01653717
CD19	B-cell malignancies	CD28-CD3ζ	Baylor College of Medicine	I/II	NCT00840853
CD19	ALL, CLL, NHL	CD28-CD3ζ	Baylor College of Medicine	I	NCT00586391
CD19	ALL, CLL, NHL	CD28-CD3ζ	Baylor College of Medicine	I	NCT02050347
CD19	B-cell malignancies	CD28-CD3ζ	National Cancer Institute	I	NCT01593696
CD19	CLL	CD28-CD3ζ and CD137-CD3ζ	MSKCC/ University of Pennsylvania	I/II	NCT00466531
CD19	CLL	CD28-CD3ζ	MSKCC	I	NCT01416974
CD19	ALL	CD28-CD3ζ	MSKCC	I	NCT01860937
CD19	NHL	CD28-CD3ζ	Kite Pharma, Inc.	I/II	NCT02348216
CD19	ALL	CD28-CD3ζ	Kite Pharma, Inc.	I/II	NCT02614066
CD19	ALL	CD28-CD3ζ	Kite Pharma, Inc	I/II	NCT02625480
CD19	ALL	CD137-CD3ζ	University of Pennsylvania	II	NCT02030847
CD19	ALL	CD28-CD3ζ	MSKCC	I	NCT01430390
CD19	B-cell malignancies	NI	M.D. Anderson Cancer Center	I	NCT02529813
CD19	NHL	CD137-CD3ζ	Juno Therapeutics, Inc	I	NCT02631044
CD19	B-cell malignancies	CD28-CD3ζ	Shanghai Tongji Hospital,	I/II	NCT02537977

CD19	B-cell malignancies	CD137-CD3ζ	Shanghai GeneChem Co., Ltd.	I/II	NCT02672501
CD19	NHL	CD28-CD3ζ	Jichi Medical University	I/II	NCT02134262
CD19	B-cell malignancies	NI	Beijing Doing Biomedical Co., Ltd.	I	NCT02546739
CD19	B-cell malignancies	NI	Beijing Doing Biomedical Co., Ltd.	I	NCT02656147
CD19	B-cell malignancies	CD137-CD3ζ and CD3ζ	Chinese PLA General Hospital	I/II	NCT01864889
CD19	Mantle cell lymphoma	CD137-CD3ζ	Chinese PLA General Hospital	I/II	NCT02081937
CD19	B-cell malignancies	CD28-CD3ζ	Shenzhen Second People's Hospital	I	NCT02456350
CD19	Leukaemia, Lymphoma	CD137-CD3ζ	Seattle Children's Hospital	I/II	NCT02028455
CD19	ALL	CD3ζ	University College London	I/II	NCT01195480
CD19	ALL, Burkitt’s lymphoma	NI	University College London	I	NCT02443831
CD19	NHL	CD28-CD3ζ	City of Hope	I	NCT01815749
CD19	B-cell malignancies	CD28-CD137-CD3ζ	Uppsala University	I/II	NCT02132624
CD19	B-cell malignancies	CD137-CD3ζ	University of Pennsylvania	I	NCT01029366
CD19	NHL	CD3ζ	Professor Robert Hawkins, Christie Hospital NHS Foundation Trust	I	NCT01493453
CD19	B-ALL	CD28-CD3ζ	MSKCC	I	NCT01044069

CD19	B-ALL	CD137-CD3ζ	Juno Therapeutics, Inc.	I	NCT02535364
CD19	DLBCL	CD137-CD3ζ	Novartis Pharmaceuticals	II	NCT02445248
CD19	DLBCL	NI	University College London	I	NCT02431988
CD19	B-cell leukaemia	CD28-CD3ζ	Second Military Medical University	I/II	NCT02644655
CD19	NHL	CD28-CD3ζ	City of Hope	I	NCT02051257
CD19	B-cell leukaemia and lymphoma	NI	Southwest Hospital, China	I	NCT02349698
CD19	cHL	CD137-CD3ζ	University of Pennsylvania	I	NCT02277522
CD19	CD19+ lymphomas	CD137-CD3ζ	University of Pennsylvania	II	NCT02030834
CD19	cHL	CD137-CD3ζ	University of Pennsylvania	0	NCT02624258
CD19	B-cell lymphomas	CD27-CD3ζ	Peking University	I/II	NCT02247609
CD19	B-cell lymphomas	CD28-CD3ζ	Xinqiao Hospital of Chongqing	I/II	NCT02652910
CD20	CD20+ leukemia and lymphoma	CD137-CD3ζ	Chinese PLA General Hospital	I/II	NCT01735604
CD22	ALL	CD137-CD3ζ	University of Pennsylvania	I	NCT02588456
CD22	B-cell malignancies	CD137-CD3ζ	University of Pennsylvania	I	NCT02650414
CD22	B-cell malignancies	CD137-CD28-CD3ζ	National Cancer Institute	I	NCT02315612
CD30	HL, NHL	CD28-CD3ζ	Baylor College of Medicine	I	NCT01316146
CD30	CD30+ lymphoma	CD28-CD3ζ	UNC Lineberger Comprehensive Cancer Center	I	NCT02663297

CD30	CD30+ lymphoma	CD27-CD3ζ	Peking University	I/II	NCT02274584
CD30	NHL, HL	CD28-CD3ζ	Baylor College of Medicine	I	NCT01192464
CD30	Mycosis fungoides/CTCL	CD28-CD3ζ	University of Cologne	I	NCT01645293
CD30	CD30+ lymphomas	NI	Chinese PLA General Hospital	I/II	NCT02259556
CD33	AML	CD137-CD3ζ	Chinese PLA General Hospital	I/II	NCT01864902
CD123	AML	CD28-CD3ζ	City of Hope Medical Center	I	NCT02159495
CD123	AML	CD137-CD3ζ	University of Pennsylvania	0	NCT02623582
CD133	Solid Tumours	CD137-CD3ζ	Chinese PLA General Hospital	I	NCT02541370
CD138	MM	CD137-CD3ζ	Chinese PLA General Hospital	I/II	NCT01886976
CD171	Neuroblastoma	CD137-CD3ζ	Seattle Children's Hospital	I	NCT02311621
BCMA	MM	NI	bluebird bio	I	NCT02658929
BCMA	MM	CD137-CD3ζ	University of Pennsylvania	0	NCT02546167
IL13Rα	Glioma	CD137-CD3ζ	City of Hope Medical Center	I	NCT02208362
κ light chain	NHL, CLL, MM	CD28-CD3ζ	Baylor College of Medicine	I	NCT00881920
Lewis Y	AML, MM	CD28-CD3ζ	Peter MacCullum Cancer Center, Australia	I	NCT01716364
GD2	Non-neuroblastoma solid tumors	CD137-CD28-CD3ζ	National Cancer Institute	I	NCT02107963
EGFRvIII	Glioblastoma	NI	University of Pennsylvania	I	NCT02209376

GD2	Neuroblastoma	CD28-OX40-CD3ζ	Baylor College of Medicine	I	NCT01822652
HER2	Sarcoma	CD28-CD3ζ	Baylor College of Medicine	I	NCT00902044
GD2	Sarcoma	CD28-OX40-CD3ζ	Baylor College of Medicine	I	NCT01953900
ErbB Family	SCCHN	CD28-CD3ζ	King's College London	I	NCT01818323
HER2	GBM	CD28-CD3ζ	Baylor College of Medicine	I	NCT01109095
Mesothelin	Solid Tumours	CD137-CD3ζ	University of Pennsylvania	I	NCT02159716
Mesothelin	Solid Tumours	CD137-CD3ζ	Chinese PLA General Hospital	I	NCT02580747
Mesothelin and CD19	Pancreatic cancer	CD137-CD3ζ	University of Pennsylvania	I	NCT02465983
MUC1	Solid Tumours	NI	PersonGen Biomedicine (Suzhou) Co., Ltd.	I/II	NCT02617134
MUC1	Solid Tumours	NI	PersonGen Biomedicine (Suzhou) Co., Ltd	I/II	NCT02587689
EGFRvIII	Glioblastoma	CD28-CD3ζ	National Cancer Institute	I/II	NCT01454596
EGFRvIII	Glioblastoma	NI	Gary Archer Ph.D.	I	NCT02664363
HER2	HER2+ Tumours	CD28-CD3ζ	Baylor College of Medicine	I	NCT00889954
NKG2D Ligands	AML, MS, MM	CD28-CD3ζ	Celdara Medical, LLC	I	NCT02203825
EphA2	EphA2+ Malignant Glioma	NI	Fuda Cancer Hospital, Guangzhou	I/II	NCT02575261
GD2	Neuroblastoma	NI	Children's Mercy Hospital Kansas City	I	NCT01460901

GD2	Neuroblastoma	CD28-OX40- CD3ζ	Baylor College of Medicine	I	NCT02439788
FAP	MPM	CD28-CD3ζ	University of Zurich	I	NCT01722149
EGFR	EGFR+ Solid Tumours	CD137-CD3ζ	Chinese PLA General Hospital	I/II	NCT01869166
EGFR	Malignant glioma	NI	RenJi Hospital	I	NCT02331693
GPC3	HCC	NI	RenJi Hospital	I	NCT02395250
HER2	Breast Cancer	CD28-CD3ζ	Fuda Cancer Hospital, Guangzhou	I/II	NCT02547961
HER2	HER2+ Solid Tumours	CD137-CD3ζ	Chinese PLA General Hospital	I/II	NCT01935843
HER2	Glioblastoma	CD28-CD3ζ	Baylor College of Medicine	I	NCT02442297
IL13Rα2	Glioma	CD137-CD3ζ	City of Hope	I	NCT02208362
CEA	Adenocarcinomas	CD28-CD3ζ	Roger Williams Medical Center	II	NCT01723306
CEA	CEA+ Tumours	NI	Southwest Hospital, China	I	NCT02349724

*www.clinicaltrials.gov Search terms: chimeric antigen receptor, chimeric T-cell. Accessed 14/02/2016

ALL - acute lymphoblastic leukaemia; AML - acute myeloid leukaemia; B-ALL - B cell acute lymphocytic leukaemia; CAR, chimeric antigen receptor; CEA - carcinoembryonic antigen; CLL - chronic lymphocytic leukaemia; CR - complete response; DLBCL - Diffuse Large B-Cell Lymphoma; EGFR – epidermal growth factor receptor; FAP – fibroblast activation protein; GD2 – ganglioside D2; GPC3 - glypican-3; HCC - hepatocellular carcinoma; MM – multiple myeloma; MS - Myelodysplastic Syndrome; MPM - Malignant Pleural Mesothelioma; MSKCC – Memorial Sloan Kettering Cancer Center; NHL - non-Hodgkin's lymphoma; NI – no information; SCCHN - Squamous Cell Cancer of the Head and Neck; GBM - Glioblastoma multiforme.

Chapter 2 Materials and Methods

2.1 Molecular Biology Techniques

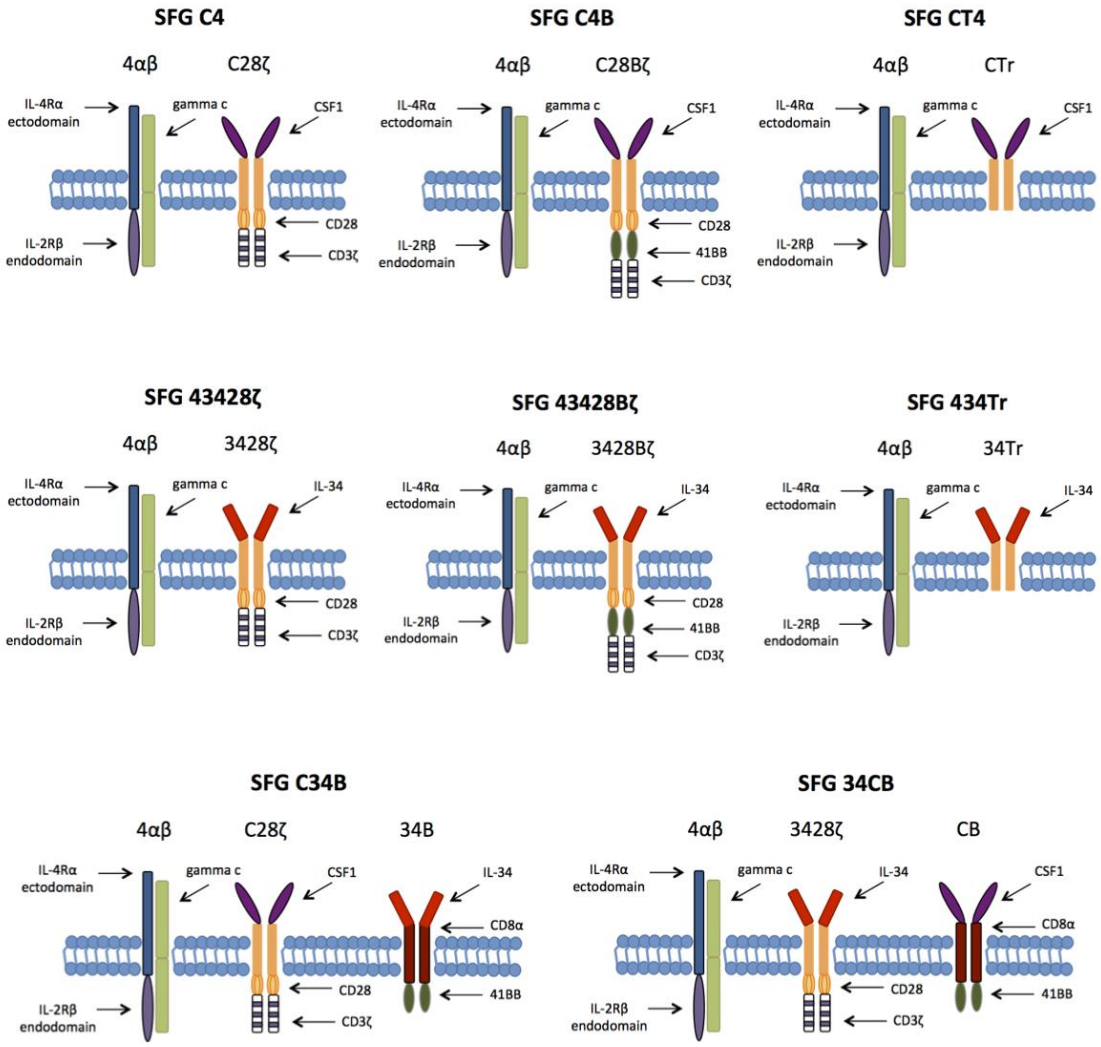

Figure 2.1 A schematic representation of the various chimeric antigen receptor constructs used in this thesis.

CSF-1 = colony-stimulating factor-1, IL-34 = interleukin 34, IL-4Rα = Interleukin-4 receptor alpha subunit, IL-2Rβ = Interleukin-2 receptor beta subunit, CD3ζ = CD3 zeta chain, CD8α = CD8 alpha chain, gamma c = common gamma chain.

2.1.1 Generation of CAR Constructs

The constructs SFG C28ζ and SFG CTr were produced by Dr. Scott Wilkie prior to the commencement of this PhD. All other constructs were designed and cloned over the course of the project using the Polymerase Incomplete Primer Extension (PIPE) cloning method (please refer to section 2.1.2). All retroviral constructs are shown schematically in Figure 2.2 (page 80). Successful cloning was confirmed by restriction pattern agarose gel analysis and sequencing identified no mutations within the coding sequences (Source Bioscience, UK).

C28ζ and CTr were cloned in the SFG retroviral vector as NcoI/XhoI fragments, ensuring that their start codons are in the precise place (the naturally occurring NcoI site) previously occupied by the deleted *env* gene. Gene expression is achieved from the Moloney murine leukaemia virus (MoMLV) long terminal repeat (LTR), which has promoter activity and virus packaging of the RNA is ensured by the MoMLV ψ packaging signal, which is flanked by splice donor and acceptor sites.

2.1.1.1 SFG C28ζ construct

SFG C28ζ comprises of a human fusion gene encoding the CD8α chain leader sequence (amino acids (AA) 1 to 18), CSF-1 (AA 19 to 178), the partial extracellular, transmembrane and intracellular domain of CD28 (AA 179 to 285) and the intracellular domain of the CD3 zeta (CD3ζ) chain (AA 286 to 397).

2.1.1.2 SFG CTr construct

SFG CTr is designed as a matched truncated control for SFG C28ζ. The endodomain in CTr has been truncated to remove the entire CD3ζ sequence and all but the three most N-terminal amino acids of the CD28 intracellular domain. Consequently, CTr is a non-signalling construct.

2.1.1.3 SFG C4 construct

The SFG C4 (4αβ + C28ζ) construct (Figure 2.1 and Figure 2.2) is defined by the co-expression of the C28ζ CAR with the chimeric cytokine receptor 4αβ [246]. The chimeric cytokine receptor 4αβ is a fusion molecule comprising of IL-4Rα ectodomain (AA 1 to 233) and the shared IL-2/15Rβ endodomain (AA 241 to 551). It was designed to achieve selective IL-4-driven proliferation of CAR^+ T-cells in which 4αβ is co-expressed. Dual expression of both constructs using the same promoter was achieved by the introduction of a self-cleaving 2A peptide sequence between the 4αβ and C28ζ coding regions. This peptide was derived from the insect virus *Thosea asigna* and is therefore referred as a T2A sequence [247]. The T2A sequence permits dual polypeptide expression from the same mRNA molecule by inducing a ribosomal 'skip', in which a peptide bond between the two encoded polypeptides is 'missed' [248]. The stop codon at the 3' end of the 4αβ sequence has been removed to ensure full expression. Since the T2A peptide leaves a short peptide overhang on the C-terminus of the upstream encoded polypeptide (in this case 4αβ), a furin cleavage site was introduced upstream of the T2A sequence to remove this sequence (Figure 2.2). Construction of C4 was achieved by means of the PIPE cloning method (please refer to section 2.1.2). Briefly, 40 bp C28ζ-specific primers (all listed in Table 2.1) were used for PCR SFG C28ζ vector linearization and generation of single-stranded 5′-ends by PIPE. Simultaneously, the 4αβ sequence was PCR amplified using a pair of 40 bp primers with 5′-C28ζ-end overlapping sequences, thereby generating single-stranded C28ζ-end homologous products by PIPE. In a following step, the PIPE products were mixed and the single-stranded overlapping sequences annealed and assembled as a complete SFG C4 construct.

2.1.1.4 SFG C4B construct

The SFG C4B (4αβ + C28Bζ) construct (Figure 2.1 and 2.2) is defined by the co-expression of the C28Bζ CAR with the chimeric cytokine receptor 4αβ. The new CAR C28Bζ is a 3rd generation CAR comprising of a human fusion gene encoding the CD8

alpha chain leader sequence (AA 1 to 18), the CSF-1 peptide (AA 19 to 178), the partial extracellular, transmembrane and intracellular domains of CD28 (AA 179 to 285), followed by the CD137 (4-1BB) endodomain (AA 286 to 327) and the intracellular domain of the CD3 zeta (CD3ζ) chain (328 to 439 bases). Construction was achieved by means of PIPE cloning (please refer to section 2.1.2). In short, 40 bp C4-specific primers (Table 2.1) were used for PCR SFG C4 linearization at the site of fusion between the intracellular domains of CD28 and CD3ζ within the C28ζ construct, thereby generating single-stranded 5′-ends. Simultaneously, the 4-1BB sequence was PCR amplified using a pair of 40 bp primers with 5′-end overlapping sequences, thereby generating single-stranded C4-end homologous products, which were then used in a enzyme-free ligation to generate the SFG C4B construct.

2.1.1.5 SFG CT4 construct

The SFG CT4 (4αβ + CTr) construct (Figure 2.1 and 2.2) was designed as a matched truncated control of C4 and C4B. The chimeric cytokine receptor 4αβ was cloned upstream of the CTr construct, providing means of selective expansion of CAR-transduced T-cells. Construction of SFG CT4 was achieved using the same PIPE cloning strategy used for the generation of SFG C4 (see 2.1.1.3).

2.1.1.6 SFG C34B construct

The SFG C34B (4αβ + C28ζ + 34B) construct was designed to explore the possibility of dual CAR-based targeting of CSF-1R (Figure 2.1 and 2.2). To test this, a fusion molecule termed 34B was designed. It was engineered as a fusion between the human IL-34 signalling peptide (AA 1 to 20), human IL-34 peptide (AA 21 to 245), the extracellular and transmembrane domains of CD8α (AA 246 to 312) and the 4-1BB signalling endodomain (AA 313 to 355). Expression of all three elements was achieved with the insertion of a second T2A peptide and furin cleavage site, separating C28ζ from 34B. To avoid the introduction of a large direct repeat which would induce proviral instability, the second T2A DNA sequence was codon “wobbled” to be as different as possible from the first T2A

sequence, while maintaining the encoded protein sequence. The 34B construct, along with the second T2A DNA sequence, upstream of it, were designed and codon optimised as a cDNA cassette, which was synthesised by GenScript. Construction of SFG C34B was achieved using the PIPE cloning method. As described previously (see section 2.1.2 and 2.1.1.3) 40 bp self-complementary primers (Table 2.1) were used to linearize SFG C4 and PCR amplify the cDNA cassette. The PCR products were then mixed to assemble the complete SFG C34B construct.

2.1.1.7 SFG 43428ζ construct

The SFG 43428ζ (4αβ + 3428z) construct (Figure 2.1 and 2.2) is defined by the co-expression of a new 2nd generation CAR termed 3428z with the chimeric cytokine receptor 4αβ. The 3428ζ construct differs from C28ζ in only the targeting moiety, in which the CSF-1 peptide has been replaced with full length human IL-34, and in the signal peptide, in which the IL-34 leader sequence (bases 1-60) has been used. Construction of this new second generation CAR was achieved by means of the PIPE cloning (please refer to section 2.1.2). This time the PIPE method was utilized for swapping the CSF-1 targeting moiety in C28ζ with IL-34. To achieve this, three primer pairs were designed (Table 2.1). The first two vector-specific primer pairs, flanking the existing CSF-1, were used for amplification of two vector fragments, subsequently treated by *Dpn*I to destroy the *Escherichia (E.) coli*-derived PCR template. The last primer pair, with 5′-vector-fragment-end overlapping sequences, was used for amplification of the incoming IL-34 sequence. The three PCR products were mixed together and transformed into chemically competent *E. coli* cells.

2.1.1.8 SFG 43428Bζ construct

The SFG 43428Bζ (4αβ + 3428Bζ) construct (Figure 2.1 and 2.2) is defined by the co-expression of a new 3rd generation CAR termed 3428Bζ with the chimeric cytokine receptor 4αβ. The 3428Bζ construct differs from C4B in only the targeting moiety, in which the CSF-1 peptide has been replaced with full length human IL-34, and in the signal

peptide, in which the IL-34 leader sequence (bases 1-60) has been used. The same PIPE technique was employed for its construction as is described in section 2.1.1.7.

2.1.1.9 SFG 434Tr construct

The SFG 434Tr (4αβ + 34Tr) construct (Figure 2.1 and 2.2) is defined by the co-expression of the non-signalling 34Tr construct and the chimeric cytokine receptor 4αβ. It is designed as a matched truncated control for SFG 43428ζ and SFG 43428Bζ. A similar PIPE-based cloning strategy as the one described in section 2.1.1.7, involving swapping of the targeting moiety CSF1 in CTr with the IL-34 peptide, was used for the construction of 34Tr.

2.1.1.10 SFG 34CB construct

The SFG 34CB (4αβ + 3428ζ + CB) construct is a second dual CAR directed against CSF-1R. In the closely related SFG C34B (described previously in section 2.1.1.6), signal 1 and 2 (CD28) are provided upon binding of CSF-1 to the target and an additional signal 2 (4-1BB) comes from IL-34 binding to CSF-1R. By contrast, in SFG 34CB these two targeting moieties have been exchanged. In the first fusion, CD28 and CD3ζ have been joined to IL-34. This molecule has been co-expressed with a second fusion in which CSF-1 has been joined to the CD8α hinge and transmembrane domain followed by the intracellular domain of 4-1BB (Figure 2.1 and 2.2). To generate the SFG 34CB construct, four primer pairs were designed (Table 2.1). The first two vector-specific primer pairs, flanking the existing CSF-1 and IL-34 sequences, were used for amplification of 2 vector fragments. The second two primer pairs, with 5′-vector-fragment-end overlapping sequences, were used for amplification of the incoming IL-34 and CSF-1 sequences with swapped places. The four PCR products were used in an enzyme-free ligation to generate the SFG 34CB construct.

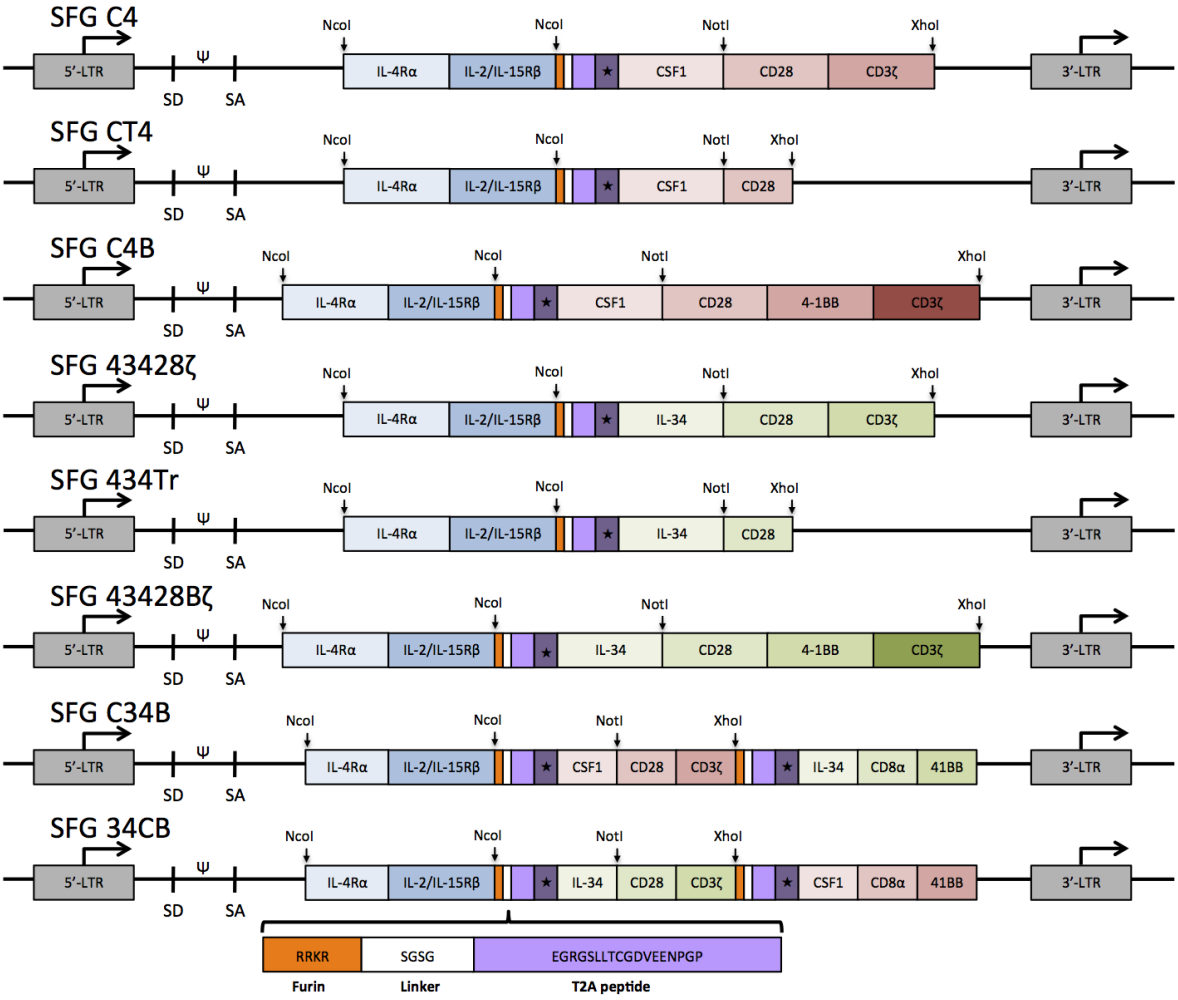

Figure 2.2 A schematic of the SFG retroviral vector containing the 4αβ chimeric cytokine receptor and the various CAR constructs used in this thesis.

Individual coding sequences are separated using T2A peptides derived from the *Thosea asigna* insect virus, which induces a ribosomal 'skip' and therefore misses a peptide bond between the C-terminal glycine and proline. Attachment of the T2A peptide sequence at the C-terminus of the upstream construct is prevented by the presence of a furin cleavage site, which is linked to the T2A peptide by a serine-glycine linker. LTR = long terminal repeat.

2.1.2 Polymerase Incomplete Primer Extension (PIPE) Cloning

The PIPE cloning method is a PCR-based alternative to the conventional restriction enzyme- and ligation-dependent cloning methods [249]. It eliminates the use of restriction enzymes and ligation, and thus the incorporation of restriction sites, which could encode extra, unwanted residues into expressed proteins [250]. The PIPE method relies on the inefficiency of the amplification process in the final cycles of a PCR reaction, possibly due to the decreasing availability of deoxynucleotide triphosphates (dNTPs), which results in the generation of partially single-stranded (PIPE) PCR products with overhanging 5`ends [251]. Using appropriate primer design these 5` overhanging ends can be used as “sticky ends”. To achieve this a set of vector-specific primers were used for PCR vector linearization and another set of primers with 5’-vector-end overlapping sequences were used for insert amplification, generating incomplete extension products by PIPE (Figure 2.3). The PIPE products were subsequently treated by Dpn I (NEB) digestion according to the manufacturer’s instructions in order to destroy *E. coli*-derived vector template, thus reducing background contamination. The unpurified PIPE products were mixed at a 1:1 molar ratio, followed by a 30 minute incubation at 60°C. Finally, 2µl from the mixture was used to transform TOP10F’ competent cells.

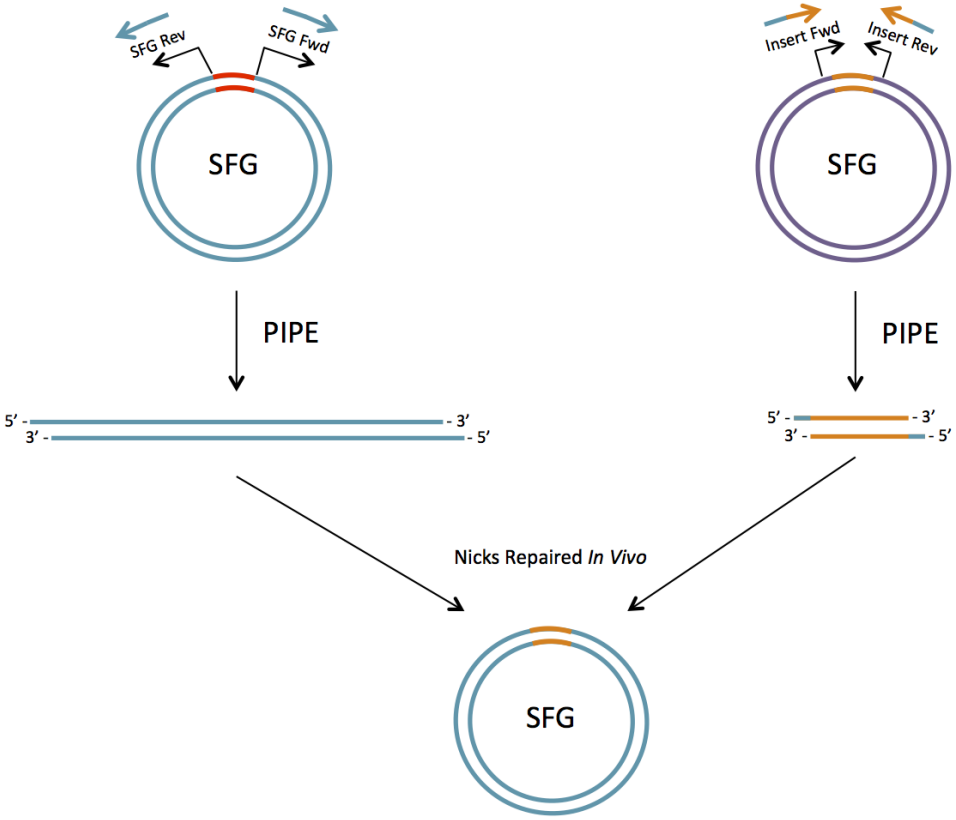

Figure 2.3 Schematic representation of PIPE cloning.

A set of vector-specific primers were designed for SFG linearization. In parallel, the desired insert was amplified with another set of 5' SFG-end homologous primers. The PIPE products were mixed together and assembled into a new insert containing SFG vector.

2.1.2.1 Materials, Reagents and Equipment

- Primers (please refer to Table 2.1)
- Template
- Nuclease-free water
- Phusion High-Fidelity DNA Mastermix (Thermo Scientific, UK)
- Eppendorf Mastercycler Gradient PCR Machine

2.1.2.2 Protocol

1. A 50 µL reaction mixture as detailed below was produced:

Nuclease-free water	XµL
2x Phusion PCR MasterMix	25µL
Forward primer	2.5µL (10µM)
Reverse primer	2.5µL (10µM)
Template DNA	XµL (10ng)

2. Samples were subjected to the following PCR programme:

Initial denaturation	98°C	30 sec	
Denaturation	98°C	10 sec	30 cycles
Annealing	60°C	30 sec	
Extension	72°C	15-30 sec/kb	
Store	4°C	hold	

2.1.3 Restriction Enzyme Digestion

DNA digestion and restriction patterns were used to accurately verify successful cloning and presence of inserts.

2.1.3.1 Materials, Reagents and Equipment

- Restriction enzymes (NEB, UK)
- 10x Restriction enzyme buffers (NEB, UK)
- 100x Bovine Serum Albumin (BSA) (NEB, UK)

- Nuclease-free water
- DNA template
- Eppendorf Mastercycler Gradient PCR machine
- Ice

2.1.3.2 Protocol

1. A 20µL reaction mixture was produced for a double digest. All components were kept on ice while the reaction was set up.

   XµL (1µg) DNA

   XµL Nuclease free water

   2µL 10x NEB Buffer

   0.5µL Enzyme 1 (1U)

   0.5µL Enzyme 2 (1U)

   1µL 1 in 10 diluted BSA

2. Reaction mixtures were incubated for one hour in a PCR machine at 37^{o}C.
3. To each reaction mixture was added 4µL of 6x DNA loading buffer.
4. The sample was run on an agarose gel.

Table 2.1 Primers used for PIPE cloning

SFG C4 and CT4	F1	5’-CCACCTCTGACTTGAGCGTCGATTTTTGTGATGCTCGTCA-3’
	R1	5’-CCATGGCAGTCTAGAGGATGGTCCACCCCCGGGGTCGGCA-3’
	F2	5’-CCATGGCTCTCCCAGTGACTGCCCTACTGCTTCCCCTAGC-3’
	R2	5’-GACGCTCAAGTCAGAGGTGGCGAAACCCGACAGGACTATA-3’
	F3	5’-CATCCTCTAGACTGCCATGGGCTGGCTGTGTTCCGGCCTG-3’
	R3	5’-AGTCACTGGGAGAGCCATGGGTCCGGGGTTCTCTTCCACG-3’
SFG C34B	F1	5’-TGCAGGCCCTGCCCCCTCGCAGGAGGAAGAGAAGTGGATC-3’
	R1	5’-GATCCCTCGAGTGGCTGTTATTACAGCTCGCAGCCGCCCT-3’
	F2	5’-TAACAGCCACTCGAGGGATCCGGATTAGTCCAATTTGTTA-3’
	R2	5’-TCTGACGCTCAGTGGAACGAAAACTCACGTTAAGGGATTT-3’
	F3	5’-TCGTTCCACTGAGCGTCAGACCCCGTAGAAAAGATCAAAG-3’
	R3	5’-GAGCCTGTAAGTGAGCTTGGAGAGAGGGGCTGTTAGTAAC-3’
	F4	5’-CCAAGCTCACTTACAGGCTCTCTACTTAGTCCAGCACGAA-3’
	R4	5’-GCGAGGGGGCAGGGCCTGCATGTGAAGGGCGTCGTAGGTG-3’
SFG C4B	F1	5’-AGAGTGAAGTTCAGCAGGAGCGCAGAGCCCCCCGCGTACC-3’
	R1	5’-AGCTTTGGTAACAGGAATATTGCAGCATTCATGCACATTG-3’
	F2	5’-CAATGTGCATGAATGCTGCAATATTCCTGTTACCAAAGCT-3’
	R2	5’-GCGGCCGCTCCCTCGGACTGCCTCTCATGGCCTTGGCTGG-3’
	F3	5’-CAGTCCGAGGGAGCGGCCGCAATTGAAGTTATGTATCCTC-3’
	R3	5’-CTCCTGCTGAACTTCACTCTCAGCTCGCAGCCGCCCTCCT-3’
SFG 43428ζ and 434Tr	F1	5’-AATTGAAGTTATGTATCCTCCTCCTTACCTAGACAATGAG-3’
	R1	5’-ATCAGCTCACTCAAAGGCGGTAATACGGTTATCCACAGAA-3’
	F2	5’-CCGCCTTTGAGTGAGCTGATACCGCTCGCCGCAGCCGAAC-3’
	R2	5’-GGGTCCGGGGTTCTCTTCCACGTCGCCGCAGGTCAGCAGG-3’
	F3	5’-TGGAAGAGAACCCCGGACCCATGCCTAGAGGCTTCACATG-3’
	R3	5’-GAGGATACATAACTTCAATTGCGGCCGCAGGCAGCAGTCC-3’

SFG 43428BζSFG 43428Bζ	F1	5’-AGCTTTGGTAACAGGAATATTGCAGCATTCATGCACATTG-3’
	R1	5’-AGCTTTGGTAACAGGAATATTGCAGCATTCATGCACATTG-3’
	F2	5’-CAATGTGCATGAATGCTGCAATATTCCTGTTACCAAAGCT-3’
	R2	5’-GCGGCCGCAGGCAGCAGTCCCTCGCCTTGGGCTCTCACAG-3’
	F3	5’-GGACTGCTGCCTGCGGCCGCAATCGAGGTGGAGCAGAAGC-3’
	R3	5’-CTCCTGCTGAACTTCACTCTCAGCTCGCACCCGCCCTCTT-3’
SFG 34CB	F1	5’-GTCAGTGAGCGAGGAAGCGGAAGAGCGCCCAATACGCAAA-3’
	R1	5’-GGGTCCGGGGTTCTCTTCCACGTCGCCGCAGGTCAGCAGG-3’
	F2	5’-TGGAAGAGAACCCCGGACCCATGCCTAGAGGCTTCACATG-3’
	R2	5’-GAGGATACATAACTTCAATTGCGGCCGCAGGCAGCAGTCC-3’
	F3	5’-AATTGAAGTTATGTATCCTCCTCCTTACCTAGACAATGAG-3’
	R3	5’-GGGCCCGGGGTTCTCTTCCACATCTCCACATGTCAGGAGA-3’
	F4	5’-TGGAAGAGAACCCCGGGCCCATGGCTCTCCCAGTGACTGC-3’
	R4	5’-GCGCTGGCGTCGTGGTGGGTGCGGCCGCTCCCTCGGACTG-3’
	F5	5’-ACCCACCACGACGCCAGCGCCGCGACCACCAACCCCGGCG-3’
	R5	5’-TTTGCGTATTGGGCGCTCTTCCGCTTCCTCGCTCACTGAC-3’

2.1.4 Separation of DNA Fragments by Agarose Gel Electrophoresis

Agarose gel electrophoresis was used for separation of DNA fragments by size. Migration rates are dependent on the pore size of the gel, which is determined by the agarose concentration. Optimal resolution of the fragments of interest was achieved by using 1% agarose, which ensures 0.25 – 12kb range of separation.

2.1.4.1 Materials, Reagents and Equipment

- Electrophoresis grade Agarose (MP Biomedicals, UK)
- 10x TBE buffer (please see below)
- 6x DNA loading buffer (please see below)
- Ethidium Bromide (Sigma-Aldrich, UK)
- 1 kb DNA ladder (NEB, UK)
- Gel Mould (Biorad, UK)
- Gel Comb (Biorad, UK)
- Gel Tank (Biorad, UK)
- Microwave
- UV Transilluminator (UVI Tech, UK)

Buffers and solutions:

10x TBE: 108g Tris-base, 55g boric acid, 9.3g EDTA in 1L deionised water

6x DNA Loading Buffer: Distilled water, 40% (w/v) sucrose, 0.25% (w/v) bromophenol blue, 0.25% (w/v) xylene cyanol

2.1.4.2 Protocol

1. One gramme of agarose was mixed with 100mL 1xTBE and heated in a microwave until completely dissolved.
2. After cooling under cold running water, 0.30µg/mL ethidium bromide was added and the mixture swirled vigorously to ensure even distribution.

3. The gel was poured into a pre-cast mould, a comb inserted and the mixture was left to set at room temperature.
4. Prior to loading, samples were mixed 5:1 with 6x DNA loading buffer. In addition to the samples, a 1kb DNA ladder was loaded to allow the size of migrating DNA fragments to be estimated.
5. The gel was run at 5-8 V/cm until sufficient migration (as visualised by the loading dye) had occurred.
6. The DNA was visualised with UV light at 254 nm using a UV transilluminator.

2.1.5 Transformation of Escherichia coli TOP10F' Strain

Replenishment of plasmid stocks and selection of newly produced vectors was achieved by introducing the plasmid into chemically competent *E. coli.* All steps followed common microbiological practice, using a Bunsen burner to provide sterile conditions.

2.1.5.1 Materials, Reagents and Equipment

- TOP10F' *E. coli* (Invitrogen, UK)
- Plasmid DNA
- Agar plates
- Super Optimal broth with Catabolite repression (SOC) (Sigma-Aldrich, UK)
- Water bath set at 42^{o}C
- Ice
- Oven set at 37^{o}C
- Bunsen burner
- Excella E-25 incubator shaker
- Glass spreaders
- 100% Ethanol (Fisher Scientific, UK)

Buffers and solutions:

SOC Media = 20g bacto tryptone, 5g bacto yeast extract, 10mM Sodium Chloride (NaCl), 2.5mM Potassium Chloride (KCl), 10mM Magnesium Chloride ($MgCl_2$), 10mM Magnesium Sulphate ($MgSO_4$), 20mM Glucose.

2.1.5.2 Protocol

1. One vial of TOP10F' *E. coli* was thawed on ice.
2. 1µg Plasmid DNA was added to the *E. coli* and incubated for 30 minutes on ice.
3. Bacteria were heat shocked at 42°C for 90 seconds and subsequently incubated on ice for 5 minutes.
4. Following addition of 300µL SOC media, samples were shaken at 220rpm for one hour at 37°C.
5. Simultaneously, agar plates containing ampicillin were dried in an oven at 37°C.
6. The *E. coli* were spread onto the pre-dried plate and incubated at 37°C overnight.

2.1.6 Production of Agar Plates

2.1.6.1 Materials, Reagents and Equipment

- LB agar (Novagen, UK)
- Ampicillin (Sigma-Aldrich, UK)
- Microwave oven
- Non-tissue culture treated 10cm Petri-dishes (Fisher Scientific, UK)
- Bunsen burner

Buffers and solutions:

Agar = 5g yeast extract, 10g peptone from casein, 10g NaCl in 1L deionised water

2.1.6.2 Protocol

1. 500mL agar was melted in a microwave oven for 20min at 40% maximum power to obtain a molten solution.
2. After cooling down, a selective antibiotic (100mg ampicillin) was added and mixed thoroughly.
3. The solution was distributed evenly over 20 Petri dishes and left to solidify at room temperature.
4. Petri dishes were stored at 4°C.

2.1.7 Selection of Bacterial Clones

2.1.7.1 Materials, Reagents and Equipment

- Luria-broth (L-broth)
- Ampicillin (Sigma Aldrich, UK))
- 50mL Conical Centrifuge Tubes (Fisher Scientific, UK)
- 20µL pipette tips
- Excella E-25 incubator shaker

Buffers and solutions:

L-broth: 10g tryptone, 5g yeast extract, 0.5g NaCl

2.1.7.2 Protocol

1. 5mL of L-broth, containing 100µg of Ampicillin was aliquotted into 50mL Falcon tubes.
2. Single bacterial colonies were picked using a pipette tip and submerged in the L-broth.
3. The tubes were shaken at 220rpm for 16 hours at 37°C prior to being centrifuged at 3000g for 10 minutes to pellet the bacteria. The supernatant was discarded and the pellet subjected to plasmid isolation.

2.1.8 Storage of Bacterial Clones

2.1.8.1 Materials, Reagents and Equipment

- 100% glycerol (Sigma-Aldrich, UK)
- 850µL bacterial culture
- cryo-vials

2.1.8.2 Protocol

1. 150µl sterile 100% glycerol and 850µl of the bacterial culture (frozen stock is 15% glycerol) were added to a sterile, labelled cryo-vial and mixed well.
2. Frozen stock of bacterial clones was stored at -80°C.

2.1.9 Isolation of Plasmid DNA from *E. coli* – MiniPrep

Plasmid DNA was extracted from the bacterial cultures using a QIAprep Spin Miniprep kit. The procedure is based on Birnboim and Doly's rapid alkaline lysis protocol [252], in which bacterial lysis is achieved using sodium dodecyl sulphate (SDS) in the presence of 200mM sodium hydroxide (NaOH). The strong alkaline environment resulted in denaturation of proteins and chromosomal DNA and ensured their co-precipitation with SDS upon neutralization of the solution and conversion to high salt environment by the addition of potassium acetate. The supercoiled conformation of the plasmid DNA prevented separation of the DNA strands, thereby ensuring that it remained in solution. Contaminating RNA was eliminated by both the addition of RNAse A to the initial re-suspension buffer and precipitation in the high salt environment of the neutralization buffer. Any remaining impurities were removed by running the aqueous phase through a column containing a silica membrane. The neutralization buffer contained the chaotropic salt, guanidine hydrochloride, which induced dehydration of the plasmid DNA, allowing it to bind strongly to the silica membrane, whilst other contaminating factors were removed in the flow-through. Following two further wash steps with chaotropic salt and ethanol

containing buffers, the purified plasmid DNA was eluted from the column using a low salt buffer.

2.1.9.1 Materials, Reagents and Equipment

- QIAprep spin Miniprep kit (Qiagen, UK)
- Pelleted TOP10F' *E. coli*
- 1.5mL Eppendorf tubes
- Eppendorf 5415R refrigerated Micro-centrifuge

Buffers and solutions:

Buffer P1 = 50mM Tris-HCl (pH 8), 10mM EDTA, added 100µg/mL RNAse A

Buffer P2 = 200mM NaOH, 1% (w/v) SDS

Buffer EB = 10mM Tris-HCl (pH 8.5)

NOTE: Qiagen does not publish the full composition of the neutralizing N3 buffer, buffer PB or buffer PE. Buffer N3 is known to contain guanidine hydrochloride (as the source of chaotropic salt) and acetic acid (probably in the form of potassium acetate) to neutralize the alkaline environment caused by the NaOH in buffer P2. Buffer PB also contains guanidine hydrochloride, along with isopropanol. No details regarding the composition of buffer PE have been released.

2.1.9.2 Protocol

1. Pelleted bacteria were re-suspended in 250µL buffer P1.
2. An equal volume of buffer P2 was added and the sample was gently inverted approximately 10 times to ensure complete mixing.
3. 350µL buffer N3 was added to each sample and complete mixing was achieved through gentle inversion.
4. Centrifugation at 15,700g pelleted the white precipitate in each sample.

5. The aqueous phase was carefully transferred to a QIAprep spin column and the white precipitate discarded.
6. Following centrifugation at 15,700g, each column was washed with 500µL buffer PB and centrifuged at 15,700g, before discarding the eluate.
7. Each column was washed with 750µL buffer PE and centrifuged at 15,700g and the eluate was again discarded.
8. After an additional centrifugation at 15,700g to remove any residual ethanol, the DNA was eluted in 50µL buffer EB through centrifugation at 15,700g.
9. The concentration of the isolated DNA was determined and stored at -20°C.

2.1.10 Isolation of Plasmid DNA – Maxi-Prep

Maxi-preps were used for the isolation of highly concentrated plasmid DNA. As with mini-preps, the process relies on bacterial lysis under strong alkaline conditions, with proteins and chromosomal DNA removed by precipitation upon neutralisation and conversion to a high salt environment. RNA impurities were removed through the addition of RNase A in the initial re-suspension buffer. Once insoluble contaminants had been removed via centrifugation, the supernatant (containing the plasmid DNA) was subjected to anion-exchange chromatography. The negatively charged plasmid DNA binds strongly to the positively charged diethylaminoethyl (DEAE) resin beads, until eluted using a high-salt containing buffer. Intermediate washes with buffers of increasing salt concentrations ensured the removal of remaining contaminants. Once eluted, the DNA was precipitated and desalted using a series of alcohol washes before being dissolved in TE buffer.

2.1.10.1 Materials, Reagents and Equipment

- 100mL TOP10F' bacteria containing wanted plasmid
- QIAGEN Plasmid Maxi Kit
- 1.5mL Eppendorf tubes
- Oak Ridge polycarbonate centrifuge tubes

- Oak Ridge polypropylene copolymer centrifuge tubes
- Sorvall RC 5B Centrifuge
- 70% Ethanol
- Isopropanol

Buffers and Solutions

Buffer P1 = 50mM Tris.HCl (pH 8.0), 10mM EDTA, 100μg/mL RNase A

Buffer P2 = 200mM NaOH, 1% (w/v) SDS

Buffer P3 = 3M Potassium Acetate

Buffer QBT = 750mM NaCl, 50mM 3-(N-Morpholino)-propanesulfonic acid (MOPS), 15% (v/v) isopropanol, 0.15% (v/v) Triton X-100

Buffer QC = 1M NaCl, 50mM MOPS, 15% (v/v) isopropanol

Buffer QF = 1.25M NaCl, 50mM Tris.HCl (pH 8.5), 15% (v/v) isopropanol

TE Buffer = 10mM Tris.HCl (pH 8), 1mM EDTA.

2.1.10.2 Protocol

1. Once pelleted, the bacteria were re-suspended in 10 mL buffer P1 and bacterial lysis was induced by addition of an equal volume of buffer P2. Mixing ensured complete lysis.
2. Pre-chilled buffer P3 (10 mL) was added after a maximum of five minutes lysis and the solution was well mixed to ensure complete neutralisation.
3. The solution was incubated on ice for approximately 15 minutes before being centrifuged at 20,200 g for 30 minutes at 4°C.
4. The supernatant was decanted into a fresh polycarbonate centrifuge tube and centrifuged at 20,200 g for 15 minutes at 4 °C to ensure complete removal of all insoluble contaminants.
5. The resulting supernatant was added to a pre-equilibrated QIAGEN-tip 500 and left to filter by gravity flow.

6. The tip was washed twice using 30 mL buffer QC before the plasmid DNA was eluted into a polypropylene copolymer centrifuge tube using 15 mL buffer QF.
7. The DNA was precipitated by adding 10.5 mL isopropanol and pelleted by centrifugation for 30 minutes at 17,700 g and 4°C.
8. The pellet was washed with 5 mL 70% ethanol to remove the salt and the DNA pelleted by centrifugation at 20,000 g for 10 minutes.
9. After removal of the supernatant and air-drying of the DNA pellet at 37°C for approximately five minutes, the DNA was re-suspended in 200 μL of TE buffer.
10. Once the concentration of DNA had been calculated it was stored at -20°C until required.

2.1.11 Sequencing

All the new constructs were sent for sequencing (SourceBioscience, UK) to confirm successful cloning. The results were analyzed with 4Peaks software and sequence alignment was performed on SerialCloner 2.5 software.

2.2 Cell Culture Techniques

2.2.1 Common Medias and Solutions

D10 Media: 500mL Dulbecco's Modified Eagle Medium (DMEM) (Lonza, UK)
50mL Foetal Calf Serum (Sigma-Aldrich, UK)
200mM GlutaMAX (Gibco, UK)
50,000U Penicillin (Gibco, UK)
50mg Streptomycin (Gibco, UK)

RBS Media: 500mL Roswell Park Memorial Institute (RPMI) Medium (Lonza, UK)
50mL Foetal Calf Serum
200mM GlutaMAX
50,000U Penicillin

50mg Streptomycin

R10 Media: 500mL Roswell Park Memorial Institute (RPMI) Medium

50mL Human Male AB Serum (Gibco, UK)

200mM GlutaMAX

50,000U Penicillin

50mg Streptomycin

CPDA: Citrate Phosphate Dextrose Adenine Solution (Gibco, UK)

Anticoagulant solution used in 1:9 ratio with whole blood.

Trypsin: 0.25% Trypsin-EDTA (Gibco, UK)

CDB: Cell Dissociation Buffer (Invitrogen Life Tech, UK)

Isotonic, and enzyme-free solution of salts, chelating agents, and cell-conditioning agents in Ca^{2+} and Mg^{2+}-free phosphate-buffered saline

1x PBS: Phosphate Buffer Saline (Biochrom AG, UK)

9.55g/L PBS in deionised water

2.2.2 Cell Lines

All cells were incubated at 37°C, 95%O_2/5% CO_2, unless otherwise stated.

2.2.2.1 Materials, Reagents and Equipment

- R10 media
- D10 media
- Interleukin-2 (IL-2) (Novartis, UK)
- Interleukin-4 (IL-4) (Gentaur, UK)

- Tetracycline (Calbiochem, UK)
- Puromycin (Merck, UK)
- 6-well tissue culture-treated plates (Greiner Bio-one, UK)
- Tissue-culture treated Petri dishes (Greiner Bio-one, UK)

2.2.2.2 Tumour Cell Lines

To confirm the ability of CAR^+ T-cells to target CSF-1R, 8 different cell lines (listed below) were used. All lymphoma cell lines (a generous gift from Dr Stephan Mathas, Max-Delbrück-Center for Molecular Medicine, Berlin, Germany) were grown in RBS media in flasks while the breast cancer cell lines were propagated in D10 in serial dilutions and monolayers were passaged when appropriate.

KM-H2: human Hodgkin's lymphoma cell line, established from the pleural effusion of a 37-year old man with Hodgkin's disease (mixed cellularity type) in 1974, characterized by IgG4 rearrangement [253].

K299: human $CD30^+$ Anaplastic large cell lymphoma (ALCL) cell line, positive for t(2;5)(p23;q35), established from the peripheral blood of a 25-year-old man [254].

K299 FMS: has been developed during this PhD by transducing K299 with SFG retroviral vector (please refer to section 2.2.3.1) containing the c-*fms* gene. Consequently, K299 FMS expresses high levels of CSF-1R (Figure 5.8, A).

DEL: human $CD30^+$ ALCL cell line, negative for t(2;5)(p23;q35), established from the pleural effusion of a 12-year-old boy with malignant histiocytosis in 1987 [255].

FE-PD: human $CD30^+$ ALCL cell line, negative for t(2;5)(p23;q35), established from the peripheral blood of a 46-year-old woman, originally diagnosed with Hodgkin's disease [256].

JB6: human $CD30^+$ ALCL cell line, positive for t(2;5)(p23;q35), established from the peripheral blood of a 12-year-old boy [257].

L540: human Hodgkin's lymphoma cell line, established from the bone marrow of a 20-year-old woman with Hodgkin's disease (nodular sclerosis type), characterised by rearranged TCR gene [258].

T47D: established from a pleural effusion in a woman with breast cancer. It is both oestrogen and progesterone receptor positive [259].

T47D FMS: has been developed in the lab prior to the start of this PhD by transducing T47D with SFG retroviral vector (please refer to section 2.2.3.1) containing the c-*fms* gene. Consequently, T47D FMS expresses high levels of CSF-1R making it an ideal positive control for CAR functionality assessment.

Note: The six lymphoma cell lines (KM-H2, K299, DEL, FE-PD, JB6 and L540) have been transduced with an SFG retroviral vector (please refer to section 2.2.3.1) encoding for genes for firefly luciferase (ffLuc) and tdTomato, allowing for ease of tracking in co-cultivation experiments as well as for *in vivo* imaging by bioluminescence.

2.2.2.3 Retroviral Packaging Cell Lines

Packaging cell lines are designed to synthesize and provide all retroviral proteins required for assembly of high-titre infectious virus, but should not produce any replication-competent virus. To ensure no virion replication post infection, replication-defective vectors are used, in which the coding regions for the 4 genes *gag*, *pro*, *pol* and *env*, which are crucial for the completion of the retroviral life cycle, are deleted and replaced with the DNA sequence intended for transfer. Instead, those genes are expressed *in trans,* within the packaging cell line, which thereby provides all of the required proteins for viral

assembly. The retroviral genomic sequence (containing the desired gene) is subsequently packaged into viruses, which are capable of infecting their target cells and delivering the DNA of interest, but then fail to continue the typical lytic pathway that leads to cell lysis and death.

The genome of every retrovirus consists of two RNA copies. These encode for the four specific genes mentioned above (*gag*, *pro*, *pol* and *env*) [260], which are crucial for the completion of the retroviral life cycle. The gag sequence encodes for the three main structural proteins: matrix (MA), capsid (CA) and nucleocapsid (NC) proteins. The pro sequence, encodes for proteases (PR) responsible for cleaving Gag and Gag-Pro-Pol during particles assembly, budding and maturation. The pol sequence encodes for the enzymes reverse transcriptase (RT) and integrase (IN), the former catalyzing the reverse transcription of the viral genome from RNA to DNA during the infection process and the latter responsible for integrating the proviral DNA into the host cell genome. The env sequence encodes for both surface (SU) and transmembrane (TM) subunits of the envelope glycoprotein. This is initially synthesized as a single polypeptide which undergoes cleavage by a cell-encoded protease to yield both subunits. All of the structural proteins of the virion are derived from three polyproteins: Gag, Gag-Pro-Pol, and Env (Figure 2.4). All viral proteins (MA, CA, NC, PR, RT and IN) are initially linked within the Gag and Gag-Pro-Pol proteins. The Gag protein is capable of directing budding at the plasma membrane, and the Pro-Pol polyproteins are incorporated into the resulting particle because they are linked to Gag. Subsequently, after budding the Gag and Gag-Pro-Pol proteins are cleaved by the viral protease to produce the mature, infectious virion.

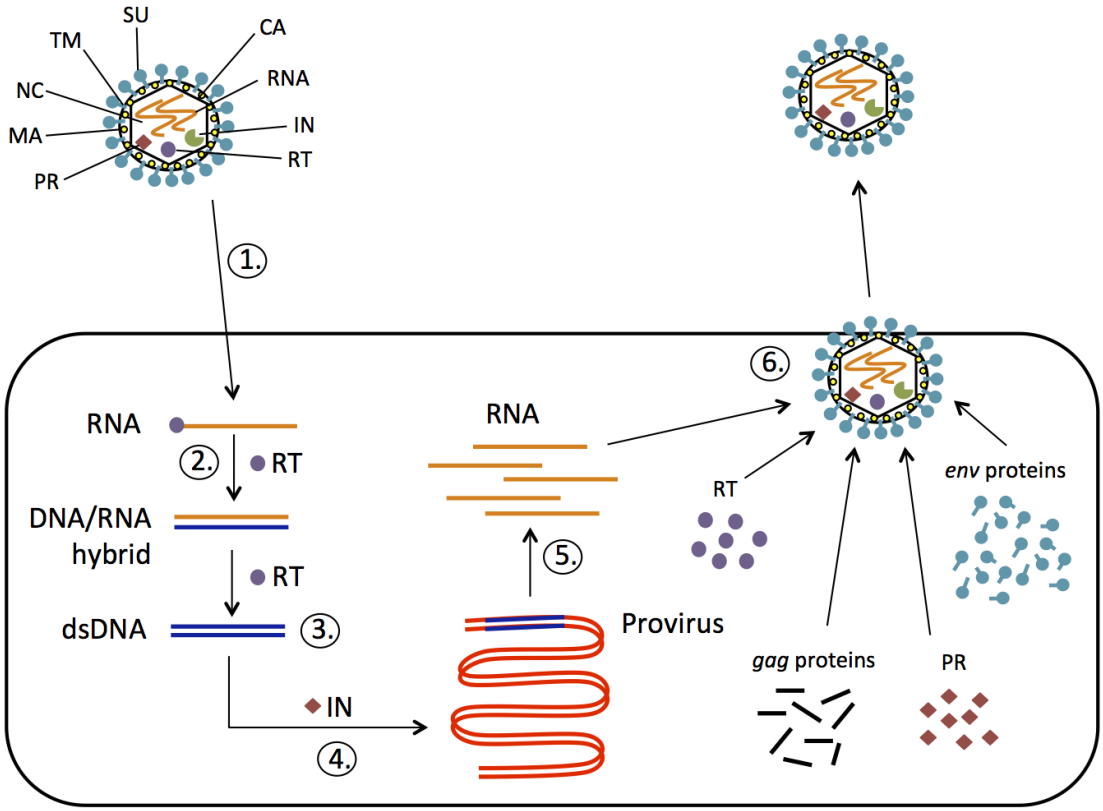

Figure 2.4 Retroviral life cycle.

Upon target cell infection, (step 1), the viral particle envelope and capsid are disassembled, releasing the viral genome and proteins into cytoplasm. The viral reverse transcriptase (RT) binds to a transfer RNA (tRNA) binding site in the 5' LTR and synthesizes a complementary DNA strand (step 2). The template viral RNA is then degraded by the RNase H subunit of the reverse transcriptase allowing for synthesis of a second DNA strand (step 3). The resulting double stranded DNA (dsDNA) is integrated as a provirus into the host genome by the viral integrase (IN) (step 4). The host RNA polymerase transcribes the viral RNA (step 5), which is then exported from the nucleus and transcribed to give the gag, pro, pol and env proteins. These proteins, along with two copies of the untranslated viral RNA are packaged into a new viral particle (step 6), which subsequently buds from the target cell. MA – matrix proteins, CA – capsid proteins, NC - nucleocapsid proteins, PR – protease, RT – reverse transcriptase, IN – integrase, SU – surface proteins, TM – transmembrane proteins.

To minimise the risk of producing replication-competent virus the *gag-pro-pol* and *env* genes are expressed on separate plasmids within the retroviral packaging cell line. The *pro* and *pol* genes are always expressed on the same plasmid as *gag* due to the fact that they are transcribed as a single *gag-pro-pol* mRNA transcript. Therefore three separate recombination events would need to occur before all genes are expressed *in cis*. To further decrease the risk of restoring replicative competence, heterologous promoters like CMV's have been used [261, 262]. Thereby *gag-pro-pol* genes are expressed from a single construct driven by a heterologous promoter. The retroviral vector contains a cassette for transgene expression typically driven by the 5'LTR promoter [263] while the envelope expression is supplied by a third independent construct usually driven by a heterologous promoter.

Three different types of retroviral packaging cell lines were used throughout this PhD, depending on the target cell species and the necessary viral tropism.

H29D: The H29D retroviral packaging cell line (293GPG in reference [264]) is based on the human embryonic kidney adenoviral 5-transformed cell line (HEK 293, [265]) This packaging cell line expresses the MoMLV *gag-pol* genes under the control of the cytomegalovirus (CMV) immediately early (IE) promotor. Expression of the vesicular stomatitis virus-G (VSV-G) *env* proteins results in the production of viral particle displaying a broad tropism. Since constitutive expression of the VSV-G envelope protein is toxic, controlled expression was achieved by placing the VSV-G coding sequence under the control of a tetracycline-repressed promoter. Initiation of transcription from this promoter is dependent upon the binding of a tetracycline-transactivator (tTa) molecule. However, in the presence of tetracycline this binding is inhibited. Therefore, to prevent constitutive expression of the VSV-G *env* protein, H29D cells were maintained in D10 media supplemented with 2µg/mL tetracycline. Fresh media and tetracycline were provided every three days and the cells were passaged when confluent. Tetracycline was removed from the media for the production of VSV-pseudotyped virus and the toxicity of this

envelope protein meant that fresh H29D transductions were required for each preparation of fresh virus.

PG13: retroviral packaging cell line based on mouse embryonic fibroblast cell line, NIH 3T3, that has been transfected to express Moloney Murine Leukaemia Virus (MoMLV) *gag-pol* protein and Gibbon Ape Leukaemia Virus (GaLV) *env* protein (European Collection of Cell Cultures) [266]. PG13 viral particles are capable of infecting human cells and are used to produce stably expressing PG13 clones as the GaLV is not toxic to the cells. The PG13 packaging cells were grown in D10 media in serially diluted cultures and were passaged when confluent.

293Vec RD114: retroviral packaging cell line based on the HEK 293 cell line, that has been transfected to express MoMLV *gag-pol* protein and feline leukaemia virus (RD114) *env* protein (BioVec Pharma) [267]. 293Vec RD114 produced retroviral vectors are pseudotyped by RD114 virus envelope protein and are capable of infecting human cells with titres of up to 0.5 x 10^7 infectious units per ml. Stable 293Vec RD114 clones were produced and grown in D10 media in serially diluted cultures and were passaged when confluent.

2.2.3 Retroviral Vectors

Efficient gene transduction depends on the inclusion in the retroviral vector of a number of *cis*-acting viral elements such as (1) a promoter and polyadenylation signal; (2) a viral packaging signal (ψ) required for packaging of the mRNA transcript into new viral particles; (3) signals required for reverse transcription, including a transfer RNA-binding site (PBS) and polypurine tract (PPT) for initiation of first- and second-strand DNA synthesis, and a repeated (R) region at both ends of the viral RNA required for transfer of DNA synthesis between templates; and (4) short, partially inverted repeats located at the termini of the viral LTRs required for integration (Figure 2.5).

All the CAR constructs in this thesis have been cloned in the SFG retroviral vector.

2.2.3.1 SFG

The SFG retroviral vector is based on the MFG vector [268], in which gene expression is driven by the MoMLV LTRs and the presence of the MoMLV ψ packaging signal ensures efficient packaging of the RNA into the virus. The presence of the splice donor and splice acceptor sites allow the production of the sub-genomic RNA transcripts usually required for the translation of the *env* gene [269]. The gene of interest is inserted at a naturally occurring *NcoI* restriction site, ensuring that its start codon is in the precise place previously occupied by the deleted *env* gene. This vector does not contain a eukaryotic cell-compatible selectable marker gene.

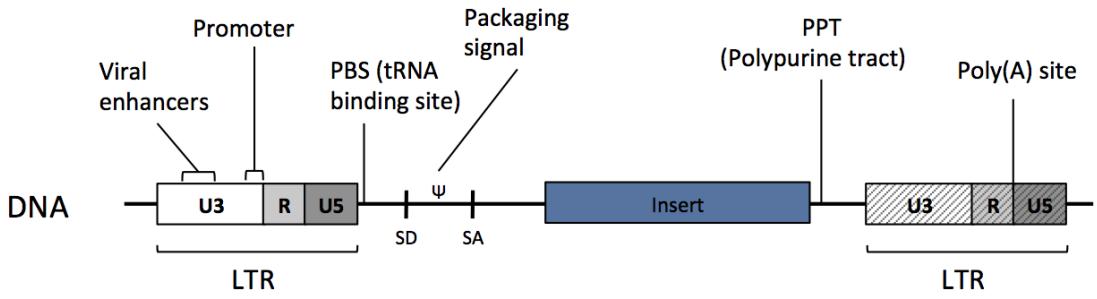

Figure 2.5 Critical *cis*-acting elements in retroviral vectors and vector replication cycle.

Critical *cis*-acting elements in retroviral vectors are indicated in the figure. After one round of viral replication, the U3 regions in both LTRs are derived from the original 3′LTR U3 region and both U5 regions are derived from the U5 region originally present in the 5′LTR in the plasmid. Usually, R sequences arise from the 5′plasmid LTR, but they may also include 3′plasmid LTR sequences. (U3) Unique 3′LTR RNA; (U5) unique 5′LTR RNA; (R) repeat at both ends of the viral RNA; (poly[A]) polyadenylation; (LTR) long terminal repeat. Image is adapted from Figure 1, Retroviruses, 1st edition [270].

2.2.4 Production of Retroviral Packaging Cell Lines

2.2.4.1 Materials, Reagents and Equipment

- H29D cells
- D10 medium
- Plasmid DNA
- Polyethylenimine (PEI) (Sigma, UK)
- Vortex
- PG13 cells
- H29D retroviral supernatant
- Plasmid of interest
- Serum free media (DMEM without supplements)

2.2.4.2 Transfection of H29D Cells

1. Tetracycline was removed from the H29D cells a minimum of two hours prior to transfection by replacing the tetracycline-containing D10 with fresh D10 only.
2. Total plasmid DNA was diluted in a sterile tube in serum-free DMEM (volume of media was 10% of final volume in culture vessel).
3. PEI (1µg/µL) was added to the diluted DNA and mixed immediately by vortexing or pipetting. The volume of PEI used was based on a 3:1 ratio of PEI(µg):total DNA(µg).
    a. **6 well dish:** 9µl of PEI (1µg/µl) = 9µg PEI + 3µg DNA
    b. **10cm dish:** 21µl of PEI (1µg/µl) = 21µg PEI + 7µg DNA
    c. **15cm dish:** 33µl of PEI (1µg/µl) = 33ug PEI + 11ug DNA
4. The mixture was incubated at room temperature for 20 minutes, before being added drop-wise to the H29D cells.
5. After gentle rocking ensuring complete mixing of the transfection mixture, the cells were incubated for 3 hours at 37^{o}C.
6. After 3 hours, the media was replaced with fresh D10.

7. Supernatants were harvested daily from day 3-7 and either directly used to infect target cells or snap frozen in an ethanol bath. Removed supernatants were replaced daily with fresh D10 media.

2.2.4.3 PG13 and 293Vec RD114 Infection

1. The media was removed from empty PG13 or 293Vec RD114 cells and replaced with 3mL H29D supernatant containing the VSV-pseudotyped virions.
2. The packaging cells were subsequently incubated for 72 hours before they were analysed for transgene expression using flow cytometry.
3. PG13 or 293Vec RD114 populations in which >80% of cells were expressing the virus of interest were used as stable packaging cell lines.

2.2.5 Human Peripheral Blood Mononuclear Cell Isolation and Activation

Peripheral blood mononuclear cells (PBMCs) were isolated from healthy donors by density gradient centrifugation using Ficoll Paque Plus (GE Healthcare, UK). Recruitment of healthy volunteer donors for this purpose was approved by the Guy's Hospital Research Ethics Committee (09/H0804/92; Use of Donor Blood Samples for Pre-Clinical Development of Active and Passive Immunotherapy for Cancer and 09/H0707/086; Generation of clinical grade T-cells for adoptive cell therapy).

2.2.5.1 Materials, Reagents and Equipment

- Fresh blood
- Citrate-Dextrose solution (ACD)
- 50mL Syringe (BD Bioscience, UK)
- Butterfly needle
- 50mL Falcon tubes (Fisher Scientific, UK)
- Ficoll-Paque Plus (GE Healthcare, UK)
- Pasteur Pipettes (SLS, UK)

- Anti-CD3/Anti-CD28 Dynabeads (Invitrogen, UK)
- R10 media
- PBS
- Eppendorf centrifuge

2.2.5.2 Protocol

- 15mL Ficoll-Paque was aliquotted into two separate 50mL Falcon tubes.
- Fresh Blood (25-50mL) (anticoagulated with 1x citrate-dextrose solution) was slowly layered onto the Ficoll-Paque and was centrifuged at 400g for 30 minutes (acc = 0, dec = 0).
- The PBMC layer, present at the interface between the Ficoll-Paque and the plasma, was transferred into fresh 50mL Falcon tubes using a Pasteur pipette and diluted to a final volume of 50mL in pre-warmed PBS and centrifuged for 10 minutes at 300g.
- The cell pellet was re-suspended in 50mL pre-warmed PBS and centrifuged for 10 minutes at 300g.
- Following aspiration of the supernatant, the cell pellet was re-suspended in 10mL R10 media and cells were counted.
- Cells were re-suspended in R10 media at a concentration of 3 x 10^6 cells/mL and activated with anti-CD3/anti-CD28 paramagnetic Dynabeads at a 1:3 cell:bead ratio.

2.2.6 Production of RetroNectin Plates

In order to improve T-cell transduction rates, the plates used were pre-treated with RetroNectin. RetroNectin is a fragment of the extracellular matrix protein fibronectin that binds the target T-cell through a CS-1 domain and a cell-binding domain (CBD), which interacts with the VLA-4 and VLA-5 integrin receptors respectively. Attachment of the virus to the heparin-binding domain present in RetroNectin between the CS-1 and CBD causes

co-localisation of the target cell and the virus, thus greatly improving gene transfer efficiency [271, 272].

2.2.6.1 Materials, Reagents and Equipment

- RetroNectin (TaKaRa, UK)
- Non-tissue culture treated 6-well plates (VWR, UK)
- PBS
- Pasteur pipettes

2.2.6.2 Protocol

1. 200µg of RetroNectin was re-suspended in 12mL PBS/plate
2. 2mL of the resulting solution was transferred using a Pasteur pipette into each well of a non-tissue culture treated 6-well plate, thereby giving coverage of approximately 3.5µg/cm^2
3. Plates were incubated for a minimum of 2 hours at room temperature or 24 hours at 4°C prior to use.
4. When the plate was to be used, unbound RetroNectin was transferred to a new plate using a Pasteur pipette. RetroNectin was used for a maximum of two transductions.

2.2.7 Retroviral Transduction of Human T-cells

To introduce the CAR constructs into T-cells, they were subjected to retroviral-mediated transduction. This ensured integration of the inserted coding DNA into the host T-cell genome, thereby permitting stable CAR expression.

2.2.7.1 Materials, Reagents and Equipment

- Activated T-cells
- PG13 or 293Vec RD114 cells

- RetroNectin-coated plate
- Pasteur pipettes
- Trypan blue (Gibco, UK)
- Centrifuge

2.2.7.2 Protocol

1. After the unbound RetroNectin had been transferred to a fresh plate using a Pasteur pipette, each well was coated with 3mL of retrovirus-containing supernatant from the desired packaging cell line.
2. Activated T-cells were counted using trypan-blue exclusion and 1 x 10^6 viable cells added to each well.
3. Each well was supplemented with 100U/mL of IL-2.
4. Plates were centrifuged for one hour at 50g.
5. Cells were subsequently incubated for 96 hours, after which the transduction rate was determined using flow cytometry.

2.2.8 Assessment of CAR^+ T-cell Anti-Tumour Efficacy

In order to demonstrate the ability of CAR^+ T-cells to recognise and destroy CSF-1R-expressing targets, they were co-cultured with a variety of human tumour cell lines. Target recognition was monitored by measuring cytokine release, whilst anti-tumour activity was quantitated either using an MTT (3-[4,5-dimethylthiazol-2-yl]-2,5- diphenyltetrazolium bromide; thiazolyl blue) assay (please refer to section 2.2.9.1), a luciferase assay (please refer to section 2.2.9.3) or by CFSE (carboxyfluorescein succinimidyl ester) staining of lymphoma cell lines (please refer to section 2.2.9.2).

2.2.8.1 Materials, Reagents and Equipment

- Transduced T-cells
- Tumour cells

- R10 media
- rhIL-4
- rhIL-2
- 24-well cell culture plate (Fisher Scientific, UK)

2.2.8.2 Protocol

1. Tumour cells were seeded into a 24-well cell culture plate and were either allowed to reach confluence (T47D / T47D FMS) or 1 x 10^6 cells (lymphoma cell lines) were seeded per well.
2. T-cells were counted using trypan-blue exclusion and re-suspended in R10 media at a concentration of 1 x 10^6 cells/mL and gently pipetted onto the surface of the confluent tumour monolayer.
3. After 24 and/or 48h hours of incubation, 500µL supernatant was removed for analysis of cytokine (IL-2 and interferon (IFN)-γ) secretion.
4. Depending upon the experiment, the T-cells were either:
    a. supplied with fresh R10 until the desired monolayer destruction was achieved. Alternatively, lymphoma cells were regularly monitored for target cell destruction by flow cytometry (lymphoma cell lines were CFSE labelled in advance) or luminescence assay (lymphoma cell lines were transduced to express firefly luciferase),
    b. removed, counted and re-stimulated on a fresh tumour monolayer,
    c. removed, counted and probed for enrichment of the CAR using flow cytometry.

2.2.9 Quantification of Tumour-Cell Lysis

2.2.9.1 MTT Assay

Anti-tumour activity of CAR^+ T-cells against adherent cancer cell lines (T47D / T47D FMS) was quantified using an MTT assay. MTT is a water soluble tetrazolium salt yielding a

yellowing solution when prepared in media. Mitochondrial dehydrogenases of viable cells cleave the tetrazolium ring in dissolved MTT, yielding purple formazan crystals, which are insoluble in aqueous solutions. The crystals are dissolved in acidified isopropanol. The resulting purple solution is spectrophotometrically measured at a wavelength of 570nm. Since dead cells do not cause this change, the number of viable cells determines the amount of formazan formed, indicating the degree of cytotoxicity caused [273].

2.2.9.1.1 Materials, reagents and equipment

- MTT (Sigma-Aldrich, UK)
- PBS
- DMSO (VWR, UK)
- FLUOstar Omega (BMT Labtech, UK)
- Omega Software (version 1.20) (BMT Labtech, UK)

2.2.9.1.2 Protocol

1. MTT was reconstituted in PBS at a concentration of 5mg/mL.
2. Medium was aspirated from the co-culture and wells were washed with 500µL PBS.
3. MTT stock solution was diluted 1/10 (to a concentration of 500µg/mL) in D10 media and 500µL (250µg) was added to each well.
4. Cell cultures were incubated for 2-4 hours at 37°C and 5% CO_2.
5. The supernatant was aspirated and the formed formazan crystals were dissolved in 300µL DMSO.
6. Absorbance was measured spectrophotometrically at 570nm.
7. Relative cell viability was calculated using the following equation:

Viability = absorbance of test well / average absorbance of untreated tumour monolayer

8. The data was presented either as percentage viable cells or percentage lysis. This was calculated using the following equations:

$$\text{Percentage viable cells} = \text{viability} * 100$$

$$\text{Percentage lysis} = 100 - \text{percentage viable cells}$$

2.2.9.2 CFSE Labelling of Lymphoma Cell Lines

Quantification of lymphoma cell destruction by CAR-transduced T-cells was achieved by CFSE labelling the lymphoma cell lines prior to co-culture with the effector cells. CFSE crosses intact cell membranes and was used for target cell tracking. Once inside the cells, intracellular esterases cleave the acetate groups to yield the fluorescent carboxyfluorescein molecule. The dye is then cross-linked to intracellular proteins. Target cell death was measured as disappearance of the CFSE fluorescent signal.

2.2.9.2.1 Materials, Reagents and Equipment

- CFSE (eBioscience, UK)
- PBS
- 15 mL Falcon tubes (Fisher Scientific, UK)
- RBS media

2.2.9.2.2 Protocol

1. Lymphoma cells were washed twice with PBS to remove any serum.
2. Cells were re-suspended at 5-10 x 10^6 cell/mL in PBS.
3. CFSE was added to a final concentration of 1µM and cells were incubated for 10min at room temperature.
4. Labelling was stopped by adding 10mL cold RBS and cells were incubated on ice for 5min.
5. Cells were washed 3 times with RBS.
6. CFSE-labelled cells were used for CAR + T-cell co-culture within 24h.

7. CFSE-labelled lymphoma cells were co-cultured with CAR$^+$ T-cells at 1:1 ratio in a 6-well plate.
8. Lymphoma cells were monitored daily for target cell destruction by flow cytometry.

2.2.9.3 Luciferase Assay

A more elegant alternative to the target cell CFSE labelling was achieved by stably expressing both a firefly luciferase enzyme and the red fluorescent protein tandem dimer (td)Tomato in the lymphoma cell lines. Expression of both genes was achieved using the SFG retroviral vector. Tandem dimer Tomato is a bright red fluorescent protein with emission wavelength of 581nm. It was used as a fluorescent reporter for the identification of tumour cells within a co-culture with CAR$^+$ T-cells. Firefly luciferase catalyses the conversion of a molecule of D-luciferin to an electronically 'excited' molecule of oxyluciferin when in the presence of magnesium, ATP and oxygen. The subsequent relaxation of this oxyluciferin molecule to a lower energy state results in the release of a single photon, which can be detected by a super-cooled 'charged-coupled device' (CCD) camera or a luminometer [274-276]. Since dead cells cannot catalyze this reaction, the number of viable cells determined the amount of luminescence detected, indicating the degree of cytotoxicity caused.

2.2.9.3.1 Materials, Reagents and Equipment

- D-Luciferin (Perkin Elmer, UK)
- PBS
- RBS media
- Co-cultured cells
- OptiPlate white opaque 96-well luminometer plates (Perkin Elmer, UK)
- FLUOstar Omega
- Omega Software (version 1.20)

2.2.9.3.2 Protocol

1. D-Luciferin was reconstituted in PBS at a concentration of 30mg/mL and filter sterilized through a 0.2µm filter.
2. The stock D-luciferin was diluted in pre-warmed RBS media and added to the co-culture wells at a final concentration of 0.3mg/mL.
3. Luminescence was measured on FLUOstar Omega luminescence detection system.
4. Luminescence values were compared with untreated lymphoma cells.

2.3 *In vivo* Models

All *in vivo* experimentation was done in accordance with the UK Home Office guidelines as stated in the project license (license number 70/7794) and personal license (license number I9CED56C0) that governed this work.

2.3.1 Development of an *in vivo* Lymphoma Model

In order to test the anti-tumour potential of CAR-transduced T-cells *in vivo*, it was necessary to establish a suitable xenograft model. Luciferase-expressing tumour cells were administered via various routes and monitored for growth and ease of imaging.

2.3.1.1 Materials, Reagents and Equipment

- D-Luciferin
- 1mL insulin syringes (29G x 13mm) (Terumo, UK)
- IVIS Lumina II bioluminescent imaging platform (Caliper Life sciences, UK)
- Isofluorane anaesthetic (Baxter, UK)
- 25G syringes (BD Microlance, UK)

2.3.1.2 Protocol

1. SCID/Beige mice were randomised into the required number of groups and were inoculated with the following number of tumour cells re-suspended in 200µL PBS.
    a. 5×10^6 intraperitoneally (i.p.)
    b. 10×10^6 intravenously (i.v.)
    c. 5×10^6 intravenously (i.v.)
    d. 2×10^6 intravenously (i.v.)
    e. 1×10^6 intravenously (i.v.)
    f. 0.5×10^6 intravenously (i.v.)
2. Tumour growth was monitored using bioluminescence imaging (BLI) at appropriate time-points for the duration of the study.

2.3.2 Bioluminescence Imaging

Bioluminescence imaging (BLI) is a sensitive, non-invasive technique for monitoring tumour growth *in vivo*. After delivery of the D-luciferin substrate, the luciferase-expressing tumours are visualised *in-situ* whilst the mice are under general anaesthesia.

2.3.2.1 Materials, Reagents and Equipment

- D-luciferin
- Isoflurane
- IVIS Lumina II imaging platform
- 1mL insulin syringes (29G x 13mm)

2.3.2.2 Protocol

1. Mice were injected i.p. with 3mg (200µL) D-luciferin and placed back in their cages for seven minutes.
2. Mice were anesthetised with 3-4% gaseous isoflourane and transferred to the IVIS Lumina platform

3. Nine images of increasing duration (1s, 2s, 5s, 10s, 30s, 45s, 60s, 120s, 300s) were taken using small binning. Throughout imaging mice were maintained under anaesthesia with 1.5% isoflourane and were kept warm.
4. The mice were returned to their cages once the imaging was completed and were monitored until they had regained consciousness.

2.3.3 Target Retention in *In Vivo* Lymphoma Models

Prior to testing the therapeutic efficacy of CAR-grafted T-cells, it was important to assess whether surface CSF-1R expression was maintained following the *in vivo* passage of lymphoma cells.

2.3.3.1 Materials, Reagents and Equipment

- Saline solution
- Cell strainer 40μm (Falcon, UK)
- Petri dish
- Flow cytometer BD Canto II and LSRFortessa Flow Cytometers (BD, UK)
- Ice
- Antibodies (please refer to section 2.4.2)

2.3.3.2 Protocol

1. Tumours were resected from tumour-bearing SCID/Beige mice post-mortem and transferred to a vial of saline solution.
2. Each tumour was passed through a cell strainer ensuring single cell suspension (mechanical disaggregation).
3. The resulting tumour cell suspension was subsequently probed for the presence of CSF-1R on lymphoma cells, as detailed in section 2.4.

2.3.4 Therapeutic Study

In order to test the therapeutic potential of CSF-1R re-targeted T-cells, they were administered to tumour-bearing mice and the growth of the tumour was subsequently monitored.

2.3.4.1 Materials, reagents and equipment

- D-luciferin
- Isoflurane
- IVIS Lumina II imaging platform
- 1 mL insulin syringes (29 G x 13 mm)
- 25 G syringes

2.3.4.2 Protocol

1. On Day 0, thirty female SCID/Beige mice were inoculated intravenously with 2 x 10^6 sK299 LT or alternatively with 2 x 10^6 K299 FMS LT tumour cells. The mice underwent BLI following tumour cell inoculation in order to confirm successful tumour cell delivery. These mice were subsequently used in the proceeding study.
2. Six days post-tumour inoculation, the mice were imaged to confirm tumour take. Mice were subsequently sorted into six groups depending upon the level of tumour signal. Each group displayed a similar average signal level.
3. On the same day, the groups were treated as follows;
    a. 20 x 10^6 (or alternatively 10 x 10^6) C4B$^+$ T-cells i.v. (n=5)
    b. 20 x 10^6 (or alternatively 10 x 10^6) C34B$^+$ T-cells i.v. (n=5)
    c. 20 x 10^6 (or alternatively 10 x 10^6) 43428Bζ$^+$ T-cells i.v. (n=5)
    d. 20 x 10^6 (or alternatively 10 x 10^6) 34CB T-cells i.v. (n=5)
    e. 20 x 10^6 (or alternatively 10 x 10^6) UT T-cells i.v. (n=5)
    f. PBS i.v. (n=5)
4. Mice were imaged regularly for the duration of the study.

2.3.5 Assessment of target retention by sK299 LT and K299 FMS LT tumours

As stable *in vivo* expression of CSF-1R by the tumour is central to its continued targeting, it was important to assess whether surface CSF-1R expression was maintained following *in vivo* passage.

2.3.5.1 Materials, reagents and equipment

- Saline solution
- Petri dish
- Scalpel
- Cell strainer
- Antibodies
- Flow cytometer BD Canto II and LSRFortessa Flow Cytometers (BD, UK)
- Ice

2.3.5.2 Protocol

1. Tumours were resected from SCID/Beige mice post-mortem and immediately transferred in a vial of saline solution and placed on ice.
2. Each tumour was placed on a Petri dish, cut into pieces with a scalpel and put through a cell strainer to obtain single cell suspension (mechanical disaggregation).
3. The resulting tumour cell suspension was then probed for surface level of expression of CSF-1R, as detailed in section 2.4.

2.4 Flow Cytometry

Multicolour flow cytometry was used to detect cell surface protein expression and thereby to assess CAR expression and immunophenotype of transduced T-cells in addition to target expression on tumour cells.

2.4.1 Materials, Reagents and Equipment

- Antibodies (please refer to section 2.4.2)
- FACSCanto II and LSRFortessa Flow Cytometers (BD, UK)
- Diva software (BD, UK)
- 5mL polystyrene round-bottom flow cytometry tubes (BD Falcon, UK)
- Cell Dissociation Buffer (Gibco, UK)
- Trypsin/EDTA (Gibco, UK)

2.4.2 Antibodies

Staining for human CSF-1-based CARs

Polyclonal goat anti-human CSF1 500ng/μL (Sigma-Aldrich, UK)

Anti-goat Ig FITC-conjugated 1μg/μL (DAKO, UK)

Staining for human IL-34-based CARs:

Mouse anti-human IL-34 (clone 1D12) (Abcam, UK)

Goat anti-mouse IgG PE-conjugated (Invitrogen, UK)

Staining for human 4αβ:

Mouse IgG_1 anti-human CD124 PE-conjugated (BD Pharmingen, UK)

Staining for human CSF-1R:

Rat anti-human CSF-1R (clone 3-4A4) (Santa-Cruz, UK)

Goat anti-rat IgG PE-conjugated (Invitrogen, UK)

Staining for human memory T-cell phenotype:

Mouse anti-human CD8 PE-Cy7-conjugated (BioLegend, UK)

Mouse anti-human CD45RO PerCP-Cy5.5-conjugated (BioLegend, UK)

Mouse anti-human CCR7 APC-conjugated (BioLegend, UK)

Mouse anti-human CD28 FITC-conjugated (BioLegend, UK)

Mouse anti-human CD27 APC-Cy7-conjugated (BioLegend, UK)

DAPI (4',6-diamidino-2-phenylindole) viability stain

Staining for human T-cell anergy:

Mouse anti-human CD8 PE-Cy7-conjugated (BioLegend, UK)

Mouse anti-human PD1 APC-Cy7-conjugated (BioLegend, UK)

Mouse anti-human TIM3 PerCP-conjugated (BioLegend, UK)

Mouse anti-human LAG3 APC-conjugated (R&D, UK)

Mouse anti-human 2B4 FITC-conjugated (BioLegend, UK)

DAPI viability stain (Life Technology, UK)

Staining for mouse macrophages:

Rat anti-mouse CD16/CD32 (Fc receptor block) (BioLegend, UK)

Rat anti-mouse CD11b PE-Cy7-conjugated (BioLegend, UK)

Rat anti-mouse F4/80 PerCP-conjugated (BioLegend, UK)

DAPI viability stain (Life Technology, UK)

Staining for mouse myeloid derived suppressor cells:

Rat anti-mouse CD16/CD32 (Fc receptor block) (BioLegend, UK)

Rat anti-mouse CD11b PE-Cy7-conjugated (BioLegend, UK)

Rat anti-mouse GR1 APC-conjugated (BioLegend, UK)

DAPI viability stain (Life Technology, UK)

2.4.3 Protocol

1. A pre-determined number of cells (1×10^5 – 1×10^6) were placed in a flow-cytometry tube and incubated with previously titrated primary antibody for 30 minutes on ice.

2. Samples were washed using 2mL cold PBS, and centrifuged at 300g for 5 minutes until pelleted.
3. Each sample was incubated with 3-7µg (fluorophore-conjugated) secondary antibody for 30 minutes on ice in the dark.
4. Samples were again washed with cold PBS, centrifuged and subsequently re-suspended in 300µL PBS immediately prior to analysis. Samples were kept in the dark and on ice until analysed by flow cytometry.

NOTE: When directly conjugated antibodies were used for staining, cells were re-suspended in 300µL PBS after completion of 1. and 2. above and then analysed by flow cytometry.

2.5 Detection of Cytokine Release

2.5.1 Enzyme-Linked Immunosorbent Assay (ELISA)

The enzyme linked immunosorbent assay (ELISA) was used for the detection and quantification of cytokine release in the co-culture supernatants, which occurred as a result of target engagement by the CAR and subsequent CAR^+ T-cell activation. Plates were pre-coated with a 'capture' antibody specific for the cytokine of interest (IL-2 or IFN-γ). Once bound to the capture antibody the cytokine was detected using a second, biotin-labelled, antibody and subsequently with avidin-labelled horseradish peroxidase (HRP). Visualisation was achieved using a 3,5,3',5'-tetramethylbenzadine (TMB)/hydrogen peroxide solution. Oxidation of the colourless TMB reagent to a blue solution (an equilibrium between the TMB cation radical and the diamine-diimine charge transfer complex [277]) highlighted assay progression. After 15 min the reaction was stopped using 2M sulphuric acid. The reduction in pH induced formation of the yellow diimine product and prevented further development by denaturation of the HRP. Plates were subsequently read at 450nm and the concentrations of each sample calculated with respect to the known concentrations of the standard curve.

2.5.1.1 Materials, Reagents and Equipment

- High-binding flat-bottom 96-well ELISA plates (Iwaki, UK)
- IFN-γ Ready-Set-Go ELISA Kit (eBioscience, UK)
- IL-2 Ready-Set-Go ELISA kit (eBioscience, UK)
- IL-34 Duoset ELISA Kit (R&D Systems, UK)
- M-CSF Duoset ELISA Kit (R&D Systems, UK)
- Colour Reagent A (Stabilised Peroxide Solution) (R&D Systems, UK)
- Colour Reagent B (Stabilised TMB Reagent) (R&D Systems, UK)
- Wash Buffer (please see below)
- Sulphuric Acid (H_2SO_4) (BDH, UK)
- Fluostar Omega plate reader
- Omega Software (version 1.20)
- MARS data analysis software (version 1.20 R2)

Buffer and solutions:

Wash buffer = PBS + 0.05% Tween-20

2.5.1.2 Protocol

1. A 96-well ELISA plate was coated with 100µl/well of capture antibody diluted 1/250 in coating buffer. The plate was sealed and incubated at 4^{o}C overnight.
2. The plate was washed 5 times with 300µl/well wash buffer and blocked with 200µl/well of 1x assay diluent for 1 hour at room temperature.
3. The plate was washed as described above.
4. Standard curve samples were serially diluted in a two-fold manner in assay diluent. A seven point standard curve ranging from 500pg/mL to 3.9pg/mL was plated in triplicate. Background absorbance was measured by plating assay diluent alone.

Supernatant samples from co-cultivation were diluted between 1:20 to 1:200 in assay diluent prior to plating in triplicate. The plate was sealed and incubated overnight at 4^{o}C.

5. The plate was washed as described above.
6. Detection antibody was diluted 1/250 and 100µl/well were added.
7. The plate was incubated for 1 hour at room temperature.
8. Wash step executed as in step 3.
9. Avidin-HRP was diluted 1/250 and 100µl/well were added.
10. The plate was incubated for 30 min at room temperature.
11. Wash step executed as in step 3.
12. 100µl/well of TMB substrate solution was added to each well and the plate was incubated for 15 min.
13. The reaction was stopped by adding 50µl/well of stop solution (2M H_2SO_4)
14. Absorbance was read at 450nm using the Fluostar Omega plate reader.
15. Standard curves and cytokine concentrations were calculated using the MARS data analysis software.

2.6 Immunoblot analysis

Analysis of protein expression using western blot has been used to confirm expression of the various CAR constructs in T-cells and of the CSF-1R receptor in the lymphoma cell lines.

2.6.1 Materials, Reagents and Equipment

- RIPA lysis buffer (please see below)
- cOmplete, mini, EDTA-free Protease inhibitor cocktail tablets (Roche, UK)
- Whole Cell Lysates
- NuPAGE Novex 4-12% Bis-Tris Protein Gels (Life Technologies, UK)
- NuPAGE MOPS SDS Running Buffer (20X) (Life Technologies, UK)

- Transfer buffer (please see below)
- Loading buffer (please see below)
- TBST buffer (please see below)
- Glycine (MP Biomedicals, UK)
- Tris Base (Fisher Scientific, UK)
- Nitrocellulose membrane (PALL Life Sciences, UK)
- Antibodies (please see section 2.6.2)
- Enhanced Chemiluminescence (ECL) Kit (GE Healthcare, UK)
- Distilled water
- Full range rainbow recombinant protein markers (GE Healthcare, UK)
- High performance Chemiluminescent Hyperfilm (GE Healthcare, UK)
- Optimax X-ray developer (Jet, UK)
- Methanol (Fisher Scientific, UK)
- Ponceau S Solution (Sigma, UK)
- Skimmed milk powder (Oxoid, UK)
- Electrophoresis tank (Invitrogen, UK)
- Whatman 3MM Chr paper (SLS, UK)
- Techne Dri-blok DB-2A heated block (Techne, UK)
- Saran wrap (Dow, UK)

Buffers and Solutions

RIPA lysis buffer = 50mM Tris.HCl pH 7.5, 150mM NaCl, 1% NP-40, 1% sodium deoxycholate, 0.1% SDS, 1x Protease inhibitor cocktail tablet.

Loading Buffer = 50 mM Tris.HCl, 100 mM DTT, 2% (w/v) SDS, 0.1% (w/v) bromophenol blue, 10% (v/v) glycerol.

TBST = 50mM Tris, 150mM NaCl, 0.05% Tween-20

Transfer Buffer = 39 mM Glycine, 48 mM Tris base, 0.037% (w/v) SDS, 20% (v/v) methanol.

Blocking Buffer = TBS, 5% (w/v) skimmed milk powder

NOTE: Roche do not release the details of the protease inhibitors contained within the cOmplete, mini, EDTA-free protease inhibitor cocktail tablets.

The SDS in SDS-PAGE electrophoresis is responsible for both denaturing the proteins in the sample as well as for providing them with a net negative charge. Therefore protein separation is determined by differences in size, which is influenced by the percentage of polyacrylamide present within the resolving gel [278]. The proteins were separated on pre-cast reducing 4-12% NuPAGE gradient gels using MOPS running buffer, which allowed for a separation range of 15 to 260 kDa.

2.6.2 Antibodies

Probing for human CSF-1R

Rabbit anti-human CSF-1R polyclonal antibody*

Goat anti-rabbit HRP-conjugated antibody (Dako, UK)

*Generous gift from Dr Nicholas Dibb, Hammersmith Hospital Campus, Imperial College London

Probing for human PTPζ

Rabbit anti-human PTPζ (Santa Cruz, UK)

Goat anti-rabbit HRP-conjugated antibody (Dako, UK)

Probing for human KU-70 (loading control)

Goat anti-human KU-70 antibody (Santa Cruz, UK)

Rabbit anti-goat HRP-conjugated antibody (Dako, UK)

Probing for CAR constructs

Mouse anti-human CD247 (CD3ζ) (BD, UK)

Goat anti-mouse HRP-conjugated antibody (Dako, UK)

2.6.3 Protocol

1. Whole cell lysates were produced by syringe homogenization of the cells in RIPA lysis buffer.
2. Cell lysates were thawed and centrifuged at 16,200 g to pellet the insoluble material.
3. A sufficient volume of supernatant was removed and mixed 3:1 with the protein-loading buffer before being boiled at 90 °C for 10 minutes.
4. Lysates were centrifuged at 16,200 g before being loaded into the wells of the pre-casted gel.
5. The gel was run at 20V/cm for 120 minutes.
6. Proteins were transferred from the polyacrylamide gel to a nitrocellulose membrane using the Mini Trans-Blot system (Bio-Rad) at 30V/90mA overnight at 4^{o}C.
7. The membrane was blocked for 1 hour at room temperature in blocking buffer to prevent non-specific binding.
8. The primary antibody was diluted to the recommended concentration in blocking buffer and incubated with the membrane for 1 hour at room temperature.
9. The membrane was washed three times for 10 min each in TBST.
10. An HRP-conjugated secondary antibody was diluted to the recommended concentration in blocking buffer and incubated with the membrane for 1 hour at room temperature.
11. Following an additional three washes in TBST, the membrane was covered with a pre-mixed ECL solution.
12. After 1 min incubation, excess ECL solution was drained and the membrane covered in Saran wrap.

13. The membrane was fixed inside a film cassette and a chemiluminescent hyperfilm placed on top (in the dark).
14. After a sufficient exposure time had been observed, the film was removed and developed using a Jet Optimax X-ray developer. Membranes were often exposed for differing durations in order to optimise the signal gained.

Densitometry analysis of western blots was performed using ImageJ 4.1 software (National Institute of Health, USA).

2.7 Statistical Analysis

To investigate for statistical significance, unless stated otherwise, values were subjected to a two-way ANOVA, followed by a Bonferroni post-hoc test and p-values < 0.05 were taken as significant. Data was analysed using Graphpad Prism software (version 5).

Chapter 3 Investigation into CSF-1R expression in cHL and ALCL

3.1 Introduction

Cancer cells employ a variety of mechanisms to evade apoptosis and senescence. Pre-eminent among these is the aberrant co-expression of growth factors and their ligands, forming an autocrine growth loop that promotes tumour formation and progression. One growth loop whose transforming potential has been repeatedly demonstrated is the CSF-1/CSF-1R axis [279].

3.1.1 The CSF-1/CSF-1R axis in cancer

Expression of CSF-1 and/or CSF-1R has been documented in several human malignancies including breast, cervical, endometrial, ovarian, lung, prostate and kidney cancer, as well as in classical Hodgkin's lymphoma (cHL) and anaplastic large cell lymphoma (ALCL) [34, 280-283]. Indeed, elevated serum levels of CSF-1 have been demonstrated in patients with breast [284, 285], ovarian [286, 287], colorectal [288, 289] and pancreatic cancer [290] and Hodgkin's lymphoma [291-293]. The oncogenic potential of the CSF-1/CSF-1R axis generally results from the co-expression of the growth factor and its receptor rather than mutations that render the receptor constitutively active [294]. In this respect, CSF-1R can be activated either in an autocrine manner (e.g. co-expressed with CSF-1 by the tumour cells) or in a paracrine manner – for example where CSF-1 is secreted by cancer-associated fibroblasts. The transforming potential of the CSF-1/CSF-1R axis has been confirmed by expressing *c-fms* in CSF-1-producing fibroblasts and epithelial cells, resulting in tumour formation in Balb/c mice [279]. The role of the CSF-1R/CSF-1 axis has been most extensively studied in breast and ovarian cancer, with a few recent reports of its involvement in the pathogenesis of cHL and ALCL.

3.1.1.1 Breast cancer

Among epithelial cancers, the role of CSF-1/CSF-1R has been most extensively studied in breast cancer. Normally, breast tissue does not express CSF-1R and only low levels of CSF-1 are detected [294, 295]. By contrast, serum CSF-1 levels are elevated in patients with metastatic breast cancer [295] and may be 10 fold higher than normal in advanced disease [294]. Furthermore, 58% of all human breast tumours express CSF-1R [296] and at least 85% of invasive breast carcinomas express *c-fms* [281, 295] while 36% co-express both the receptor and CSF-1 [297].

In the context of breast cancer risk, a large cohort breast cancer tissue array revealed a strong association between *c-fms* expression and both lymph node metastasis and poor survival of breast cancer patients [298]. In support of this, an independent study has linked *c-fms* over-expression in breast cancer to invasive and metastatic properties [299]. In an elegant study using mice in which the polyoma middle T antigen is expressed under the mouse mammary tumour virus promoter, Lin *et al.* revealed a causal relationship between the CSF-1/CSF-1R axis and metastatic dissemination [299]. When these mice were crossed onto the op/op background, the resultant absence of CSF-1 did not affect the growth of primary mammary tumours, but retarded both tumour cell invasion and formation of lung metastases. Restoration of CSF-1 expression in the mammary epithelium alone restored tumour progression and metastasis. Similarly, disease progression was accelerated when CSF-1 was over-expressed in wild type mice [299].

Consistent with its role in tumour progression and metastasis, the expression of CSF-1R and its ligand CSF-1 in neoplastic epithelial cells has been strongly correlated with poor prognosis and is predictive for ipsilateral recurrence in breast cancer patients [298, 300]. In addition, CSF-1 has been reported to stimulate angiogenesis through recruitment of macrophages, which in turn secrete pro-angiogenic factors (eg VEGF), growth factors (eg epidermal growth factor) and matrix metalloproteases (MMPs) important for invasion and motility of tumour cells [301]. In *CSF1* nullizygous mice, angiogenesis is markedly blunted

whereas forced CSF-1 over-expression causes increased tumour vessel density and oncogenicity [302, 303].

Apart from promoting angiogenesis, CSF-1-educated tumour-associated macrophages (TAM) have a central role in supporting tumour cell survival, proliferation, motility and drug resistance as well as suppressing anti-tumour immunity [304]. The production and recruitment of TAMs is regulated by the CSF-1/CSF-1R axis. Interruption of the axis through CSF-1 antisense oligonucleotides [301], CSF-1R and CSF-1 small interfering RNA (siRNA) [301] or anti-CSF-1 antibody [305] resulted in up to 50% suppression of growth of human MCF-7 mammary carcinoma cell xenografts in mice. This was accompanied by inhibition of host-derived macrophage recruitment to those tumours and hence inhibition of MMPs and VEGF production [301]. Furthermore, anti-CSF-1 treatment reversed the chemo-resistance of MCF-7 xenografts, suggesting a role for CSF-1 in drug-resistance [305]. In keeping with these data, down-regulation of CSF-1 targeting miRNA (MiR-130a) was reported in several chemo-resistant ovarian cancer cell lines [306].

Collectively, these data supports the paradigm that the CSF-1/CSF-1R axis plays a crucial role in regulation of tumourigenesis and angiogenesis via its effect on tumour-surrounding stroma, contributing to both permissive and instructive signals to tumour growth and progression.

3.1.1.2 Ovarian cancer

Broadly similar findings have been observed in studies of the role of CSF-1/CSF-1R axis in ovarian cancer progression, as described above for breast cancer. Expression of CSF-1 has been detected in 75% of primary ovarian tumours and 69% of metastases while 92% of primary tumours and 83% of metastases express CSF-1R [307]. Co-expression of this ligand/ receptor pair by metastatic deposits is an independent poor prognostic factor, shortening the mean time to recurrence by 11 months (from 24.1 +/- 3.9 to 13.5 +/- 4 months) [307]. Furthermore, elevated CSF-1 levels in serum and ascitic fluid has been

associated with poor outcome in this disease [308, 309]. Indeed, measurement of serum CSF-1 is one of a number of candidate biomarkers that has been proposed to aid the early detection of ovarian cancer [310].

The pro-tumourigenic effects of the CSF-1/CSF-1R axis in ovarian cancer was demonstrated by over-expression of CSF-1 in c-*fms*$^{+}$ ovarian cancer cells. As a result, cells became more invasive, motile, adhesive and tumourigenic *in vivo* [311]. These phenotypic changes were all reversed upon disruption of the autocrine loop using antisense oligomer therapy directed against c-*fms* and CSF-1 mRNA knock down [311].

The mechanisms by which CSF1/ CSF-1R promotes ovarian cancer progression remain under investigation. One relevant candidate is urokinase plasminogen activator (uPA) [312]. This serine protease is a CSF-1-inducible mediator of tissue re-modelling and is known to play a significant role in ovarian tumour invasion and metastasis. Both uPA and the related plasminogen activator inhibitor-1 (PAI-1) have been shown to be elevated in malignant ovarian tumours, compared to benign counterparts or normal ovarian epithelium [313, 314]. Furthermore, antisense inhibition of uPA reduces the metastatic peritoneal spread of human ovarian cancer in nude mice [315].

In contrast to malignant ovarian tumours, co-expression of CSF-1/ CSF-1R is not found in non-invasive tumours [316]. Furthermore, minimal to non-existent expression of CSF-1 or CSF-1R has been detected in normal ovarian epithelium [316]. These considerations raise the possibility that targeting of the CSF-1/CSF-1R axis may achieve therapeutic benefit in this disease.

3.1.1.3 Classical Hodgkin's lymphoma and anaplastic large cell lymphoma

Aberrant CSF-1R expression has also been reported in both Hodgkin and Reed-Sternberg (HRS) cell lines and primary HRS and ALCL cells. This represents an example of lineage-inappropriate expression of downstream genes that promote survival of a lymphoid

neoplasm [34]. The mechanism underlying deregulated expression in cHL and ALCL is remarkable because expression of CSF-1R transcripts, unlike in epithelial cancers, is driven by an endogenous long terminal repeat (LTR) sequence upstream of the CSF-1R gene [34]. Specifically, Lamprecht *et al*. have demonstrated that the promoter of the *THE1B* LTR is aberrantly activated, both due to demethylation of the region and also DNA methylation-induced silencing of the gene that encodes the *THE1B* LTR transcriptional repressor CBFA2T3 [34]. Aberrantly expressed CSF-1R is generally constitutively activated, most likely due to an autocrine and paracrine CSF-1 loops. Furthermore, CSF-1R signalling was demonstrated to be necessary for HRS cell growth and survival [34].

In the same study, it was shown that that CSF-1R expression is restricted to cHL and anaplastic large cell lymphoma (ALCL) since the promoter of the *THE1B* LTR is not activated in most non-Hodgkin's lymphomas. In light of these findings, quantification of CSF-1R transcripts may aid in both diagnosis and detection of minimal residual disease in treated cHL or ALCL patients [34].

In terms of prognostic value, CSF-1R expression in HRS cells is significantly correlated with treatment failure. In multivariate analysis of 132 cHL patients, Steidl *et al*. have demonstrated that a combined score of CSF-1R expression and high number of $CD68^+$ infiltrating macrophages is an independent predictor of short progression-free survival. [317]

Expression of CSF-1 is also linked to cHL progression, both as an autocrine HRS cell growth factor and as a stimulus to monocyte/ macrophage growth and survival [35, 317]. Only few studies have examined circulating CSF-1 levels in cHL patients, but collected data suggest that patients present with significantly higher levels than healthy persons. Furthermore, among cHL patients, those with bulky mediastinal mass and systemic symptoms showed most profoundly increased CSF-1 levels [292, 318].

Collectively these data suggest that in cHL and ALCL, the CSF-1/CSF-1R axis is linked to lineage infidelity, cellular reprogramming and treatment resistance, raising the possibility that CSF-1R expression and signalling may constitute new therapeutic targets for these lymphomas. Consequently, further investigations are required in order to determine whether targeting of the CSF-1/CSF-1R axis may achieve therapeutic benefit in these diseases.

3.2 Results

3.2.1 CSF-1R expression by a panel of cHL and ALCL cell lines

In order to determine the suitability of CSF-1R as a therapeutic target in cHL and ALCL, its expression profile on a panel of six human lymphoma cell lines was investigated (Figure 3.1). Western blotting analysis demonstrated the expected two bands at approximately 165kDa and 140kDa in all six cases, albeit at variable intensity. These band sizes correlate well with those reported for the two major glycosylated variants of human CSF-1R (Figure 3.1, A) [319]. The lower band seen in all lanes in this blot (top panel) is believed to represent an undefined protein that is cross-reactive with this polyclonal antiserum. A loading control is shown in the bottom panel. To confirm these results, flow cytometry was undertaken after incubation of these cells with a CSF-1R-specific monoclonal antibody. This analysis confirmed that CSF-1R was detectable on the cell surface of these tumour cells, at varying levels of expression (Figure 3.1, B). The human breast cancer cell line T47D has been previously reported to lack CSF-1R expression and was therefore used as a negative control for these analyses [320]. In order to create a positive control, the parental T47D cell line was genetically engineered to express high levels of CSF-1R (T47D FMS), as confirmed by both western blotting and flow cytometry (Figure 3.1, A and C).

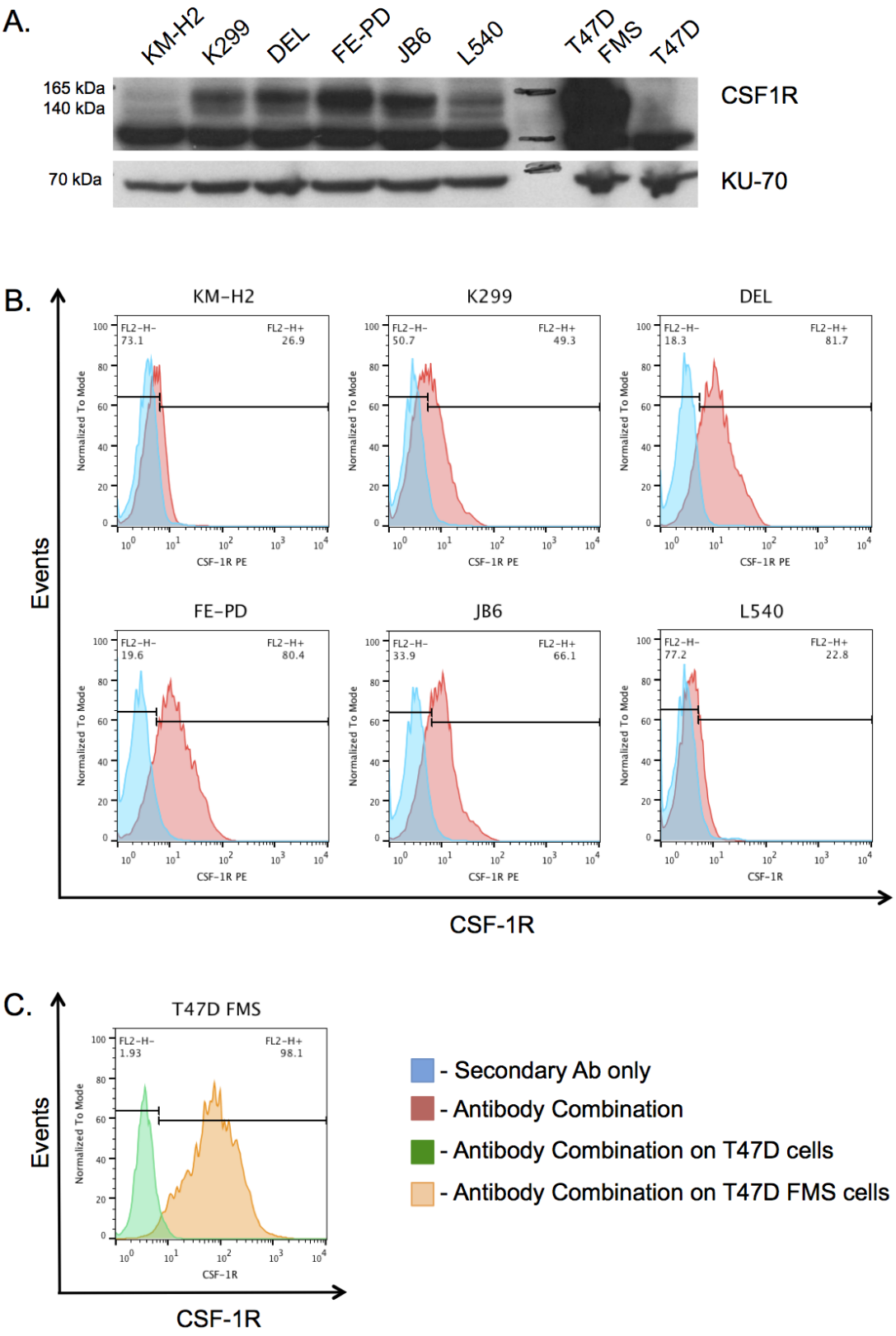

Figure 3.1 CSF-1R expression by a panel of cHL and ALCL cell lines.

(A) Each lymphoma cell line as well as T47D and T47D FMS (5 x 10^6 cells) were lysed in reducing lysis buffer. The lysates were separated using SDS-PAGE and protein was transferred onto a nitrocellulose membrane. The presence of CSF-1R was (legend continues on next page)

3.2.2 Ligand expression by the panel of lymphoma cell lines

Given the transforming potential of CSF-1R upon its co-expression with CSF-1 (see section 3.1.1), I next investigated the expression of both CSF-1R ligands (CSF-1 and IL-34) in the panel of cHL and ALCL cell lines (Figure 3.2). In accordance with published data, the cHL cell lines KM-H2 and L540 both produced low levels of CSF-1 [34]. Notably however, IL-34 production was detected by 5 of the 6 lymphoma cell lines tested. Furthermore, cell culture supernatants were collected for ELISA in the absence of anti-CSF-1R blocking antibody, raising the possibility that the detected cytokine levels are a proportion of the amount produced due to continuous internalization of the ligand-receptor complex.

---

detected using a polyclonal primary antibody, followed by an HRP-conjugated anti-rabbit IgG antibody and subsequent development using enhanced chemiluminescence (top panel). The lysates were also probed for the presence of the nuclear membrane protein, KU-70, as a loading control (bottom panel). **(B)** The panel of lymphoma cell lines was probed for the cell surface expression of CSF-1R using a monoclonal rat anti-human CSF-1R antibody followed by a goat anti-rat PE conjugated secondary antibody (red histograms). Cells were also stained using the secondary antibody only (blue histograms) to show the specificity of staining. **(C)** The parental T47D breast cancer cell line (green histogram) and T47D FMS, a derivative that has been genetically engineered to express high levels of CSF-1R (orange histogram) were both stained with the same antibody combination. Results are representative of 2 (**A**) and 7 (**B and C**) independent replicates.

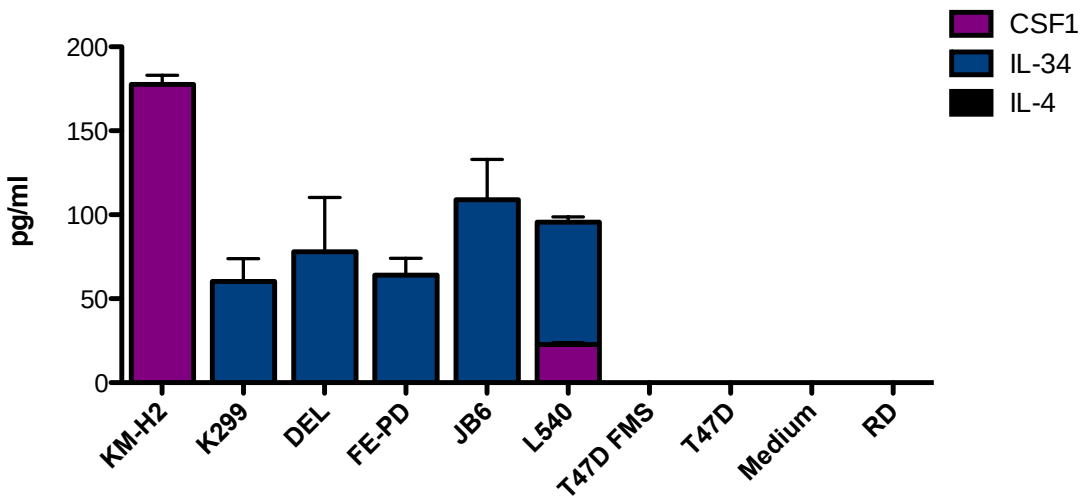

Figure 3.2 CSF-1 and IL-34 expression by the panel of lymphoma cell lines.

For collection of cell culture supernatants for ELISA, cells were plated at 0.8 x 10^6 cells/ml, and supernatants were collected after 48 hours. As controls, standard medium and the reagent diluent for the standards (RD) were included. Data are presented as mean ± standard deviation from three independent experiments.

3.2.3 PTPζ expression by the panel of lymphoma cell lines

Since it was established that 5/6 lymphoma cell lines secrete IL-34, it was of crucial importance to determine whether they also express the alternative IL-34 receptor, PTPζ [131]. The PTPζ receptor is primarily expressed on neural progenitors and glial cells. [132] Unsurprisingly, IL-34 is highly expressed in the brain and has an important role in microglial development [133].

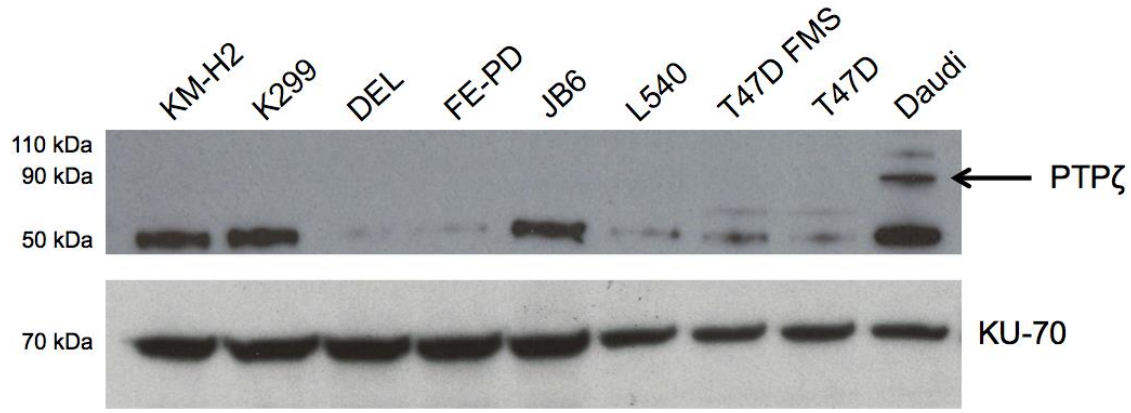

Figure 3.3 PTPζ expression by a panel of cHL and ALCL cell lines.

Each lymphoma cell line as well as T47D and T47D FMS (5 x 10^6 cells) was lysed in reducing lysis buffer. The Daudi cell line was used as a positive control as recommended by the anti-PTPζ antibody supplier**.** The lysates were separated using SDS-PAGE and the protein subsequently transferred onto a nitrocellulose membrane. The presence of PTPζ was detected using a polyclonal primary antibody, followed by an HRP-conjugated anti-rabbit IgG antibody and subsequent development using enhanced chemiluminescence (top panel). The lysates were also probed for the presence of the nuclear membrane protein, KU-70, as a loading control (bottom panel).

In order to investigate PTPζ expression, each lymphoma cell line (5 x 10^6 cells) was lysed under reducing conditions and probed for the receptor by western blotting (Figure 3.3). Importantly, the Daudi cell line was used as a positive control as recommended by the antibody supplier. As expected, a band at approximately 90 kDa was detected in the Daudi lane, which correlated well with the reported size of PTPζ (Figure 3.3). However, none of the lymphoma cell lines showed evidence of expressing this receptor. Absence of PTPζ expression, even though confirmed by western blotting, could not be further verified using flow cytometry because no suitable antibody was available for this purpose.

3.2.4 Investigation of the ability of corticosteroids to up-regulate CSF-1R expression by lymphoma cells

Recently, it has been demonstrated that dexamethasone induces substantial up-regulation of CSF-1R expression at mRNA and protein levels in a number of breast cancer cell lines [321-323]. This effect has been attributed to the presence of functional glucocorticoid response elements in both c-*fms* promoters, which mediate this effect via binding to the glucocorticoid receptor [323]. In order to investigate whether dexamethasone treatment can similarly induce up-regulation of CSF-1R expression in cHL and ALCL cells, the previously described panel of lymphoma cell lines was treated with 1μM dexamethasone. Cells were lysed every 12 hours under reducing conditions and western blots were probed for the expression of CSF-1R (Figure 3.4). As indicated by the bar graphs, dexamethasone treatment did not induce a significant upregulation of CSF-1R expression in these cells with the exception of the FE-PD cell line at 48h (Figure 3.4, D). These results were verified using flow cytometry analysis of cell surface CSF-1R expression (Figure 3.5).

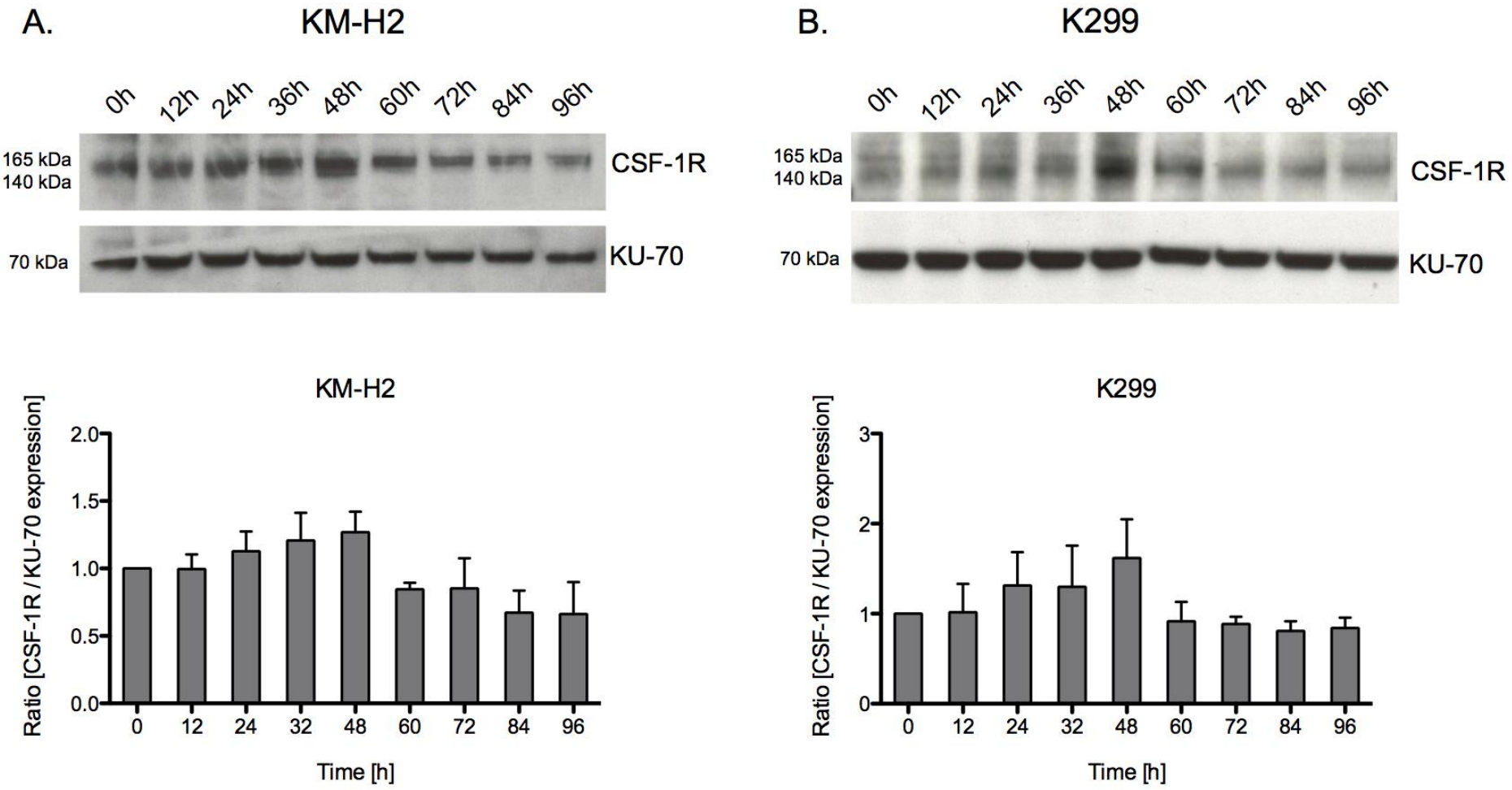

Figure 3.4 Time course of CSF-1R expression level post dexamethasone treatment. (figure and legend continue on page 141)

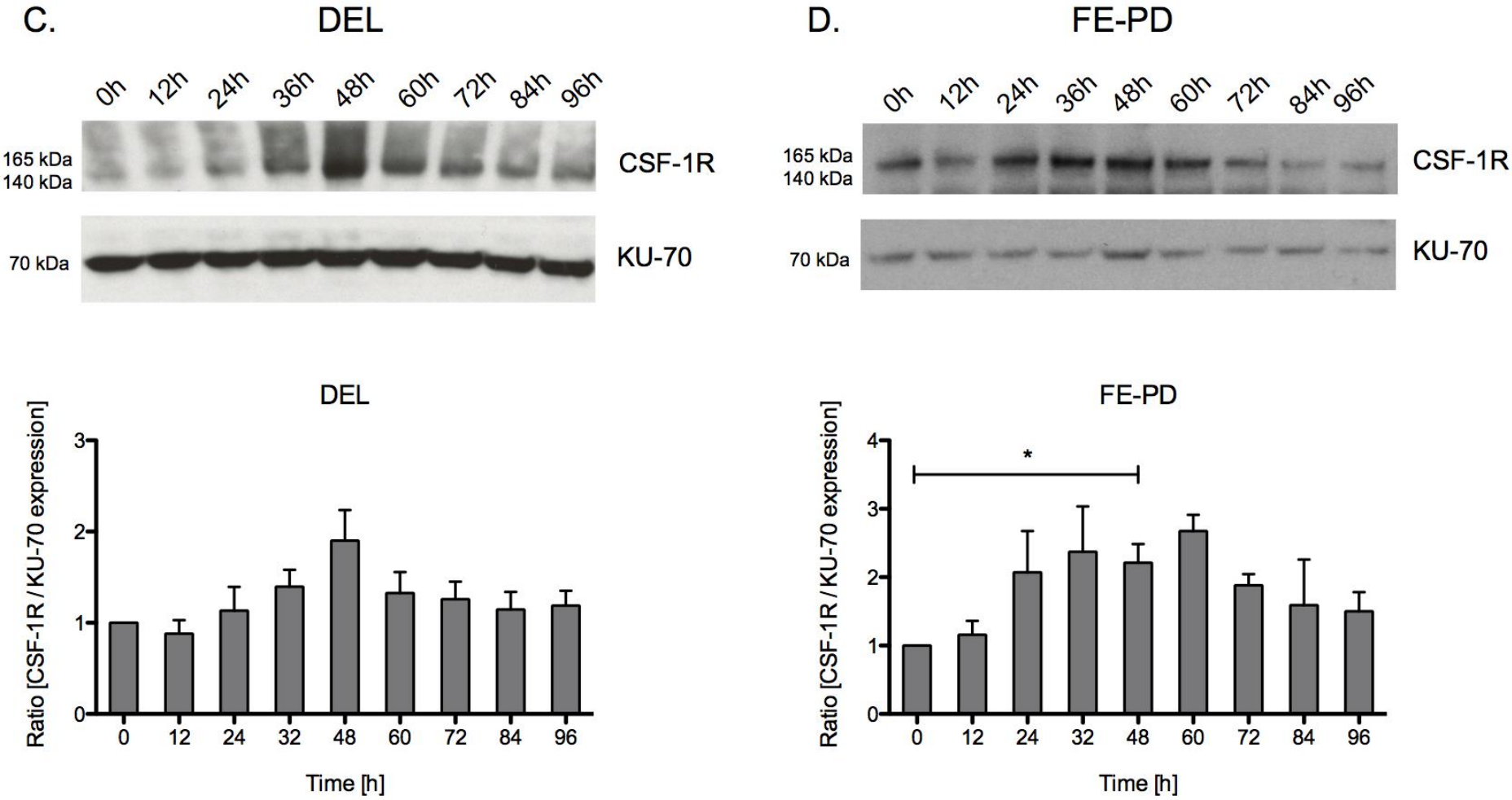
C.
DEL
0h
12h
24h
36h
48h
60h
72h
84h
96h
165 kDa
140 kDa
CSF-1R
70 kDa
KU-70
D.
FE-PD
0h
12h
24h
36h
48h
60h
72h
84h
96h
165 kDa
140 kDa
CSF-1R
70 kDa
KU-70
DEL
Ratio [CSF-1R / KU-70 expression]
0
1
2
3
0
12
24
32
48
60
72
84
96
Time [h]
FE-PD
*
Ratio [CSF-1R / KU-70 expression]
0
1
2
3
4
0
12
24
32
48
60
72
84
96
Time [h]

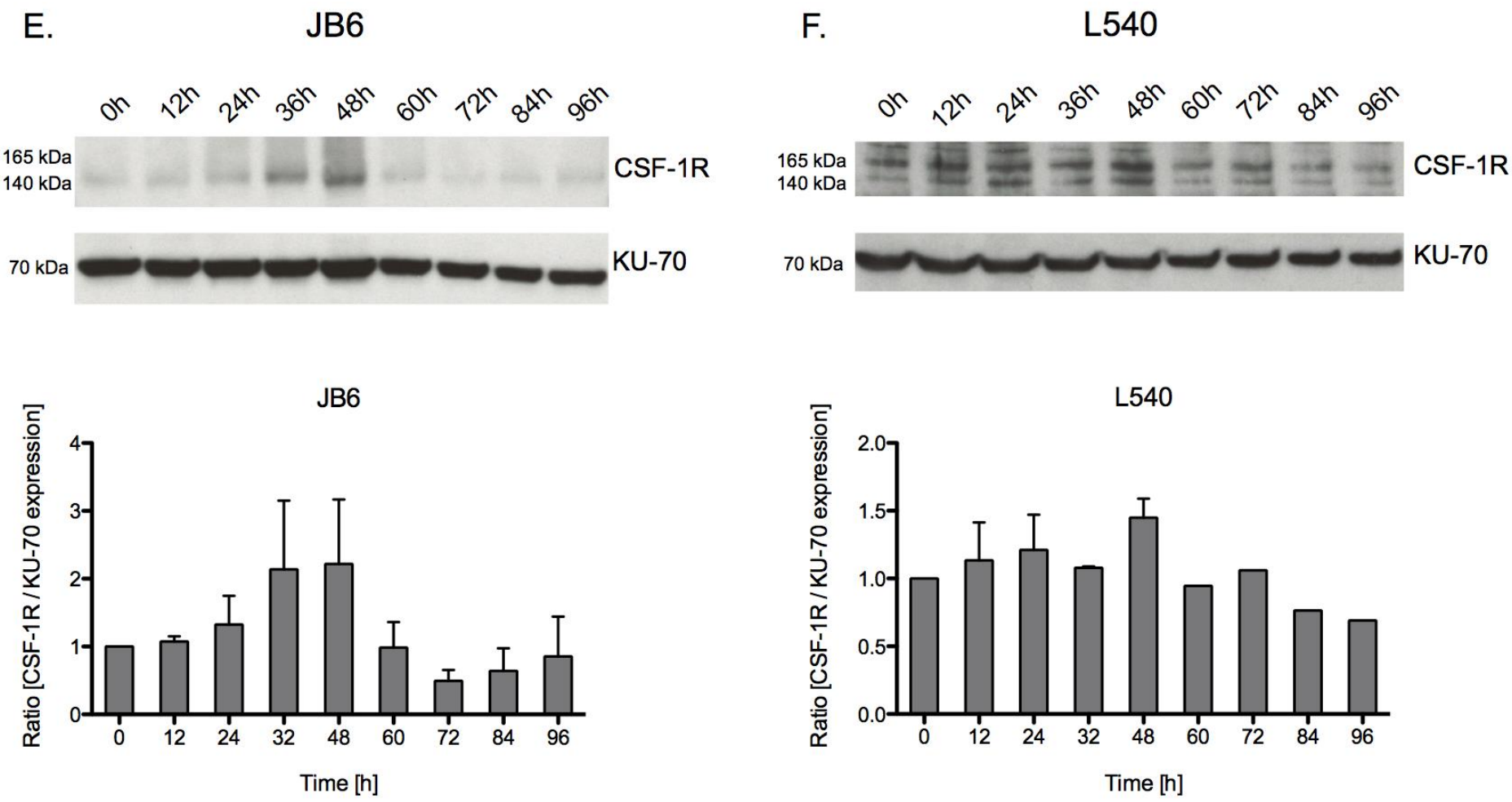
E.
JB6
0h
12h
24h
36h
48h
60h
72h
84h
96h
165 kDa
140 kDa
CSF-1R
70 kDa
KU-70
F.
L540
JB6
Ratio [CSF-1R / KU-70 expression]
Time [h]
L540

3.2.5 Investigation of the ability of corticosteroids to up-regulate CSF-1R expression by human monocyte-derived macrophages

Colony stimulating factor-1 receptor is naturally expressed on macrophages and a small subset of monocytes ($CD14^+CD16^+$). In order to characterize the effect of systemic administration of dexamethasone on CSF-1R expression level on macrophages, an *in vitro* assay was carried out. Human monocytes were isolated from PBMC using $CD14^+$ magnetic selection and differentiated to either M1 (in the presence of 20 ng/ml recombinant human GM-CSF [324]) or M2 macrophages (in the presence of 50 ng/ml recombinant human CSF-1 [324]) [325]. After 7-day culture in the described above conditions, macrophages were immunophenotyped to confirm M1 or M2 polarisation (Appendix, Figure S1) and were then exposed to 1μM dexamethasone or alternatively left in medium for further 48h. Macrophages were then lysed in reducing conditions and probed for CSF-1R expression. As indicated in Figure 3.6, dexamethasone treatment induced up-regulation of CSF-1R protein level in both M1 and M2 macrophages after 48 hours.

Indicated lymphoma cells were exposed to 1μM dexamethasone and 5 x 10^6 cells were lysed in reducing lysis buffer every 12 hours for 4 days. Lysates were separated using SDS-PAGE and the protein subsequently transferred onto a nitrocellulose membrane. The presence of CSF-1R was detected using a polyclonal primary antibody, followed by an HRP-conjugated anti-rabbit IgG antibody and subsequent development using enhanced chemiluminescence (top panel). The lysates were also probed for the presence of the nuclear membrane protein, KU-70, as a loading control (bottom panel). A representative western blot is shown for each cell line. Bar graphs were obtained by densitometry analysis (ImageJ) performed on three independent replicate experiments. Data were expressed as a ratio between CSF-1R and KU-70 expression (normalized to 0h time point), and shown as mean ± SD. Data were analysed by Student's *t*-test. * = $p<0.05$ relative to 0h time point.

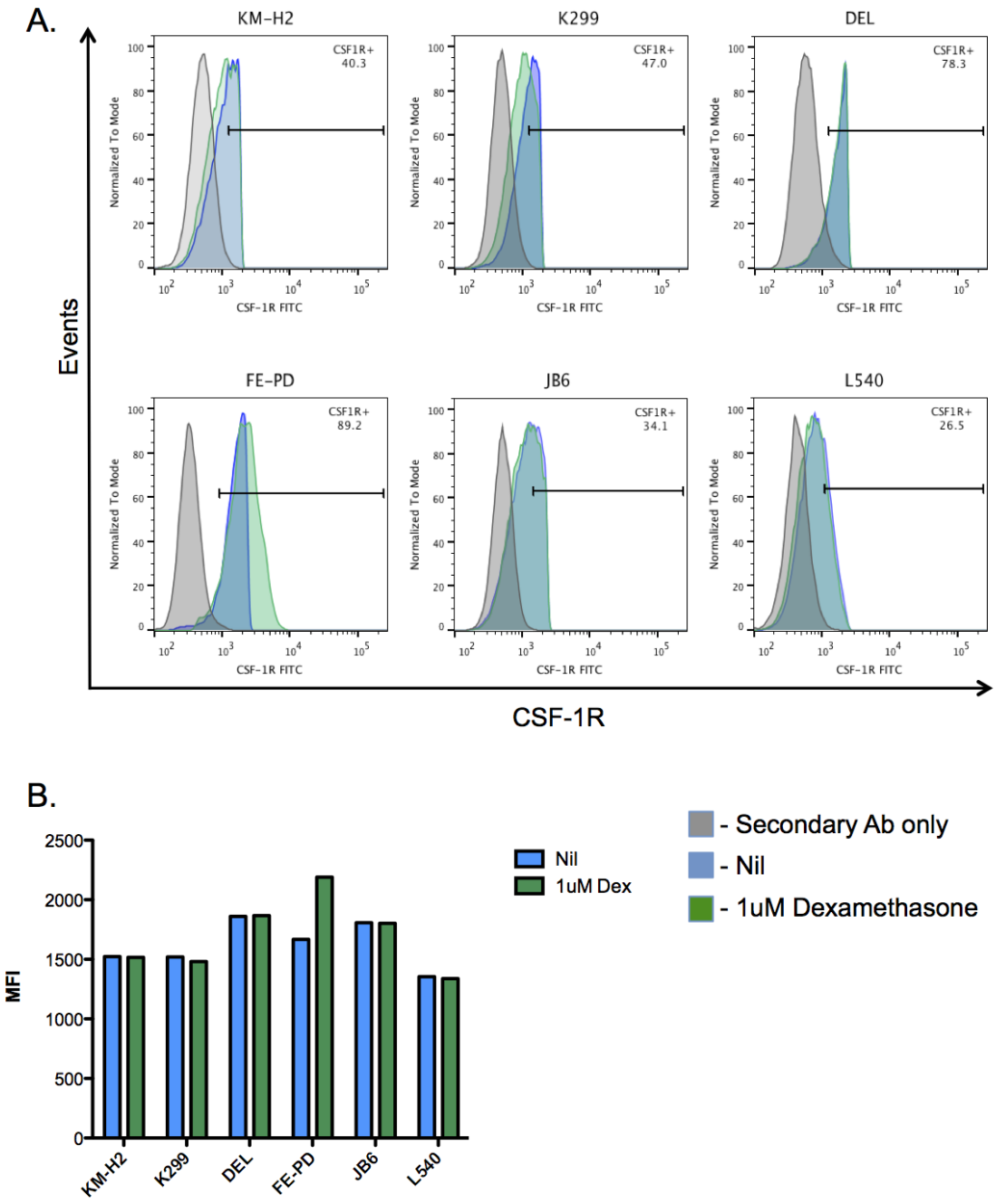

Figure 3.5. Surface CSF-1R expression by lymphoma cells cultured +/- dexamethasone.

(A) The panel of six lymphoma cell lines was either treated with 1μM dexamethasone or left untreated for 48 hours. Next, cell surface CSF-1R expression was determined by flow cytometry. The presence of CSF-1R was detected using a rat monoclonal anti-human CSF-1R antibody, followed by a FITC-conjugated secondary antibody (blue histogram – in the absence of dexamethasone treatment at 48h; green histogram – following exposure to 1μM dexamethasone for 48h). Cells were also stained using the secondary antibody only (grey histograms) to show the specificity of staining. **(B)** Median fluorescence intensity was plotted for each cell line in both conditions.

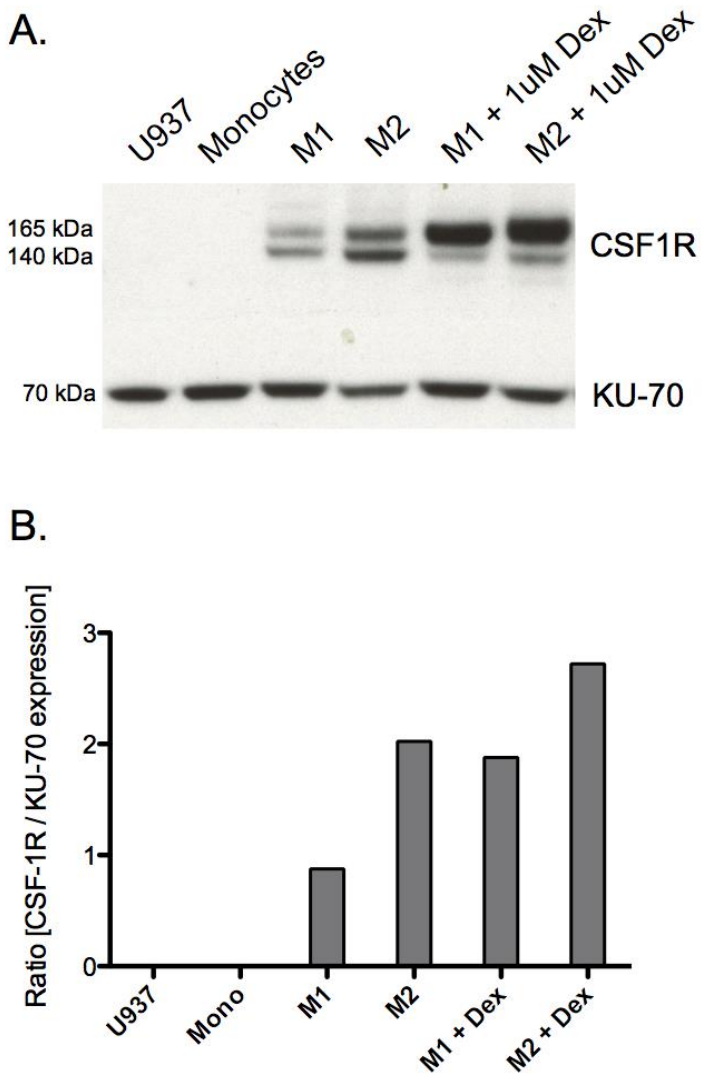

Figure 3.6 CSF-1R expression by human monocyte-derived macrophages cultured +/- dexamethasone.

MACS-separated $CD14^+$ human monocytes were differentiated into M1 or M2 macrophages by cultivation for 7 days in GM-CSF or CSF-1 respectively. For the next 48h, cells were cultured in presence or absence of 1μM dexamethasone and levels of CSF-1R protein were analysed by western blotting. Lysates produced under reducing conditions were separated using SDS-PAGE and subsequently transferred onto a nitrocellulose membrane. The presence of CSF-1R protein was determined using a rabbit anti-CSF-1R primary antibody, followed by a goat anti-rabbit IgG HRP-conjugated secondary antibody. The presence of bound secondary antibody was detected using enhanced chemiluminescence (ECL) **(A, top panel)**. The lysates were also probed for the presence of the nuclear membrane protein, KU-70, as a loading control **(A, bottom panel)**. Bar graphs were obtained by densitometric analysis (ImageJ) of western blot data **(B)**.

3.3 Discussion

In order to elucidate whether CSF-1R expression in cHL and ALCL would be amenable to CAR-re-directed T-cells, a panel of 6 lymphoma cell lines (2 cHL, 2 ALK^+ ALCL, 2 ALK^- ALCL cell lines) was probed for CSF-1R expression by western blotting (assessing total relative levels of expression; Figure 3.1, A) and flow cytometry (providing comparative information on cell surface expression; Figure 3.1, B). Varying levels of CSF-1R expression were detected in all six lymphoma cell lines. Additionally, an autocrine loop was confirmed by CSF-1 and IL-34 ELISA (Figure 3.2). Expression levels of both ligands was determined in the absence of anti-CSF-1R blocking antibody, raising the possibility that the detected cytokine levels underestimate the true amount produced due to continuous internalization of the ligand-receptor complex. Importantly, while the involvement of CSF-1 in the pathogenesis of cHL and ALCL has been reported previously, these results suggest for the first time a role for IL-34 in this process [35, 292, 318, 326]. However the role of IL-34 in cHL and ALCL has not been addressed in this project and warrants further study. Knocking down IL-34 by si/shRNA would shed light on its involvement in proliferation and migration, as well as on its potential role as a mediator of cellular cross talk and an influential factor in the tumour microenvironment.

Colony-stimulating factor-1 receptor has been shown to translocate to the nucleus in both breast cancer cell lines and patient tumour samples where it acts as a transcriptional factor [327]. It is hypothesized that since CSF-1R does not contain a nuclear localization signal (NLS) it can only translocate into the nucleus when complexed with CSF-1, which does contain an NLS [327]. Once in the nucleus, CSF-1R binds to the promoter region of CSF-1 thus not only driving a self-sustaining loop by regulating CSF-1 expression but also shedding light on its association with treatment resistance and poor prognosis. No such role has been described in the literature for the CSF-1R/ IL-34 receptor-ligand complex. Upon entering the IL-34 amino acid sequence

in the online database NucPred (http://www.sbc.su.se/~maccallr/nucpred), which predicts putative NLS's in any given amino acid sequence, a score of 0.22 was generated for IL-34, suggesting that it lacks a NLS [328]. NucPred assigns a likelihood score of 1 to an amino-acid sequence with a known well-defined NLS. Sequences, which score $\geq$ 0.7 with NucPred have been shown to be 81% correct with a coverage of 44%. By contrast, when CSF-1R was run, the NLS score obtained was 0.15, while CSF-1 (Gene ID: 1435; isoform 1) was scored as 0.63. These data strongly suggest that an NLS is lacking in CSF-1R but present in CSF-1 and, by implication, the complex of this cytokine with its receptor. By contrast, this situation would not be expected to apply to IL-34 when complexed with CSF-1R. This hypothesis can be tested by provision of exogenous CSF-1 or IL-34 in a CSF-1R expressing model system, in which nuclear localization of CSF-1R will be confirmed by immunofluorescence.

Recently, a novel IL-34 receptor was identified termed PTPζ [131]. Physiological expression of PTPζ is largely restricted to the central nervous system and this receptor is overexpressed in some malignancies, most notably in glioblastomas [329-331]. Furthermore, increased expression levels of PTPζ in astroctyomas has been correlated with a poor clinical prognosis. [330] Functionally, PTPζ is known to facilitate tumour cell adhesion and migration through interactions with extracellular matrix components and the growth factor pleiotrophin [332, 333]. Given the detected IL-34 production by the lymphoma cell lines and in light of its role in glioblastomas, PTPζ expression level was investigated in the panel of lymphoma cell lines (Figure 3.3). While none of the lymphoma cell lines showed evidence of PTPζ expression, a band of the expected size (approximately 90 kDa) was detected in the Daudi cell line, which served as a positive control. Consequently, it was concluded that all six lymphoma cell lines express variable levels of CSF-1R, but not PTPζ, and secrete either one or both ligands for the former receptor. Therefore, the limiting step in targeting CSF-1R in this system would be the availability of the receptor on the cell surface, which is determined by its expression level and the rate of receptor-ligand complex internalization.

The mature CSF-1R is relatively stable in the absence of CSF-1 and IL-34 with a half-life of three to four hours [334]. However, upon ligand binding, receptor expression is down-regulated rapidly (receptor-ligand complex half-life ≈ 5 min) [335] by internalization of the ligand-receptor complex. This provides a mechanism for attenuation of the growth factor receptor signalling [336]. In contrast to other tyrosine kinase receptor-ligand complexes that are subjected to proteasome-dependent proteolytic process (e.g. Platelet-derived Growth Factor β –Receptor [337], Met [338], Epidermal Growth Factor [339]), CSF-1R is degraded lysosomally. Upon interaction of c-cbl with the C-terminal Y969 of CSF-1R, the receptor complex becomes ubiquitinated and, after association with clathrin-dependent coated pits, it is pinocytosed and subsequently degraded in lysosomes [334, 340]. For the purpose of CSF-1R targeting using CAR-engineered T-cells, the rapid rate of internalization of the ligand-receptor complex is potentially unfavourable. Consequently, I considered the use of agents such as glucocorticoids that are known to up-regulate steady state expression of this receptor at the cell surface.

Gluccorticoids (GC) are a class of pharmaceuticals that attenuate many aspects of the inflammatory process. These agents bind to glucocorticoid receptors (GR), which associate with glucocorticoid response elements (GREs) that are found in the promoters of many target genes. In turn, these complexes recruit co-activator proteins to increase histone acetylation, thereby allowing enhanced gene transcription to occur [341]. Expression of several anti-inflammatory genes is increased in this manner, including IL-10, inhibitor of -κB (IκBα) and MAPK-phosphatase-1. In addition, glucocorticoids have been reported to inhibit the transcription of a number of inflammatory cytokines (e.g. IL-1β, IL-2, IL-3, IL-4, IL-5, IL-6, IL-11, TNF-α and GM-CSF) and chemokines (e.g. IL-8, RANTES, MCP-1, MCP-3, MCP-4 and MIP-1α) [342]. This results in disruption of immune cell recruitment (neutrophils, monocytes,

macrophages, T-cells and granulocytes) to the site of inflammation as well as in inhibition of their activation and consequent proliferation.

Exposure to GC, including dexamethasone, results in *c-fms* overexpression through the activation of a GR-mediated pathway. This effect has been attributed to functional GREs located in both *c-fms* promoters [323]. The *c-fms* gene has two described promoters, separately directing expression in monocytic and trophoblast cell lineages. In placental trophoblasts, the c-*fms* transcript is initiated from the first promoter, which is 26 kb upstream of exon 2 and includes a non coding first exon, while in the monocytic lineage CSF-1R expression is initiated from the second *c-fms* promoter, immediately upstream of exon 2 [119, 323, 343]. As demonstrated by Roberts *et al*., both promoters of the *c-fms* gene contain functional GREs, which can mediate the observed GC effect through the glucocorticoid receptor [343].

Expression of c-*fms* has been reported to be dramatically up-regulated by GC both in breast cancer cell lines *in vitro* as well as in breast cancer metastasis *in vivo* [295, 321, 344]. Even low physiological levels of GC induce elevated c-*fms* expression *in vivo* [345]. In cHL and ALCL, unlike in epithelial cancers, CSF-1R expression is driven by an aberrantly activated endogenous LTR, located ~6.2 kb upstream of the monocytic lineage promoter [34]. In order to investigate whether dexamethasone treatment can induce similar up-regulation of c-*fms* expression in cHL and ALCL, the panel of lymphoma cell lines was treated with 1μM dexamethasone. Cells were lysed every 12 hours under reducing conditions and probed for the expression of CSF-1R. Analysis of the band intensities from 3 separate donors (shown in the bar graphs), indicates transient, but not statistically significant (with the exception of the FE-PD cell line) CSF-1R up-regulation at 48h (Figure 3.4). More importantly, surface level of CSF-1R expression was not affected by dexamethasone treatment (with the exception of the FE-PD cell line), as indicated by flow cytometry (Figure 3.5). Taken together, these results suggest that in the context of cHL and ALCL dexamethasone treatment would

fail to confer a therapeutic benefit related to targeting CSF-1R using CAR-engineered T-cells (Appendix, Figure S2).

Glucocorticoid receptors are largely expressed in inflammatory cells, notably macrophages, which play a key role in inflammation [346]. As expected, dexamethasone treatment of human monocyte derived macrophages resulted in marked up-regulation of CSF-1R at 48h (Figure 3.6).

Overall, the data presented in this chapter show that CSF-1R is an attractive candidate target in cHL and ALCL. However, it is also a challenging target in these diseases owing to the endogenous production of both ligands (CSF-1 and IL-34), feeding into an autocrine loop that is likely to promote rapid internalisation of the ligand-receptor complex. Furthermore, dexamethasone treatment of the panel of lymphoma cell lines failed to induce a significant up-regulation of CSF-1R expression, unlike the situation observed in dexamethasone-treated macrophages. Consequently, I next set out to examine if CAR T-cells would be able to detect cell surface expression of CSF-1R by cHL and ALCL cells, despite the presence of endogenous ligands produced by these lymphoma cells.

Chapter 4 Design, cloning and *in vitro* characterization of CSF-1R-targeted chimeric antigen receptors

4.1 Introduction

In recent years, we have witnessed a sea-change in the manner with which cellular therapies are viewed by the clinical community and the pharmaceutical industry. Building on the exciting momentum engendered by CD19 CAR T-cells, there is every prospect that genetically engineered lymphocytes will provide a rich source of new medicines to treat human disease.

Several challenges will guide the next stages of development of CAR T-cell immunotherapy of cancer. First, development of effective therapeutic regimens for solid tumours will require renewed efforts to address the problem of the tumour microenvironment, which imposes a hypoxic, metabolic and immunological ambiance that is poorly conducive to effective immunotherapy. A number of approaches to address this issue have been presented below and doubtless several more strategies will emerge in the near future.

4.1.1 Recent developments in pre-clinical CAR engineering

Several new approaches have been described recently that aim to refine the precision, potency and safety of immunotherapy using CAR T-cells.

4.1.1.1 Dual Targeting Using CAR T-cells

One emerging strategy involves the separation of signalling domains between two co-expressed CARs with distinct target specificities, thereby delivering complementary signals *in trans* (Figure 4.1, B). Exemplifying this approach, HER2- and MUC1-specific CARs were co-expressed that signal through CD3ζ and CD28 respectively [347]. Tumour cell lysis and efficient T-cell proliferation was only achieved upon interaction

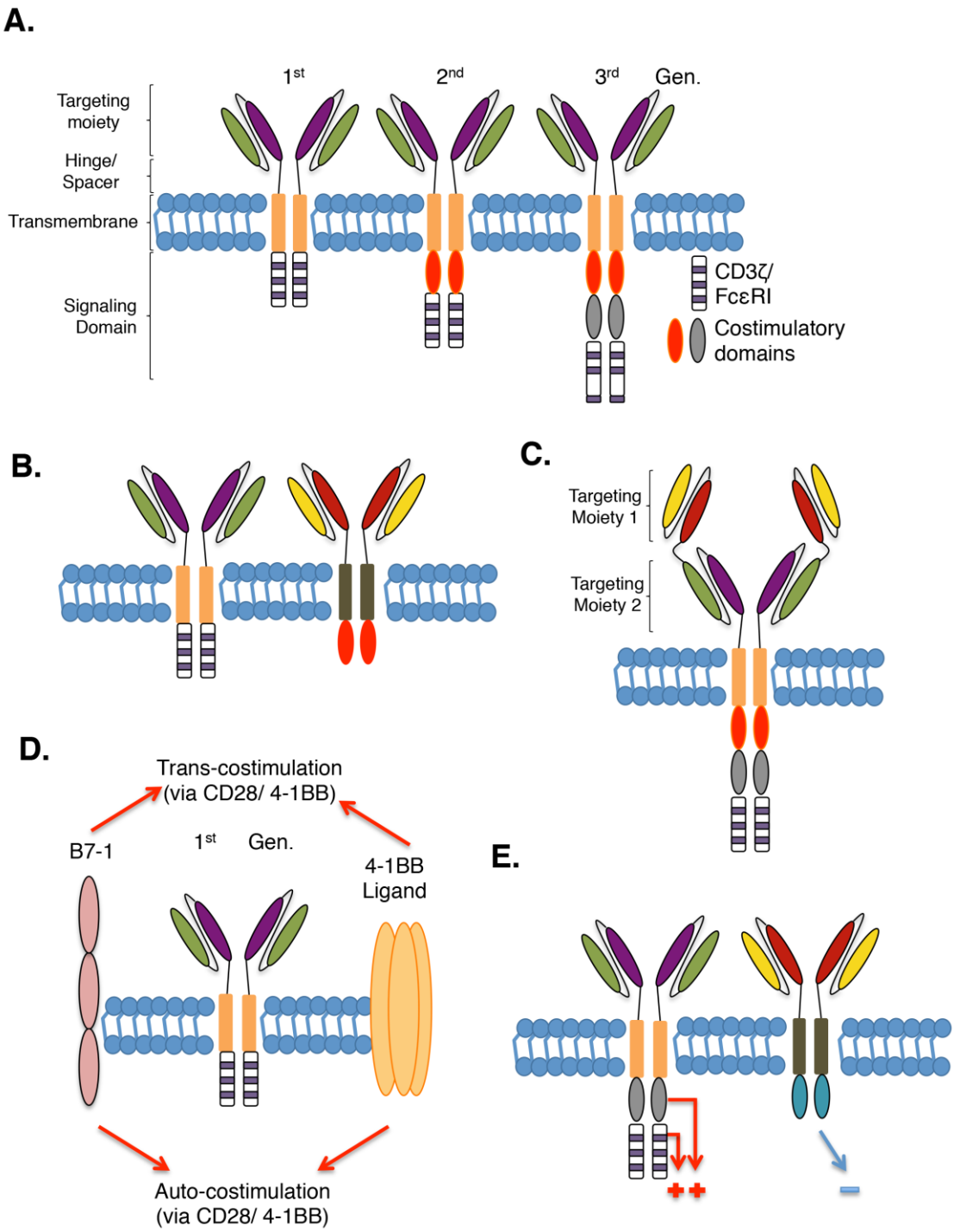

Figure 4.1 Chimeric antigen receptor configurations.

(A) First generation CARs contain a single endodomain module that delivers signal 1, most commonly CD3ζ or FcεR1. Second and third generation CARs contain in addition either one or two co-stimulatory modules respectively. (legend continues on next page)

with cells that expressed both CAR targets. Recently Kloss *et al*. [348] refined this strategy using a model in which CARs for two prostate cancer antigens were co-expressed. Each CAR promoted sub-optimal T-cell activation when engaged alone. However, potent anti-tumor activity was observed upon simultaneous target binding. Such a dual targeting system can potentially reduce reactivity against healthy tissues that may express single targets but, on the other hand, it may also increase the possibility of tumour escape through antigen loss. The latter is illustrated by the unfortunate outgrowth of $CD19^{neg}$ blast cells in a number of patients with acute lymphoblastic leukaemia (ALL) following treatment with CD19-targeted CAR T-cells (Table 1.4) [202, 210].

(B) Dual targeted CARs bind to distinct targets and signal via complementary endodomains (e.g. providing signal 1 and 2 respectively). **(C)** "TanCARs" contain two targeting moieties, joined in tandem in the CAR ectodomain. **(D)** An alternative device to deliver co-stimulation to CAR T-cells entails the co-expression of one or more co-stimulatory ligands. In the example shown, the CAR T-cells co-express B7-1 and 4-1BB ligand, which can provide co-stimulation by engagement of CD28 and 4-1BB, both in the same T-cell (auto-costimulation) and neighbouring T-cells (trans-costimulation). **(E)** Inhibitory CARs may be co-expressed that serve to attenuate positive signals delivered by activating CARs. By this means, T-cell activation can be restricted to target cells that only express the ligand for the activating but not the inhibitory CAR.

A further modification of the dual targeting approach involves the expression of CARs that can simultaneously bind to more than one target molecule in tandem (Figure 4.1, C). Such “TanCARs” are designed as a single CAR molecule in which two or more scFvs are joined using a linker, thereby conferring a plurality of target specificities [349]. An advantage of the TanCAR approach is that T-cells exhibit cytolytic activity against tumour cells that express only one of the targets while synergistic enhancement of effector function may be achieved when more than one antigen is encountered [349].

A further dual targeting system entails the co-expression of one or more co-stimulatory ligands with a first generation CAR (Figure 4.1, D). This approach has proven to be strongly efficacious in some pre-clinical models [350] although concerns remain that such constitutive co-stimulation may promote autoimmune toxicity.

4.1.1.2 Optimizing safety of CAR T-cells

Clinical experience with CAR T-cells has highlighted the significant risk of these cells to induce cytokine release syndrome (CRS) and other on-target toxicities. Consequently, a number of “suicide gene” systems have been developed that can be co-expressed with the CAR of interest and which may be activated when required in a pharmacologically-regulated manner. Greatest clinical experience has been gained with the herpes simplex virus thymidine kinase gene, which confers sensitivity to ganciclovir, but which is immunogenic when infused in immune competent recipients [351]. An increasingly used alternative is inducible caspase 9, which can be activated by a chemical inducer of dimerization and leads to extraordinarily rapid ablation of gene-modified cells [352, 353]. Thirdly, an epitope tag may be co-expressed in CAR T-cells, allowing their elimination upon administration of a clinically licensed monoclonal antibody [354, 355].

While all of these ablative strategies have their merits, it is ultimately preferable to devise safer systems that would not require the elimination of therapeutically active cells. Some recent developments suggest that this may be an attainable goal. Since there is a paucity of tumour-specific targets, CAR T-cells are commonly engineered to bind molecules that are over-expressed in transformed cells, but are found at lower levels in healthy tissues. Consequently, it is desirable to enable therapeutically active cells to discriminate between tumour cells that express targets at high levels while ignoring healthy tissues where lower amounts may be present. One strategy to achieve this entails the co-expression of activating and inhibitory CARs in the same lymphoid population (Figure 4.1, E) [356]. The principle underlying this approach is that a potent inhibitory CAR (e.g. containing a PD-1 endodomain) can be used to neutralize the activating signal delivered by a co-expressed CAR in healthy tissues in which both targets are co-expressed at comparable levels. By contrast, if a transformed cell only expresses the target recognized by the activating CAR, but not that bound by its inhibitory counterpart, then tumour cell destruction occurs. Clinically applicable systems that exploit this principle have great potential to facilitate the safer development of CAR T-cell immunotherapy for common solid tumour types.

4.1.1.3 Potentiating CAR T-cells by co-expression of cytokines

While CAR T-cells have achieved notable successes against haematological malignancy, impact against solid tumours has proven more elusive. However, several strategies that are undergoing experimental development may help to address this deficit. One approach entails the co-expression of a tumour-specific CAR and a cytokine that can potentiate anti-tumour activity. Several groups have co-expressed CARs with IL-12, [357-360] a cytokine that exerts pleiotropic supportive effects upon innate immune cells within the tumour microenvironment [359]. Use of IL-12-expressing CAR T-cells obviated the need for prior lymphodepletion in one model system [361]. Alternatively, *in vivo* longevity and potency of CAR T-cells may be enhanced by co-

expression of a common gamma cytokine in these cells, such as IL-2, IL-7, IL-15 or IL-21 [362, 363].

4.1.1.4 Potentiating CAR T-cells by co-expression of cytokine receptors

Persistence of CAR T-cells may also be enhanced by co-transfer of genes that confer responsiveness to a cytokine that can be administered with therapeutic intent, such as IL-7 [364] or IL-4 [365]. Alternatively, responsiveness may be conferred in a similar manner to cytokines that are naturally over-produced in the tumor microenvironment, such as IL-4 [365] or colony-stimulating factor-1 (CSF-1) [366].

4.1.1.5 Potentiating CAR T-cells by co-expression of chemokine receptors

In a related approach, migration of CAR T-cells to the tumour microenvironment may be enhanced by co-expression of a receptor that confers responsiveness to one or more tumour-associated chemokines (e.g. CXCR2, which binds several chemokines including CXCL1 and 8; [367, 368] CCR2b, which binds CCL2; [369, 370] or CCR4, which binds CCL17) [371]. Alternatively, T-cells may be harnessed to undergo chemotactic migration in response to other tumour-derived cytokines (e.g. by expression of CSF-1 receptor, which binds CSF-1) [372].

4.1.1.6 Optimizing differentiation status of CAR T-cells

Another approach to improve efficacy of CAR T-cell immunotherapy involves the use of specific lymphoid subsets that have greater potential for *in vivo* persistence, such as central memory T-cells [373]. Indeed, recent evidence suggests that T-cells lying between the naive and central memory stages of differentiation may be even more suitable for this purpose [374, 375]. These so-called memory stem cell T-cells (T_{SCM}) express a $CD45RA^{+}CD62L^{+}CCR7^{+}CD95^{+}$ phenotype and can be propagated *ex vivo* after CD3/CD28 engagement in the presence of IL-7 and IL-15. This expansion protocol allows for both a high efficiency expansion with retention of self-renewal

potential, rendering these cells of great interest for use in adoptive T-cell immunotherapy [376, 377].

In summary, a large number of innovative approaches continues to be described that have the potential to enhance the efficacy of CAR T-cell immunotherapy. This provides a rich pipeline of candidate approaches for future clinical evaluation across a spectrum of malignant disorders.

4.2 Results

I set out to develop a CAR-based immunotherapeutic approach directed against the up-regulated expression of CSF-1R in cHL and ALCL. Both naturally occurring CSF-1R ligands were used as antigen recognition domains in the design of a panel of eight CSF-1R targeting CARs, which can be provisionally divided into 3 groups:

- CSF-1-based CARs – CSF-1 was used as a targeting moiety for the construction of a second generation CAR (CD28-CD3ζ) termed “C4”, a third generation CAR (CD28-4-1BB-CD3ζ) termed “C4B” and a truncated CAR with no signalling domains, named “CT4”.
- IL-34-based CARs – this group comprises a truncated CAR (“434Tr”), a second (“43428ζ”) and a third generation (“43428Bζ”) CARs similar to the CSF-1-based CARs, but employing IL-34 as antigen-recognition domain.
- Double targeting CARs – employ both CSF-1 and IL-34 as targeting domains, which are coupled to CD28-CD3ζ and 4-1BB, or vice versa (termed “C34B” and “34CB” respectively). The dual targeted CAR combinations were then stoichiometrically co-expressed in the same T-cell population using a *Thosea Asigna (*T)2A-containing retroviral vector.

Please refer to Figure 2.1 (page 74) and Figure 2.2 (page 80) for schematic representation of the various CSF-1R-targeting CAR constructs used in this chapter.

4.2.1 Cloning of CSF-1R-targeting CAR constructs

All CARs have been expressed using the SFG onco-retroviral expression vector [268]. All constructs apart from SFG C28ζ and SFG CTr were designed and cloned over the course of the project using the Polymerase Incomplete Primer Extension (PIPE) cloning method (please refer to section 2.1.2).

Construction of SFG C4 (4αβ + C28ζ) was achieved by PIPE PCR. Two fragments of the SFG C28ζ plasmid containing PIPE overhangs were amplified and are denoted as fragment 1 (4819 bp) and fragment 2 (2756 bp) (Figure 4.2, A and B). Then, the 4αβ-furin-T2A cassette was PIPE PCR amplified from the SFG T4 plasmid (courtesy of Dr David Davies, King's College London) to generate a 4αβ fragment (1714 bp) with PIPE overhangs. Next, all PIPE PCR products were subjected to DpnI digestion in order to destroy any remaining intact SFG template, which would contaminate the subsequent ligation reaction. Following the DpnI digestion, the three un-purified self-complementary PIPE PCR products were mixed in 1:1:1 molar ratio, incubated at 60^{o}C for 30 min and transformed into *E.coli*. Successful transformants were verified by analytical digestion with NcoI/NotI and run on 1% agarose gel (Figure 4.3, A). Restriction digestion yielded the following 3 bands, which were separated by agarose gel electrophoresis: SFG backbone (≈7000 bp), 4αβ (≈1700 bp) and the targeting moiety CSF-1 (≈500 bp). All bands were of the predicted sizes. A similar cloning strategy was employed for SFG CT4 using SFG CTr as template (Figure 4.3, A).

The construct SFG C34B (4αβ + C28ζ + 34B) was designed to explore the possibilities of dual CAR-based targeting of CSF-1R (Figure 2.1 and 2.2). In order to construct this, a second CSF-1R-targeting CAR was designed, termed 34B. The 34B construct was designed together with a second codon “wobbled” T2A DNA sequence, placed in the upstream position. Sequences were codon optimised as a cDNA cassette, which was synthesised by GenScript. Cloning of SFG C34B was achieved by PIPE PCR linearising SFG C4 and PIPE PCR amplifying the cDNA cassette. The self-

complementary PIPE PCR products were then mixed to assemble the complete SFG C34B construct. Successful cloning was confirmed by restriction pattern agarose gel analysis. An NcoI/XhoI restriction digestion generated the predicted 3 bands as follows: SFG backbone (≈6300 bp), 4αβ (≈1700 bp) and both CAR cDNAs contained within one band (≈2400 bp) (Figure 4.3, B).

The constructs SFG 43428ζ (4αβ + 3428ζ) and SFG 434Tr (4αβ + 34Tr) were PIPE cloned by swapping the CSF-1 targeting moiety in SFG C28ζ and SFG CTr respectively with IL-34. To achieve this, three primer pairs were designed (please refer to Table 2.1). The first two vector-specific primer pairs, flanking the existing CSF-1, were used for amplification of two vector fragments, while the last primer pair, with 5′-vector-fragment-end overlapping sequences, was used for amplification of the incoming IL-34 sequence. Successful transformants were characterized by loss of the second NcoI site flanking 4αβ and upon NcoI/XhoI restriction digestion generated 2 bands, separated on a gel: SFG backbone (≈6000 bp) and 4αβ + CAR in one band (for SFG 43428ζ ≈3100 bp while for SFG 434Tr ≈2700 bp) both bands with the predicted sizes (Figure 4.3, C and D).

To generate the SFG 34CB construct (4αβ + 3428ζ + CB), the SFG C34B construct was used as template and four primer pairs were designed. The first two vector-specific primer pairs, flanking the existing CSF-1 and IL-34 sequences, were used for amplification of 2 vector fragments. The second two primer pairs, with 5′-vector-fragment-end overlapping sequences, were used for amplification of the incoming IL-34 and CSF-1 sequences with swapped places. The four PCR products were used in an enzyme-free ligation to generate the SFG 34CB construct. Successful cloning was verified by BamHI restriction digestion, which generated 3 bands, separated on a gel: SFG backbone + 4αβ in one band (≈7700bp), 3428ζ (≈1800bp) and CB (≈950bp) all of them with the predicted sizes (Figure 4.2, E).

For the construction of SFG C4B (4αβ + C28Bζ) and SFG 43428Bζ (4αβ + 3428Bζ), SFG C4 and SFG 43428ζ were used as templates respectively. In each case template-specific primers were used for PCR SFG template linearization at the site of fusion between the intracellular domains of CD28 and CD3ζ within the C28ζ construct or the 3428ζ construct, thereby generating single-stranded 5′-ends. Simultaneously, the 4-1BB sequence was PCR amplified using a pair of 40 bp primers with 5′-end overlapping sequences, thereby generating single-stranded template-end homologous products, which were then used in a enzyme-free ligation to generate the SFG C4B and SFG 43428Bζ constructs. Successful cloning was confirmed by restriction pattern agarose gel analysis. A NotI/XhoI restriction digestion generated 2 bands: SFG backbone along with 4αβ and the targeting moiety from the respective CAR (≈9000 bp), and a smaller band representing the signalling domains CD28 + 41BB + CD3ζ (≈800bp) (Figure 4.3, F).

All SFG constructs were subsequently sequenced and no mutations were identified within the coding regions (Source Bioscience).

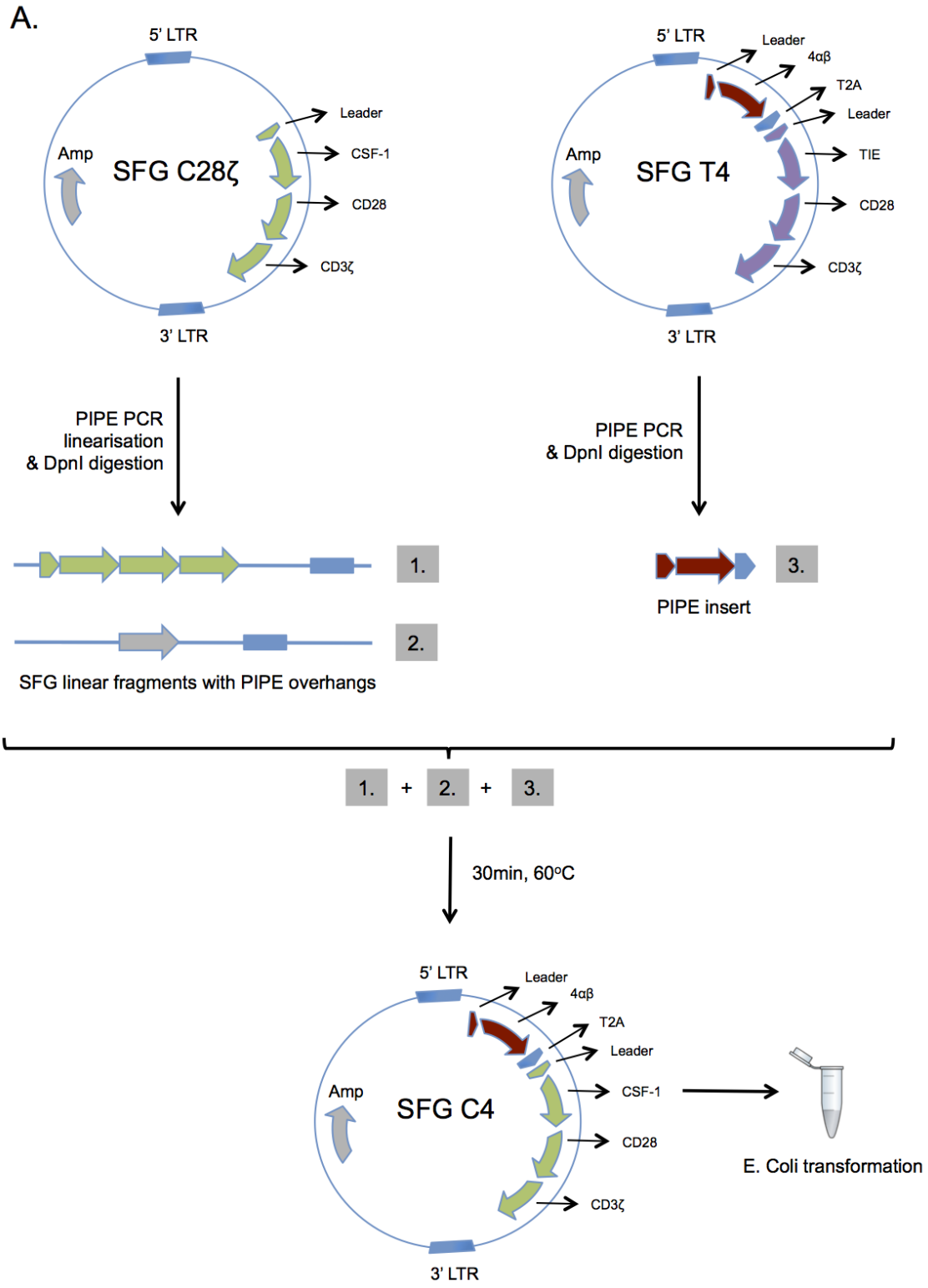

Figure 4.2 Schematic representation of SFG C4 PIPE cloning strategy.

(figure and legend continue on next page)

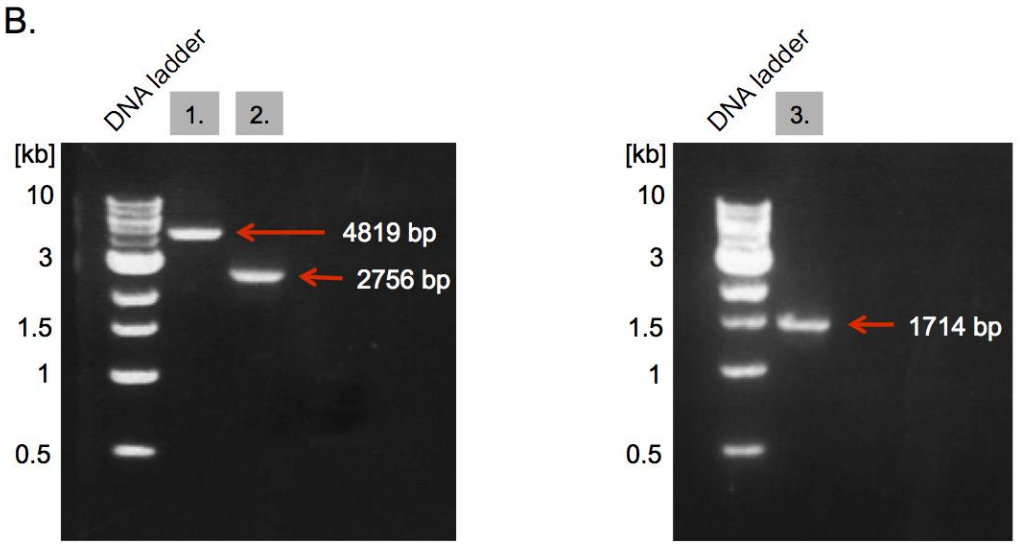

(A) SFG C28ζ was linearised using PIPE PCR (fragment 1 and 2). Simultaneously, the 4αβ-furin-T2A cassette was PIPE PCR amplified generating fragment 3. The resultant three PIPE PCR products were subjected to DpnI digestion and incubated for 30min at 60^{o}C and then transformed into *E. coli*. **(B)** PIPE PCR products were run on 1% agarose gel electrophoresis to confirm correct size prior to proceeding to the ligation reaction.

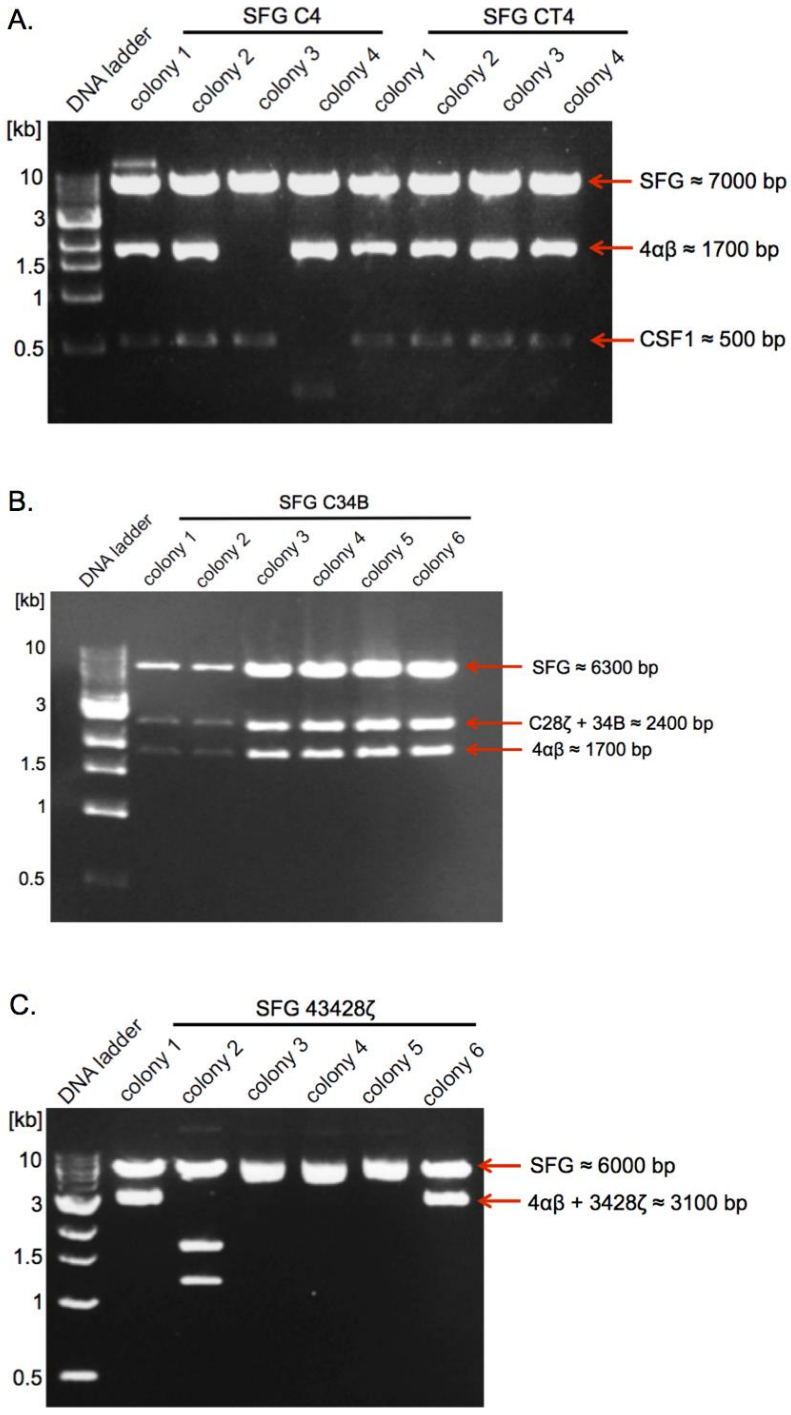

Figure 4.3 Restriction pattern agarose gel analysis of SFG C4, C4B, CT4, C34B, 43428ζ, 43428Bζ, 434Tr and 34CB.

Successful transformants were verified by analytical digestion with appropriate restriction enzymes so that the pattern of fragments on the gel can indicate if the plasmid contains the expected size insert sequence. (figure and legend continue on next page)

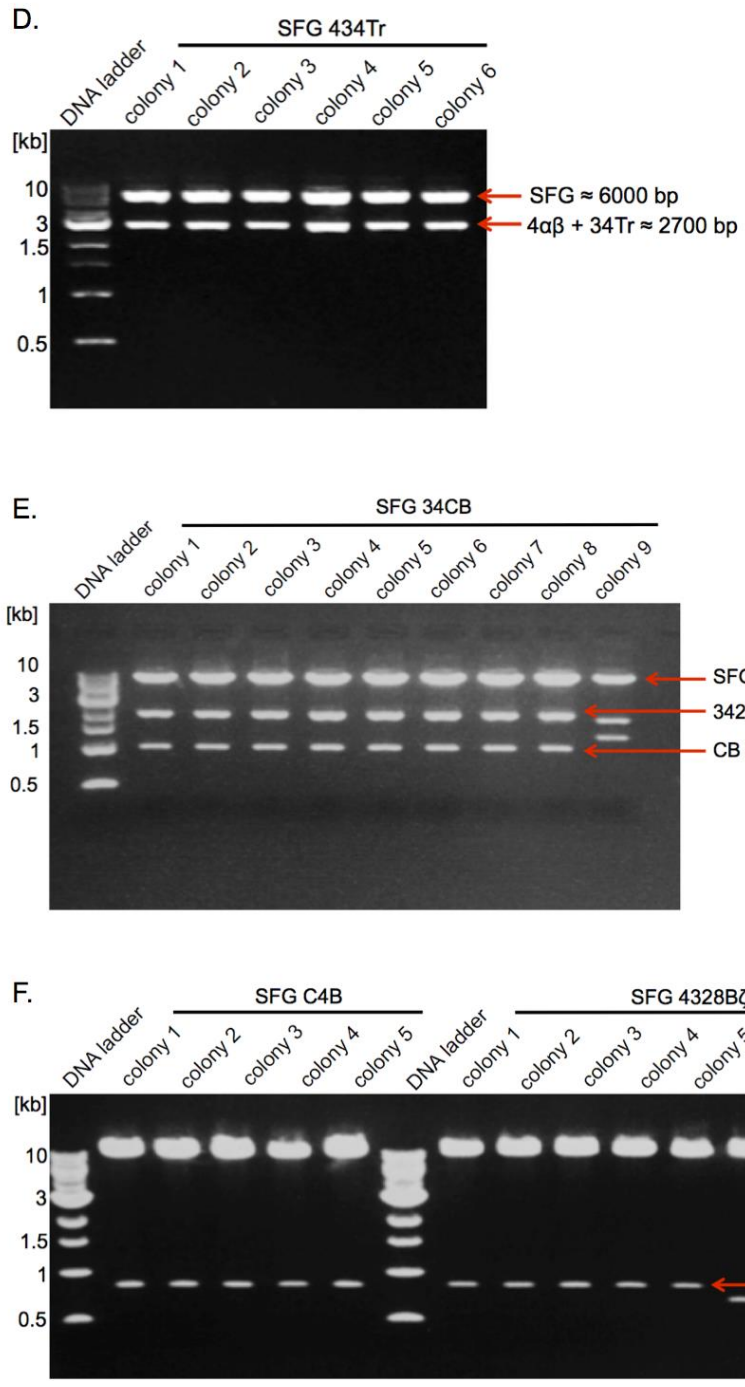

(A) NcoI/NotI restriction digestion of SFG C4 and SFG CT4 generated 3 bands with the predicted sizes: SFG backbone (≈7000 bp), 4αβ (≈1700 bp) and the targeting moiety CSF-1 (≈500 bp). **(B)** SFG C34B was subjected to NcoI/XhoI restriction digestion yielding 3 bands of expected sizes: SFG backbone (≈6300 bp), 4αβ (≈1700 bp) and both CARs in one band (≈2400 bp). **(C) and (D)** SFG 43428ζ and 434Tr were digested with NcoI/XhoI generating 2 bands, separated on a gel: SFG backbone (≈6000 bp) and 4αβ + CAR in one band (for SFG 43428ζ ≈3100 bp while for SFG 434Tr ≈2700 bp). (legend continues on next page)

4.2.2 Establishing stable CAR-expressing retroviral packaging cell lines

In general, gene transfer undertaken in this project has been achieved using engineered retroviruses, thereby permitting stable CAR expression. This has been achieved through the establishment of two stable CAR-expressing retroviral packaging cell lines derived from PG13 and 293Vec RD114 cell lines (see section 2.2.2.3). Of note, 293Vec RD114 packaging cell line produces about 100-fold higher viral titres than PG13 cells do. Both retroviral packaging cell lines were generated in a two-step process involving transfection of H29D retroviral packaging cells (see section 2.2.2.3) and subsequent PG13 or 293Vec RD114 retroviral transduction using the transiently produced H29D-derived viral particles (Figure 4.4 and 4.5).

(E) SFG 34CB was digested with BamHI and run on a 1% gel. Upon restriction, 3 bands were visible on a gel: SFG backbone + 4αβ in one band (≈7700bp), 3428ζ (≈1800bp) and CB (≈950bp) all of them with the predicted sizes. **(F)** SFG C4B and SFG 43428Bζ were digested with NotI/XhoI generating 2 bands, separated on a gel: SFG backbone along with 4αβ and the targeting moiety from the respective CAR (≈9000 bp), and a smaller band representing the signalling domains CD28 + 41BB + CD3ζ (≈800bp). All bands were of the predicted sizes.

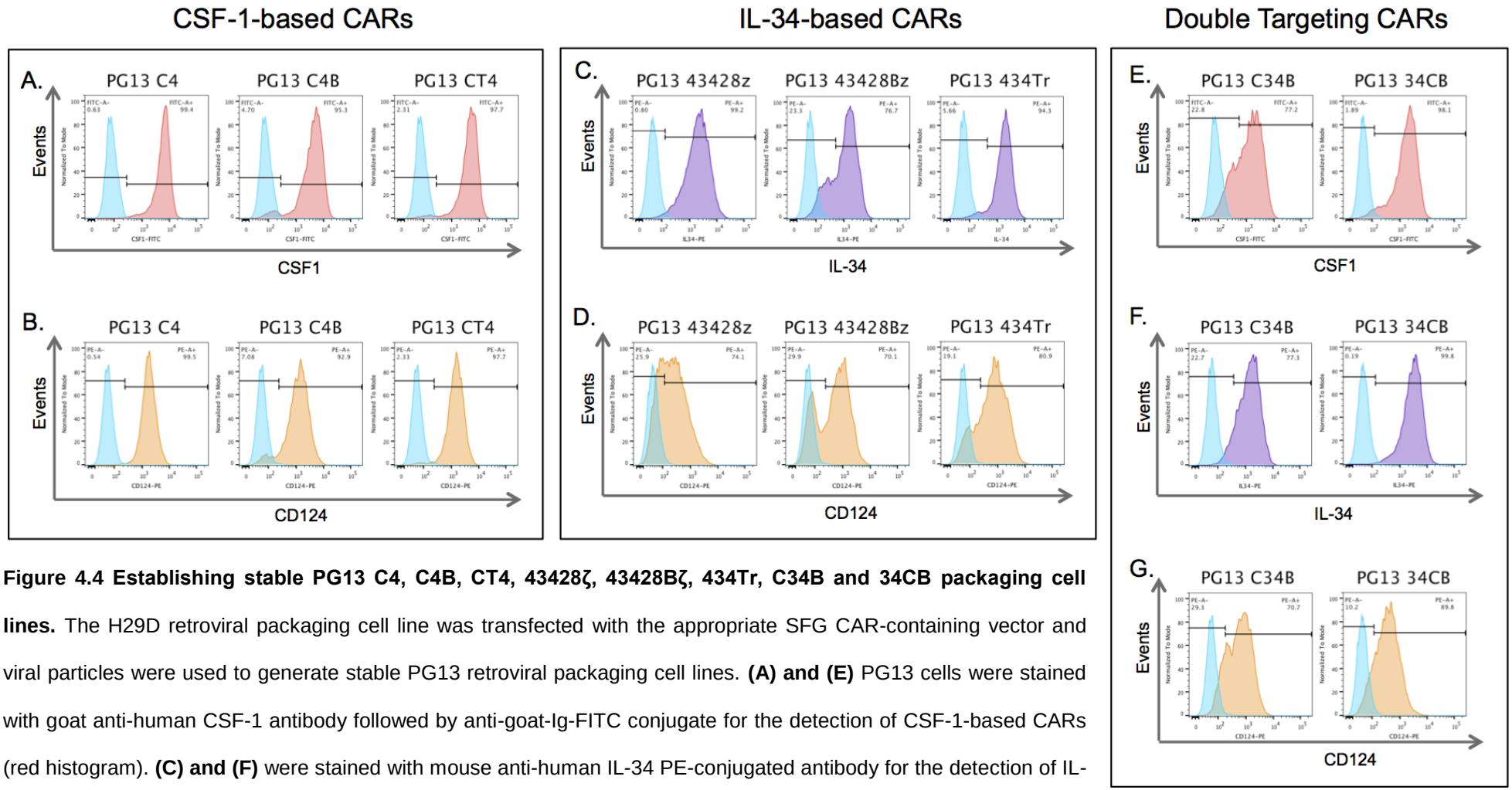

Figure 4.4 Establishing stable PG13 C4, C4B, CT4, 43428ζ, 43428Bζ, 434Tr, C34B and 34CB packaging cell lines. The H29D retroviral packaging cell line was transfected with the appropriate SFG CAR-containing vector and viral particles were used to generate stable PG13 retroviral packaging cell lines. **(A) and (E)** PG13 cells were stained with goat anti-human CSF-1 antibody followed by anti-goat-Ig-FITC conjugate for the detection of CSF-1-based CARs (red histogram). **(C) and (F)** were stained with mouse anti-human IL-34 PE-conjugated antibody for the detection of IL-34-based constructs (purple histogram). **(B), (D) and (G)** PG13 cells were stained with anti-IL4Rα-PE for the detection of 4αβ (orange histogram). The blue histogram shows the same staining on empty (parental) PG13 cells.

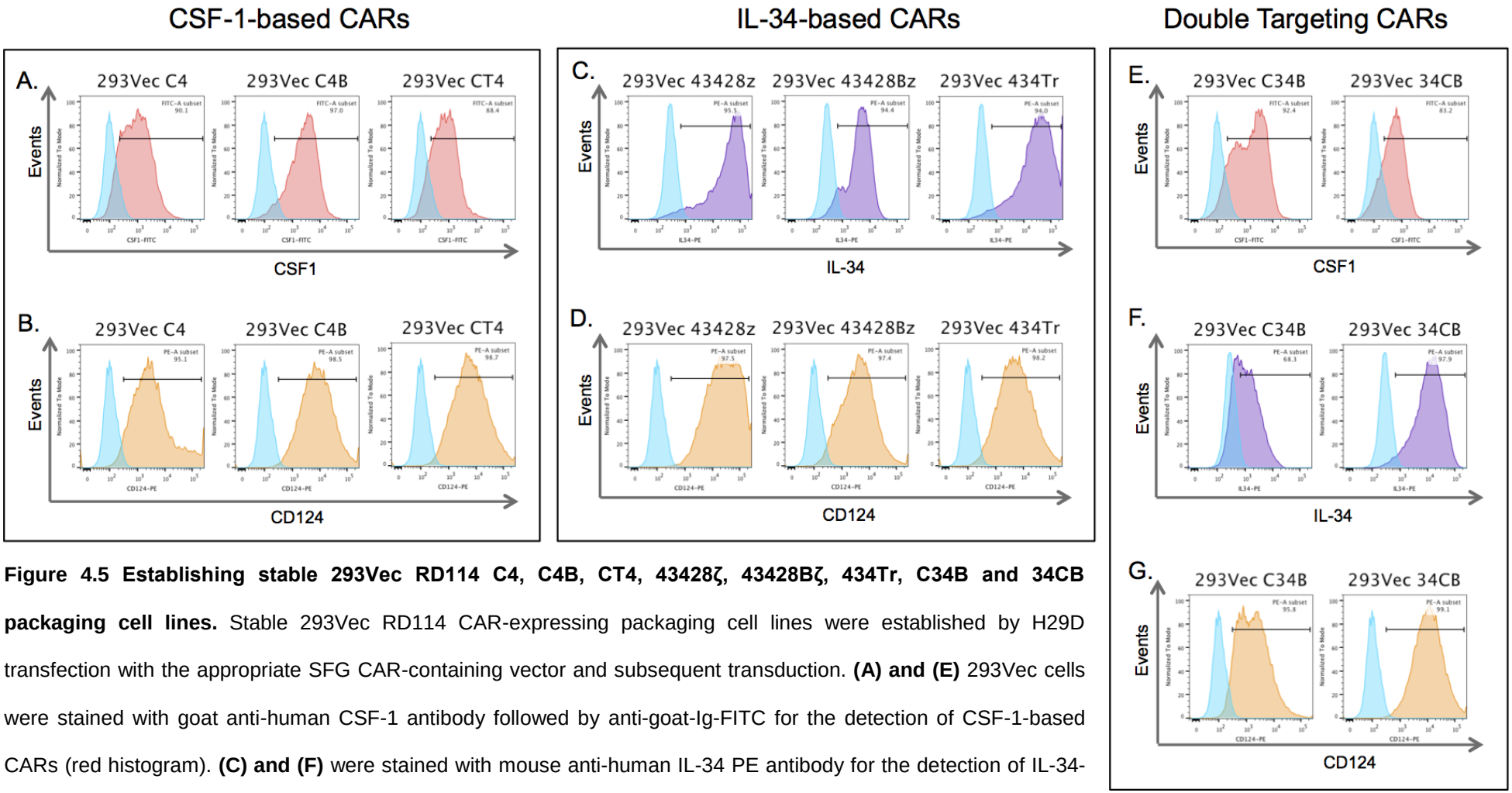

Figure 4.5 Establishing stable 293Vec RD114 C4, C4B, CT4, 43428ζ, 43428Bζ, 434Tr, C34B and 34CB packaging cell lines. Stable 293Vec RD114 CAR-expressing packaging cell lines were established by H29D transfection with the appropriate SFG CAR-containing vector and subsequent transduction. **(A) and (E)** 293Vec cells were stained with goat anti-human CSF-1 antibody followed by anti-goat-Ig-FITC for the detection of CSF-1-based CARs (red histogram). **(C) and (F)** were stained with mouse anti-human IL-34 PE antibody for the detection of IL-34-based constructs (purple histogram). **(B), (D) and (G)** 293Vec cells were stained with anti-IL4Rα-PE for the detection of 4αβ (orange histogram). The blue histogram shows the same staining on empty 293Vec RD114 cells.

4.2.3 Expression of CSF-1R-targeting CARs on primary human T-cells

Prior to testing the anti-tumour activity of the CSF-1R-targeting CARs, it was crucial to demonstrate their stable expression in primary human T-cells. Following gamma retroviral-mediated gene transfer from PG13 or 293Vec RD114 packaging cell lines, T-cells were tested for cell surface expression of the CARs using flow cytometry. As shown in Figure 4.6, A, the CARs could be detected at the cell surface, thus indicating that the constructs were expressed, folded and trafficked correctly to the plasma membrane.

The expression of the 4αβ construct by T-cells provides means for selective expansion and enrichment of CAR^+ T-cells in the presence of IL-4 [378]. Consequently, when cultured in the presence of IL-4 for 12 days, the CAR^+ T-cells received an IL-2/IL-15-like signal, thereby gaining a distinct proliferative advantage over untransduced T-cells. This resulted in the selective enrichment of the CSF-1R-targeting CAR^+ T-cell population, even in the absence of antigen (Figure 4.6, B).

To further confirm CAR expression, T-cells were lysed following retroviral-mediated gene transfer and investigated for the presence of the genetically engineered receptor using western blotting. Samples were run under reducing conditions to allow for the detection of monomeric CAR chains. Lysates were probed for the presence of the CAR through detection of the CD3ζ chain. The presence of 44-55kDa bands within the C4, C4B, C34B, 43428ζ, 43428Bζ and 34CB samples correlate well with the predicted molecular weights of the CAR constructs (44kDa, 48kDa, 44 kDa, 51kDa, 55kDa and 51kDa respectively) for all but the double targeting constructs C34B and 34CB, which travelled as 2kDa heavier bands than their predicted molecular weight (Figure 4.6, C). The absence of banding within the CT4 and 434Tr samples was expected due to the lack of the CD3ζ domain. The endogenous CD3ζ chain (16kDa) served as a convenient loading control.

As shown on Figure 4.6, D, the average T-cell transduction efficiency was comparable across the panel of CSF1-R-targeting CARs, following IL-4-mediated enrichment for 12 days. These data have been normalized against untransduced T-cells from the same donors stained using the same antibody combination.

Taken together, these data demonstrate that T-cells can be efficiently transduced to express a variety of CSF-1R-targeted CARs. Moreover, CAR expression remained stable for a number of days, even in the absence of antigen, which is crucial for the CAR^+ T-cells' ability to provide prolonged anti-tumour effect.

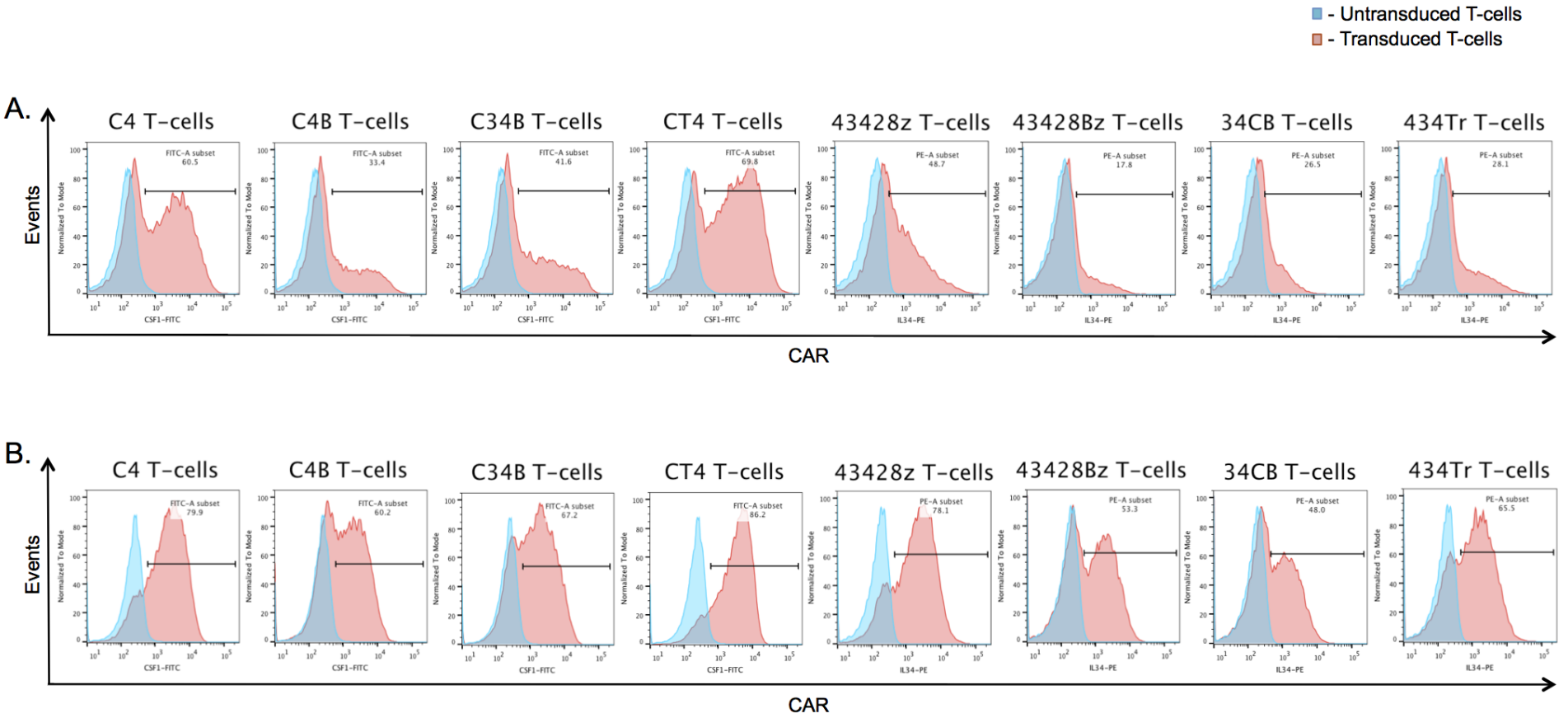

Figure 4.6 Expression of a panel of CSF-1R-targeting CARs in primary human T-cells.

Expression of various CAR constructs was detected at the cell surface of primary human T-cells as assessed by flow cytometry at Day 3 post T-cell transduction **(A)** and after 12 days expansion in the presence of 30ng/mL IL-4 **(B)**. The presence of CSF-1-based CARs was detected (figure and legend continue on next page)

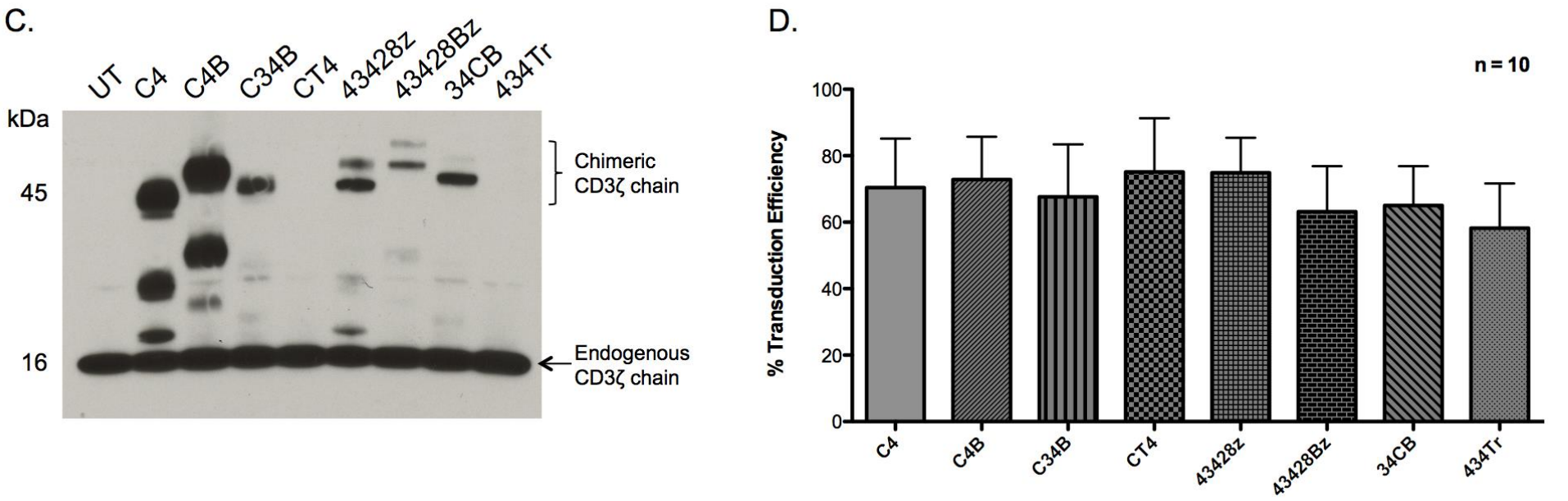

using a goat polyclonal anti-human CSF-1 antibody, followed by a FITC-conjugated secondary antibody (pink histogram). Level of expression of IL-34-based CARs was assessed using mouse anti-human IL-34 antibody directly conjugated to PE. The level of expression in both cases was compared to untransduced T-cells probed with the same antibody combinations (blue histogram). **(C)** CAR-grafted T-cells were lysed under reducing conditions and the lysates probed for the presence of the CAR using SDS-PAGE. Detection of the CAR and the CD3ζ chain loading control was achieved using a mouse monoclonal anti-human CD3ζ antibody followed by a rabbit anti-mouse IgG HRP-conjugated secondary antibody and subsequent development using enhanced chemiluminescence (ECL). **(D)** Average T-cell transduction efficiency for the different CAR constructs was calculated from 10 separate experiments. Data are presented as mean ± standard deviation and depict % CAR T-cell positivity after culture of the transduced T-cells in IL-4 for 12 days.

4.2.4 Validation of the anti-tumour potential of CSF-1R-targeted CAR$^+$ T-cells

In order to determine the cytotoxic activity of CSF-1R-targeted CAR$^+$ T-cells, experiments were performed with human breast cancer monolayers that were discordant for target antigen expression. This was achieved by co-cultivating CAR$^+$ T-cells with T47D breast cancer cells and T47D FMS, a derivative that has been genetically engineered to express high levels of CSF-1R (Figure 3.1, C).

An MTT assay was used to measure tumour cell destruction, which negatively correlates with formazan dye production. In this assay, mitochondrial dehydrogenase-catalysed conversion of a tetrazolium salt to a formazan dye indicates metabolic activity and therefore the presence of viable cells. The absorbance of the formazan dye product may be subsequently quantified and compared to the maximal formazan dye production (as determined by target cells grown in the absence of T-cells), providing a measure of target cell viability (please refer to section 2.2.9.1 for more details).

As shown in Figure 4.7, A, co-culture of T47D FMS with CSF-1R re-directed CAR$^+$ T-cells overnight at a 1:1 ratio resulted in complete target cell lysis in the presence of C4$^+$, C4B$^+$, C34B$^+$, 43428ζ$^+$, 43428Bζ$^+$ and 34CB$^+$ T-cells, while no cytotoxicity was recorded in the control groups (CT4$^+$, 434Tr$^+$ and UT T-cells). No significant destruction of the parental T47D cell line was detected (Figure 4.7, B). These data confirm that both CSF-1 and IL-34-targeted CARs can specifically engage CSF-1R-expressing tumour cells, leading to their destruction.

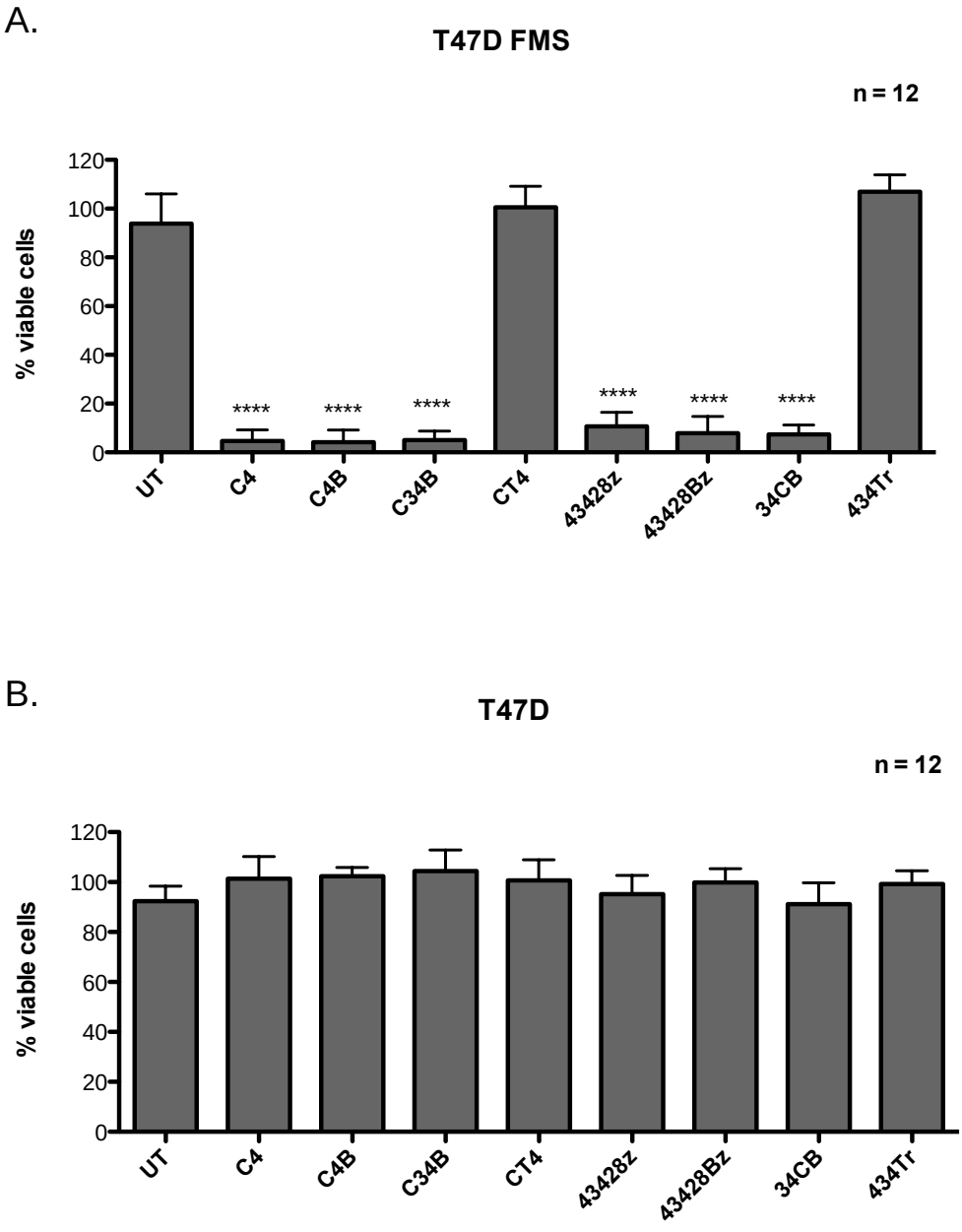

Figure 4.7 Target cell destruction following T-cell co-culture.

Human T-cells were engineered to express the indicated CARs and were cultured in IL-4 for 12 days. Engineered T-cells were then co-cultivated overnight (1:1 ratio) with T47D FMS (**A**) or T47D (**B**) target cells. Residual tumour cell viability was determined using the MTT assay. Following gentle removal of T-cells by washing, the monolayers were incubated with a tetrazolium salt solution for 2 hours and the production of a formazan dye measured by absorbance at 570nm thereafter. Data were normalized against the maximal formazan dye production, as generated by tumour cells grown in the absence of T-cells. Normalization was achieved using the following equation: (legend continues on next page)

4.2.5 Antigen-specific activation of CSF-1R-targeted T-cells

The activation of CSF-1R re-targeted CAR^+ T-cells in the presence or absence of the target (T47D FMS/ T47D co-cultures) was compared to that achieved with untransduced T-cells and the matched signalling-incompetent truncated CAR constructs. During the co-culture period, T-cell activation was monitored by measurement of the release of IFN-γ (Figure 4.8, A) and IL-2 (Figure 4.8, B). Significantly higher levels of both cytokines were produced upon co-culture of $C4^+$, $C4B^+$, $C34B^+$, $43428ζ^+$, $43428Bζ^+$ and $34CB^+$ T-cells with the T47D FMS monolayer, when compared to matched co-cultures with untransduced, $CT4^+$ or $434Tr^+$ control T-cells. No cytokine release was detected when CAR T-cells were cultured alone or co-cultivated with unmodified T47D cells (Figure 4.8), thereby confirming that CAR^+ T-cell activation was antigen dependent.

Tumour cell viability = (Sample MTT value/Average no T-cell MTT value)*100

Data were analysed using one-way ANOVA followed by a Tukey post-hoc test and were presented as mean ± standard deviation of 12 independent replicate experiments.

**** = $p<0.0001$ and is relative to UT T-cells.

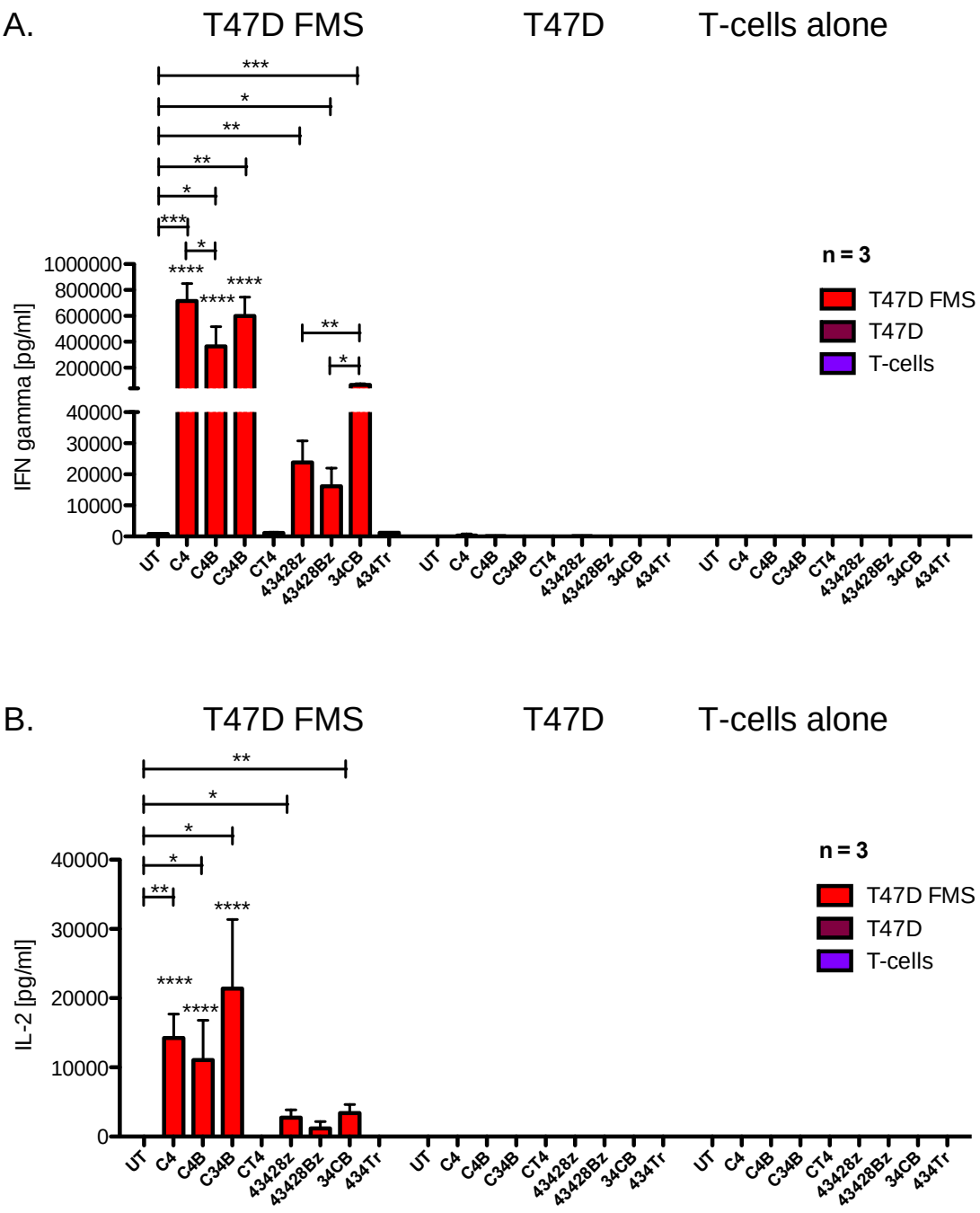

Figure 4.8 Antigen-dependent production of IFN-γ and IL-2 by CAR⁺ T-cells.

A panel of CSF-1R-targeting CAR-engrafted and untransduced (UT) T-cells were co-cultured with T47D FMS and T47D cell lines. Supernatants were removed after 24 hours and analysed for IFN-γ **(A)** and IL-2 **(B)** release using a sandwich ELISA. Data is presented as mean ± standard deviation from three independent experiments. **** = p<0.0001; *** = p<0.001; ** = p<0.01; * = p<0.05. Unless indicated otherwise, asterisks above a bar indicate that the CAR⁺ T-cells secrete significantly more cytokine on that particular cell line than on any other cell line or in the absence of monolayer.

4.2.6 Proliferative capacity of CSF-1R re-targeted T-cells upon serial re-stimulation

In order to investigate the ability of CSF-1R re-targeted CARs to promote T-cell proliferation upon multiple rounds of *in vitro* antigen exposure, co-culture experiments were performed with T47D FMS breast cancer cells. T-cells were subjected to successive rounds of antigen stimulation in the absence of exogenous cytokines. Stimulation was provided by weekly culture on T47D FMS monolayers and T-cell numbers were enumerated at the indicated intervals (Figure 4.9).

Pooled data from 7 similar replicate experiments are shown in Figure 4.9, indicating the fold expansion of CAR T-cells that occurred in the week after each cycle of stimulation. At the time of each re-stimulation cycle, T-cells were tested for their ability to kill T47D FMS and unmodified T47D monolayers (Figure 4.10). One day after each cycle of stimulation, supernatant was removed from these cultures and tested for IL-2 and IFN-γ content by ELISA (Figure 4.11). As shown on Figures 4.9, 4.10 and 4.11, the double targeting C34B CAR repeatedly outperformed conventional second and third generation CARs by maintaining high proliferative capacity, cytotoxic potential and ability to release IFN-γ and IL-2 over 15 repeated rounds of antigen stimulation.

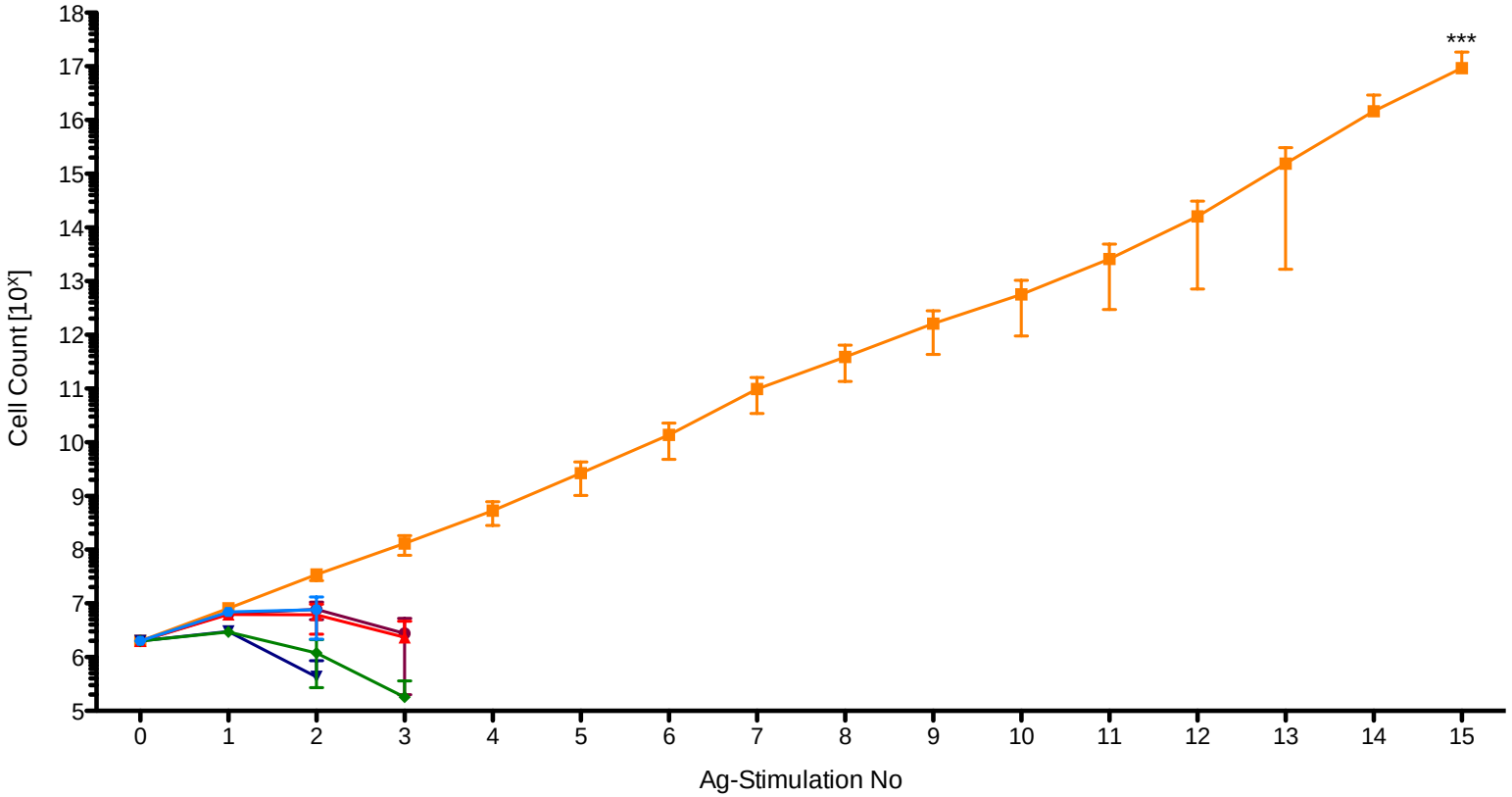

Figure 4.9 Antigen (Ag)-dependent proliferation of CAR$^+$ T-cells.

Human T-cells were engineered to express the indicated CARs. CAR T-cells were subjected to successive rounds of antigen stimulation (fresh T47D FMS monolayers at 7-day intervals) in the absence of exogenous cytokines and T-cell numbers were enumerated at the indicated intervals. Data were presented as mean ± SD from seven independent experiments. *** = p<0.001.

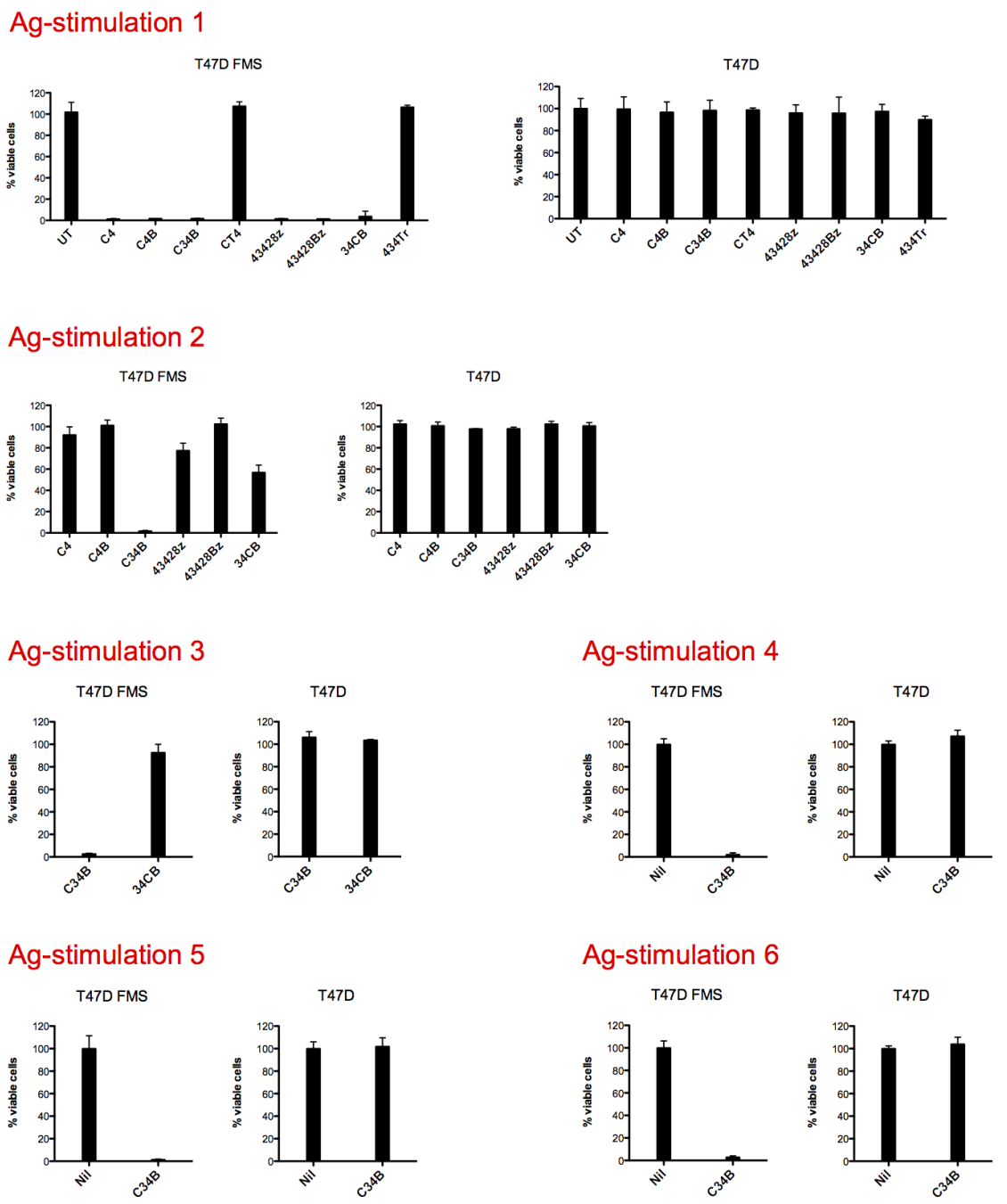

Figure 4.10 Antigen (Ag)-specific cytotoxicity of CAR$^+$ T-cells is maintained upon serial re-stimulation.

A panel of CSF-1R-targeting CAR-grafted T-cells were subjected to successive rounds of stimulation in the absence of exogenous cytokine support either in the presence (T47D FMS monolayer) or absence (T47D monolayer) of the antigen. At the time of each re-stimulation cycle, cell viability following overnight incubation with CAR$^+$ or untransduced T-cells (1:1 ratio) was quantified using the MTT assay. (figure and legend continue on next page)

Ag-stimulation 7

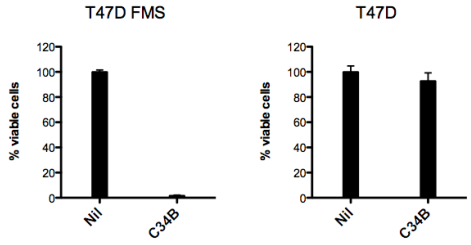

Ag-stimulation 8

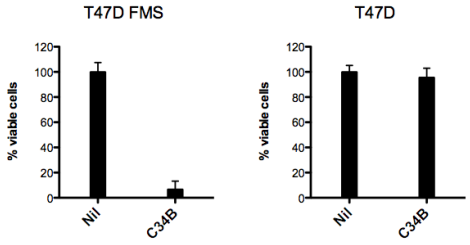

Ag-stimulation 9

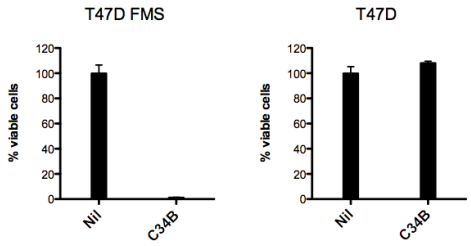

Ag-stimulation 10

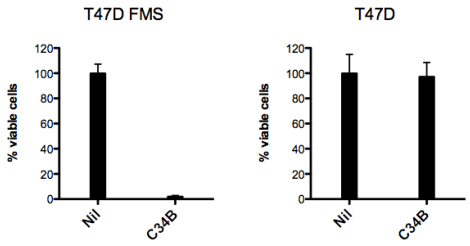

Ag-stimulation 11

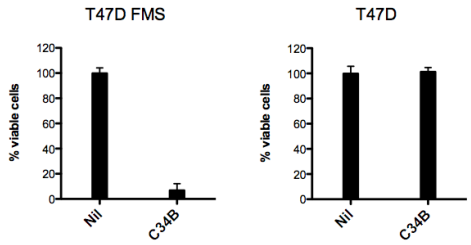

Ag-stimulation 12

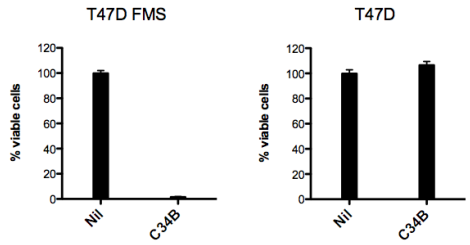

Ag-stimulation 13

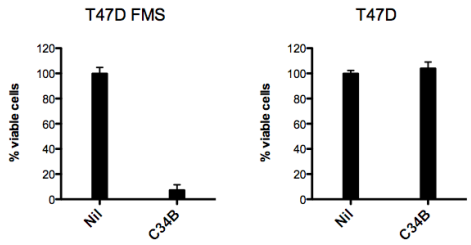

Ag-stimulation 14

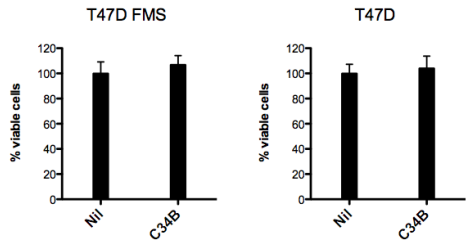

Normalization was achieved using the following equation:

Tumour cell viability = (Sample MTT value/Average no T-cell MTT value)*100

Upon each cycle of re-stimulation, cytotoxicity was quantified at 24h with the exception of the last Ag-stimulation (Ag-stimulation 14), which was measured at 72h. Data are representative of seven experiments and are presented as mean ± standard deviation of triplicates.

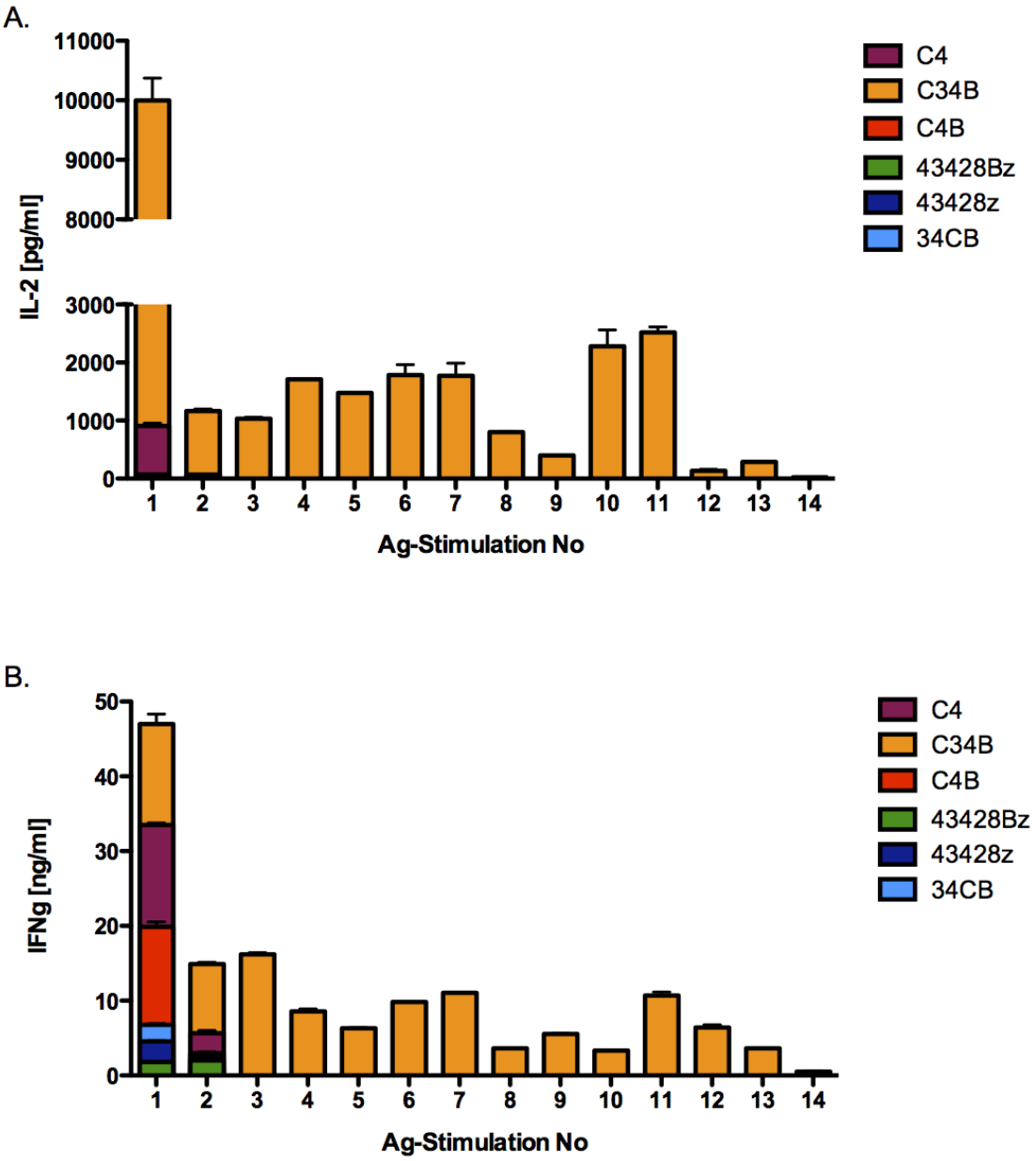

Figure 4.11 Antigen-specific cytokine release by CAR$^+$ T-cells is maintained upon serial re-stimulation.

A panel of CSF-1R-targeting CAR-grafted T-cells were subjected to successive rounds of stimulation on T47D FMS monolayers, in the absence of exogenous cytokine support. One day after each cycle of stimulation, supernatant was removed from these cultures and tested for IL-2 **(A)** and IFN-γ **(B)** release by sandwich ELISA. Data are representative of seven experiments and are presented as mean ± standard deviation from triplicates.

4.2.7 Targeting cHL and ALCL cell lines using CSF-1R re-targeted T-cells

In order to investigate whether CSF-1R re-targeted T-cells have the ability to recognize lymphoma cells *in vitro*, a series of co-culture experiments were undertaken with a panel of cHL and ALCL lymphoma cell lines. One possible way of determining the cytotoxic potential of T-cells is by target cell labelling prior to co-culture with T-cells. Common labelling reagents include the radioisotope ^{51}chromium [149], the fluorescent ester calcein-acetoxymethyl (calcein-AM) [379] and carboxyfluorescein succinimidyl ester (CFSE) [380].

A more elegant alternative to the target cell CFSE labelling approach (Appendix, Figure S3) was achieved by stably expressing both a firefly luciferase enzyme and the red fluorescent protein tdTomato in the lymphoma cell lines. Expression of both genes from one open reading frame was achieved by inserting a furin cleavage site followed by a flexible serine-glycine linker and a T2A sequence between them. Both genes were cloned as a single cDNA cassette, flanked by NcoI/XhoI restriction sites within the SFG retroviral vector (SFG LuciTom) (Figure 4.12, A). The tdTomato red fluorescent protein emits bright red fluorescence at a peak wavelength of 581nm. It was used as a fluorescent reporter for the identification of tumour cells within a co-culture with CAR$^+$ T-cells. Firefly luciferase catalyses the conversion of a molecule of D-luciferin to an electronically 'excited' molecule of oxyluciferin when in the presence of magnesium, ATP and oxygen. Since dead cells cannot catalyze this reaction, the number of viable cells determined the amount of luminescence detected, indicating the degree of cytotoxicity caused (please refer to section 2.2.9.3 for more details).

A PG13 LuciTom retroviral packaging cell line was generated in a two-step process involving H29D transfection and subsequent PG13 retroviral transduction (Figure 4.12, B). The PG13-derived viral particles were then used to establish stable expression of the SFG LuciTom construct in the panel of lymphoma cell lines (Figure 4.12, C, D and E). Transduced lymphoma cells were then cell sorted to achieve >90% LuciTom$^+$ (LT$^+$)

expression in the population. Furthermore, LuciTom expression was maintained over a prolonged period in culture, highlighting successful integration of the cDNA into the recipient genome.

As the overall aim of this project was to determine whether CSF-1R re-targeted T-cells represent a potential therapy for cHL and ALCL, it was important to determine their ability to destroy cHL and ALCL cell lines *in vitro*. Lymphoma cell lines were co-cultured at a 1:1 ratio with CAR^+ or untransduced (UT) T-cells and co-cultures were probed for luciferase activity at 24h, 48h, 72h, 96h, 120h, and 144h, providing a measure of target cell viability. The data was normalized against the maximal luminescence, as shown by tumour cells grown in the absence of T-cells. As shown on Figure 4.13, 4.14, 4.15, 4.16, 4.17 and 4.18 co-culture of CAR^+ T-cells resulted in variable clearance of the target cells – from complete destruction (DEL cell line at 48h) to 50% residual viable cells (K299 cell line at 144h). Results are representative of 5 separate experiments. Overall, CSF-1-based CARs elicited higher target cell lysis than IL-34-based CARs, with no significant difference in the cytotoxic potency of second and third generation CARs within each group (Appendix, Table S1). Importantly, there was no reduction in lymphoma cell viability upon incubation with either $CT4^+$, $434Tr^+$ or UT T-cells, when compared to target cells grown in the absence of T-cells.

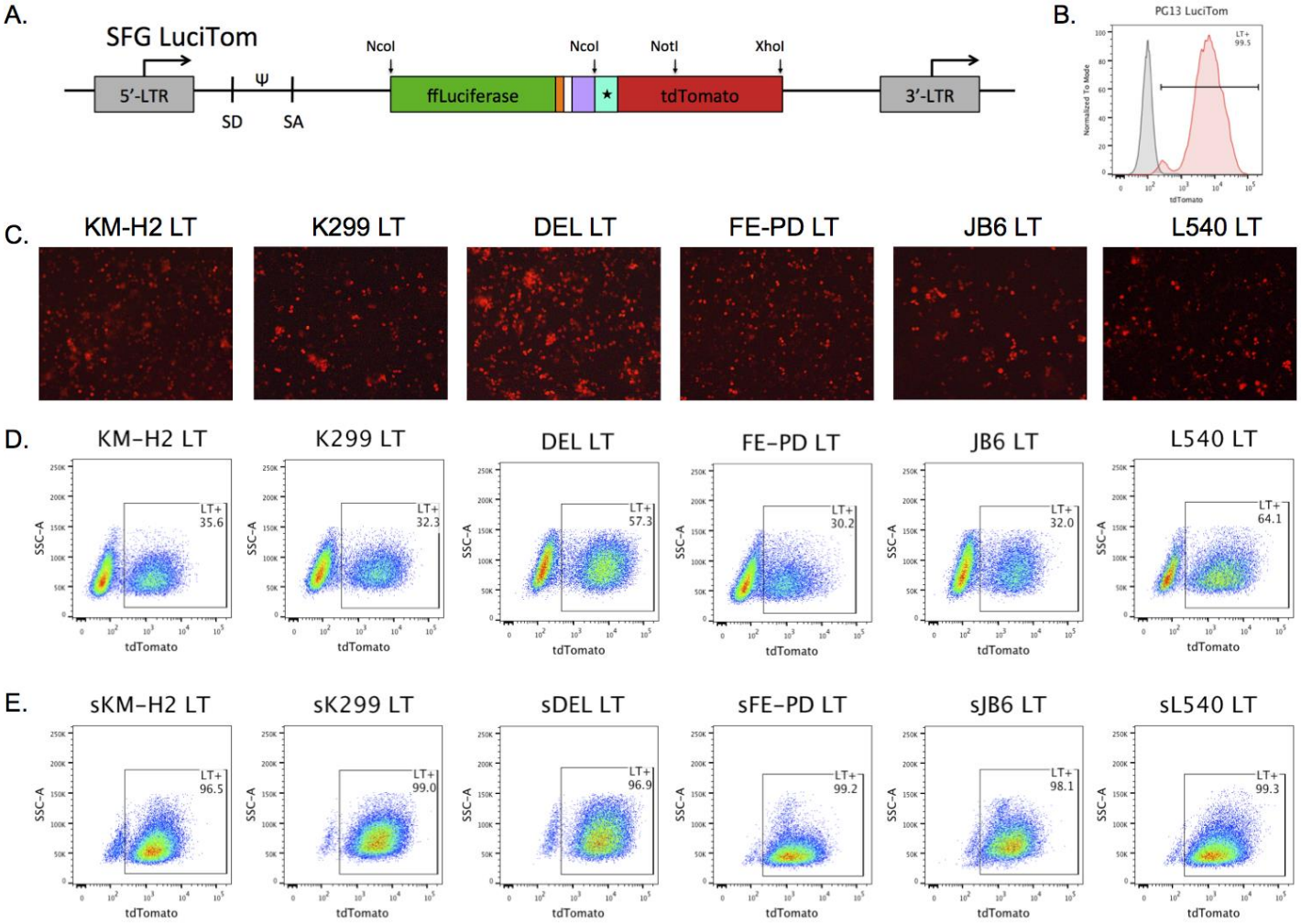

Figure 4.12 Stable expression of the SFG LuciTom construct in lymphoma cell lines. (legend continues on next page)

4.2.8 Determination of CSF-1R re-targeted T-cell activation on cHL and ALCL cell lines.

The secretion of IFN-γ and IL-2 by CSF-1R re-targeted T-cells was dependent upon recognition of target antigen, as indicated by detection of high levels of both cytokines following co-culture with T47D FMS cells. Furthermore, CAR-transduced cells were not constitutively active as demonstrated by the lack of cytokine secretion upon co-culture with T47D cells (Figure 4.8).

To investigate whether expression of CSF-1R-targeted CARs enabled re-direction of T-cell specificity against cHL and ALCL, engineered T-cells were co-cultured with a panel of lymphoma cell lines (Figure 4.19 and 4.20). A substantially (and in many cases significantly) greater concentration of IFN-γ (Figure 4.19) and IL-2 (Figure 4.20) was detected in the co-cultures with $C4^+$, $C4B^+$, $C34B^+$, $43428\zeta^+$, $43428B\zeta^+$ and $34CB^+$ T-cells when compared to $CT4^+$, $434Tr^+$ or UT T-cells. No statistically significant differences in cytokine production were detected between double targeting, second and third generation CARs or between CSF-1-based and IL-34-based CAR-grafted T-cells (Appendix, Table S2).

Taken together, cytotoxicity and cytokine release data show that CSF-1R re-targeted T-cells but not control T-cells can be specifically re-directed *in vitro* against cHL and ALCL cell lines.

(A) Structure of the SFG LuciTom retroviral vector. Stoichiometric co-expression of ffLuciferase and tdTomato is achieved through the use of a T2A sequence. **(B)** A stable PG13 LuciTom expressing retroviral packaging cell line was established, as verified by flow cytometry and the collected viral particles were used for transduction of a panel of lymphoma cell lines. Successful transduction was verified by fluorescence microscopy **(C)** and flow cytometry **(D)**. Transduced lymphoma cell lines were annotated with "LT" after their name (e.g. DEL LT) and, following cell sorting for tdTomato expression, "s" was added to the name (e.g. sDEL LT) **(E)**.

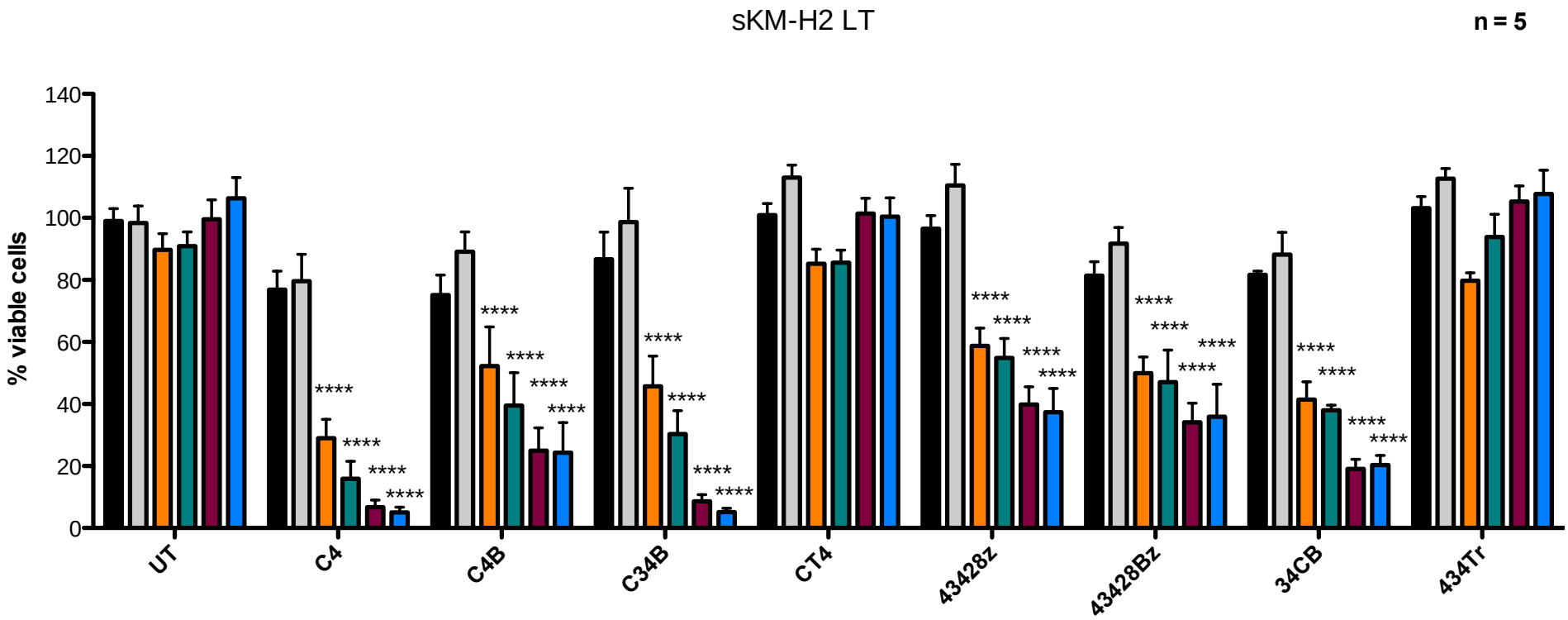

Figure 4.13 Cytotoxicity of CSF-1R-retargeted T-cells against the KM-H2 cell line *in vitro.*

The cHL cell line KM-H2 was co-cultured with a panel of CAR-grafted T-cells at a 1:1 ratio for the indicated period of time. The level of target cell viability following co-culture was monitored using a luciferase assay. Data were normalised against the maximal luminescence, as shown by tumour cells grown in the absence of T-cells. Normalization was achieved using the following equation: Tumour cell viability = (Sample luminescence value / Average luminescence value when no T-cells added)*100. Data are presented as mean ± SD from five independent experiments. **** = $p<0.0001$; *** = $p<0.001$; ** = $p<0.01$; * = $p<0.05$ relative to UT T-cells at any given time point.

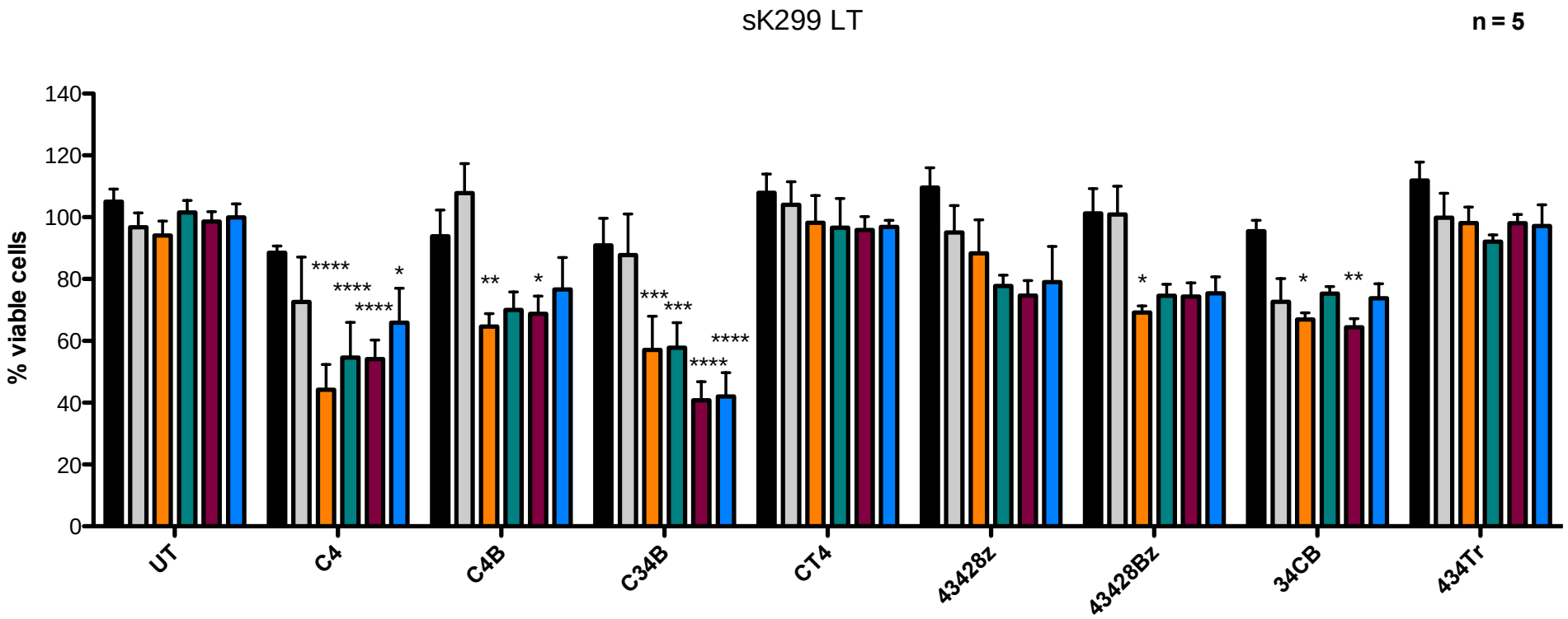

Figure 4.14 Cytotoxicity of CSF-1R-retargeted T-cells against the K299 cell line *in vitro.*

The ALCL cell line K299 was co-cultured with a panel of CAR-grafted T-cells at a 1:1 ratio for the indicated period of time. The level of target cell viability following co-culture was monitored using a luciferase assay. Data were normalised against the maximal luminescence, as shown by tumour cells grown in the absence of T-cells. Normalisation was achieved using the following equation: Tumour cell viability = (Sample luminescence value / Average luminescence value when no T-cells added)*100**.** Data are presented as mean ± SD from five independent experiments. **** = $p<0.0001$; *** = $p<0.001$; ** = $p<0.01$; * = $p<0.05$ relative to UT T-cells at any given time point.

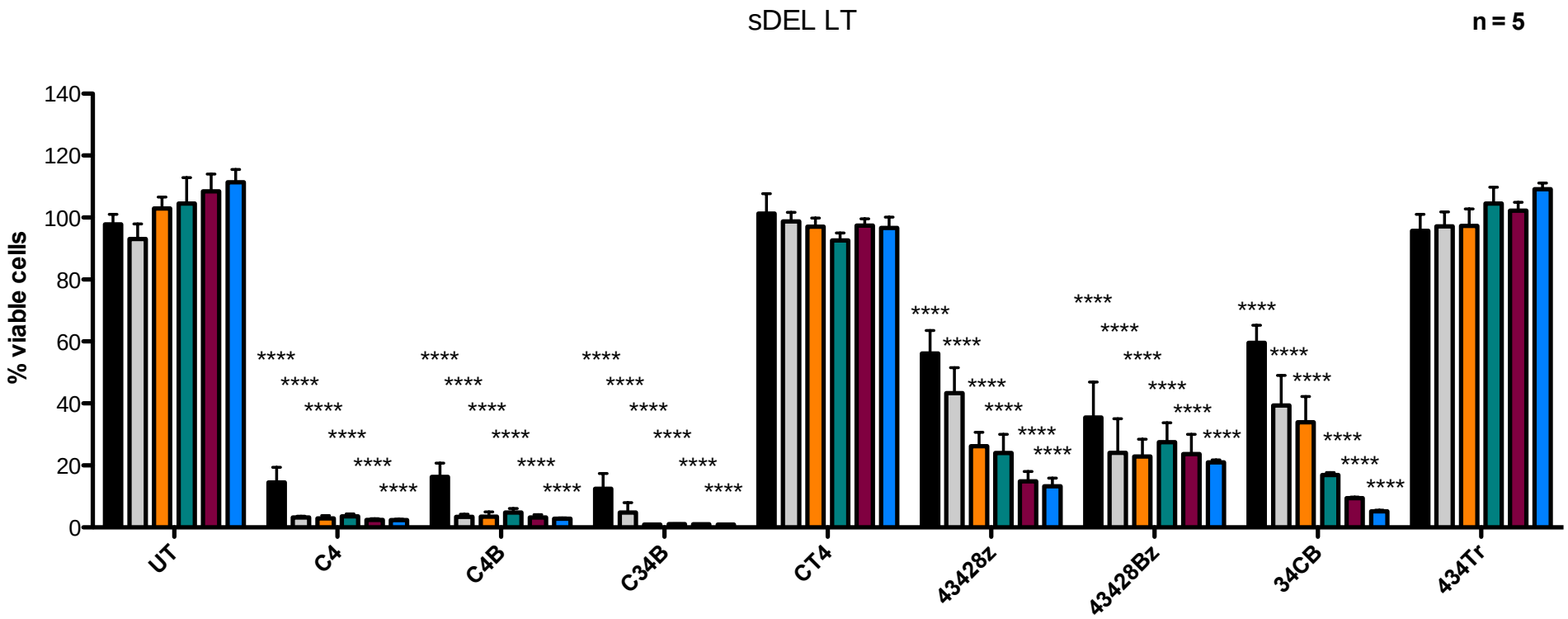

Figure 4.15 Cytotoxicity of CSF-1R-retargeted T-cells against the DEL cell line *in vitro*.

The ALCL cell line DEL was co-cultured with a panel of CAR-grafted T-cells at a 1:1 ratio for the indicated period of time. The level of target cell viability following co-culture was monitored using a luciferase assay. Data were normalised against the maximal luminescence, as shown by tumour cells grown in the absence of T-cells. Normalisation was achieved using the following equation: Tumour cell viability = (Sample luminescence value / Average luminescence value when no T-cells added)*100. Data are presented as mean ± SD from five independent experiments. **** = p<0.0001; *** = p<0.001; ** = p<0.01; * = p<0.05 relative to UT T-cells at any given time point.

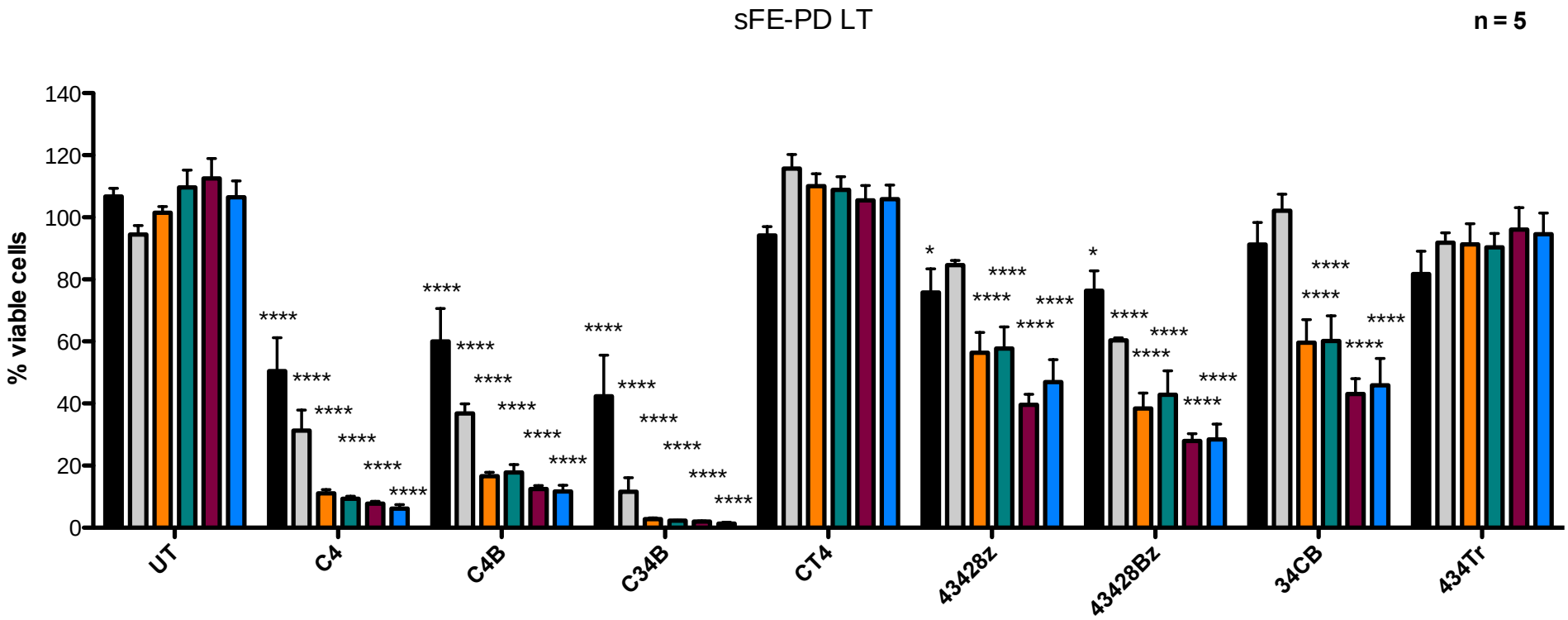

Figure 4.16 Cytotoxicity of CSF-1R-retargeted T-cells against the FE-PD cell line *in vitro*.

The ALCL cell line FE-PD was co-cultured with a panel of CAR-grafted T-cells at a 1:1 ratio for the indicated period of time. The level of target cell viability following co-culture was monitored using a luciferase assay. Data were normalised against the maximal luminescence, as shown by tumour cells grown in the absence of T-cells. Normalisation was achieved using the following equation: Tumour cell viability = (Sample luminescence value / Average luminescence value when no T-cells added)*100**.** Data are presented as mean ± SD from five independent experiments. **** = p<0.0001; *** = p<0.001; ** = p<0.01; * = p<0.05 relative to UT T-cells at any given time point.

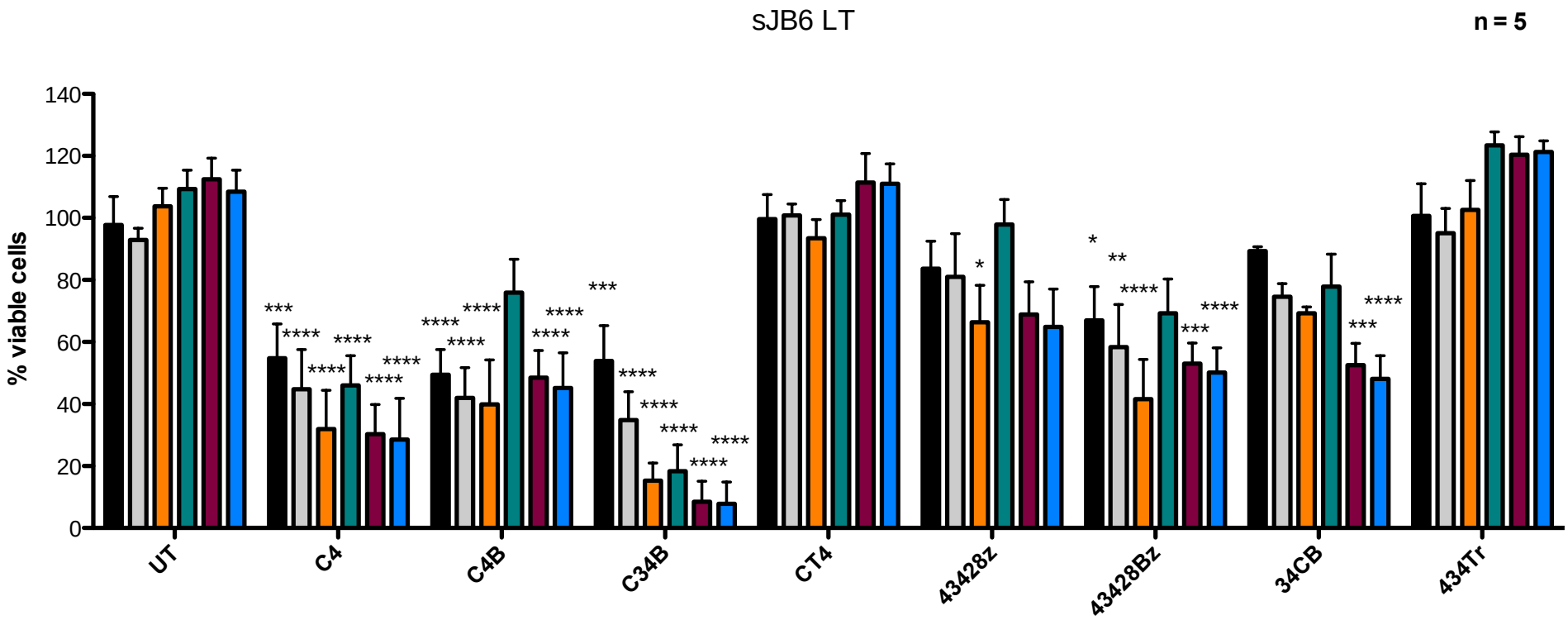

Figure 4.17 Cytotoxicity of CSF-1R-retargeted T-cells against the JB6 cell line *in vitro.*

The ALCL cell line JB6 was co-cultured with a panel of CAR-grafted T-cells at a 1:1 ratio for the indicated period of time. The level of target cell viability following co-culture was monitored using a luciferase assay. Data were normalised against the maximal luminescence, as shown by tumour cells grown in the absence of T-cells. Normalisation was achieved using the following equation: Tumour cell viability = (Sample luminescence value / Average luminescence value when no T-cells added)*100. Data are presented as mean ± SD from five independent experiments. **** = p<0.0001; *** = p<0.001; ** = p<0.01; * = p<0.05 relative to UT T-cells at any given time point.

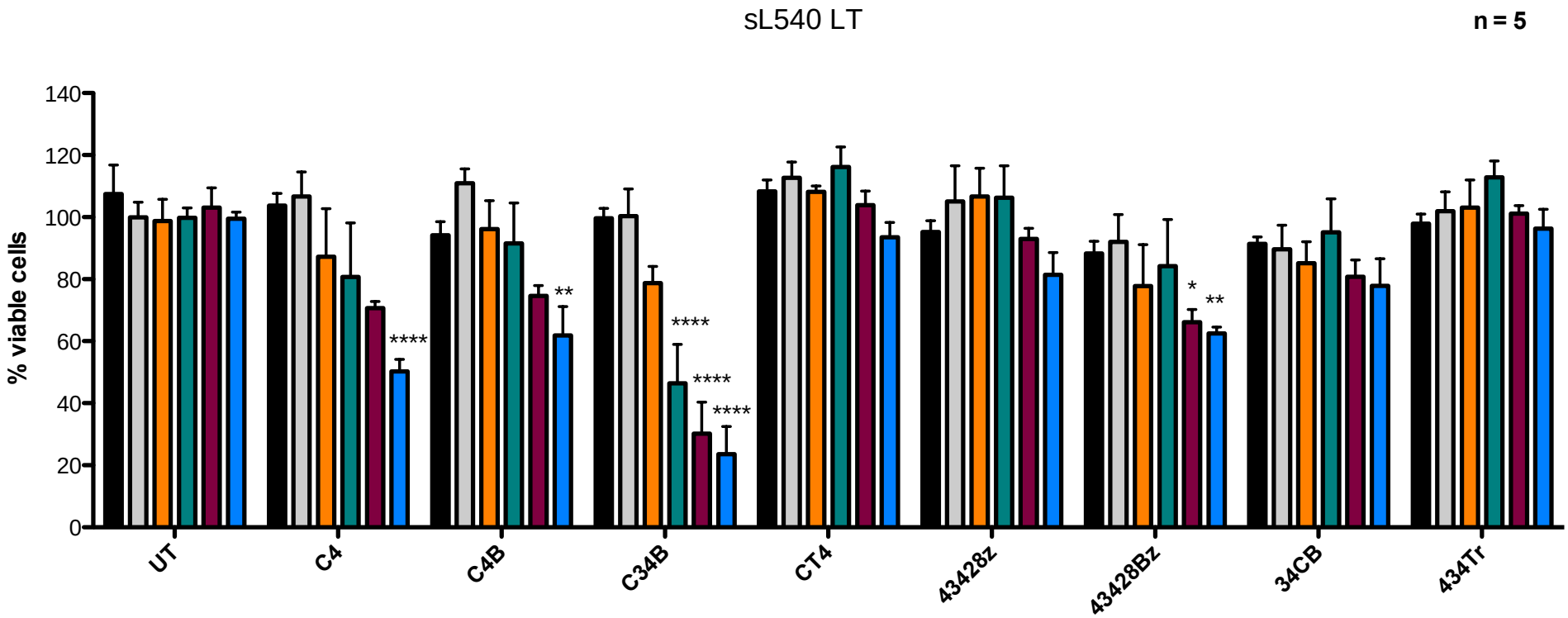

Figure 4.18 Cytotoxicity of CSF-1R-retargeted T-cells against the L540 cell line *in vitro*.

The cHL cell line L540 was co-cultured with a panel of CAR-grafted T-cells at a 1:1 ratio for the indicated period of time. The level of target cell viability following co-culture was monitored using a luciferase assay. Data were normalised against the maximal luminescence, as shown by tumour cells grown in the absence of T-cells. Normalisation was achieved using the following equation: Tumour cell viability = (Sample luminescence value / Average luminescence value when no T-cells added)*100. Data are presented as mean ± SD from five independent experiments. **** = p<0.0001; *** = p<0.001; ** = p<0.01; * = p<0.05 relative to UT T-cells at any given time point.

4.3 Discussion

The overall aim of this project was to investigate whether T-cells can be genetically re-targeted against CSF-1R and consequently to test the feasibility of this approach, as a novel CAR-based adoptive T-cell therapy for cHL and ALCL.

A major obstacle to effective CAR-based T-cell immunotherapy of cancer is poor survival *in vivo* of the genetically modified infused cells. T-cell expansion is generally induced by IL-2. However IL-2 is toxic when administered in high doses and furthermore it exerts similar stimulatory effects on gene modified, non-gene modified and regulatory T cells (Treg). The 4αβ chimeric cytokine receptor addresses exactly this limitation. It is designed as a fusion protein of the IL-4 receptor alpha (IL-4Rα) ectodomain and the common beta subunit (β_C) shared by IL-2 and IL-15 (Figure 2.1, page 74) [365]. Upon administration of IL-4 (a poor T-cell mitogen), 4αβ heterodimerises with the common gamma chain (γ_C) delivering proliferation signals selectively to 4αβ$^+$ T-cells. Thus 4αβ$^+$ T-cells achieve a strong selective advantage over untransduced cells when cultured in IL-4, which makes 4αβ a useful tool for *ex vivo* expansion and enrichment of CAR$^+$ T-cells. Additionally some tumours secrete IL-4 in the immediate microenvironment, which could theoretically induce 4αβ-CAR$^+$ T-cell trafficking towards the tumour site followed by local expansion and survival of the genetically modified T-cells. In the case of cHL, primary HRS cells have been shown to express IL-4Rα but no endogenous IL-4 production has been detected. However, low levels of IL-4 have been detected within the reactive infiltrate but there is no evidence that it acts as a growth factor for Hodgkin's Reed Sternberg (HRS) cells [381]. In the context of ALCL, endogenous IL-4 secretion has been the subject of little investigation. One study has outlined that five out of eight ALCL cell lines express low levels of IL-4 [382]. In light of these findings, stoichiometric co-expression of 4αβ and CSF-1R-targeting CAR was sought to support CAR-based immunotherapy of CSF-1R-expressing malignancies.

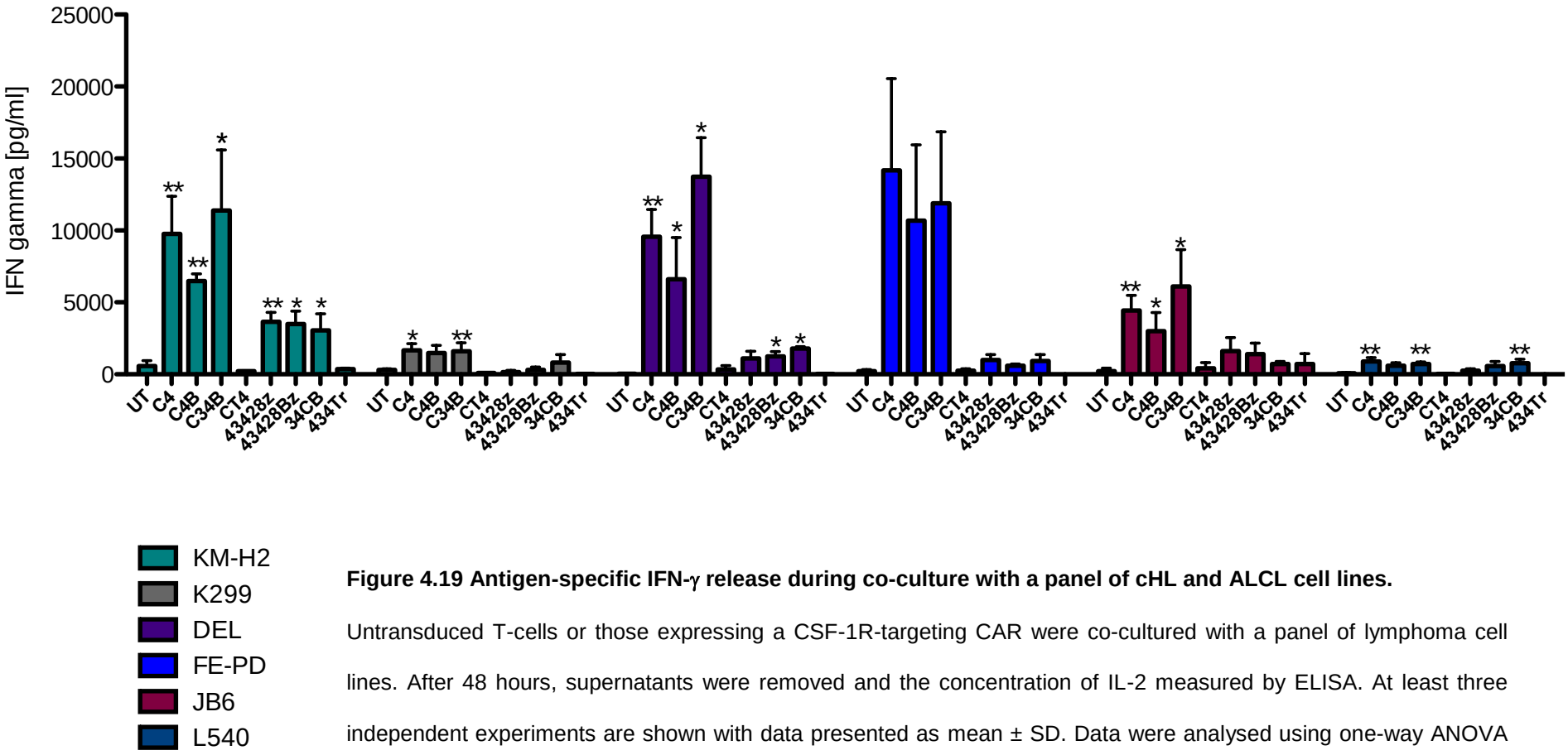

Figure 4.19 Antigen-specific IFN-γ release during co-culture with a panel of cHL and ALCL cell lines.

Untransduced T-cells or those expressing a CSF-1R-targeting CAR were co-cultured with a panel of lymphoma cell lines. After 48 hours, supernatants were removed and the concentration of IL-2 measured by ELISA. At least three independent experiments are shown with data presented as mean ± SD. Data were analysed using one-way ANOVA followed by a Tukey post-hoc test. *p<0.05; **p<0.01; ***p<0.001.

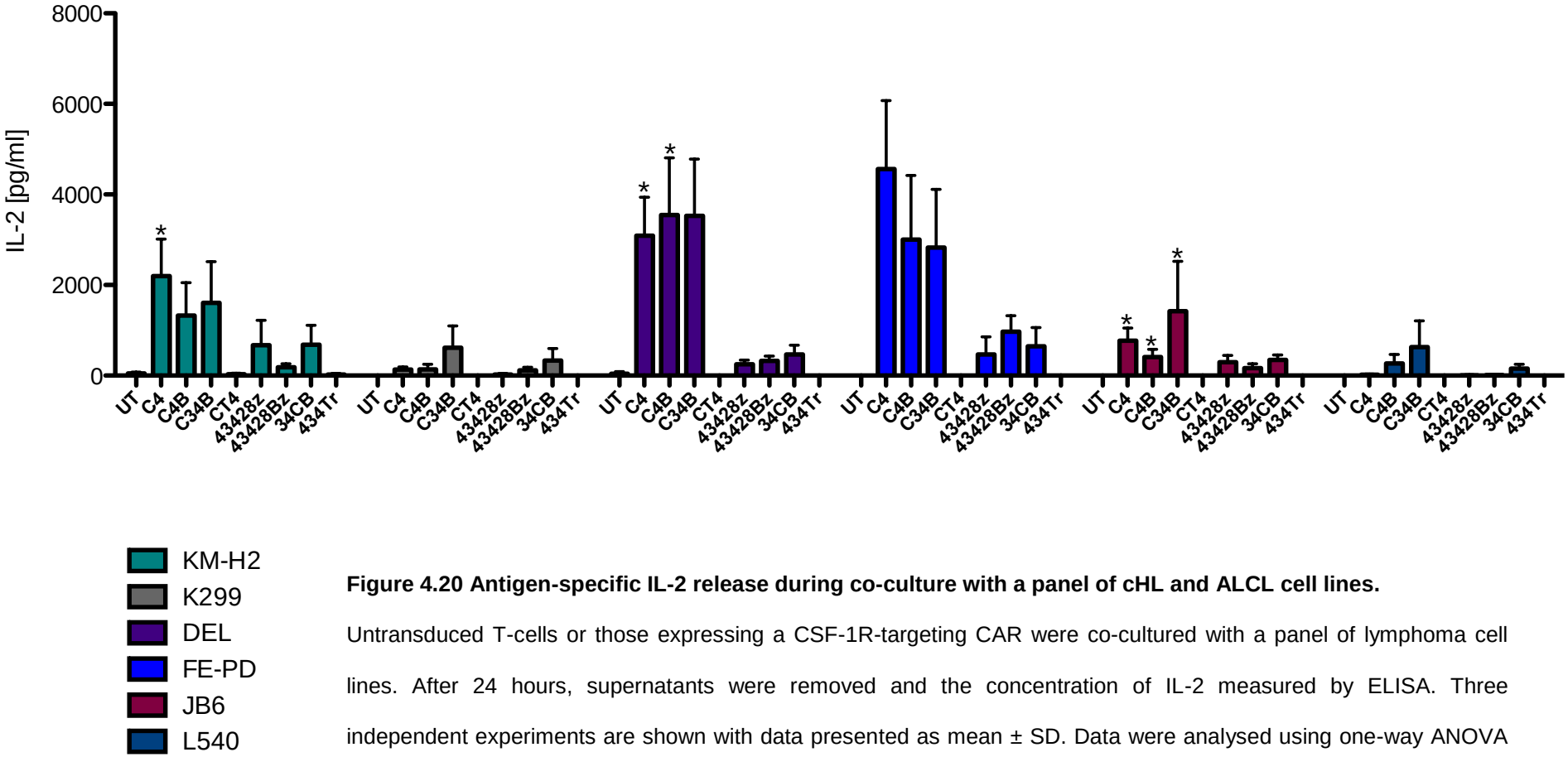

Figure 4.20 Antigen-specific IL-2 release during co-culture with a panel of cHL and ALCL cell lines.

Untransduced T-cells or those expressing a CSF-1R-targeting CAR were co-cultured with a panel of lymphoma cell lines. After 24 hours, supernatants were removed and the concentration of IL-2 measured by ELISA. Three independent experiments are shown with data presented as mean ± SD. Data were analysed using one-way ANOVA followed by a Tukey post-hoc test. *p<0.05; **p<0.01; ***p<0.001.

A panel of eight CSF-1R-targeting CARs were cloned using the PIPE cloning method, which is a PCR-based alternative to the conventional restriction enzyme- and ligation-dependent cloning methods (Figure 4.2 and 4.3) [249]. This approach eliminates the use of restriction enzymes and ligation, and thus the incorporation of restriction sites, which could encode extra, unwanted residues into expressed proteins [250]. To enable stoichiometric co-expression of 4αβ and a CSF-1R targeting CAR in the same cell, a self-cleaving 2A peptide sequence was introduced between the two constructs.

For the design of the panel of CSF-1R-targeting CARs, both naturally occurring CSF-1R ligands (CSF-1 and IL-34) were used as antigen-recognition domains. Please refer to Figure 2.1 (page 74) and Figure 2.2 (page 80) for schematic representation of the various CSF-1R-targeting CAR constructs used in this chapter. Taking into consideration that IL-34 has been reported to have considerably higher affinity towards the target than CSF-1 does, double targeting, second and third generation CARs utilizing each of those peptides as targeting moieties have been engineered [102]. This approach was undertaken in an attempt to explore the potential impact that target-binding affinity could have on CAR function, both in the context of a single CAR and a co-expressed pair of fusion receptors.

In order to achieve stable transduction of human T-cells, two CAR-expressing retroviral packaging cell lines have been generated – PG13 and 293Vec RD114. Successful generation of CAR-expressing packaging cell lines was confirmed by flow cytometry. Cell surface expression of both 4αβ and each CAR construct was confirmed in retroviral packaging cells. Despite expecting stoichiometric co-expression of 4αβ and each CAR in the same cell, slight variations in mean fluorescence intensity (MFI) were observed, which could be attributed to the different binding affinities of the antibodies used (Figure 4.4 and 4.5).

Prior to investigating whether T-cells can be genetically re-targeted against CSF-1R, it was of initial importance to demonstrate that the panel of eight CARs can be expressed at the T-cell surface following gamma retroviral-mediated gene transfer. This was confirmed by flow cytometry on a number of occasions (Figure 4.6, A) and suggests correct folding and trafficking of all chimeric constructs to the plasma membrane. The 4αβ chimeric cytokine receptor proved useful as a device to achieve selective expansion and enrichment of CAR^+ T-cells, as demonstrated by increase in the percentage of CAR^+ T-cells when grown in IL-4 in the absence of antigen (Figure 4.6, B). This enabled experiments to be performed using T-cell populations in which the proportion of gene-modified cells was similar. Furthermore, CAR expression was maintained over the 12-day culture period in IL-4, highlighting successful integration of the receptor cDNA into the recipient T-cell genome.

Further analysis of CAR expression in primary human T-cells was performed by western blotting analysis (Figure 4.6, C). Whole cell lysates were run on SDS-PAGE under reducing conditions, subjected to immunoblotting and then probed using a CD3ζ-specific antibody. The lower band (16kDa) is the endogenous CD3ζ chain, which was used as a loading control. The monomeric CAR chains were detected at the expected molecular weight for all but the double targeting constructs C34B and 34CB, which were seen as 46kDa and 53kDa bands respectively as opposed to the predicted 44kDa (C34B) and 51kDa (34CB). The most likely explanation for this discrepancy is a non-functional second furin cleavage site leading to inclusion of the T2A sequence at the C-terminal end of the C28ζ and 3428ζ constructs respectively. Even though not desirable, this fusion does not seem to interfere with T-cell activation or cytotoxicity as demonstrated in Figure 4.7 and 4.8.

Despite using the 4αβ chimeric cytokine receptor for enrichment of CAR-grafted T-cells, the level of T-cell transduction varied between experiments and between the constructs being expressed (Figure 4.6, D). This in part can be attributed to intrinsic

difference associated with using T-cells from a variety of donors. For example, donor cell responsiveness to activation with anti-CD3/28 beads is central to effective T-cell transduction because retrovirally mediated infection is dependent on progression through the cell cycle. Additionally, viral titres were not determined prior to T-cell transduction, allowing for different levels of virus exposure of the recipient T-cells. Lastly, the surface level of expression of the GALV receptor, Pit1 and the RD114 receptor, RDR, may have varied between donors, accounting for inter-donor variation of the transduction efficiency [383, 384].

In order to assess whether T-cells can be genetically re-targeted against CSF-1R, co-cultures were set up with T47D FMS cells, which have been shown to express high levels of the target CSF-1R in a stable manner. Cancer cell destruction was measured in an MTT assay. As shown on Figure 4.7, A, overnight co-culture of T47D FMS with CSF-1R re-targeted CAR^+ T-cells resulted in complete target cell lysis in the presence of $C4^+$, $C4B^+$, $C34B^+$, $43428\zeta^+$, $43428B\zeta^+$ and $34CB^+$ T-cells. No significant destruction was detected against the parental T47D cell line, which does not express the target CSF-1R and thus serves as a negative control (Figure 4.7, B).

Destruction of the T47D FMS monolayers was correlated with preceding CAR^+ T-cell activation. The release of significant amounts of both IFN-γ (Figure 4.8, A) and IL-2 (Figure 4.8, B) by CSF-1R-targeting T-cells ($C4^+$, $C4B^+$, $C34B^+$, $43428\zeta^+$, $43428B\zeta^+$ and $34CB^+$ T-cells), but not by control T-cell populations ($CT4^+$, $434Tr^+$ and UT T-cells) shows that these CARs must be able to bind the target receptor and are subsequently capable of activating primary human T-cells. This is further strengthened by the fact that CAR^+ T-cell activation occurred only in the presence of the antigen (T47D FMS cells) and not upon co-culture with the negative control T47D cell line ($CSF\text{-}1R^{NEG}$) or in the absence of monolayer (T-cells group), thereby confirming that activation of these T-cells must be occurring through the CARs themselves.

Despite similar cytotoxicity exerted by all signalling-capable CSF-1 and IL-34-based CARs, cytokine release as measured by ELISA revealed a considerable difference between those two groups. Although not statistically significant, there was a trend towards release of greater concentrations of both IFN-γ and IL-2 by CSF-1-based CAR^+ T-cells compared to IL-34-based CAR^+ T-cells. This observation can be attributed to a number of factors. Differences in transduction efficiency and CAR density on the cell surface provide one possible explanation, but given that all CAR^+ T-cells were expanded and enriched in IL-4 that seems unlikely. It is important to note that immunophenotyping of the CAR^+ T-cells was not undertaken. Therefore the possibility of CAR molecules being predominantly expressed in different T-cell subsets cannot be ruled out, though it is highly unlikely given that T-cell transduction was achieved using identical viruses. The most probable explanation for the observed differences in T-cell activation lies in the CAR design itself. The higher affinity of IL-34 interaction with the target might prove an impediment to serial target engagement and disengagement by CAR^+ T-cells. In fact, a similar phenomenon has been described with TCR-peptide-MHC (TCR-pMHC) interaction. In an elegant study, Valitutti and colleagues have demonstrated that a single pMHC complex appears to engage and downregulate up to 200 TCR molecules per T-cell in a process they refer to as “serial triggering” [385]. This serial triggering of TCRs has since been widely accepted as central to optimal signalling of the T-cell. Consequently, long TCR-pMHC lifetimes of dissociation might prevent serial triggering and thus signalling. In support of this notion are a number of studies demonstrating that T-cells that have TCRs with higher affinity or slower off-rates for pMHC exhibit reduced activity for the pMHC [386-389]. Of particular interest is a recent study that examined two different class I-reactive T-cell systems concluding that higher affinity (slower off-rates) for a pMHC yielded reduced activity [390]. Taking these findings into account it was suggested that the higher affinity of IL-34 interaction with the target is the most probable cause for the lower biological activity of these CAR-grafted T-cells.

Interestingly, no considerable differences in cytokine release or cytotoxicity were observed between double targeting, second or third generation CARs in the CSF-1-based group (Figure 4.8, A). In the IL-34-based group however, significantly higher concentration of IFN-γ, but not IL-2, was produced by the double targeting CAR 34CB in comparison to either second or third generation CARs. This observation could reflect the improved activation status of 34CB$^+$ T-cells as a result of the second CSF-1-based CAR providing co-stimulation through 4-1BB upon target recognition.

As T-cell proliferation is a key aspect of the activation process, it was used as an additional marker to assess efficient target engagement and optimal T-cell activation. All signalling-competent CSF-1R-targeting CAR constructs showed identical cytolytic capacity *in vitro* upon encountering the target for the first time (Figure 4.7). However, upon exposing CAR-grafted T-cells to successive rounds of antigen stimulation (in the absence of exogenous cytokines), while at the same time measuring their proliferative capacity, the C34B CAR repeatedly outperformed matched second and third generation CARs (Figure 4.9). In addition, the proliferation of the C34B$^+$ T-cells, ability to maintain their cytotoxic potency and to release IL-2 was maintained over 15 repeated rounds of stimulation with antigen-expressing tumour cells (Figure 4.9, 4.10 and 4.11). Interestingly, the proliferative advantage of C34B$^+$ T-cells was not retained in 34CB-bearing T-cells. This underlines the importance of fine-tuning signal transduction upon CAR engagement in respect to the balance of co-stimulatory signals provided and their functional outcome. Although more needs to be learned about CD28 and 4-1BB function as co-stimulatory domains within CARs, recent data indicates that CD28 signalling results in brisk proliferative response and boost effector functions, whereas 4-1BB signalling induces a progressive T-cell accumulation which may compensate for reduced immediate potency [391]. Consequently, in the setting of double targeting CARs, CAR affinity, along with CAR expression levels, will determine the potency of the constructs. Since IL-34 has higher affinity for the target than CSF-1 (coincidentally 34 times higher), target engagement by the C34B construct would

provide predominant signalling through 4-1BB while in the 34CB construct intracellular signal transduction would predominantly employ CD28 and CD3ζ signalling. This could potentially account for the superior *in vitro* proliferative capacity of C34B- over 34CB-grafted T-cells.

The reason for the striking difference in expansion and retention of *in vitro* cytotoxicity and cytokine release by $C34B^+$ T-cell compared to those expressing other CAR constructs warrants further discussion. One possibility is that target-dependent activation of CAR^+ T-cells may also have resulted in different levels of T-cell death. Indeed, it has been suggested that T-cell apoptosis, through activation-induced cell death (AICD), may be a downstream effect of IFN-γ release [392, 393]. Consequently, it was hypothesised that whilst second and third generation CAR^+ T-cells were undergoing proliferation, a number of them may also have been eliminated through AICD, while $C34B^+$ T-cells were being protected. Contrary to this, however, is the fact that all CAR^+ T-cell populations produce very similar levels of IFN-γ (Figure 4.8). Furthermore, no significant differences in Fas ligand expression, a marker of AICD, were detected in double targeting CAR^+ T-cells in comparison to conventional second and third generation CAR^+ T-cells post-activation (Appendix, Figure S4) [394]. The sustained functionality of $C34B^+$ T-cells upon repeated *in vitro* stimulation can most probably be attributed to the arrangement of the elements in the double targeting CAR, which may be facilitating activity. For example, by definition, one of the co-stimulatory modules in a 3rd generation CAR (in this case 4-1BB) must be placed away from its natural location close to the inner leaflet of the plasma membrane. This may cause it not to signal normally owing to impaired access to obligate membrane-associated partner molecules. Alternatively, close proximity of 2 co-stimulatory signalling modules in a 3rd generation CAR, like CD28 and 4-1BB in C4B and 43428Bζ, might lead to steric issues, preventing full engagement of one or more downstream signalling pathways. Both of these issues are avoided in the arrangement of the double targeting CARs, where the signalling moieties have been fused directly to a transmembrane

domain, ensuring that they are both adjacent to the plasma membrane within the cell. Furthermore, they may be spaced within the cell so that they will not interact sterically with each other. Overall, despite similar cytotoxicity exerted by all signalling-competent CSF-1 and IL-34-based CARs, repeated antigen re-stimulations revealed that the double targeting C34B CAR maintains proliferative capacity, cytotoxic potency and ability to release IL-2 for several more rounds of antigen-stimulation than any other CAR configuration tested.

Following proof of successful CAR^+ T-cell re-direction against a CSF-1R-expressing cell line (T47D FMS cells) (Figure 4.7), it was crucial to demonstrate that this retargeting was maintained against cHL and ALCL cell lines. In order to allow for *in vitro* measurement of target cell destruction and *in vivo* quantification of tumour burden, the lymphoma cell lines were transduced to stably express firefly luciferase (ffLuc) and the fluorescent protein tdTomato (Figure 4.12). Following flow sorting for transduced cells, lymphoma cell lines were co-cultured in 1:1 ratio with CAR^+ T-cells and co-cultures were probed every 24h for 6 days. As shown on Figure 4.13, 4.14, 4.15, 4.16, 4.17 and 4.18 co-culture of CAR^+ T-cells resulted in variable level of clearance of the target cells, correlating with the surface level of expression of CSF-1R on the lymphoma cell lines (Figure 3.1). The high level of CSF-1R expression on DEL and FE-PD cell lines resulted in complete clearance of the cancer cells within 24h and 72h respectively. Substantial target cell lysis was also observed with KM-H2 and JB6 cell lines. By contrast, the modest function of CAR^+ T-cells against K299 and L540 cells may have resulted from the low level of CSF-1R expression by these cells (Figure 3.1, A and B). This observation raises the possibility that the activation of CAR^+ T-cells requires CSF-1R expression by the target cells to be above a certain level. If correct, this may be beneficial for clinical translation of CAR^+ T-cells as it suggests that low levels of CSF-1R expressed by healthy tissues may be below the activation threshold, therefore reducing the potential for “on-target” toxicity.

One potential impediment to CSF-1R targeting of the lymphoma cell lines is the previously documented (Figure 3.2) endogenous expression of either one or both CSF-1R ligands, which may induce receptor down-regulation by internalization of the receptor-ligand complex.

An important observation is that across the six-lymphoma cell lines, consistently, the IL-34-based CAR-grafted T-cells exerted inferior cytotoxicity compared to CSF-1-based CAR-transduced T-cells. This can be attributed to the poorer activation of IL-34-based CAR^+ T-cells, which has already been observed upon co-culture with the positive control T47D FMS (discussed in detail above) but was also confirmed by the detection of minimal cytokine release upon engagement with the lymphoma cell lines (Figure 4.19 and 4.20). In general, levels of IFN-γ and IL-2 were significantly lower in lymphoma co-cultures than following co-culture with cells that ectopically express CSF-1R, a finding that is likely to reflect the higher levels of cell surface CSF-1R expression and the lack of endogenous CSF-1R ligand secretion by the latter.

No significant differences in cytokine release or cytotoxicity were observed in co-cultures of T47D FMS (on first cycle of Ag-stimulation) or lymphoma cells with T-cells engineered to express second or third generation CARs or double targeting CARs in either the CSF1- or IL-34-based groups.

Overall, the data presented in this chapter demonstrate that CSF-1R-targeted CAR^+ T-cells can be effectively and specifically redirected against a panel of cHL and ALCL cell lines *in vitro*, unlike control CAR^+ or untransduced T-cells. Furthermore, CSF-1-based CAR^+ T-cells undergo more robust activation upon target engagement in comparison to IL-34-based CAR^+ T-cells, which can most likely be attributed to the higher affinity of CSF-1R interaction of the latter. Lastly, C34B-grafted T-cells exhibited enhanced proliferative capacity upon successive rounds of re-stimulation while maintaining their cytotoxic potency and ability to release IL-2. This suggests that providing co-stimulation

in trans results in favourable spatial and temporal differences in the recruitment, kinetics and regulation of co-stimulation. However, simply adopting the double targeting strategy does not translate into augmented functionality, as illustrated by the 34CB construct. This raises the possibility that fine-tuning of the relative affinities of dual targeted receptors for their targets may be necessary to achieve optimal potency of the constructs. Taken together, these data warrant investigation of the *in vivo* anti-tumour activity of CSF-1R-retargeted CAR T-cells against lymphoma xenografts that express this target.

Chapter 5 Determining the anti-tumour potential of CSF-1R-targeting CAR$^+$ T-cells *in vivo*

5.1 Introduction

The CSF-1/CSF-1R axis has been demonstrated to play a key role in supporting tumour cell survival, proliferation and enhanced motility (discussed in details in section 3.1). Expression of CSF-1R has been reported in diverse cancer types. In cHL and ALCL, CSF-1R expression has been shown to originate from an aberrantly activated endogenous long terminal repeat (LTR) suggesting that the origin of the unnatural CSF-1R expression found on HRS and ALCL cells is loss of epigenetic control [141, 142]. Aberrant CSF-1R expression is also commonly documented in tumours of epithelial origin such as breast [143, 144] and ovarian cancer [145]. Additionally, CSF-1R expression has been strongly associated with poor prognosis in those cancers, which makes it an attractive target for cancer immunotherapy [146-148].

5.1.1 Targeting the CSF-1/CSF-1R axis in cancer

The majority of tumour-associated antigens (TAA) are not restricted to the tumour alone but are also expressed on non-diseased tissue. Instead, it is usually the relative expression levels that differ between malignant and healthy tissue. Consequently, as complete avoidance of toxicity can be difficult to achieve, therapeutic targeting of TAA needs to achieve a satisfactory balance whereby sufficient benefit is achieved while avoiding unacceptable toxicities. As discussed in section 1.3, CSF-1R expression is restricted to cells of the mononuclear phagocyte lineage. In order to assess the potential toxicities associated with targeting this antigen, Hume and colleagues have developed the 'MacGreen' transgenic mouse, in which an enhanced green fluorescent protein (EGFP) reporter gene is driven by the *Csf1r* promoter, allowing for visualisation of the participation of CSF-1R$^+$ cells in tumour progression and metastasis [395]. This mouse model was used for assessment of the number, phenotype and fate of CSF-1R$^+$

cells upon administration of an anti-CSF-1R M279 antibody, which resulted in selective reduction of $Ly6C^-$ stationary monocytes, but not of their precursors $Ly6C^+$ inflammatory monocytes [396]. Furthermore, antibody-mediated targeting of CSF-1R did not affect $Ly6C^+$ inflammatory monocytes numbers nor did it abrogate their recruitment or function in LPS-induced lung inflammation, wound healing and acute graft versus host disease. It did, however, decrease the number of tumour-associated macrophages (TAMs) in syngeneic mesothelioma and Lewis lung carcinoma tumour models, despite the fact that tumours were established prior to starting treatment. This work shed further light on the consequences of targeting CSF-1R, confirming its role in the maturation of monocytes into tissue resident macrophages though at the same time indicating that CSF-1R signalling may not be absolutely necessary for monocyte production or for effective function of inflammatory monocytes. These findings reinforce CSF-1R as an attractive target for drug discovery.

Current development of targeted therapies in oncology concerns principally two types of agents: monoclonal antibodies (Mabs) and tyrosine kinase inhibitors (TKIs).

5.1.1.1 Tyrosine kinase inhibitors

At present there are 28 tyrosine kinase inhibitors that have been approved for cancer treatment in the clinic, of which half were approved in the last 3 years, and more than 100 kinase inhibitors are at different stages of clinical development [397]. Most of those inhibitors compete with ATP for the ATP-binding site [136]. Clinically relevant receptor TKIs known to inhibit CSF-1R are imatinib, dasatinib, nilotinib, pazopanib, sorafenib and sunitinib [398, 399]. More selective inhibitors are tandutinib [400] (phase II), PLX-3397 (phase III), PLX-5622 (phase I) and JNJ-28312141 (phase I); and the research tool compounds GW-2580 [401], and Ki-20227 [402]. Imatinib has been shown in a case report to induce complete remission in relapsing diffuse type tenosynovial giant cell tumour (dt-GCT), a rare proliferative disorder affecting synovial joints and tendon sheaths [403]. The observed complete response has been attributed to its ability to

block CSF-1R activation, inhibiting the paracrine loop responsible for the growth of these tumours [404]. However, further studies assessing the efficacy of imatinib [405] and subsequently of related TKIs such as nilotinib [406] showed tumour shrinkages in only a few cases of patients with dt-GCT [407]. Unfortunately kinase inhibitors are well known to engage multiple off-targets usually among structurally similar kinases from the same family, which is a major limitation for their widespread use.

5.1.1.2 Antibodies

Currently there are 3 monoclonal antibodies targeting CSF-1R in Phase I clinical trials. Ries and colleagues generated a high-affinity, humanized anti-CSF-1R monoclonal antibody termed RG7155 that inhibited both ligand-dependent and ligand-independent activation of CSF-1R by blocking receptor dimerization [408]. Treatment with RG7155 selectively induced apoptosis of M2-like macrophages but not M1-like macrophages *in vitro*. In animal models of colorectal adenocarcinoma and fibrosarcoma, CSF-1R blockade depleted TAMs and resulted in a relative increase in cytotoxic effector $CD8^+$ T-cells and a decrease in $CD4^+FOXP3^+$ regulatory T-cells and ultimately delayed tumour growth and metastasis. Consistent with this finding, in a phase I study of patients with locally advanced and/or metastatic ovarian and breast carcinoma, RG7155 treatment significantly diminished $CSF\text{-}1R^+$ and $CD68/CD163^+$ TAMs and triggered a shift toward an increased CD8/CD4 T-cell ratio [409]. Disease stabilization was observed in 6/40 patients with ovarian or breast cancer. Additionally, 28 patients with dt-GCT were recruited and treated in the same trial (NCT01494688) and objective response was observed in 24 of them. RG7155 treatment also led to significant reduction of surrogate skin tissue resident macrophages and rapid elimination of $CD14^+CD16^+$ peripheral monocytes. Overall RG7155 treatment was well tolerated with only 18% patients (21/114) experiencing grade 3/4 adverse events (asthenia, peripheral edema and pyrexia). These results strongly suggest that TAMs represent a promising therapeutic target in various solid tumours and support further testing of CSF-1R blockade in combination with chemotherapeutic agents or immunotherapies.

RG7155 is currently being tested in combination with an anti-PD1 (MPDL3280A) monoclonal antibody in a Phase Ib study for locally advanced or metastatic solid tumours (NCT02323191).

The other two monoclonal antibodies (Mabs) targeting CSF-1R (named IMC-CS4 and FPA008) are both currently in Phase I evaluation in patients with advanced solid tumours and PVNS/dt-GCT (NCT01346358 and NCT02471716 respectively). Results from both trials are still currently pending.

Colony stimulating factor-1 receptor is a major therapeutic target in cancer due to its overexpression in a number of different malignancies. Preliminary results from CSF-1R-targeting Mabs in Phase I, even though not sufficient for evaluating the overall safety profile of targeting this receptor, are encouraging. Taken together, these data reinforce CSF-1R as an attractive therapeutic target for cancer immunotherapy.

5.2 Results

The overall goal of this PhD was to determine whether CSF-1R-re-targeted T-cells represent a potential therapeutic approach for patients with refractory cHL and ALCL. A key step in the testing of every novel therapeutic anticancer agent is the evaluation of therapeutic efficacy of the agent itself using appropriate *in vivo* tumour models. Consequently, there was a need to develop a clinically relevant lymphoma mouse model that accurately represents CSF-1R-expressing lymphoma subtypes.

5.2.1 Development of an *in vivo* CSF-1R expressing lymphoma model

First, I investigated xenograft formation by six CSF-1R-expressing lymphoma cell lines, derived from both ALCL and cHL. SCID/Beige mice were inoculated i.v. with either 10 x 10^6 or 5 x 10^6 tumour cells (Figure 5.1). All six lymphoma cell lines had been transduced to stably express firefly luciferase (ffLuc) and the fluorescent protein tdTomato (Figure 4.9), thereby allowing non-invasive monitoring of tumour growth

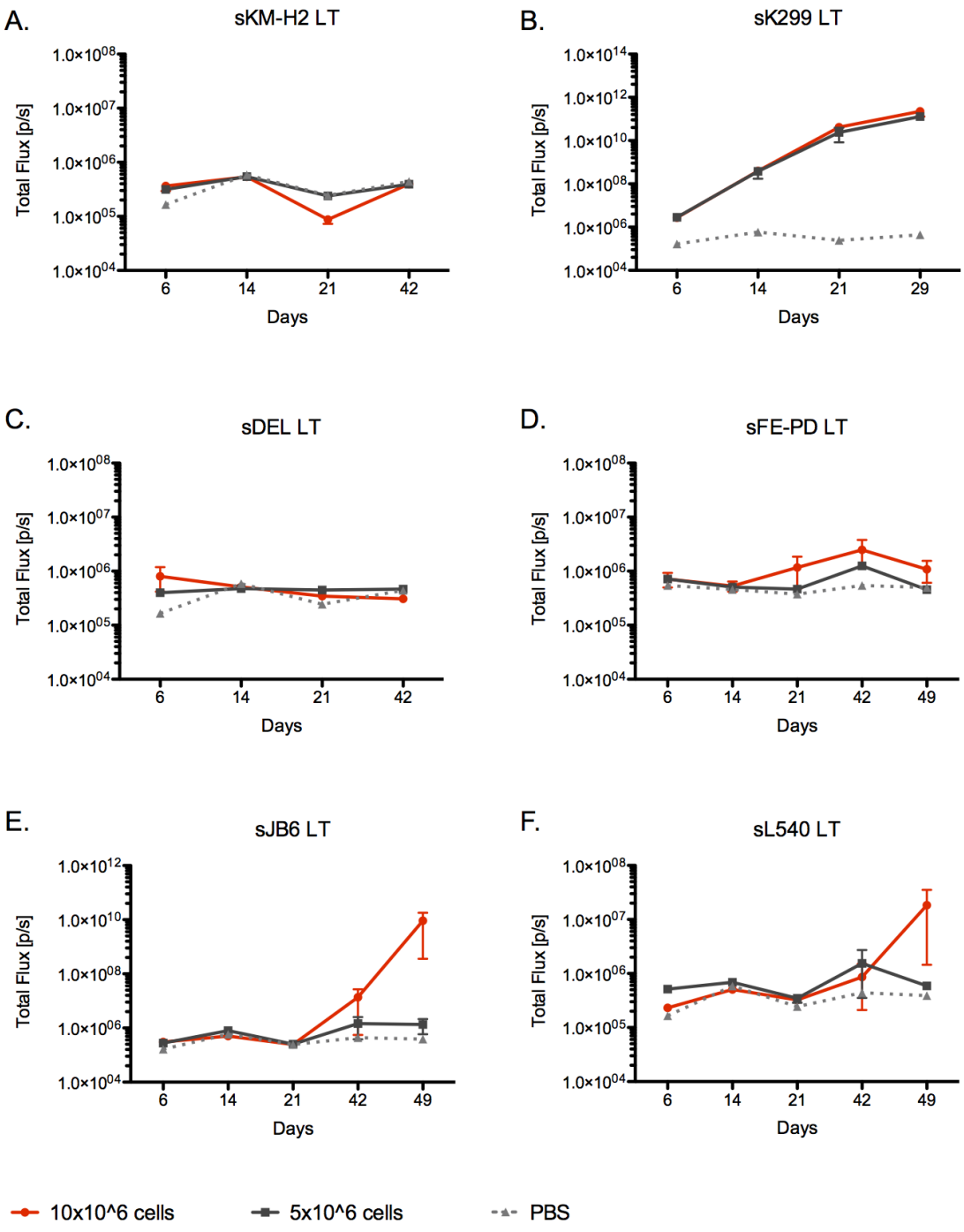

Figure 5.1 Development of a lymphoma *in vivo* model.

SCID/Beige mice (n=3 per dose) were inoculated intravenously (i.v.) with 5 x 10^6 (grey line) or 10 x 10^6 (red line) cells from the appropriate luciferase-expressing lymphoma cell line or PBS (dotted line) **(A-F)**. Tumour growth was monitored over the indicated timeframe by BLI. Quantification of luminescent signal released from each mouse was determined by drawing a region of interest (ROI) around each individual animal. Using Living Image 4.1 software, photon release within the ROI was calculated and standardised to account for the scan duration. Data are expressed as mean total photon flux (photons/s) ± standard error of the mean.

using bioluminescence imaging (BLI). Bioluminescence imaging provides a sensitive method for monitoring tumour growth *in vivo* by measuring photon release upon D-luciferin breakdown by the luciferase enzyme present within the tumour cells (please refer to section 2.3.2). Transduced lymphoma cell lines were annotated with "LT" after their name (e.g. KM-H2 LT) and following cell sorting for tdTomato they received an "s" in front of their name, which stands for "sorted" (e.g. sKM-H2 LT).

As shown in Figure 5.1, reproducible tumour engraftment within a reasonable time frame was only achieved following inoculation with the sK299 LT cell line (Figure 5.1, B). In contrast, no increase in total flux was observed in the sKM-H2 (Figure 5.1, A), sDEL LT (Figure 5.1, C) or sFE-PD LT (Figure 5.1, D) groups, when compared to baseline (PBS administration - dotted line). After a prolonged interval, a low level of signal was detected inconsistently in the sJB6 LT (n=2/3 mice) and sL540 LT (n=1/3 mice) groups, and only after injection of the higher cell dose (10 x 10^6 cells)(Figure 5.1, E and F). This experiment demonstrated that only the sK299 LT lymphoma cells achieved reproducible and robust tumour xenograft formation in SCID/Beige mice following i.v. administration of either 10 x 10^6 or 5 x 10^6 cells.

To further characterise the sK299 LT xenograft model, the number of administered cancer cells was titrated to determine the lowest number that reproducibly engraft in SCID/Beige mice. This was done in anticipation that the lower number of inoculated cancer cells would reduce tumour-related morbidity and potentially extend the therapeutic window for adoptive CAR^+ T-cell transfer. The observed growth kinetics were very similar in all five groups with a slight delay in the exponential growth phase between day 6 and day 20 in the groups that received 2 x 10^6, 1 x 10^6 and 0.5 x 10^6 cells compared to the higher dose groups (10 x 10^6 and 5 x 10^6) (Figure 5.2, A). A dose of 2 x 10^6 sK299 LT cells was chosen for all future experiments (Figure 5.2, B) since inoculation of smaller cell doses introduced greater variability in tumour engraftment

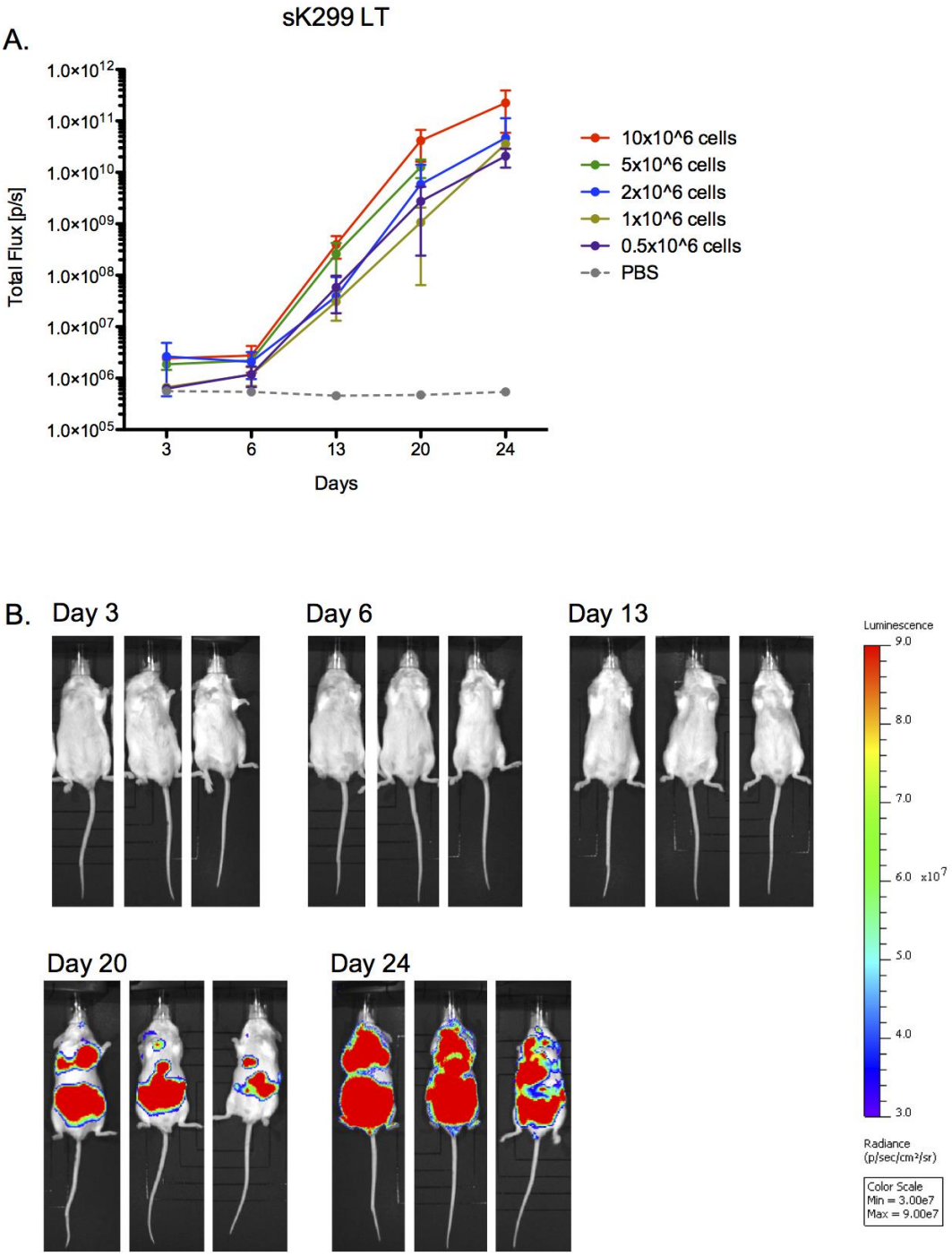

Figure 5.2 Characterisation of the sK299 LT lymphoma xenograft model.

SCID/Beige mice (n=3 per dose) were inoculated i.v. with 10 x 10^6, 5 x 10^6, 2 x 10^6, 1 x 10^6 and 0.5 x 10^6 sK299 LT cells or PBS (dotted line). **(A)** Tumour growth was monitored over the indicated timeframe by BLI. Data represent mean total photon flux (photons/s) ± SEM for each group. The images shown in **(B)** highlight tumour progression over time in the group that received 2 x 10^6 sK299 LT cells. Tumour cell dissemination to lymph nodes only was confirmed at post-mortem, with no signal detected in the heart, lungs, liver or spleen **(C)**. No tumour cells were detected in the blood or spleen as confirmed by (figure and legend continue on next page)

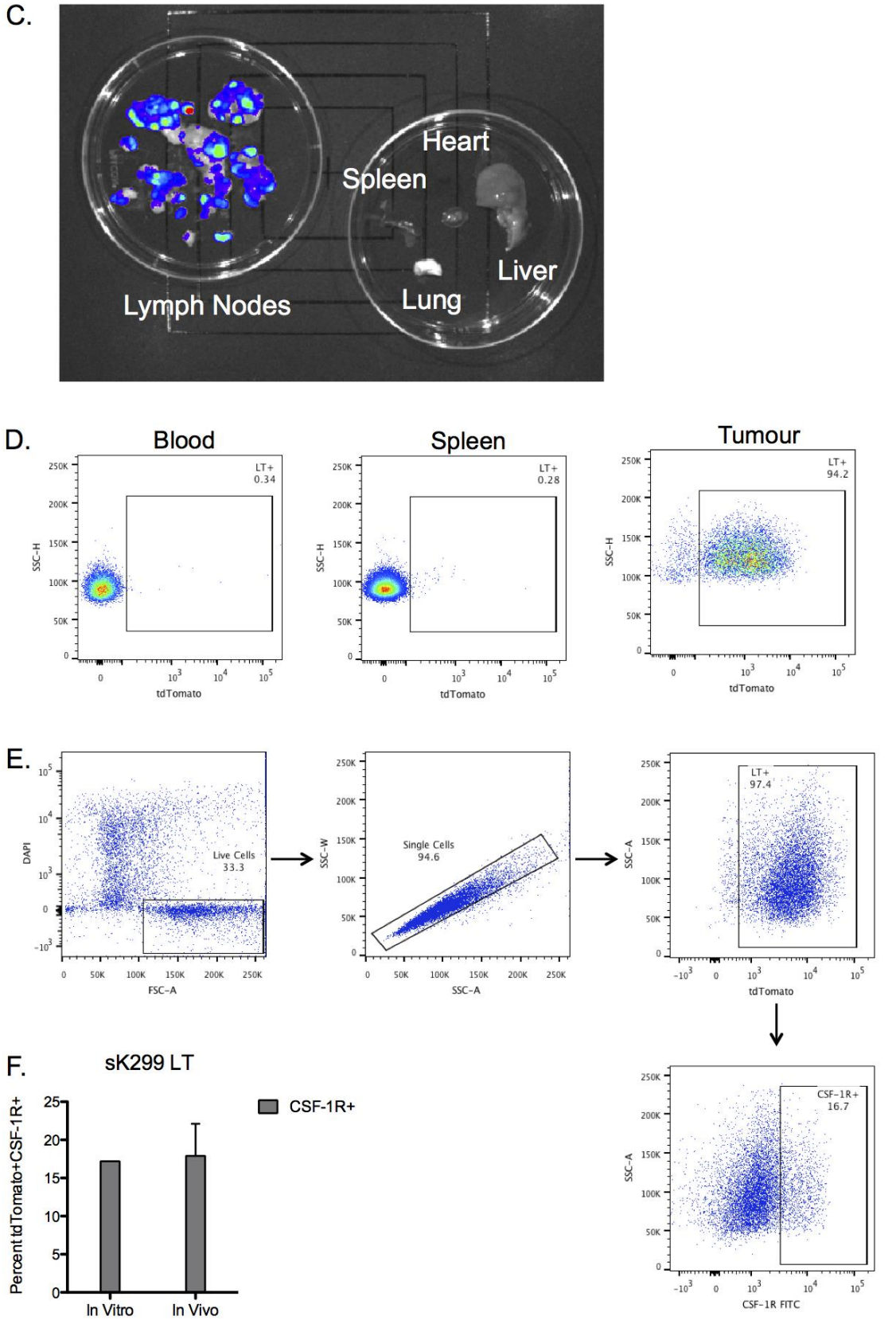

flow cytometry **(D)**. Tumours from five mice from different inoculation conditions were excised post mortem and investigated for the expression of CSF-1R by flow cytometry. To ensure retention of cell surface proteins, the tumours were mechanically disaggregated to yield a single cell suspension which was stained with a rat anti-human (legend continue on next page)

(indicated by increased size of error bars) without any additional slowing of disease progression.

Post-mortem BLI analysis indicated that the intravenously delivered sK299 LT lymphoma cells traffic to the lymph nodes where solid tumours were established, providing a clinically relevant representation of the human disease. No bioluminescence signal was detected from the excised lung, liver, spleen or heart (Figure 5.2, C). Tumour dissemination was further investigated by flow cytometry. Peripheral blood was collected and analysed along with spleen and lymph nodes for the presence of the fluorescent protein tdTomato characteristic of the infused sK299 LT cells. This analysis confirmed that tumour cells had only disseminated to lymph nodes (Figure 5.2, D).

In order to confirm that the sK299 LT tumours retain CSF-1R expression after passage *in vivo*, flow cytometry was performed on a single tumour, excised from each group post mortem (Figure 5.2, E). Mechanical separation was chosen over enzymatic digestion to achieve a single cell suspension, thereby ensuring the retention of cell surface markers. To minimize unspecific staining, all tumours were treated with mouse Fc block prior to any further staining and a viability dye (DAPI) was used to exclude background staining from dead cells. The excised tumours displayed similar levels of CSF-1R expression when compared to the sK299 LT cell line propagated at the same time *in vitro* (Figure 5.2, F). Consequently, this suggests that these tumours will remain suitable targets for CAR T-cells re-directed against CSF-1R.

CSF-1R antibody, followed by a goat anti-rat FITC conjugated secondary antibody. Non-specific binding of the antibodies was limited by using mouse Fc block prior to the staining steps. All gates were set using fluorescence minus one (FMO) controls. All tumours were gated as shown in **(E)** using DAPI as viability stain. The expression pattern of CSF-1R *in vivo* was compared with that of the sK299 LT cell line that had been cultured *in vitro* **(F)**. Data are represented as mean ± SEM.

5.2.2 Anti-tumour activity of CAR-grafted T-cells in the sK299 LT xenograft model

Mindful of the modest anti-tumour activity of CSF-1R-re-targeted T-cells against sK299 LT cells *in vitro* (Figure 4.14), I next set out to investigate their therapeutic activity *in vivo*, following adoptive transfer in SCID/Beige mice with established sK299 LT xenografts. Fifty four mice were inoculated i.v. with 2 x 10^6 sK299 LT cells (data are pooled from two separate experiments). Five days post tumour cell administration, the mice were imaged using BLI to confirm tumour engraftment and were then randomised into 6 groups with equal mean tumour burden. From this point on, treatment groups were assigned numbers and all treatment, imaging and evaluation was done in a blinded fashion. On the same day, mice were treated with either $C4B^+$, $C34B^+$, $43428B\zeta^+$, $34CB^+$ (all cultured in IL-4) or untransduced (UT) T-cells (cultured in IL-2) as control (Figure 5.5, A). Prior to infusion, the T-cells were probed for surface expression of the CAR constructs (Figure 5.3, A and B; Figure 5.4, A and B) and an infusion dose of 20 x 10^6 CAR^+ T-cells was calculated for each group according to transduction efficiency. Furthermore, cell viability and cytotoxic potential were maintained during the preparations required for T-cell infusion in mice as surplus CAR^+ but not UT T-cells conferred complete target cell lysis of T47D FMS monolayers *in vitro* (Figure 5.3, C and Figure 5.4, C). No antigen-independent killing was detected against the parental cell line T47D, which lacks target expression (Figure 5.3, D and Figure 5.4, D). To quantify tumour progression in the absence of T-cell infusion, one group of mice was treated with PBS.

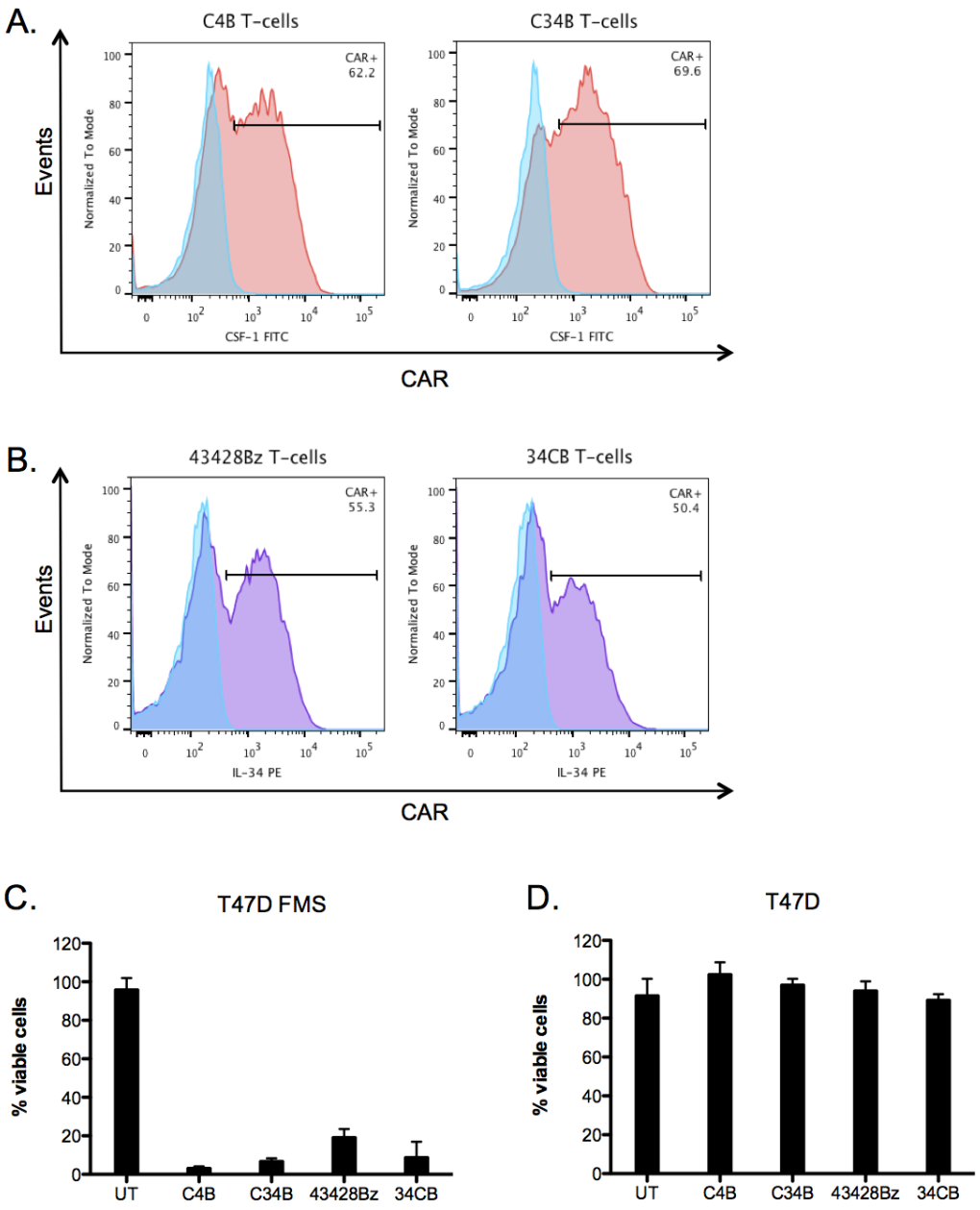

Figure 5.3 Assessing the suitability of T-cells for adoptive transfer into mice with established sK299 LT xenografts (experiment 1).

Prior to administration into mice, a small sample of each T-cell population was probed for CAR expression. Detection of the CSF-1-based CARs was achieved by flow cytometry using a goat polyclonal anti-human CSF-1 antibody, followed by a FITC-conjugated secondary antibody (pink histograms) **(A)**. The level of expression of IL-34-based CARs was assessed using mouse anti-human IL-34 antibody directly conjugated to PE (purple histograms) **(B)**. Staining was compared to untransduced T-cells probed using the same antibody combinations (blue histograms). (figure and legend continue on next page)

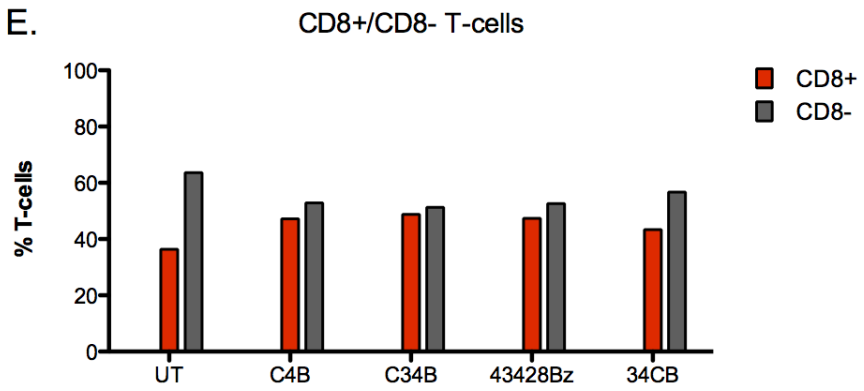

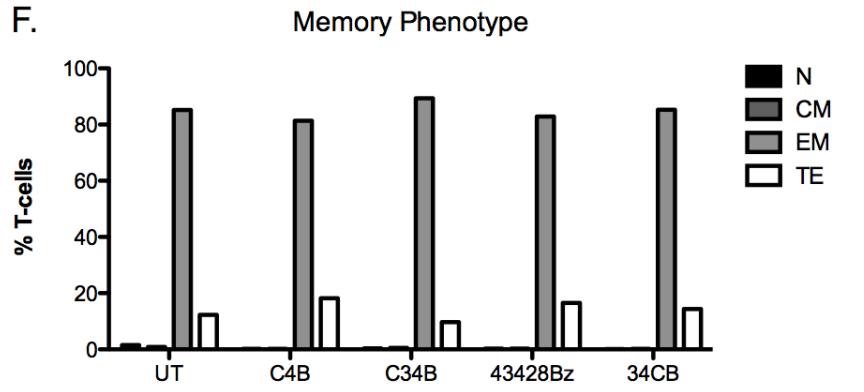

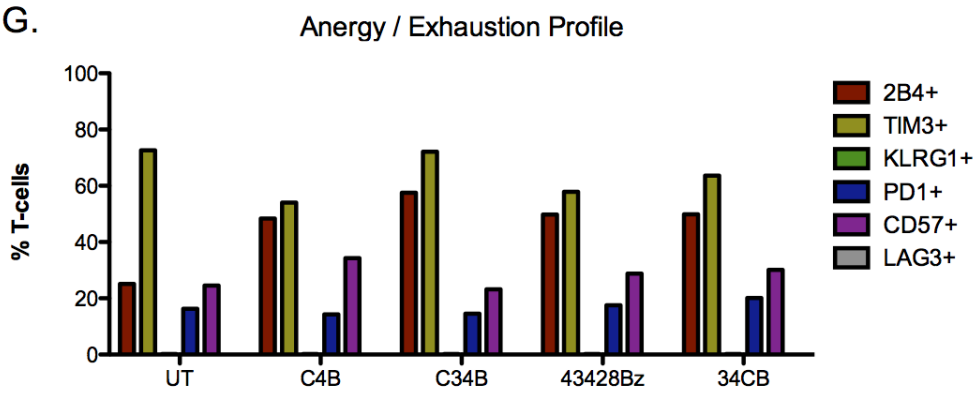

To investigate anti-tumour activity *in vitro*, surplus T-cells from the populations infused into mice were co-cultured at a 1:1 ratio with the T47D FMS and T47D cell lines **(C)** and **(D)**. Target cell destruction was measured at 24h using an MTT assay. Each sample was run in triplicate and data are presented as mean ± standard deviation. Furthermore T-cell phenotype was investigated in all CAR T-cell populations. Proportion of $CD8^+$ T-cells **(E)**, memory phenotype **(F)** and expression of a number of anergy markers **(G)** was determined by flow cytometry using a panel of directly conjugated mouse anti-human antibodies consisting of CD3 APC-Cy7, CD8 PE-Cy7, CD45RO PerCP-Cy5.5, CCR7 APC, 2B4 FITC, TIM3 PerCP-Cy5.5, KLRG1 PE, PD1 APC-Cy7, CD57 FITC and LAG3 APC.

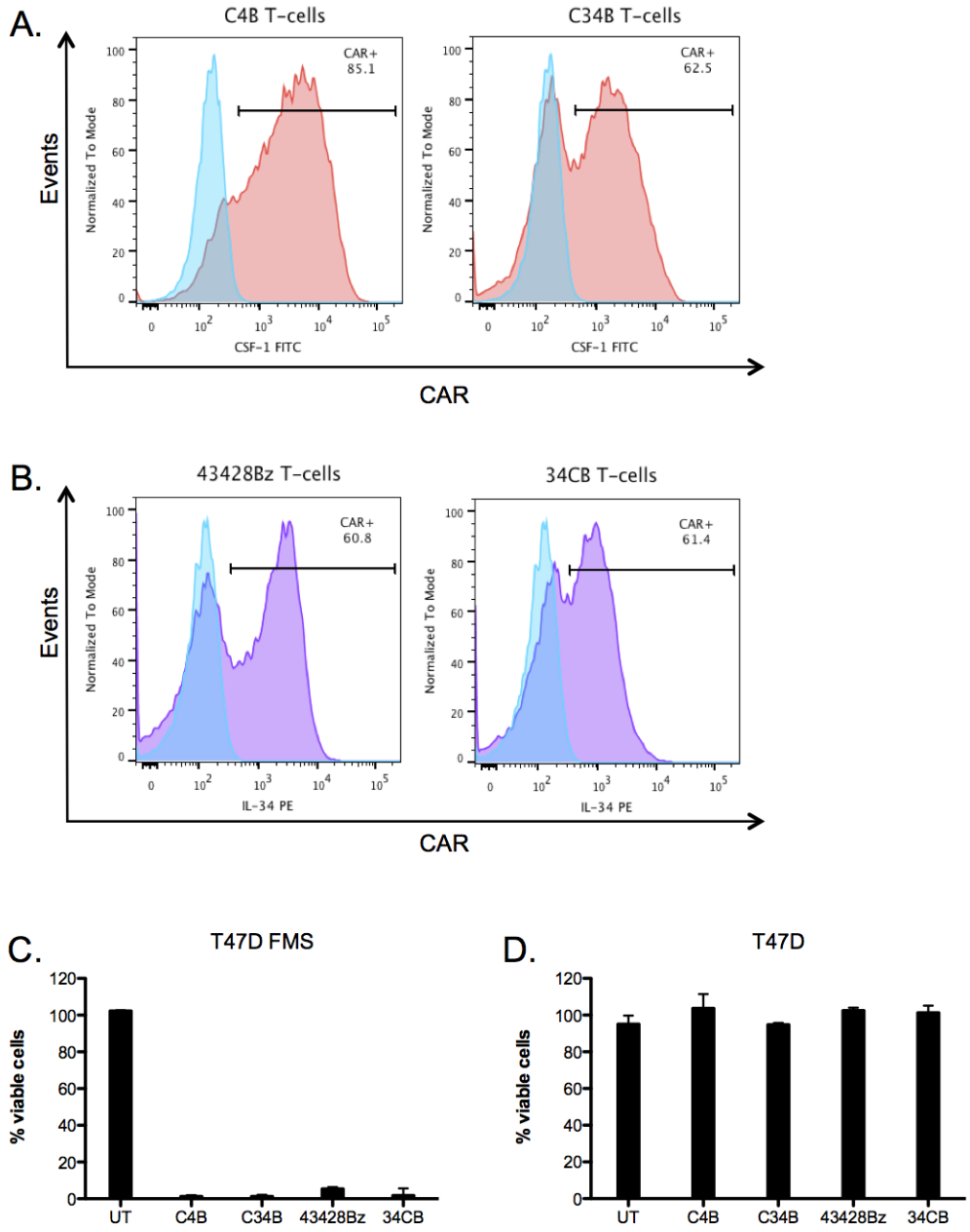

Figure 5.4 Assessing the suitability of T-cells for adoptive transfer into mice with established sK299 LT xenografts (experiment 2)

Prior to administration into mice, a small sample of each T-cell population was probed for CAR expression. Detection of the CSF-1-based CARs was achieved by flow cytometry using a goat polyclonal anti-human CSF-1 antibody, followed by a FITC-conjugated secondary antibody (pink histograms) **(A)**. The level of expression of IL-34-based CARs was assessed using mouse anti-human IL-34 antibody directly conjugated to PE (purple histograms) **(B)**. Staining was compared to untransduced T-cells probed using the same antibody combinations (blue histograms). (figure and legend continue on next page)

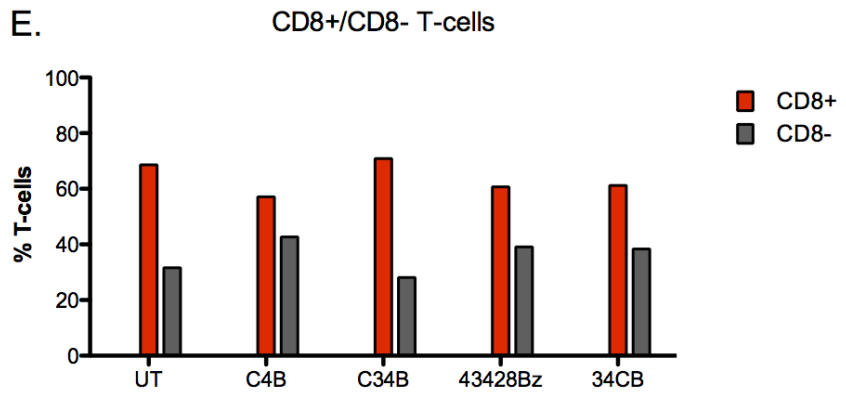

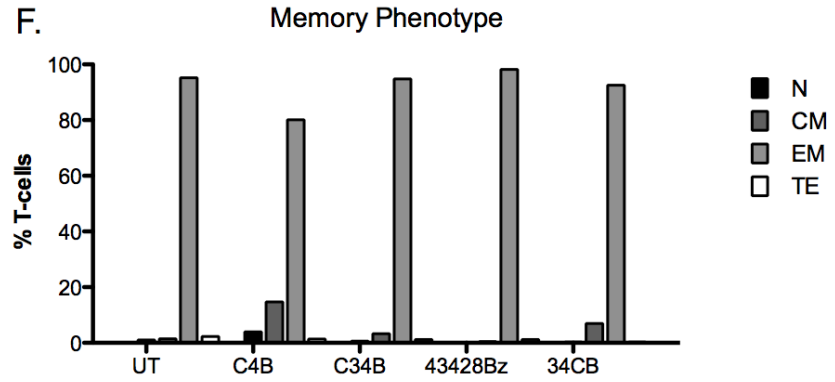

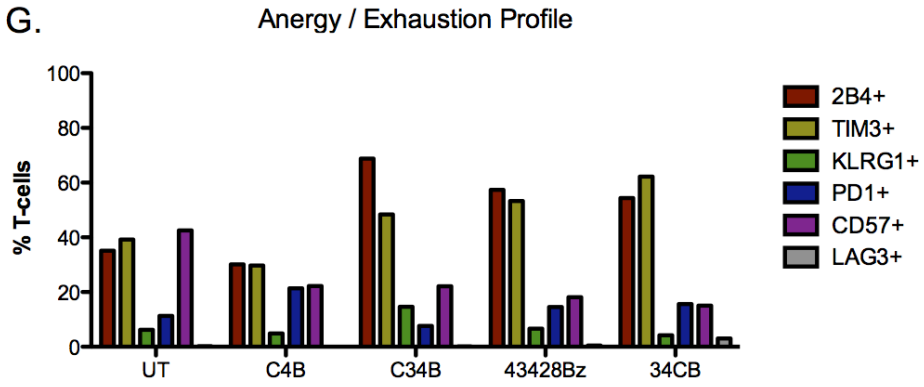

To investigate anti-tumour activity *in vitro*, surplus T-cells from the populations infused into mice were co-cultured at a 1:1 ratio with the T47D FMS and T47D cell lines **(C)** and **(D)**. Target cell destruction was measured at 24h using an MTT assay. Each sample was run in triplicate and data are presented as mean ± standard deviation. Furthermore T-cell phenotype was investigated in all CAR T-cell populations. Proportion of $CD8^+$ T-cells **(E)**, memory phenotype **(F)** and expression of a number of anergy markers **(G)** was determined by flow cytometry using a panel of directly conjugated mouse anti-human antibodies consisting of CD3 APC-Cy7, CD8 PE-Cy7, CD45RO PerCP-Cy5.5, CCR7 APC, 2B4 FITC, TIM3 PerCP-Cy5.5, KLRG1 PE, PD1 APC-Cy7, CD57 FITC and LAG3 APC.

In order to investigate the immunophenotype of the CAR^+ T-cells prior to *in vivo* administration, the expression levels of a number of cell surface markers was investigated. This analysis showed that the cells expressed a predominantly effector memory (EM) phenotype ($CD45RO^+CCR7^-$) with roughly half expressing the CD8 co-receptor (Figure 5.3, E and F; Figure 5.4, E and F). Furthermore, T-cells were stained for expression of a panel of anergy markers (2B4, TIM3, LAG3, PD1, KLRG1 and CD57) (Figure 5.3, G and Figure 5.4, G). No significant difference in the immunophenotype was noted between UT T-cells and CAR^+ T-cells despite the different expansion protocols employed (the first were expanded in IL-2 while the latter were expanded in IL-4).

Initially, it appeared that mice treated with CAR^+ T-cells showed no treatment benefit when compared to those receiving UT T-cells or PBS. However, a marked delay in tumour progression emerged in the $C34B^+$ T-cell treated group, which became statistically significant at day 24 compared to UT T-cell treated group (Figure 5.5, B). Furthermore, towards the end of the study there were 3 tumour-free long-term surviving mice in the $C34B^+$ T-cell treated group (Figure 5.5, B and D). Mice were weight regularly throughout the study. Independent of the T-cell population administered, the average weight of each group slowly increased over the course of the study indicating that no significant toxicity had occurred (Figure 5.5, C). In support of this, our group had previously shown that the SCID/Beige xenograft model could detect cytokine release syndrome induced by the adoptive transfer of CAR T-cells [240]. As highlighted in Figure 5.5 E, differences in tumour progression in individual mice were observed. One mouse in the C34B and 34CB groups showed stabilisation of tumour progression between day 24 and day 37 despite detectable high tumour burden, ultimately leading to tumour eradication in one case (C34B group) and tumour progression in the other (34CB group). Another 2 mice in the C34B group showed delayed tumour progression and 2 additional mice had no detectable tumour burden post T-cell administration.

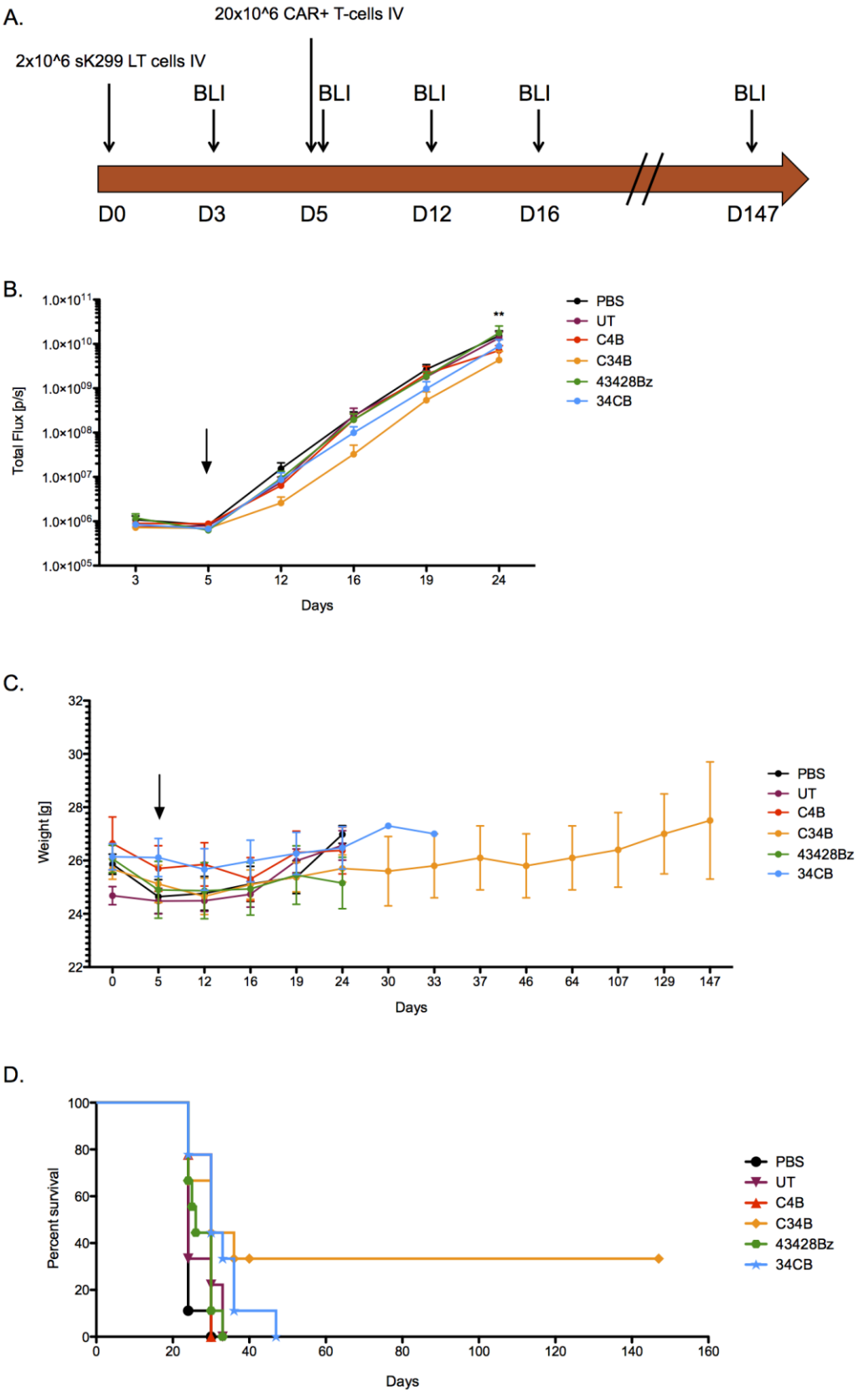

Figure 5.5 *In vivo* anti-tumour potential of CAR⁺ T-cells in the sK299 LT xenograft model.

(A) SCID/Beige mice were inoculated i.v. with 2 x 10^6 sK299 LT cells and five days later were treated i.v. with 20 x 10^6 CAR⁺ T-cells or UT T-cells or PBS (n=9). Animals were weighed **(C)** and tumour burden was monitored using BLI until (figure and legend continues on next page)

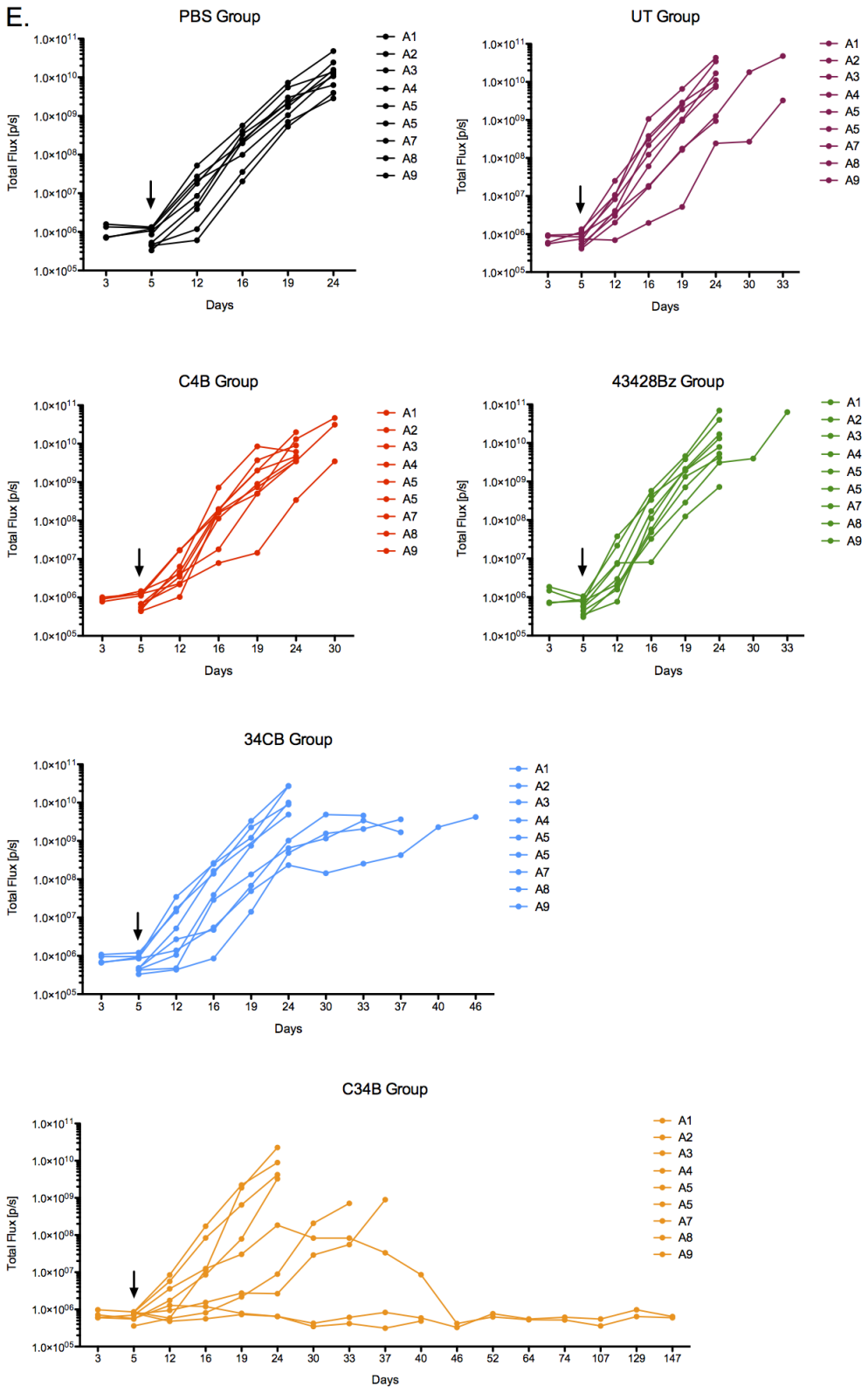

conclusion of the study **(B)**. To investigate further anti-tumour efficacy, total flux for individual animals within each group has been plotted **(E)**. Kaplan-Meier survival analysis showed difference in survival for mice treated with C34B^{+} T cells and the rest of the groups **(D)**. The data are pooled from two separate experiments and presented as mean value for each group ± SEM. ** = p<0.01; for C34B group relative to UT T-cells at day 24.

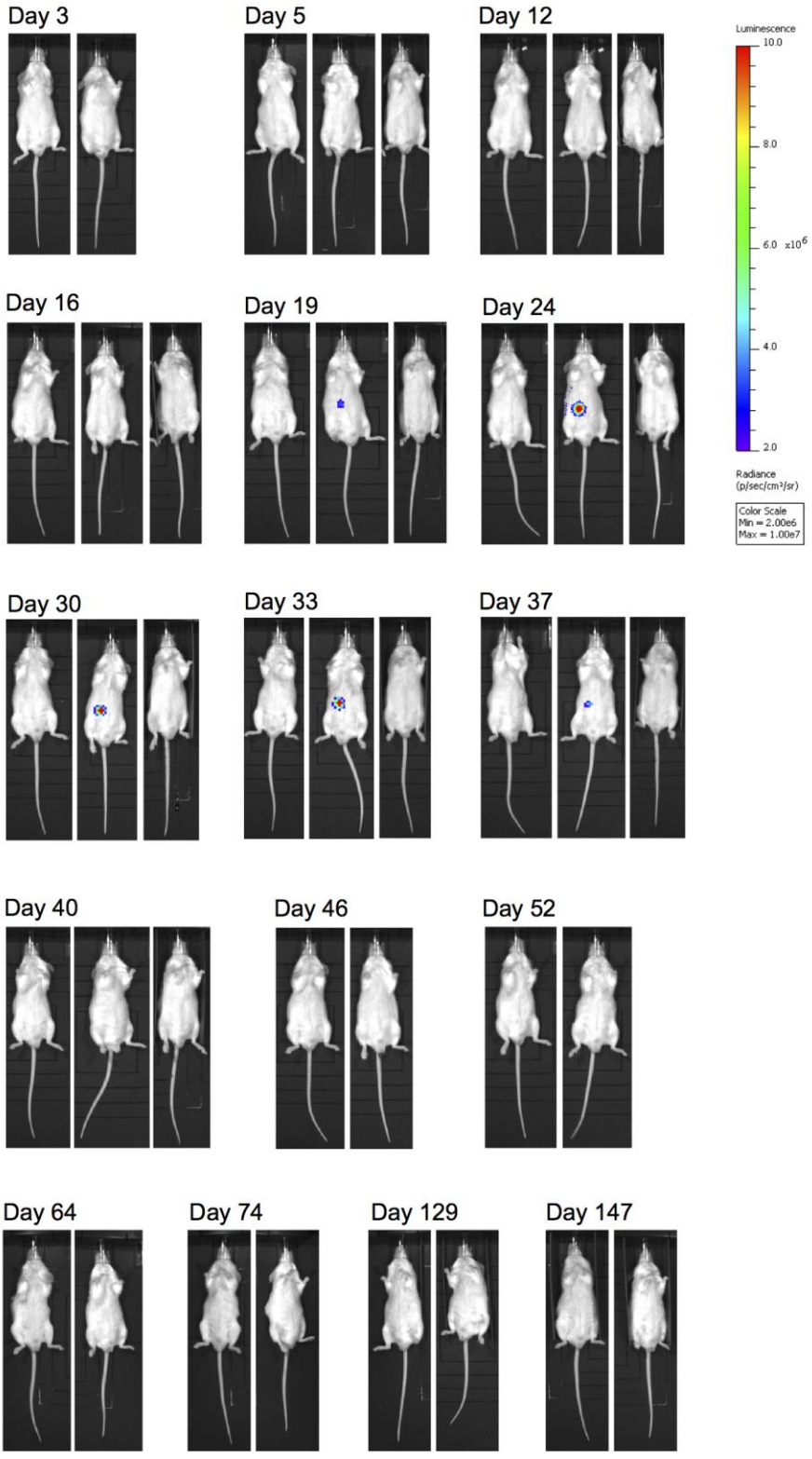

Figure 5.6 Long-term survivors from the C34B$^+$ T-cell treated group.

Three mice from the C34B$^+$ T-cell treated group remained tumour-free after initial inoculation with 2 x 10^6 sK299 LT cells followed by treatment with 20 x 10^6 C34B$^+$ T-cells 5 days later. Tumour growth was subsequently studied by BLI imaging on the indicated days. The data collected over every given time point is presented using the same scale. Mouse 3 has only been followed up for 40 days at the time of writing.

Consequently, long-term survival was achieved in 33% of the C34B group at the end of the study. Images of tumour burden as detected by BLI of the long-term survivors in the $C34B^+$ T-cell-treated group are presented in Figure 5.6.

At the end of the study, peripheral blood was collected by cardiac puncture. Tumours and spleen were excised from at least two mice per treatment group and investigated by flow cytometry for target retention post treatment and human T-cell infiltration. To ensure retention of cell surface proteins, the tumours and spleens were mechanically disaggregated to yield a single cell suspension. All samples were treated with mouse Fc block prior to staining and an identical gating strategy was employed as shown on Figure 5.2, E. Surface levels of expression of CSF-1R in the 5 treatment groups and the control PBS group was summarised on Figure 5.7 Staining for human CD3 revealed absence of viable T-cells in the peripheral blood, spleen or tumours (data not shown). Additionally, tail vein-derived peripheral blood was collected from the three long-term surviving mice from the C34B T-cell treated group (at day 30 for one mouse and day 52 for the other two post tumour inoculation) but no circulating human T-cells were detected (data not shown).

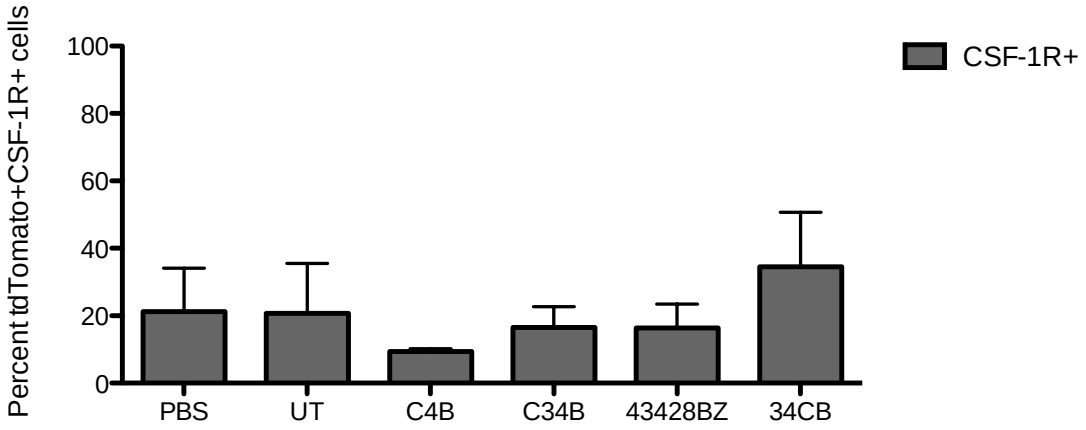

Figure 5.7 Surface levels of CSF-1R expression post treatment of the sK299 LT xenograft model.

Tumours from two to four mice per treatment group were excised during post mortem and investigated for the expression of CSF-1R by flow cytometry. Single cell suspension was achieved by mechanical disaggregation. Non-specific binding of the antibodies was limited by using mouse Fc block prior to staining with a rat anti-human CSF-1R antibody, followed by a goat anti-rat FITC conjugated secondary antibody. All gates were set using FMO controls. The employed gating strategy was described previously (Figure 5.2, E). No statistically significant difference was found between groups as determined by one-way ANOVA, followed by Bonferroni post-hoc test. Data were presented as mean ± SEM.

5.2.3 Development of K299 FMS LT xenograft lymphoma model

One possible explanation for disease progression in mice after CSF-1R re-targeted CAR T-cell treatment is inadequate target expression on tumour cells. To test this, I established a CSF-1R^{HI} expressing lymphoma model by retrovirus-mediated over-expression of CSF-1R in K299 cells, which naturally express low levels of this receptor (Figure 5.8, A). To characterise the effect of ectopic CSF-1R expression upon growth kinetics, the cell line K299 FMS LT and the parental cell line sK299 LT were cultured *in vitro* over a nine-day period and counted every third day (Figure 5.8, B). This experiment indicated that over-expression of CSF-1R had no effect on the *in vitro* growth kinetics of the K299 cell line. In order to determine whether the high level of CSF-1R expression rendered the K299 FMS LT cell line more susceptible to CSF-1R-re-targeted T-cells, a co-culture experiment was undertaken. The K299 FMS LT cell line was co-cultured at 1:1 ratio with CAR^{+} or untransduced (UT) T-cells and co-cultures were probed for luciferase activity at 24h, 48h, 72h, 96h, 120h, and 144h, providing a measure of target cell viability. Data were normalized against the maximal luminescence, as shown by tumour cells grown in the absence of T-cells. As shown on Figure 5.8 C, co-culture of CAR^{+} T-cells with the K299 FMS LT cell line resulted in considerably higher target cell lysis in comparison to co-culture with the parental cell line. Target cell lysis was accompanied by T-cell activation as indicated by IFN-γ and IL-2 release (Figure 5.8, D). Taken together, these data indicate that the K299 FMS LT cell line could be a useful model of CSF-1R^{HI}-expressing lymphoma.

In order to investigate the *in vivo* growth of the K299 FMS LT cell line, SCID/Beige mice were inoculated i.v. with either 5 x 10^6 or 2 x 10^6 tumour cells and tumour growth was compared to the parental cell line administered at the same doses (Figure 5.9, A). Tumour progression was monitored by BLI for a period of 31 days. This experiment indicated that over-expression of CSF-1R in the K299 cell line resulted in slower *in vivo* growth kinetics. As shown in Figure 5.9 A, at the higher dose (5 x 10^6 cells) K299 FMS

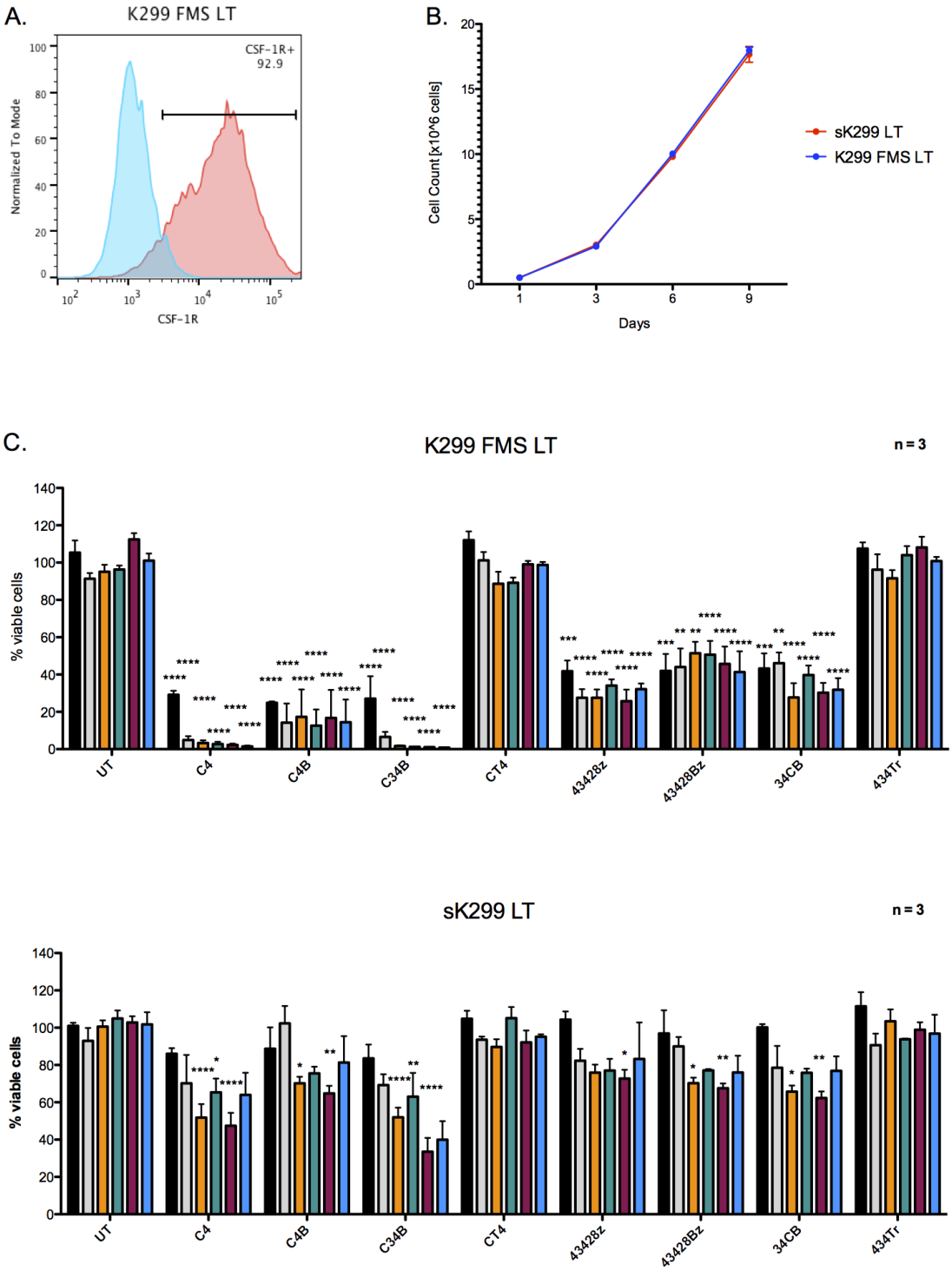

Figure 5.8 *In vitro* characterisation of the K299 FMS LT cell line.

The sK299 LT cell line has been retrovirally transduced to express high levels of CSF-1R. Successful transduction was verified by flow cytometry **(A)**. K299 FMS LT cells were stained with rat anti-human CSF-1R antibody followed by anti-rat-Ig-FITC conjugate (red histogram) or with

(figure and legend continue on foot of next page)

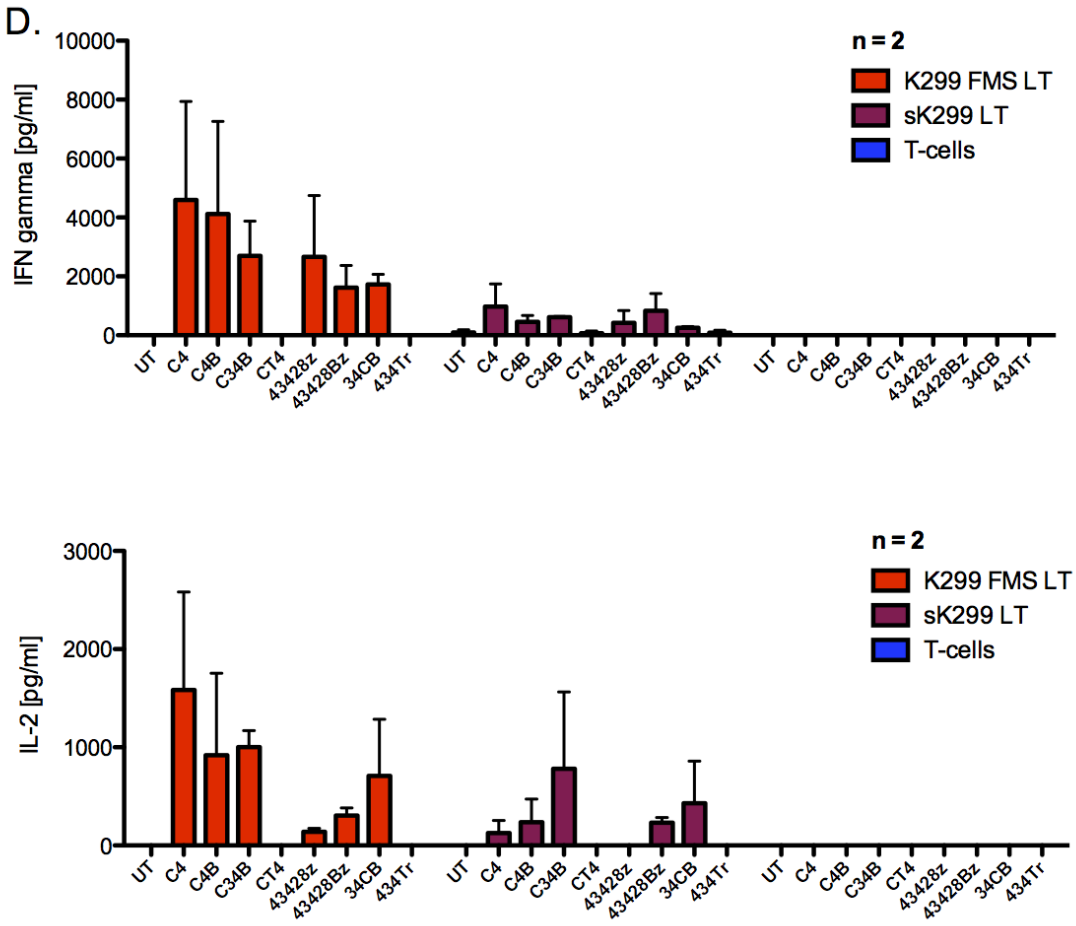

secondary antibody alone (blue histogram). The *in vitro* growth kinetics of K299 FMS LT cells was compared to sK299 LT cells **(B)**. Both cell lines were cultured at initial starting density of 0.5 x 10^6 cells per well for the indicated timeframe. Results are pooled from 3 wells. **(C)** The K299 FMS LT cell line was co-cultured with a panel of CAR-grafted T-cells at 1:1 ratio for the indicated period of time. The level of target cell viability following incubation with CAR^+ or UT T-cells was monitored using a luciferase assay. Data were normalized against the maximal luminescence, as shown by tumour cells grown in the absence of T-cells. Normalization was achieved using the following equation:

Tumour cell viability = (Sample luminescence value / Average Tumour alone luminescence value)*100

(D) Antigen-specific IFN-γ and IL-2 release were measured by ELISA at 48h and 24h respectively after co-culture with K299 FMS LT cell line. Data presented in that figure are represented as mean ± standard deviation. **** = $p<0.0001$; *** = $p<0.001$; ** = $p<0.01$; * = $p<0.05$ relative to UT T-cells at any given time point.

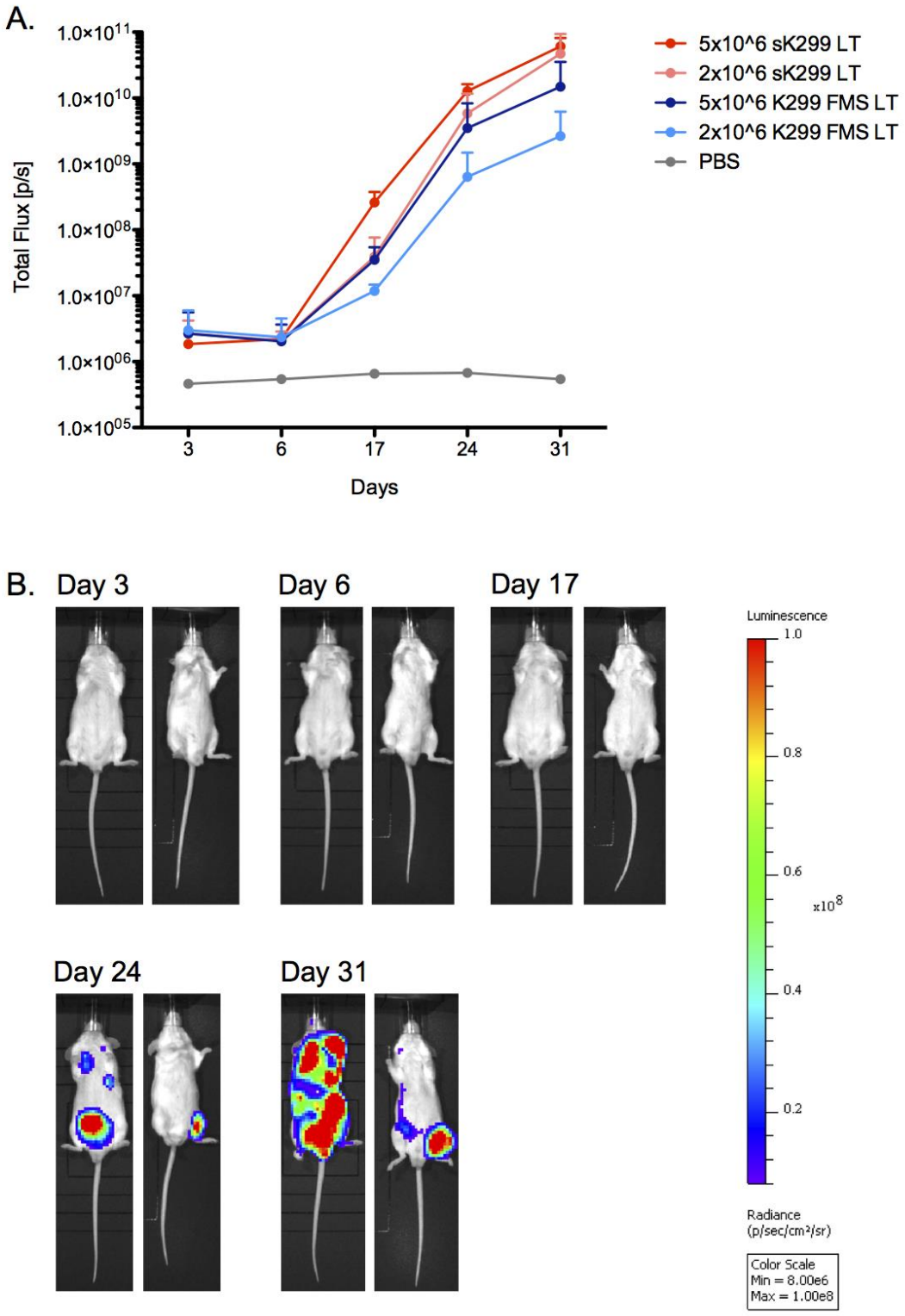

Figure 5.9 Characterisation of the K299 FMS LT *in vivo* lymphoma model.

SCID/Beige mice (n=2 per dose) were inoculated i.v. with 5 x 10^6 and 2 x 10^6 sK299 LT cells or K299 FMS LT cells or PBS. **(A)**. Tumour growth was monitored over the indicated timeframe by BLI. Data presented in the graph represent mean total photon flux (photons/s) ± SEM for each group. The images shown in **(B)** highlight tumour progression in the group that received 2 x 10^6 K299 FMS LT cells. At post-mortem analysis, (figure and legend continue on next page)

C.

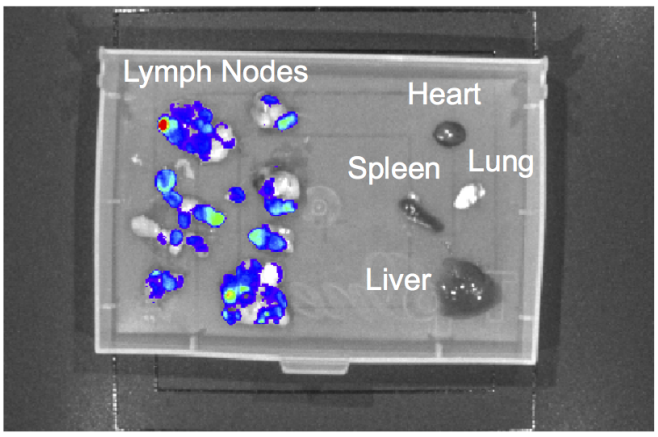

D.

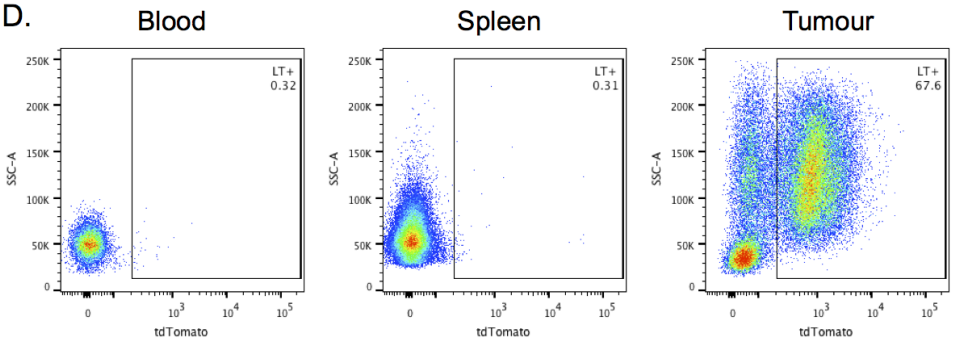

E.

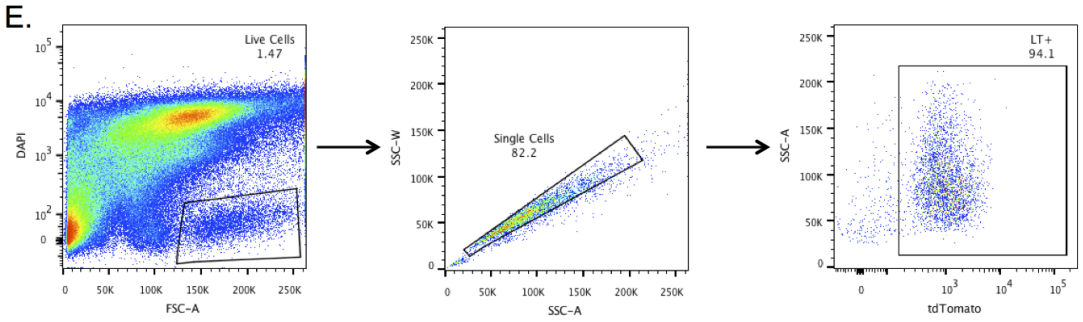

lymph node tumour cell dissemination was confirmed with no signal detected in the heart, lungs, liver or spleen **(C)**. No tumour cells were detected in the blood or spleen by flow cytometry **(D)**. Tumours from one mouse that received 2 x 10^6 K299 FMS LT cells were excised post mortem and investigated for the expression of CSF-1R by flow cytometry. Single cell suspension was achieved by mechanical disaggregation. Non-specific binding of the antibodies was limited by using mouse Fc block prior to staining with a rat anti-human CSF-1R antibody, followed by a goat anti-rat FITC secondary antibody. All gates were set using FMO controls. The employed gating strategy is shown in **(E)**. Data are represented as mean ± SEM.

LT cells grew with equivalent velocity as sK299 LT cells administered at the lower dose (2 x 10^6 cells). A dose of 2 x 10^6 K299 FMS LT cells was chosen for all future experiments.

Tumour dissemination was identical to that observed in the sK299 LT xenograft model, with solid tumours forming in the lymph nodes and no tumour detected in heart, liver, lungs, spleen or peripheral blood (Figure 5.9, C and D). The high level of CSF-1R expression, characteristic for the K299 FMS LT cell line, was maintained after *in vivo* tumour formation (Figure 5.9, E). Collected data indicated that the K299 FMS LT xenograft bearing mice would be a suitable model to test the *in vivo* therapeutic potential of CSF-1R-re-targeted T-cells.

5.2.4 Anti-tumour potential of CAR-grafted T-cells in the K299 FMS LT xenograft model

Given the high surface level of CSF-1R expression on K299 FMS LT cell line, it was hypothesized that a more significant treatment benefit could be obtained following adoptive transfer of CSF-1R-re-targeted T-cells. In order to investigate this, K299 FMS LT xenografts were established intravenously in 30 SCID/Beige mice by administering 2 x 10^6 cancer cells per mouse. Six days later the mice were imaged using BLI, randomized into groups with similar mean tumour burden and treated with either C4B$^+$, C34B$^+$, 43428Bζ$^+$, 34CB$^+$ or untransduced (UT) T-cells in a blinded manner (Figure 5.11, A). Prior to infusion, the T-cells were probed for surface level of expression of the CAR constructs (Figure 5.10, A and B) and each group was treated with 10 x 10^6 CAR$^+$ T-cells. Cell viability and antigen-specific cytotoxic potential were maintained during the preparations required for T-cell infusion as surplus CAR$^+$ but not UT T-cells elicited complete destruction of T47D FMS (Figure 5.10, C) but not of target-null T47D monolayers *in vitro* (Figure 5.10, D). To quantify tumour progression in the absence of T-cell infusion, one group of mice were treated with PBS.

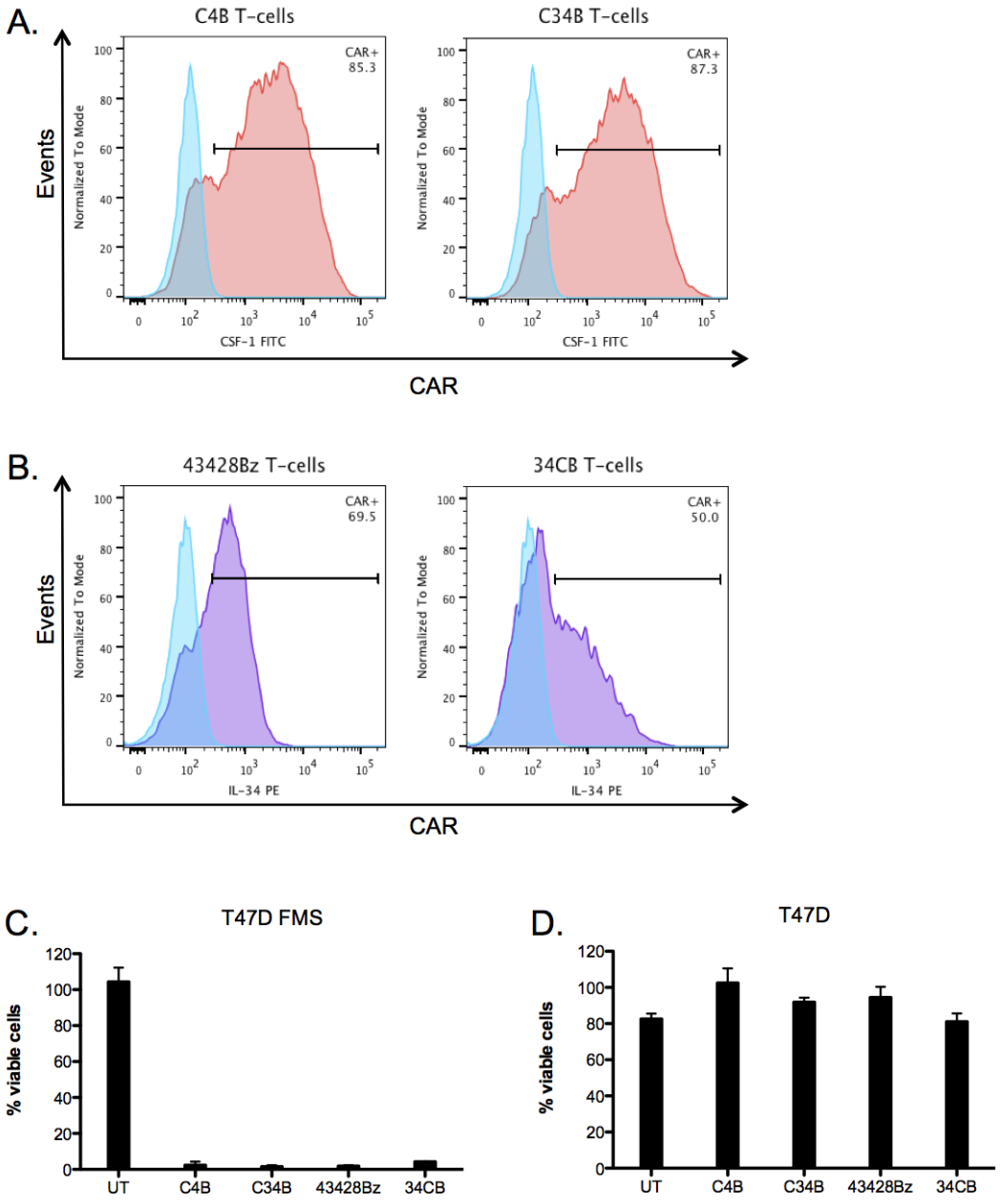

Figure 5.10 Assessing the suitability of T-cells for *in vivo* administration to K299 FMS LT xenograft bearing mice.

Transduction efficiency of each CAR$^+$ T-cell population was investigated prior to administration into mice. Detection of the CSF-1-based CARs was achieved by flow cytometry using a goat polyclonal anti-human CSF-1 antibody, followed by a FITC-conjugated secondary antibody (pink histograms) **(A)**. The level of expression of IL-34-based CARs was assessed using mouse anti-human IL-34 antibody directly conjugated to PE (purple histograms) **(B)**. Staining was compared to untransduced T-cells probed using the same antibody combinations (blue histograms). (figure and legend continue on next page)

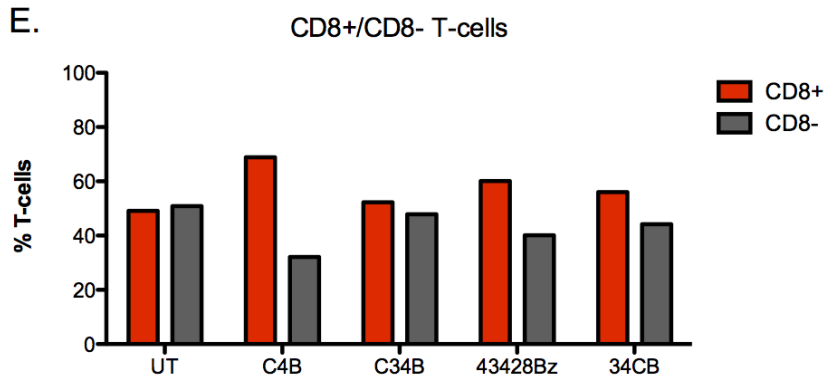

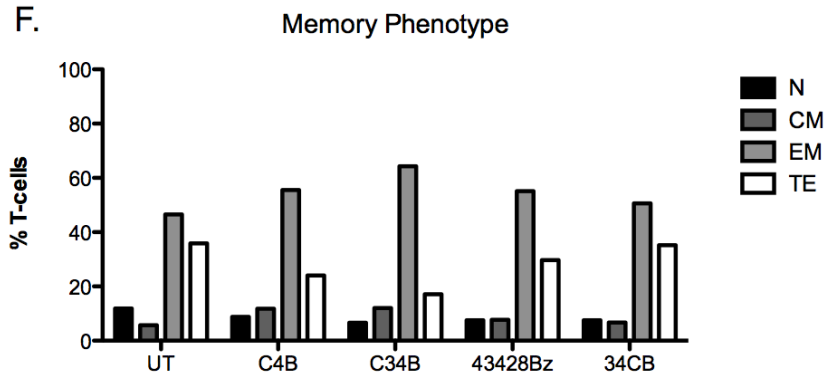

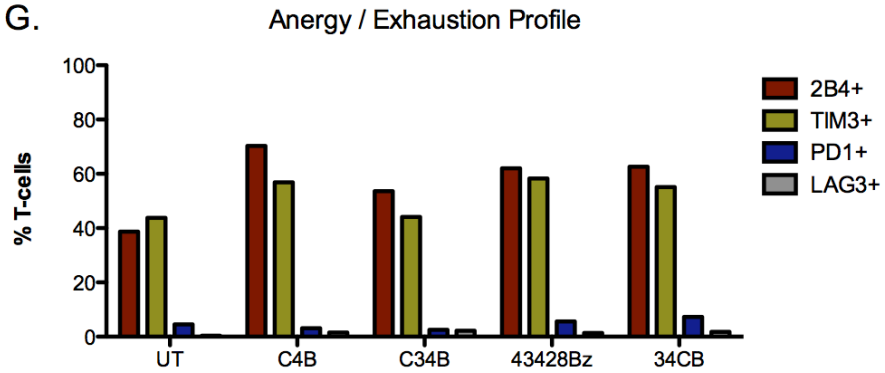

To investigate *in vitro* anti-tumour activity, surplus T-cells from the populations infused into the mice were co-cultured at 1:1 ratio with the T47D FMS and T47D cell lines **(C)** and **(D)**. Target cell destruction was measured at 24h using an MTT assay. Each sample was run in triplicate and data are presented as mean ± standard deviation. T-cell phenotype was investigated in all CAR T-cell populations. Proportion of CD8+ T-cells **(E)**, memory phenotype **(F)** and expression of a number of anergy markers **(G)** was determined by flow cytometry using a panel of directly conjugated mouse anti-human antibodies consisting of CD3 APC-Cy7, CD8 PE-Cy7, CD45RO PerCP-Cy5.5, CCR7 APC, 2B4 FITC, TIM3 PerCP-Cy5.5, PD1 APC-Cy7 and LAG3 APC.

As described previously, the immunophenotype of the CAR^+ T-cells was investigated prior to *in vivo* administration. The isolated and expanded T-cells expressed a predominantly effector memory (EM) phenotype ($CD45RO^+CCR7^-$) with roughly half of the cells expressing the CD8 co-receptor (Figure 5.10, E and F). T-cells were also probed for a number of anergy markers and as observed previously no significant difference in the immunophenotype was noted between UT T-cells and CAR^+ T-cells (Figure 5.10, G).

Despite the fact that K299 FMS LT xenografts retained high surface level of CSF-1R expression (Figure 5.9, E), mice treated with CAR^+ T-cells showed no significant therapeutic response compared to those receiving UT T-cells or PBS. There was a slight delay in tumour progression in the $C34B^+$ and $34CB^+$ T-cell treated groups, but ultimately this did not translate into a significant survival benefit (Figure 5.11, B and D). No treatment-related toxicities were observed over the duration of the study as indicated by the expected weight gain in all mice, irrespective of treatment group (Figure 5.11, C). As highlighted by Figure 5.11 E, some differences in tumour progression in individual mice were observed. Two mice in the C4B group had an initial drop in tumour burden 4 days post CAR^+ T-cell treatment and one mouse from the C34B group showed consistently slower tumour progression throughout the study.

At the end of the study, peripheral blood was collected by cardiac puncture and tumours and spleen were excised from three mice per treatment group and investigated by flow cytometry for target retention post treatment and human T-cell infiltration. As expected, no circulating T-cells were detected in the peripheral blood, spleen or tumours (data not shown) and surface levels of expression of CSF-1R in the 5 treatment groups and the control PBS group remained high *in vivo* (Figure 5.12). It was concluded that the poor treatment outcome despite the abundant target availability could be attributed partly to the lower number of infused CAR^+ T-cells (10×10^6 as

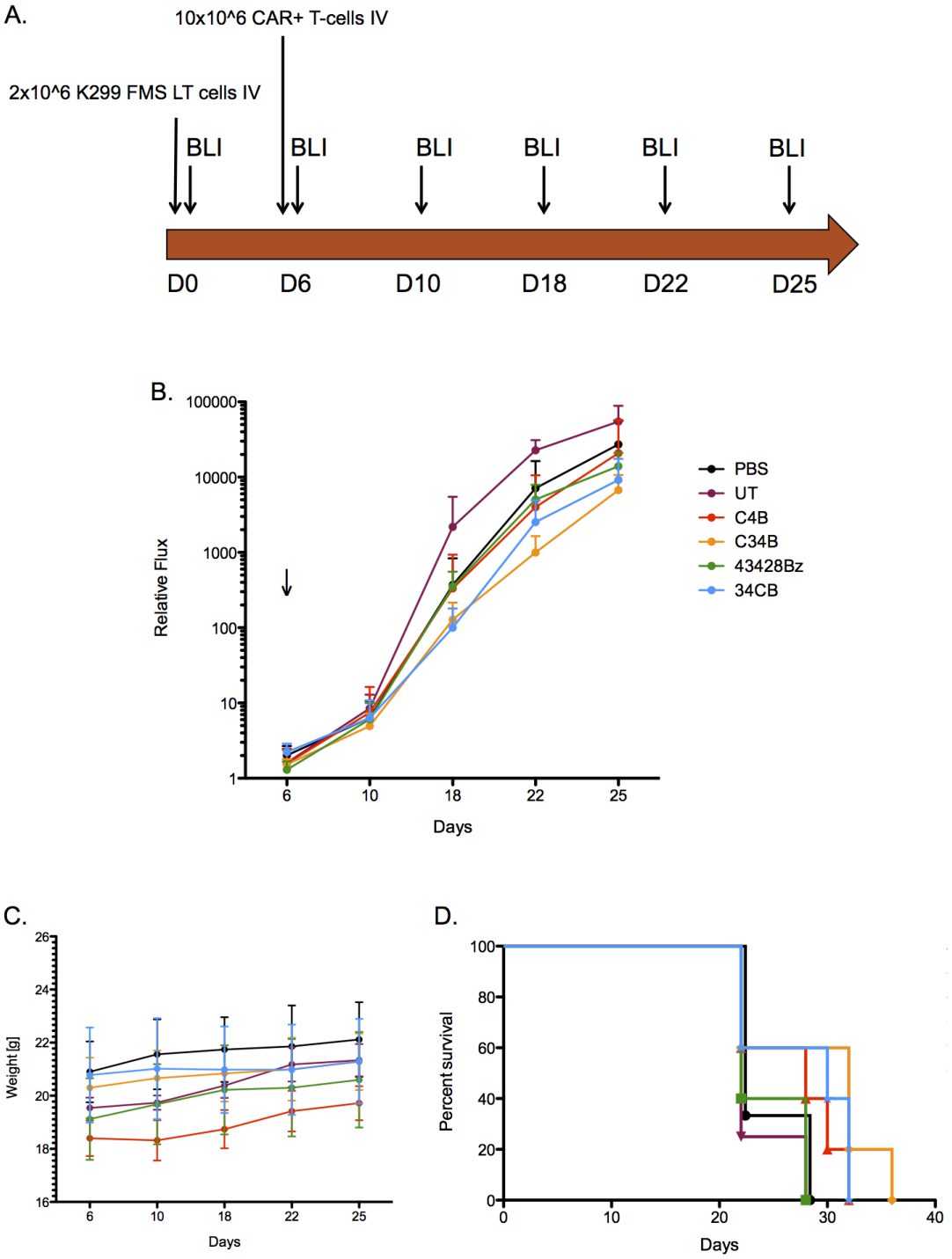

Figure 5.11 *In vivo* anti-tumour activity of CAR$^+$ T-cells in the K299 FMS LT xenograft model.

(A) 30 SCID/Beige mice were inoculated with 2 x 10^6 K299 FMS LT cells and 6 days later were treated i.v. with 10 x 10^6 CAR$^+$ T-cells or UT T-cells or PBS (n=5). Animals were weighed **(C)** and tumour burden was monitored using BLI until the conclusion of the study **(B)**. Relative flux was calculated using the following equation: (figure continues on next page)

E.

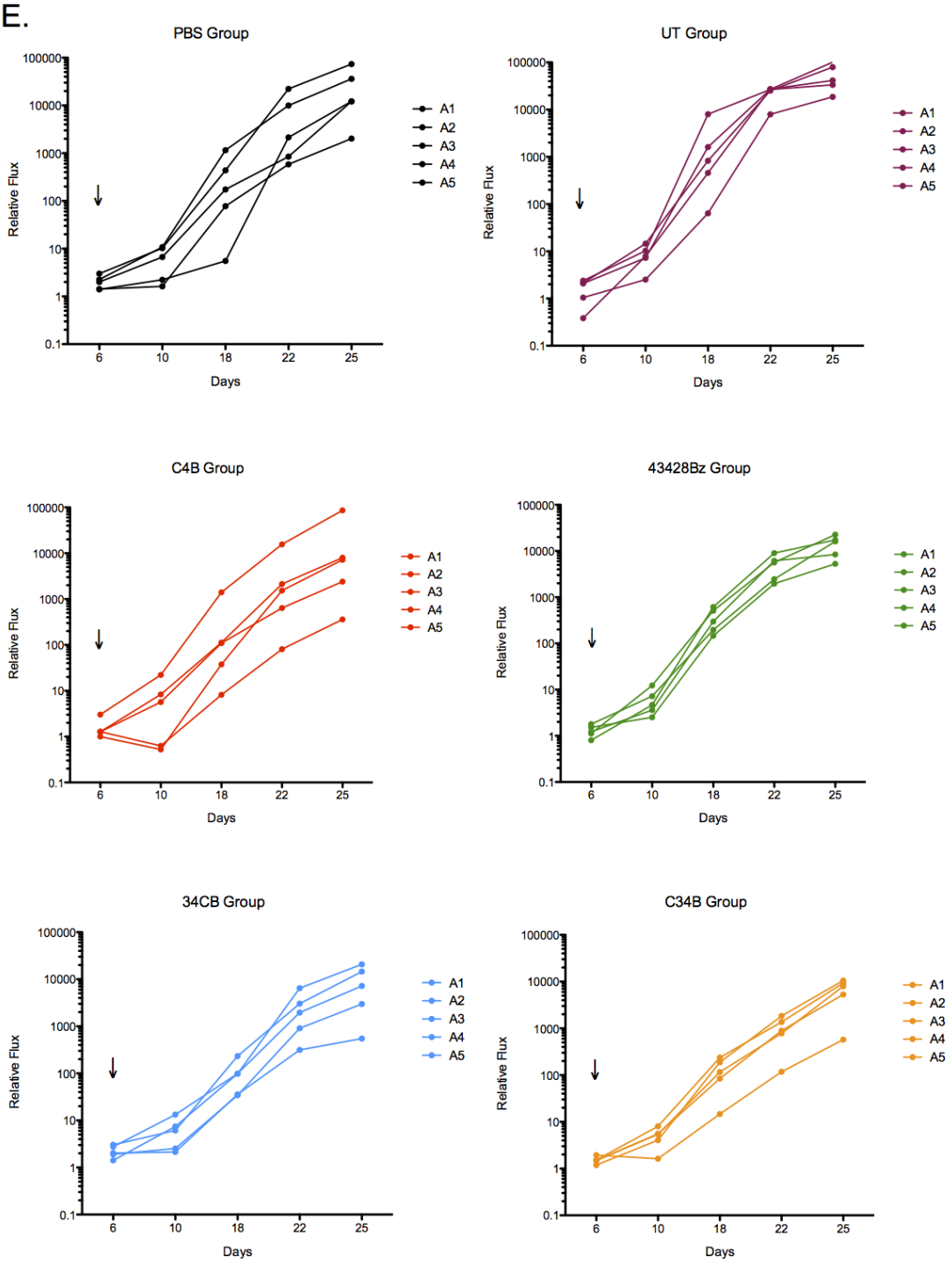

Relative Flux = (Total Flux at any given time point / Total Flux at day 0 post cancer cell administration)*100

Kaplan-Meier survival analysis showed no significant survival difference between treatment groups **(D)**. To investigate further anti-tumour efficacy within each group, total flux for individual animals have been plotted **(E)**. The data represent the mean value for each group ± SEM.

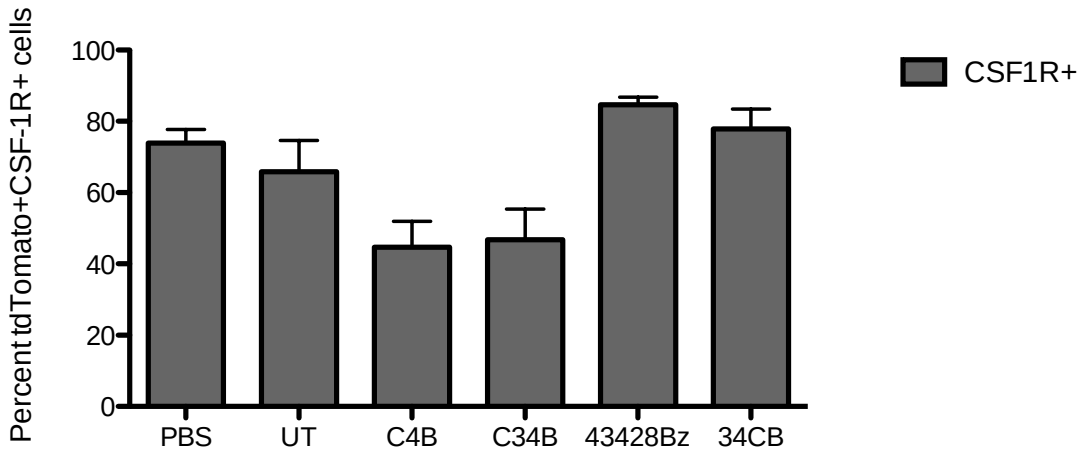

Figure 5.12 Surface levels of CSF-1R expression post treatment of the K299 FMS LT xenograft model.

Tumours from three mice per treatment group were excised post mortem and investigated for the expression of CSF-1R by flow cytometry. Single cell suspension was achieved by mechanical disaggregation. Non-specific binding of the antibodies was limited by using mouse Fc block prior to staining with a rat anti-human CSF-1R antibody, followed by a goat anti-rat FITC conjugated secondary antibody. All gates were set using FMO controls. The employed gating strategy was described previously (Figure 5.2 E). No statistically significant difference was found between groups as determined by one-way ANOVA, followed by Bonferroni post-hoc test. Data are presented as mean ± SEM.

opposed to 20 x 10^6 CAR^+ T-cells) in this experiment as well as to the general poor T-cell persistence in SCID/Beige mice.

5.3 Discussion

The major aim of this study was to evaluate the therapeutic activity of CSF-1R-re-targeted T-cells following adoptive transfer to mice with established CSF-1R-expressing human lymphoma xenografts. Therefore it was of initial importance to develop a suitable xenograft lymphoma mouse model. Subcutaneous mouse models are widely used for preclinical drug testing due to ease of tumour establishment and measurement, but they do not represent clinically relevant models of the disease. Therefore in order to assess factors such as T-cell trafficking and the suppressive tumour microenvironment upon adoptive T-cell transfer we have employed the intravenous administration route for tumour cell delivery as the closest possible representation of the clinical disease.

Out of the six lymphoma cell lines administered i.v. at 2 doses (10 x 10^6 and 5 x 10^6 cells), only the sK299 LT cell line engrafted stably, yielding a xenograft model of disseminated human $CSF\text{-}1R^+$ lymphoma in SCID/Beige mice (Figure 5.1, B). Following i.v. administration, the sK299 LT cells trafficked to the lymph nodes where solid tumours were established (Figure 5.2, C and D). In that respect, generating CAR^+ T-cells with central memory phenotype for adoptive transfer is desirable, as these cells home primarily to the lymph nodes, thereby increasing the chance for tumour encounter and eradication [410, 411]. Consequently, all T-cells were phenotyped prior to adoptive transfer but it was established that they consistently lacked CCR7 expression and exhibited predominantly effector memory T-cell phenotype (Figure 5.3, F; Figure 5.4, F and Figure 5.10, F). This could be attributed to the duration of the *in vitro* T-cell culture as well as to the cytokine milieu of the expansion protocol. At all instances, prior to *in vivo* administration transduced T-cells were expanded for 14 to 17

days in the presence of IL-4, which delivered a pseudo IL-2/IL-15 signal to transduced T-cells through the 4αβ chimeric cytokine receptor (please refer to 2.1.1.3 for more details). Alternative expansion protocols were not tested as the provided IL-4 was harnessed for its ability to induce selective expansion and enrichment of transduced T-cells [246]. One exciting possibility would be attempting to induce long-living memory stem T-cells in the presence of IL-7 and IL-15 [376, 377, 412]. These T-cells not only retain high levels of CCR7 expression but they have also been reported to have improved *in vivo* persistence when compared to T-cells expanded in IL-2 [413, 414].

To investigate their *in vivo* efficacy, CAR-grafted T-cells were adoptively transferred into mice bearing sK299 LT xenografts and their subsequent effect on tumour growth was investigated. At the same time, 3rd generation CAR^{+} T-cells were compared to double targeting CAR^{+} T-cells, for their *in vivo* persistence and therapeutic activity. The subsequent level of tumour burden displayed by CAR^{+} T-cell-treated mice was compared with those treated with UT T-cells, or with PBS alone. As demonstrated in Figure 5.5 B and E, double targeting CAR-grafted T-cells demonstrated significant anti-tumour activity *in vivo* in this model, whereas 3rd generation CAR-grafted T-cells conferred no therapeutic benefit. Mice that received one of the two alternative double targeting CAR T-cells (C34B) maintained the lowest tumour burden throughout the study, reaching significance by day 24. This result shows that double targeting CAR-grafted T-cells but not 3rd generation CAR^{+} T-cells are capable of promoting anti-tumour activity *in vivo*, in keeping with the superior performance of this CAR when tested *in vitro* (Figure 4.9; Figure 4.10 and Figure 4.11). Moreover, by the end of the study 3 mice from the C34B-treated group were tumour-free conferring 33% long-term survival of the C34B^{+} T-cell-treated group (Figure 5.5, D and Figure 5.6).

Despite the demonstrated significant anti-tumour activity *in vivo* of the C34B^{+} T-cells, 67% (6/9) of mice receiving C34B^{+} T-cells showed visible evidence of tumour at post-mortem analysis. In two of these six mice, a substantial delay in tumour progression

was observed when compared to mice treated with either UT T-cells or PBS. Nonetheless, tumour burden began to increase exponentially after day 24, indicating that the initial anti-tumour activity of C34B$^+$ T-cells in these mice did not clear the entire tumour burden. One possible explanation for this is downregulation of the target CSF-1R by tumour cells under the selective pressure of the C34B$^+$ T-cells, thereby interfering with T-cell recognition. Post-mortem analysis demonstrated that CSF-1R expression was detected in all treatment groups (Figure 5.7) and levels of expression corresponded to those found in the pilot study undertaken to investigate sK299 LT growth *in vivo* (Figure 5.2, E and F). Consequently, no *in vivo* antigen loss had occurred post CAR$^+$ T-cell treatment as demonstrated by these experiments. Despite this fact, cell surface expression of CSF-1R both *in vitro* and *in vivo* is relatively low in the sK299 LT cell line (Figure 5.2, F). This is also reflected in the modest *in vitro* anti-tumour activity of CAR$^+$ T-cells against the sK299 LT cell line (Figure 4.14). It was therefore possible that the low level of target availability was insufficient to sustain CAR$^+$ T-cell activation *in vivo* resulting in T-cell loss and/ or anergy. Since no T-cells had been detected at the end of the study or at the time of interim blood sampling, phenotyping for anergy markers was not possible.

In order to address the potential impact of low level target expression by sK299 LT tumours upon therapeutic activity of CAR$^+$ T-cells, human CSF-1R was over-expressed in these tumour cells using retroviral mediated gene transfer (Figure 5.8, A). Ectopic CSF-1R expression had no effect on the *in vitro* growth kinetics but induced slower tumour progression *in vivo* (Figure 5.8, B and Figure 5.9, A). As expected, the high level of CSF-1R expression rendered the K299 FMS LT cell line more susceptible to killing by CSF-1R-re-targeted T-cells *in vitro* (Figure 5.8, C). Target cell lysis was accompanied by CSF-1R-re-targeted T-cell activation, indicated by IFN-γ and IL-2 release (Figure 5.8, D).

Despite the fact that ectopic CSF-1R expression induced slower *in vivo* growth kinetics, it did not affect the tumour dissemination pattern observed previously with the parental cell line. As evident in Figure 5.9 C, solid tumours formed exclusively in the lymph nodes with no tumour detected in the heart, liver, lungs, spleen or peripheral blood (Figure 5.9, C and D). High cell surface expression of CSF-1R was also maintained *in vivo* in tumour-bearing mice (Figure 5.9, E). However, the observed *in vivo* anti-tumour effect of CSF-1R re-targeted CAR T-cells against the K299 FMS LT model was inferior to that seen in mice engrafted with parental sK299 LT cells (Figure 5.11, B and E). This discrepancy may in part have resulted from the different dose of CAR^+ T-cells administered in the two *in vivo* studies – while sK299 LT-xenograft-bearing mice were treated with 20 x 10^6 CAR^+ T-cells, mice engrafted with K299 FMS LT cells were administered only 10 x 10^6 CAR^+ T-cells (Figure 5.5, A and Figure 5.11, A). However, functional and phenotypic attributes of cells used in both studies were broadly similar. In both cases, T-cells had predominantly effector memory phenotype ($CD45RO^+CCR7^-$), with roughly half of the cells expressing the CD8 co-receptor, In addition, there were no significant differences observed in the expression of markers of anergy/ T-cell exhaustion (Figure 5.3, E, F and G; Figure 5.4, E, F and G; Figure 5.10, E, F and G). Furthermore, T-cell transduction efficiency for all four CAR constructs was comparable across both *in vivo* studies (Figure 5.3, A and B; Figure 5.4, A and B; Figure 5.10, A and B). Cytotoxic potential was also maintained in both cases during T-cell preparation procedures for infusion (Figure 5.3, C and D; Figure 5.4, C and D; Figure 5.10, C and D). Consequently, it was concluded that the poor *in vivo* anti-tumour activity against K299 FMS LT xenografts-bearing mice couldn't be attributed to the qualities of the T-cell product itself. This finding also suggests that expression of the CSF-1R target was not a limiting factor to the efficacy of these CAR T-cells *in vivo*.

At post-mortem analysis, CSF-1R expression was detected in all treatment groups (Figure 5.12) and levels of expression were similar to those observed in the pilot study undertaken to investigate K299 FMS LT growth *in vivo* (Figure 5.9, E). Interestingly,

C4B$^+$ and C34B$^+$ T-cell treated mice showed a considerable, yet not statistically significant decrease in cell surface target expression when compared to mice treated with UT T-cells (Figure 5.12). This observation correlates with initial treatment response observed in 2 mice in the C4B$^+$ T-cell treated group and one mouse in the C34B$^+$ T-cell group (Figure 5.11, E). It is therefore likely, that during the initial anti-tumour activity down-regulation of the target antigen has occurred at least in some tumour cells in those 2 groups. Indeed, target antigen modulation under selective pressure is one of the most important tumour escape strategies associated with treatment failure or with subsequent relapse, following the administration of a monospecific product [210, 415], including CAR T-cells [210]. Nevertheless, even though antigen loss probably played a role in the initial anti-tumour activity in the C4B$^+$ and C34B$^+$ T-cell treated groups, it is unlikely to be responsible for the observed poor anti-tumour activity against K299 FMS LT xenografts-bearing mice, as at the end of the study target antigen expression was much higher in all groups when compared to the sK299 FMS xenograft model (Figure 5.7 and Figure 5.12).

Taken together these results suggest that the high level of target expression, achieved by ectopic CSF-1R expression, is of secondary importance to the treatment response in this model. Apart from the partial antigen loss that may have occurred in two of the treatment groups, this could be attributed to the fast recycling of the receptor from the cell surface upon ligand binding.

An alternative possibility is that the T-cells may have undergone activation-induced cell death (AICD) due to being overwhelmed by the antigen [416]. Chronic stimulation of T-cells leads to the up-regulation of both Fas and Fas ligand, which are the principal mediators of AICD, leading to subsequent loss of anti-tumour activity [417]. However, no T-cells were recovered at the end of the study, which precluded further investigation into Fas/Fas ligand expression on CAR$^+$ T-cells.

In conclusion, the greater anti-tumour activity observed in mice with sK299 LT compared to sK299 FMS tumours can most probably be attributed to the larger dose of CAR^+ T-cells administered in this study. The overall treatment response in the K299 FMS LT xenograft bearing mice, even though modest when compared to the previous study with the sK299 LT model, was best in the double targeting CAR^+ T-cell treated groups, consistent with my previous observations (Figure 5.11, B). The most likely explanation for the better double targeting CAR^+ T-cell control over tumour growth when compared to third generation CAR^+ T-cells is their better survival following adoptive transfer. Although investigations into CAR^+ T-cell *in vivo* persistence (using T-cell imaging) were not undertaken, collected *in vitro* data suggest that double targeting CAR^+ T-cells, and not 3rd generation CAR^+ T-cells, retain their ability to produce IL-2 through recursive antigen re-stimulation, thereby supporting their proliferation and survival for longer (Figure 4.9, 4.10 and 4.11). Indeed, lack of sustainable T-cell persistence following adoptive transfer has been postulated as a major contributing factor to the poor responses so far seen in clinical trials [169-171, 221]. Furthermore, beneficial outcomes have been strongly correlated with more pronounced *in vivo* longevity following adoptive transfer in both animal models and patients [180, 418].

Overall, these data have shown that T-cells expressing double targeting CARs but not 3rd generation CARs retain their anti-tumour activity following adoptive transfer *in vivo*. In the case of $C34B^+$ T-cell treated mice, this response results in a significant delay in tumour growth in the sK299 LT xenograft model when compared to mice treated with UT T-cells or PBS. A major obstacle to achieving more profound *in vivo* anti-tumour activity of CAR^+ T-cells has been the aggressive nature of the lymphoma model, while at the same time, T-cell persistence post adoptive transfer has been poor. Consequently, strategies aimed at increasing the survival of CAR^+ T-cells may need to be considered for future efficacy studies in an attempt to ensure complete tumour regression and a sustained anti-tumour effect. One such strategy involves the use of more severely immune-compromised mice models. Most such models described in the

literature rely on NOD/SCID mouse strains, which contain additional mutations in the common gamma chain of the IL-2 receptor gene. This mutation can either be a truncation in the case of so-called NOG mice or a null mutation in NSG mice [419, 420]. Both strains are characterised by a similar phenotype lacking T-cells, B-cells and NK cells, while macrophages and dendritic cells are defective, thereby providing a better setting for CAR^+ T-cell engraftment and persistence post *in vivo* administration [421]. Another strategy, would be employing the 4$\alpha\beta$ expansion system *in vivo*, in particular since IL-4 has been administered to patients with diverse malignancies, including lymphoma [422, 423].

Chapter 6 General Discussion

The overall aim of this PhD was to investigate whether primary human T-cells could be genetically re-targeted against CSF-1R and whether this approach could represent a novel therapy for the treatment of cHL and ALCL.

The emerging picture of the CSF-1/CSF-1R axis in cHL and ALCL reveals its central role in tumour progression [34, 35]. The oncogenic potential of this cytokine receptor pair arises from autocrine and/or paracrine signalling, which promotes tumour cell proliferation and survival [294]. Additionally, CSF-1-secreting tumours are known to stimulate local macrophage recruitment and monocyte education to TAMs, which in turn mediate immune suppression and confer resistance to cytotoxic therapies [294]. Thus, blockade of this axis might be expected not only to directly target CSF-1R-expressing neoplastic cells, but also to abrogate the tumour permissive and immunosuppressive microenvironment.

Over the past decade, there has been an exponential increase in the number of clinical studies undertaken to evaluate the safety and efficacy of CAR T-cell based immunotherapy in patients with diverse malignant disorders. Of these, most successful trials have been directed against haematological malignancies of B-cell origin while achievements against solid cancers have been more modest. Among the major obstacles to effective CAR-based immunotherapy of cancer are poor *in vivo* longevity of the genetically modified T-cells and their sub-optimal effector function within the tumour microenvironment. Both limitations may be attributed at least in part to inefficient CAR^+ T-cell co-stimulation in the often hostile tumour microenvironment. Physiological co-stimulation of T-cells is a dynamic process that relies upon a large number of co-stimulatory molecules that display great diversity in their expression and structure and whose functions are largely context dependent [424]. However, the genetic engineering of T-cells imposes restrictions on the number of co-stimulatory

molecules that can be employed. Consequently, in an attempt to fine-tune CAR-mediated T-cell co-stimulation, a panel of eight CARs targeting CSF-1R have been designed and cloned. Two targeting moieties with distinct target affinities have been utilised to assess the impact of the rate of target engagement and target dissociation on CAR activation. Furthermore, classical second and third generation CARs have been compared to novel double targeting CARs, providing co-stimulation *in trans*.

A key starting point in the *in vitro* characterisation of the panel of CARs was the demonstration that they can all be routinely and stably expressed at the surface of primary human T-cells. This was confirmed by flow cytometry on a number of occasions, including following antigen-mediated activation, indicating successful integration of the receptor cDNA into the recipient T-cell genome. This is an important observation, as stable CAR expression is central to achieving a sustained anti-tumour response.

The targeting strategy employed in this thesis was first validated against the breast cancer cell line T47D FMS, which has been shown to express high levels of the target CSF-1R in a stable manner. Successful genetic re-targeting of T-cells was confirmed by complete target cell destruction within 24h of co-culture. Furthermore, cancer cell lysis was accompanied by CAR T-cell activation, which occurred only in the presence of the antigen (T47D FMS cells), but not in its absence (T47D cells) or in the absence of monolayer, confirming specificity of the CAR T-cell activation. A crucial observation made during these *in vitro* studies was the poorer activation of IL-34-based CARs in comparison to CSF-1-based CARs. These findings can most probably be attributed to the higher affinity of IL-34 interaction with the target, which can prove an impediment to serial target engagement and disengagement by CAR T-cells, thereby causing lower biological activity of IL-34-based CAR-grafted T-cells [385-390, 425]. An additional crucial observation was that provision of CAR-derived dual co-stimulation *in trans*, by co-expression of a pair of synergistic CARs, elicits more robust and sustained anti-

tumour activity *in vitro*. Whilst all signalling-competent CSF-1R-targeting CAR constructs showed identical cytolytic capacity upon encountering the target for the first time, successive rounds of antigen stimulations revealed that the C34B CAR repeatedly outperformed matched second and third generation CARs. The observed poor second and third generation CAR T-cell expansion and accumulation is not uncommon when weekly repeated antigen stimulations are performed in the absence of exogenous cytokine support [391]. A third crucial observation was that superior antigen-specific proliferation, cytokine secretion (IL-2 and IFN-γ) and cytotoxicity upon consecutive rounds of antigen stimulation were observed only with C34B-grafted T-cells and not in the 34CB$^+$ T-cell group. These results suggest that while providing co-stimulation *in trans* results in favourable spatial and temporal differences in the recruitment, kinetics and regulation of co-stimulation, fine-tuning of co-stimulation through the CAR affinities is necessary to achieve optimal potency of the constructs.

The ability of all signalling-competent CAR-grafted T-cells to be successfully redirected against cHL and ALCL was confirmed by their activation when co-cultivated with 6/6 lymphoma cell lines. All six lymphoma cell lines produced at least one of the natural ligands for CSF-1R. Autocrine stimulation of CSF-1R in this manner is known to induce receptor down-regulation by internalization of the receptor-ligand complex [335], which would be expected to compromise targeting of CSF-1R$^+$ lymphoma cells by CAR T-cells that have been directed against this target. Nonetheless, significant target cell lysis of all lymphoma cell lines was reproducibly observed. In an additional step, dexamethasone priming of the panel of lymphoma cell lines was tested as a device to up-regulate the expression of CSF-1R by lymphoma cells. However, this approach failed to induce significant cell surface up-regulation of the target, precluding its further use. A crucial future step in determining the translational feasibility of this approach will be to determine whether anti-tumour activity is maintained when re-directed autologous T-cells are co-cultured with primary tumour samples.

A final intention of these studies was to characterize the therapeutic impact of CSF-1R-re-targeted T-lymphocytes on *in vivo* tumour growth. A crucial observation in the preclinical evaluation of these T-cells was that double targeting CAR-grafted T-cells but not 3rd generation CAR^{+} T-cells retain their anti-tumour activity *in vivo*. Specifically, in the case of C34B^{+} T-cell treated mice, this response resulted in significant delay in tumour growth and 33% long-term survival in the sK299 LT xenograft model. The observed superior tumour growth control by double targeting CAR T-cells in comparison to 3rd generation CAR T-cells may be attributable to their enhanced survival *in vivo* following adoptive transfer. In support of this, double targeted CAR T-cells exhibited a more durable ability to undergo re-stimulation *in vitro* upon co-culture with CSF-1R-expressing lymphoma cells. In future studies, imaging of CAR re-targeted T-cells could provide valuable information on their *in vivo* longevity and bio-distribution, providing further information on this question.

Safety of CAR T-cell immunotherapy has remained problematic to date. On-target toxicity has been linked to frequent occurrence of CRS, which has been lethal on occasions [195]. All currently available CSF-1R targeted therapies have shown acceptable level of toxicity in phase 1 clinical trials [408, 409]. Grade 3/4 adverse events (asthenia, peripheral edema and pyrexia) have been reported in only 18% of patients (21/114) upon treatment with a humanised anti-CSF-1R monoclonal antibody termed RG7155. Reported toxicities include significant reduction of surrogate skin tissue resident macrophages and rapid elimination of CD14^{+}CD16^{+} peripheral monocytes, while classical CD14^{+}CD16^{-} monocytes did not show a sustained alteration.

Assessing the potential toxicities of any targeted therapy is extremely difficult in the preclinical setting owing to the need for cross-reactivity with the murine analogue of the target. However, human CSF-1 is capable of interacting with the murine as well as the human CSF-1R [426, 427], while human IL-34 interacts very inefficiently with murine

CSF-1R [426, 428]. Initial efficacy studies have revealed that CAR$^+$ T-cell treatment was very well tolerated, causing temporary loss of <5% body weight without any other side effects attributed to the treatment despite the observed anti-tumour activity. Another approach for investigating potential toxicity prior to further *in vivo* testing involves the co-culture of CAR-grafted T-cells with isolated primary monocytes and human monocyte-derived macrophages *in vitro*. Alternatively, depletion of tissue resident macrophages and/or circulating monocytes can be assessed following adoptive transfer of CAR-grafted T-cells in tumour-free murine models. Taken together, data presented in this thesis establish the principle that CSF-1R-targeted CAR$^+$ T-cells can exert anti-tumour activity against ALCL cells with acceptable safety in a mouse model in which cytokine storm can be elicited [240].

Despite encouraging results in selected haematological malignancies, a variety of discrete immune checkpoints can restrict the full potential of CAR T-cell therapy. Use of checkpoint inhibitors targeting CTLA-4 and PD-1/ PD-L1 have yielded impressive results in a select range of solid tumours, providing exciting opportunities for combinational therapy with CAR T-cells. Furthermore, the striking response to PD1 blockade as a single agent in cHL (74% overall response and 17% complete response) suggests that investigation into the potential for a combination therapy with CAR T-cells is merited [60].

Overall, the data presented within this thesis show that CAR-grafted T-cells have been successfully re-targeted against a panel of cHL and ALCL tumour cell lines *in vitro* and that this anti-tumour activity is maintained *in vivo*. An innovative approach has been developed and optimised in which the 4$\alpha\beta$ chimeric cytokine receptor is co-expressed with a pair of synergistic CARs targeted against CSF-1R. Data outlined in this thesis suggest that provision of CAR-derived dual co-stimulation *in trans* elicits more robust and sustained anti-tumour activity both *in vitro* and *in vivo*. This is accompanied by superior antigen-specific proliferation, cytokine secretion (IL-2 and IFN-γ) and

cytotoxicity upon consecutive rounds of antigen stimulation in comparison to second and third generation CARs. These encouraging findings warrant further investigations into the translational application of this technology in cHL and ALCL.

References

1. Hodgkin, (1832) On some Morbid Appearances of the Absorbent Glands and Spleen. Med Chir Trans. 17: p. 68 - 114.
2. Kuppers, R., Engert, A., and Hansmann, M.L., (2012) Hodgkin lymphoma. J Clin Invest. 122(10): p. 3439-47.
3. UK., C.R., (2013) Cancer stats incidence 2013—UK. http://www.cancerresearchuk.org/health-professional/hodgkin-lymphoma-statistics - heading-Zero. ((accessed 15/02/2016)).
4. Steidl, C., Diepstra, A., Lee, T., Chan, F.C., Farinha, P., Tan, K., Telenius, A., Barclay, L., Shah, S.P., Connors, J.M., et al., (2012) Gene expression profiling of microdissected Hodgkin Reed-Sternberg cells correlates with treatment outcome in classical Hodgkin lymphoma. Blood. 120(17): p. 3530-40.
5. Jaffe, E.S., (2009) The 2008 WHO classification of lymphomas: implications for clinical practice and translational research. Hematology Am Soc Hematol Educ Program. p. 523-31.
6. Jarrett, R.F., Krajewski, A.S., Angus, B., Freeland, J., Taylor, P.R., Taylor, G.M., and Alexander, F.E., (2003) The Scotland and Newcastle epidemiological study of Hodgkin's disease: impact of histopathological review and EBV status on incidence estimates. J Clin Pathol. 56(11): p. 811-6.
7. Harris, N.L., Jaffe, E.S., Stein, H., Banks, P.M., Chan, J.K., Cleary, M.L., Delsol, G., De Wolf-Peeters, C., Falini, B., Gatter, K.C., et al., (1994) A revised European-American classification of lymphoid neoplasms: a proposal from the International Lymphoma Study Group. Blood. 84(5): p. 1361-92.
8. Collins, G.P., Parker, A.N., Pocock, C., Kayani, I., Sureda, A., Illidge, T., Ardeshna, K., Linch, D.C., and Peggs, K.S., (2014) Guideline on the management of primary resistant and relapsed classical Hodgkin lymphoma. Br J Haematol. 164(1): p. 39-52.

9. Carbone, P.P., Kaplan, H.S., Musshoff, K., Smithers, D.W., and Tubiana, M., (1971) Report of the Committee on Hodgkin's Disease Staging Classification. Cancer Res. 31(11): p. 1860-1.

10. Lister, T.A., Crowther, D., Sutcliffe, S.B., Glatstein, E., Canellos, G.P., Young, R.C., Rosenberg, S.A., Coltman, C.A., and Tubiana, M., (1989) Report of a committee convened to discuss the evaluation and staging of patients with Hodgkin's disease: Cotswolds meeting. J Clin Oncol. 7(11): p. 1630-6.

11. Schmitz, R., Stanelle, J., Hansmann, M.L., and Kuppers, R., (2009) Pathogenesis of classical and lymphocyte-predominant Hodgkin lymphoma. Annu Rev Pathol. 4: p. 151-74.

12. Pileri, S.A., Ascani, S., Leoncini, L., Sabattini, E., Zinzani, P.L., Piccaluga, P.P., Pileri, A., Jr., Giunti, M., Falini, B., Bolis, G.B., et al., (2002) Hodgkin's lymphoma: the pathologist's viewpoint. J Clin Pathol. 55(3): p. 162-76.

13. Kuppers, R., (2009) The biology of Hodgkin's lymphoma. Nat Rev Cancer. 9(1): p. 15-27.

14. Tedoldi, S., Mottok, A., Ying, J., Paterson, J.C., Cui, Y., Facchetti, F., van Krieken, J.H., Ponzoni, M., Ozkal, S., Masir, N., et al., (2007) Selective loss of B-cell phenotype in lymphocyte predominant Hodgkin lymphoma. J Pathol. 213(4): p. 429-40.

15. Matsuki, E. and Younes, A., (2015) Lymphomagenesis in Hodgkin lymphoma. Semin Cancer Biol. 34: p. 14-21.

16. Marafioti, T., Hummel, M., Foss, H.D., Laumen, H., Korbjuhn, P., Anagnostopoulos, I., Lammert, H., Demel, G., Theil, J., Wirth, T., et al., (2000) Hodgkin and reed-sternberg cells represent an expansion of a single clone originating from a germinal center B-cell with functional immunoglobulin gene rearrangements but defective immunoglobulin transcription. Blood. 95(4): p. 1443-50.

17. Kuppers, R., Rajewsky, K., Zhao, M., Simons, G., Laumann, R., Fischer, R., and Hansmann, M.L., (1994) Hodgkin disease: Hodgkin and Reed-Sternberg

cells picked from histological sections show clonal immunoglobulin gene rearrangements and appear to be derived from B cells at various stages of development. Proc Natl Acad Sci U S A. 91(23): p. 10962-6.

18. Cabannes, E., Khan, G., Aillet, F., Jarrett, R.F., and Hay, R.T., (1999) Mutations in the IkBa gene in Hodgkin's disease suggest a tumour suppressor role for IkappaBalpha. Oncogene. 18(20): p. 3063-70.

19. Bargou, R.C., Leng, C., Krappmann, D., Emmerich, F., Mapara, M.Y., Bommert, K., Royer, H.D., Scheidereit, C., and Dorken, B., (1996) High-level nuclear NF-kappa B and Oct-2 is a common feature of cultured Hodgkin/Reed-Sternberg cells. Blood. 87(10): p. 4340-7.

20. Skinnider, B.F., Elia, A.J., Gascoyne, R.D., Patterson, B., Trumper, L., Kapp, U., and Mak, T.W., (2002) Signal transducer and activator of transcription 6 is frequently activated in Hodgkin and Reed-Sternberg cells of Hodgkin lymphoma. Blood. 99(2): p. 618-26.

21. Holtick, U., Vockerodt, M., Pinkert, D., Schoof, N., Sturzenhofecker, B., Kussebi, N., Lauber, K., Wesselborg, S., Loffler, D., Horn, F., et al., (2005) STAT3 is essential for Hodgkin lymphoma cell proliferation and is a target of tyrphostin AG17 which confers sensitization for apoptosis. Leukemia. 19(6): p. 936-44.

22. Joos, S., Granzow, M., Holtgreve-Grez, H., Siebert, R., Harder, L., Martin-Subero, J.I., Wolf, J., Adamowicz, M., Barth, T.F., Lichter, P., et al., (2003) Hodgkin's lymphoma cell lines are characterized by frequent aberrations on chromosomes 2p and 9p including REL and JAK2. Int J Cancer. 103(4): p. 489-95.

23. Weniger, M.A., Melzner, I., Menz, C.K., Wegener, S., Bucur, A.J., Dorsch, K., Mattfeldt, T., Barth, T.F., and Moller, P., (2006) Mutations of the tumor suppressor gene SOCS-1 in classical Hodgkin lymphoma are frequent and associated with nuclear phospho-STAT5 accumulation. Oncogene. 25(18): p. 2679-84.

24. Dutton, A., O'Neil, J.D., Milner, A.E., Reynolds, G.M., Starczynski, J., Crocker, J., Young, L.S., and Murray, P.G., (2004) Expression of the cellular FLICE-inhibitory protein (c-FLIP) protects Hodgkin's lymphoma cells from autonomous Fas-mediated death. Proc Natl Acad Sci U S A. 101(17): p. 6611-6.

25. Williams, H. and Crawford, D.H., (2006) Epstein-Barr virus: the impact of scientific advances on clinical practice. Blood. 107(3): p. 862-9.

26. Brauninger, A., Schmitz, R., Bechtel, D., Renne, C., Hansmann, M.L., and Kuppers, R., (2006) Molecular biology of Hodgkin's and Reed/Sternberg cells in Hodgkin's lymphoma. Int J Cancer. 118(8): p. 1853-61.

27. Bart, S.M., Johnson, T.R., DeGo, D.J., and Henning, J.D., (2013) Epstein-Barr Virus (EBV) and the effectiveness of suberoylanilide hydroxamic acid (SAHA) as a treatment for EBV infection and associated cancers. Advances in Tumour Virology. 3: p. 1-7.

28. Gulley, M.L., Eagan, P.A., Quintanilla-Martinez, L., Picado, A.L., Smir, B.N., Childs, C., Dunn, C.D., Craig, F.E., Williams, J.W., Jr., and Banks, P.M., (1994) Epstein-Barr virus DNA is abundant and monoclonal in the Reed-Sternberg cells of Hodgkin's disease: association with mixed cellularity subtype and Hispanic American ethnicity. Blood. 83(6): p. 1595-602.

29. Mancao, C., Altmann, M., Jungnickel, B., and Hammerschmidt, W., (2005) Rescue of "crippled" germinal center B cells from apoptosis by Epstein-Barr virus. Blood. 106(13): p. 4339-44.

30. Steelman, L.S., Chappell, W.H., Abrams, S.L., Kempf, R.C., Long, J., Laidler, P., Mijatovic, S., Maksimovic-Ivanic, D., Stivala, F., Mazzarino, M.C., et al., (2011) Roles of the Raf/MEK/ERK and PI3K/PTEN/Akt/mTOR pathways in controlling growth and sensitivity to therapy-implications for cancer and aging. Aging (Albany NY). 3(3): p. 192-222.

31. Thomas, S.J., Snowden, J.A., Zeidler, M.P., and Danson, S.J., (2015) The role of JAK/STAT signalling in the pathogenesis, prognosis and treatment of solid tumours. Br J Cancer. 113(3): p. 365-71.

32. Renne, C., Hansmann, M.L., and Brauninger, A., (2009) [Receptor tyrosine kinases in Hodgkin lymphoma as possible therapeutic targets]. Pathologe. 30(5): p. 393-400.

33. Renné C, W.K., Küppers R et al., (2005) Autocrine- and paracrine-activated receptor tyrosine kinases in classic Hodgkin lymphoma. Blood. 105(10): p. 4051 - 9.

34. Lamprecht, B., Walter, K., Kreher, S., Kumar, R., Hummel, M., Lenze, D., Kochert, K., Bouhlel, M.A., Richter, J., Soler, E., et al., (2010) Derepression of an endogenous long terminal repeat activates the CSF1R proto-oncogene in human lymphoma. Nat Med. 16(5): p. 571-9, 1p following 579.

35. Paietta, E., Racevskis, J., Stanley, E.R., Andreeff, M., Papenhausen, P., and Wiernik, P.H., (1990) Expression of the macrophage growth factor, CSF-1 and its receptor c-fms by a Hodgkin's disease-derived cell line and its variants. Cancer Res. 50(7): p. 2049-55.

36. Townsend, W. and Linch, D., (2012) Hodgkin's lymphoma in adults. Lancet. 380(9844): p. 836-47.

37. Board, P.D.Q.A.T.E., *Adult Hodgkin Lymphoma Treatment (PDQ(R)): Health Professional Version*, in *PDQ Cancer Information Summaries*. 2002, National Cancer Institute (US): Bethesda (MD).

38. Peters, M.V. and Middlemiss, K.C., (1958) A study of Hodgkin's disease treated by irradiation. Am J Roentgenol Radium Ther Nucl Med. 79(1): p. 114-21.

39. Kaplan, H.S., (1966) Evidence for a tumoricidal dose level in the radiotherapy of Hodgkin's disease. Cancer Res. 26(6): p. 1221-4.

40. Devita, V.T., Jr., Serpick, A.A., and Carbone, P.P., (1970) Combination chemotherapy in the treatment of advanced Hodgkin's disease. Ann Intern Med. 73(6): p. 881-95.

41. Canellos, G.P., Anderson, J.R., Propert, K.J., Nissen, N., Cooper, M.R., Henderson, E.S., Green, M.R., Gottlieb, A., and Peterson, B.A., (1992)

Chemotherapy of advanced Hodgkin's disease with MOPP, ABVD, or MOPP alternating with ABVD. N Engl J Med. 327(21): p. 1478-84.

42. Ansell, S.M., (2016) Hodgkin lymphoma: MOPP chemotherapy to PD-1 blockade and beyond. Am J Hematol. 91(1): p. 109-12.

43. Diehl, V. and Behringer, K., (2006) Could BEACOPP be the new standard for the treatment of advanced Hodgkin's lymphoma (HL)? Cancer Invest. 24(7): p. 713-7.

44. Hoppe, R.T., (1997) Hodgkin's disease: complications of therapy and excess mortality. Ann Oncol. 8 Suppl 1: p. 115-8.

45. Akhtar, S., El Weshi, A., Rahal, M., Abdelsalam, M., Al Husseini, H., and Maghfoor, I., (2010) High-dose chemotherapy and autologous stem cell transplant in adolescent patients with relapsed or refractory Hodgkin's lymphoma. Bone Marrow Transplant. 45(3): p. 476-82.

46. Baker, K.S., Gordon, B.G., Gross, T.G., Abromowitch, M.A., Lyden, E.R., Lynch, J.C., Vose, J.M., Armitage, J.O., Coccia, P.F., and Bierman, P.J., (1999) Autologous hematopoietic stem-cell transplantation for relapsed or refractory Hodgkin's disease in children and adolescents. J Clin Oncol. 17(3): p. 825-31.

47. Brice, P., (2008) Managing relapsed and refractory Hodgkin lymphoma. Br J Haematol. 141(1): p. 3-13.

48. Shadle, P.J., Allen, J.I., Geier, M.D., and Koths, K., (1989) Detection of endogenous macrophage colony-stimulating factor (M-CSF) in human blood. Exp Hematol. 17(2): p. 154-9.

49. Rehwald, U., Schulz, H., Reiser, M., Sieber, M., Staak, J.O., Morschhauser, F., Driessen, C., Rudiger, T., Muller-Hermelink, K., Diehl, V., et al., (2003) Treatment of relapsed CD20+ Hodgkin lymphoma with the monoclonal antibody rituximab is effective and well tolerated: results of a phase 2 trial of the German Hodgkin Lymphoma Study Group. Blood. 101(2): p. 420-4.

50. Ekstrand, B.C., Lucas, J.B., Horwitz, S.M., Fan, Z., Breslin, S., Hoppe, R.T., Natkunam, Y., Bartlett, N.L., and Horning, S.J., (2003) Rituximab in lymphocyte-

predominant Hodgkin disease: results of a phase 2 trial. Blood. 101(11): p. 4285-9.

51. Smith, S.M., Schoder, H., Johnson, J.L., Jung, S.H., Bartlett, N.L., and Cheson, B.D., (2013) The anti-CD80 primatized monoclonal antibody, galiximab, is well-tolerated but has limited activity in relapsed Hodgkin lymphoma: Cancer and Leukemia Group B 50602 (Alliance). Leuk Lymphoma. 54(7): p. 1405-10.

52. Fanale, M., Assouline, S., Kuruvilla, J., Solal-Celigny, P., Heo, D.S., Verhoef, G., Corradini, P., Abramson, J.S., Offner, F., Engert, A., et al., (2014) Phase IA/II, multicentre, open-label study of the CD40 antagonistic monoclonal antibody lucatumumab in adult patients with advanced non-Hodgkin or Hodgkin lymphoma. Br J Haematol. 164(2): p. 258-65.

53. LeMaistre, C.F., Saleh, M.N., Kuzel, T.M., Foss, F., Platanias, L.C., Schwartz, G., Ratain, M., Rook, A., Freytes, C.O., Craig, F., et al., (1998) Phase I trial of a ligand fusion-protein (DAB389IL-2) in lymphomas expressing the receptor for interleukin-2. Blood. 91(2): p. 399-405.

54. Dancey, G., Violet, J., Malaroda, A., Green, A.J., Sharma, S.K., Francis, R., Othman, S., Parker, S., Buscombe, J., Griffin, N., et al., (2009) A Phase I Clinical Trial of CHT-25 a 131I-Labeled Chimeric Anti-CD25 Antibody Showing Efficacy in Patients with Refractory Lymphoma. Clin Cancer Res. 15(24): p. 7701-7710.

55. Forero-Torres, A., Leonard, J.P., Younes, A., Rosenblatt, J.D., Brice, P., Bartlett, N.L., Bosly, A., Pinter-Brown, L., Kennedy, D., Sievers, E.L., et al., (2009) A Phase II study of SGN-30 (anti-CD30 mAb) in Hodgkin lymphoma or systemic anaplastic large cell lymphoma. Br J Haematol. 146(2): p. 171-9.

56. Ansell, S.M., Horwitz, S.M., Engert, A., Khan, K.D., Lin, T., Strair, R., Keler, T., Graziano, R., Blanset, D., Yellin, M., et al., (2007) Phase I/II study of an anti-CD30 monoclonal antibody (MDX-060) in Hodgkin's lymphoma and anaplastic large-cell lymphoma. J Clin Oncol. 25(19): p. 2764-9.

57. Peggs, K.S., (2015) Recent advances in antibody-based therapies for Hodgkin Lymphoma. Br J Haematol.

58. Terriou, L., Bonnet, S., Debarri, H., Demarquette, H., and Morschhauser, F., (2013) [Brentuximab vedotin: new treatment for CD30+ lymphomas]. Bull Cancer. 100(7-8): p. 775-9.

59. Younes, A., Connors, J.M., Park, S.I., Fanale, M., O'Meara, M.M., Hunder, N.N., Huebner, D., and Ansell, S.M., (2013) Brentuximab vedotin combined with ABVD or AVD for patients with newly diagnosed Hodgkin's lymphoma: a phase 1, open-label, dose-escalation study. Lancet Oncol. 14(13): p. 1348-56.

60. Ansell, S.M., Lesokhin, A.M., Borrello, I., Halwani, A., Scott, E.C., Gutierrez, M., Schuster, S.J., Millenson, M.M., Cattry, D., Freeman, G.J., et al., (2015) PD-1 blockade with nivolumab in relapsed or refractory Hodgkin's lymphoma. N Engl J Med. 372(4): p. 311-9.

61. Moskowitz, C., Ribrag, V., Michot, J., Martinelli, G., Zinzani, P.L., Gutierrez, M., Maeyer, G., Jacob, A., Giallella, K., Anderson, J., et al., (2014) PD-1 blockade with the monoclonal antibody pembrolizumab (MK-3475) in patients with classical Hodgkin lymphoma after brentuximab vedotin failure: preliminary results from a phase 1b study Blood. 124(21): p. Abstract 290.

62. Witzig, T.E., Reeder, C.B., LaPlant, B.R., Gupta, M., Johnston, P.B., Micallef, I.N., Porrata, L.F., Ansell, S.M., Colgan, J.P., Jacobsen, E.D., et al., (2011) A phase II trial of the oral mTOR inhibitor everolimus in relapsed aggressive lymphoma. Leukemia. 25(2): p. 341-7.

63. Younes, A., Sureda, A., Ben-Yehuda, D., Zinzani, P.L., Ong, T.C., Prince, H.M., Harrison, S.J., Kirschbaum, M., Johnston, P., Gallagher, J., et al., (2012) Panobinostat in patients with relapsed/refractory Hodgkin's lymphoma after autologous stem-cell transplantation: results of a phase II study. J Clin Oncol. 30(18): p. 2197-203.

64. Forero-Torres, A., Barr, P., and Diefenbach, C., (2015) A phase 1 study of INCB040093, a PI3Kd inhibitor, alone or in combination with INCB039110, a

selective JAK1 inhibitor: Interim results from patients (pts) with relapsed or refractory (r/r) classical Hodgkin lymphoma (cHL). . ASCO Annual Meeting.

65. Savoldo, B., Rooney, C.M., Di Stasi, A., Abken, H., Hombach, A., Foster, A.E., Zhang, L., Heslop, H.E., Brenner, M.K., and Dotti, G., (2007) Epstein Barr virus specific cytotoxic T lymphocytes expressing the anti-CD30zeta artificial chimeric T-cell receptor for immunotherapy of Hodgkin disease. Blood. 110(7): p. 2620-30.

66. Ramos, C.A., Ballard, B., Liu, E., Dakhova, O., Mei, Z., Liu, H., Grilley, B., Rooney, C.M., Gee, A., Chang, B.H., et al., (2015) Chimeric T Cells for Therapy of CD30+ Hodgkin and Non-Hodgkin Lymphomas. American Society of Hematology 57th Annual Meeting.

67. Stein, H., Mason, D.Y., Gerdes, J., O'Connor, N., Wainscoat, J., Pallesen, G., Gatter, K., Falini, B., Delsol, G., Lemke, H., et al., (1985) The expression of the Hodgkin's disease associated antigen Ki-1 in reactive and neoplastic lymphoid tissue: evidence that Reed-Sternberg cells and histiocytic malignancies are derived from activated lymphoid cells. Blood. 66(4): p. 848-58.

68. Swerdlow, S.H., Campo, E., Harris, N.L., Jaffe, E.S., Pileri, S.A., Stein, H., Thiele, J., and Vardiman, J.W., (2008) WHO classification of tumors of hematopoietic and lymphoid tissue. Lyon: IARC. 2.

69. Kelleher, F.C. and McDermott, R., (2010) The emerging pathogenic and therapeutic importance of the anaplastic lymphoma kinase gene. Eur J Cancer. 46(13): p. 2357-68.

70. Amin, H.M. and Lai, R., (2007) Pathobiology of ALK+ anaplastic large-cell lymphoma. Blood. 110(7): p. 2259-67.

71. Benharroch, D., Meguerian-Bedoyan, Z., Lamant, L., Amin, C., Brugieres, L., Terrier-Lacombe, M.J., Haralambieva, E., Pulford, K., Pileri, S., Morris, S.W., et al., (1998) ALK-positive lymphoma: a single disease with a broad spectrum of morphology. Blood. 91(6): p. 2076-84.

72. Brugieres, L., Deley, M.C., Pacquement, H., Meguerian-Bedoyan, Z., Terrier-Lacombe, M.J., Robert, A., Pondarre, C., Leverger, G., Devalck, C., Rodary, C., et al., (1998) CD30(+) anaplastic large-cell lymphoma in children: analysis of 82 patients enrolled in two consecutive studies of the French Society of Pediatric Oncology. Blood. 92(10): p. 3591-8.

73. Lechner, M.G., Megiel, C., Church, C.H., Angell, T.E., Russell, S.M., Sevell, R.B., Jang, J.K., Brody, G.S., and Epstein, A.L., (2012) Survival signals and targets for therapy in breast implant-associated ALK--anaplastic large cell lymphoma. Clin Cancer Res. 18(17): p. 4549-59.

74. Miranda, R.N., Aladily, T.N., Prince, H.M., Kanagal-Shamanna, R., de Jong, D., Fayad, L.E., Amin, M.B., Haideri, N., Bhagat, G., Brooks, G.S., et al., (2014) Breast implant-associated anaplastic large-cell lymphoma: long-term follow-up of 60 patients. J Clin Oncol. 32(2): p. 114-20.

75. Jarjis, R.D. and Matzen, S.H., (2015) [Breast implant-associated anaplastic large-cell lymphoma]. Ugeskr Laeger. 177(48).

76. Chang, I.W., Chen, H.K., Ma, M.C., and Huang, W.T., (2011) Anaplastic large cell lymphoma with paraneoplastic leukocytosis: a clinicopathological analysis of five cases. Apmis. 119(11): p. 794-801.

77. Lamant, L., Meggetto, F., al Saati, T., Brugieres, L., de Paillerets, B.B., Dastugue, N., Bernheim, A., Rubie, H., Terrier-Lacombe, M.J., Robert, A., et al., (1996) High incidence of the t(2;5)(p23;q35) translocation in anaplastic large cell lymphoma and its lack of detection in Hodgkin's disease. Comparison of cytogenetic analysis, reverse transcriptase-polymerase chain reaction, and P-80 immunostaining. Blood. 87(1): p. 284-91.

78. Touriol, C., Greenland, C., Lamant, L., Pulford, K., Bernard, F., Rousset, T., Mason, D.Y., and Delsol, G., (2000) Further demonstration of the diversity of chromosomal changes involving 2p23 in ALK-positive lymphoma: 2 cases expressing ALK kinase fused to CLTCL (clathrin chain polypeptide-like). Blood. 95(10): p. 3204-7.

79. Vadakara, J. and Pro, B., (2012) Targeting CD30 in anaplastic large cell lymphoma. Curr Hematol Malig Rep. 7(4): p. 285-91.

80. Marino-Enriquez, A. and Dal Cin, P., (2013) ALK as a paradigm of oncogenic promiscuity: different mechanisms of activation and different fusion partners drive tumors of different lineages. Cancer Genet. 206(11): p. 357-73.

81. Chiarle, R., Voena, C., Ambrogio, C., Piva, R., and Inghirami, G., (2008) The anaplastic lymphoma kinase in the pathogenesis of cancer. Nat Rev Cancer. 8(1): p. 11-23.

82. Parrilla Castellar, E.R., Jaffe, E.S., Said, J.W., Swerdlow, S.H., Ketterling, R.P., Knudson, R.A., Sidhu, J.S., Hsi, E.D., Karikehalli, S., Jiang, L., et al., (2014) ALK-negative anaplastic large cell lymphoma is a genetically heterogeneous disease with widely disparate clinical outcomes. 124(9): p. 1473-80.

83. Stein, H., Foss, H.D., Durkop, H., Marafioti, T., Delsol, G., Pulford, K., Pileri, S., and Falini, B., (2000) CD30(+) anaplastic large cell lymphoma: a review of its histopathologic, genetic, and clinical features. Blood. 96(12): p. 3681-95.

84. Jaffe, E.S., (2001) Anaplastic large cell lymphoma: the shifting sands of diagnostic hematopathology. Mod Pathol. 14(3): p. 219-28.

85. Pileri, S.A., Pulford, K., Mori, S., Mason, D.Y., Sabattini, E., Roncador, G., Piccioli, M., Ceccarelli, C., Piccaluga, P.P., Santini, D., et al., (1997) Frequent expression of the NPM-ALK chimeric fusion protein in anaplastic large-cell lymphoma, lympho-histiocytic type. Am J Pathol. 150(4): p. 1207-11.

86. Kinney, M.C., Collins, R.D., Greer, J.P., Whitlock, J.A., Sioutos, N., and Kadin, M.E., (1993) A small-cell-predominant variant of primary Ki-1 (CD30)+ T-cell lymphoma. Am J Surg Pathol. 17(9): p. 859-68.

87. Delsol, G., Al Saati, T., Gatter, K.C., Gerdes, J., Schwarting, R., Caveriviere, P., Rigal-Huguet, F., Robert, A., Stein, H., and Mason, D.Y., (1988) Coexpression of epithelial membrane antigen (EMA), Ki-1, and interleukin-2 receptor by anaplastic large cell lymphomas. Diagnostic value in so-called malignant histiocytosis. Am J Pathol. 130(1): p. 59-70.

88. Rosso, R., Paulli, M., Magrini, U., Kindl, S., Boveri, E., Volpato, G., Poggi, S., Baglioni, P., and Pileri, S., (1990) Anaplastic large cell lymphoma, CD30/Ki-1 positive, expressing the CD15/Leu-M1 antigen. Immunohistochemical and morphological relationships to Hodgkin's disease. Virchows Arch A Pathol Anat Histopathol. 416(3): p. 229-35.

89. Feldman, A.L., Law, M.E., Inwards, D.J., Dogan, A., McClure, R.F., and Macon, W.R., (2010) PAX5-positive T-cell anaplastic large cell lymphomas associated with extra copies of the PAX5 gene locus. Mod Pathol. 23(4): p. 593-602.

90. Juco, J., Holden, J.T., Mann, K.P., Kelley, L.G., and Li, S., (2003) Immunophenotypic analysis of anaplastic large cell lymphoma by flow cytometry. Am J Clin Pathol. 119(2): p. 205-12.

91. Fisher, R.I., Gaynor, E.R., Dahlberg, S., Oken, M.M., Grogan, T.M., Mize, E.M., Glick, J.H., Coltman, C.A., Jr., and Miller, T.P., (1993) Comparison of a standard regimen (CHOP) with three intensive chemotherapy regimens for advanced non-Hodgkin's lymphoma. N Engl J Med. 328(14): p. 1002-6.

92. Piekarz, R.L., Frye, R., Prince, H.M., Kirschbaum, M.H., Zain, J., Allen, S.L., Jaffe, E.S., Ling, A., Turner, M., Peer, C.J., et al., (2011) Phase 2 trial of romidepsin in patients with peripheral T-cell lymphoma. Blood. 117(22): p. 5827-34.

93. O'Connor, O.A., Pro, B., Pinter-Brown, L., Bartlett, N., Popplewell, L., Coiffier, B., Lechowicz, M.J., Savage, K.J., Shustov, A.R., Gisselbrecht, C., et al., (2011) Pralatrexate in patients with relapsed or refractory peripheral T-cell lymphoma: results from the pivotal PROPEL study. J Clin Oncol. 29(9): p. 1182-9.

94. Coiffier, B., Federico, M., Caballero, D., Dearden, C., Morschhauser, F., Jager, U., Trumper, L., Zucca, E., Gomes da Silva, M., Pettengell, R., et al., (2014) Therapeutic options in relapsed or refractory peripheral T-cell lymphoma. Cancer Treat Rev. 40(9): p. 1080-8.

95. Shustov, A., (2013) Novel therapies for peripheral T-cell lymphomas. Ther Adv Hematol. 4(3): p. 173-87.

96. Younes, A., Bartlett, N.L., Leonard, J.P., Kennedy, D.A., Lynch, C.M., Sievers, E.L., and Forero-Torres, A., (2010) Brentuximab vedotin (SGN-35) for relapsed CD30-positive lymphomas. N Engl J Med. 363(19): p. 1812-21.

97. Fanale, M.A., Forero-Torres, A., Rosenblatt, J.D., Advani, R.H., Franklin, A.R., Kennedy, D.A., Han, T.H., Sievers, E.L., and Bartlett, N.L., (2012) A phase I weekly dosing study of brentuximab vedotin in patients with relapsed/refractory CD30-positive hematologic malignancies. Clin Cancer Res. 18(1): p. 248-55.

98. O'Connor , O., Pro, B., Illidge, T., Trumper, L., Larsen, E., and Kennedy, D., (2013) Phase III trial of brentuximab vedotin and CHP versus CHOP in the frontline treatment of patients (pts) with CD30+ mature T-cell lymphomas (MTCL). 2013 ASCO Annual Meeting. Abstract Number: TPS8611.

99. Kwak, E.L., Bang, Y.J., Camidge, D.R., Shaw, A.T., Solomon, B., Maki, R.G., Ou, S.H., Dezube, B.J., Janne, P.A., Costa, D.B., et al., (2010) Anaplastic lymphoma kinase inhibition in non-small-cell lung cancer. N Engl J Med. 363(18): p. 1693-703.

100. Katayama, R., Shaw, A.T., Khan, T.M., Mino-Kenudson, M., Solomon, B.J., Halmos, B., Jessop, N.A., Wain, J.C., Yeo, A.T., Benes, C., et al., (2012) Mechanisms of acquired crizotinib resistance in ALK-rearranged lung Cancers. Sci Transl Med. 4(120): p. 120ra17.

101. Sherr, C.J., Rettenmier, C.W., Sacca, R., Roussel, M.F., Look, A.T., and Stanley, E.R., (1985) The c-fms proto-oncogene product is related to the receptor for the mononuclear phagocyte growth factor, CSF-1. Cell. 41(3): p. 665-76.

102. Lin, H., Lee, E., Hestir, K., Leo, C., Huang, M., Bosch, E., Halenbeck, R., Wu, G., Zhou, A., Behrens, D., et al., (2008) Discovery of a cytokine and its receptor by functional screening of the extracellular proteome. Science. 320(5877): p. 807-11.

103. Yarden, Y., Kuang, W.J., Yang-Feng, T., Coussens, L., Munemitsu, S., Dull, T.J., Chen, E., Schlessinger, J., Francke, U., and Ullrich, A., (1987) Human

proto-oncogene c-kit: a new cell surface receptor tyrosine kinase for an unidentified ligand. Embo j. 6(11): p. 3341-51.

104. Rosnet, O., Schiff, C., Pebusque, M.J., Marchetto, S., Tonnelle, C., Toiron, Y., Birg, F., and Birnbaum, D., (1993) Human FLT3/FLK2 gene: cDNA cloning and expression in hematopoietic cells. Blood. 82(4): p. 1110-9.

105. Claesson-Welsh, L., Eriksson, A., Westermark, B., and Heldin, C.H., (1989) cDNA cloning and expression of the human A-type platelet-derived growth factor (PDGF) receptor establishes structural similarity to the B-type PDGF receptor. Proc Natl Acad Sci U S A. 86(13): p. 4917-21.

106. Yarden, Y., Escobedo, J.A., Kuang, W.J., Yang-Feng, T.L., Daniel, T.O., Tremble, P.M., Chen, E.Y., Ando, M.E., Harkins, R.N., Francke, U., et al., (1986) Structure of the receptor for platelet-derived growth factor helps define a family of closely related growth factor receptors. Nature. 323(6085): p. 226-32.

107. Hubbard, S.R. and Till, J.H., (2000) Protein tyrosine kinase structure and function. Annu Rev Biochem. 69: p. 373-98.

108. van der Geer, P. and Hunter, T., (1990) Identification of tyrosine 706 in the kinase insert as the major colony-stimulating factor 1 (CSF-1)-stimulated autophosphorylation site in the CSF-1 receptor in a murine macrophage cell line. Mol Cell Biol. 10(6): p. 2991-3002.

109. Tapley, P., Kazlauskas, A., Cooper, J.A., and Rohrschneider, L.R., (1990) Macrophage colony-stimulating factor-induced tyrosine phosphorylation of c-fms proteins expressed in FDC-P1 and BALB/c 3T3 cells. Mol Cell Biol. 10(6): p. 2528-38.

110. Reedijk, M., Liu, X., van der Geer, P., Letwin, K., Waterfield, M.D., Hunter, T., and Pawson, T., (1992) Tyr721 regulates specific binding of the CSF-1 receptor kinase insert to PI 3'-kinase SH2 domains: a model for SH2-mediated receptor-target interactions. Embo j. 11(4): p. 1365-72.

111. Rohrschneider, L.R., Bourette, R.P., Lioubin, M.N., Algate, P.A., Myles, G.M., and Carlberg, K., (1997) Growth and differentiation signals regulated by the M-CSF receptor. Mol Reprod Dev. 46(1): p. 96-103.

112. Yu, W., Chen, J., Xiong, Y., Pixley, F.J., Dai, X.M., Yeung, Y.G., and Stanley, E.R., (2008) CSF-1 receptor structure/function in MacCsf1r-/- macrophages: regulation of proliferation, differentiation, and morphology. J Leukoc Biol. 84(3): p. 852-63.

113. Walter, M., Lucet, I.S., Patel, O., Broughton, S.E., Bamert, R., Williams, N.K., Fantino, E., Wilks, A.F., and Rossjohn, J., (2007) The 2.7 A crystal structure of the autoinhibited human c-Fms kinase domain. J Mol Biol. 367(3): p. 839-47.

114. Xiong, Y., Song, D., Cai, Y., Yu, W., Yeung, Y.G., and Stanley, E.R., (2011) A CSF-1 receptor phosphotyrosine 559 signaling pathway regulates receptor ubiquitination and tyrosine phosphorylation. J Biol Chem. 286(2): p. 952-60.

115. Yu, W., Chen, J., Xiong, Y., Pixley, F.J., Yeung, Y.G., and Stanley, E.R., (2012) Macrophage proliferation is regulated through CSF-1 receptor tyrosines 544, 559, and 807. J Biol Chem. 287(17): p. 13694-704.

116. Shurtleff, S.A., Downing, J.R., Rock, C.O., Hawkins, S.A., Roussel, M.F., and Sherr, C.J., (1990) Structural features of the colony-stimulating factor 1 receptor that affect its association with phosphatidylinositol 3-kinase. Embo j. 9(8): p. 2415-21.

117. Baccarini, M., Sabatini, D.M., App, H., Rapp, U.R., and Stanley, E.R., (1990) Colony stimulating factor-1 (CSF-1) stimulates temperature dependent phosphorylation and activation of the RAF-1 proto-oncogene product. Embo j. 9(11): p. 3649-57.

118. Fixe, P. and Praloran, V., (1998) M-CSF: haematopoietic growth factor or inflammatory cytokine? Cytokine. 10(1): p. 32-7.

119. Visvader, J. and Verma, I.M., (1989) Differential transcription of exon 1 of the human c-fms gene in placental trophoblasts and monocytes. Mol Cell Biol. 9(3): p. 1336-41.

120. Pixley, F.J. and Stanley, E.R., (2004) CSF-1 regulation of the wandering macrophage: complexity in action. Trends Cell Biol. 14(11): p. 628-38.

121. Fixe, P., Rougier, F., Ostyn, E., Gachard, N., Faucher, J.L., Praloran, V., and Denizot, Y., (1997) Spontaneous and inducible production of macrophage colony-stimulating factor by human bone marrow stromal cells. Eur Cytokine Netw. 8(1): p. 91-5.

122. Nohava, K., Malipiero, U., Frei, K., and Fontana, A., (1992) Neurons and neuroblastoma as a source of macrophage colony-stimulating factor. Eur J Immunol. 22(10): p. 2539-45.

123. Praloran, V., Chevalier, S., and Gascan, H., (1992) Macrophage colony-stimulating factor is produced by activated T lymphocytes in vitro and is detected in vivo in T cells from reactive lymph nodes. Blood. 79(9): p. 2500-1.

124. Praloran, V., (1991) Structure, biosynthesis and biological roles of monocyte-macrophage colony stimulating factor (CSF-1 or M-CSF). Nouv Rev Fr Hematol. 33(4): p. 323-33.

125. Price, L.K., Choi, H.U., Rosenberg, L., and Stanley, E.R., (1992) The predominant form of secreted colony stimulating factor-1 is a proteoglycan. J Biol Chem. 267(4): p. 2190-9.

126. Wiktor-Jedrzejczak, W., Bartocci, A., Ferrante, A.W., Jr., Ahmed-Ansari, A., Sell, K.W., Pollard, J.W., and Stanley, E.R., (1990) Total absence of colony-stimulating factor 1 in the macrophage-deficient osteopetrotic (op/op) mouse. Proc Natl Acad Sci U S A. 87(12): p. 4828-32.

127. Dai, X.M., Ryan, G.R., Hapel, A.J., Dominguez, M.G., Russell, R.G., Kapp, S., Sylvestre, V., and Stanley, E.R., (2002) Targeted disruption of the mouse colony-stimulating factor 1 receptor gene results in osteopetrosis, mononuclear phagocyte deficiency, increased primitive progenitor cell frequencies, and reproductive defects. Blood. 99(1): p. 111-20.

128. Niida, S., Kaku, M., Amano, H., Yoshida, H., Kataoka, H., Nishikawa, S., Tanne, K., Maeda, N., Nishikawa, S., and Kodama, H., (1999) Vascular endothelial

growth factor can substitute for macrophage colony-stimulating factor in the support of osteoclastic bone resorption. J Exp Med. 190(2): p. 293-8.

129. Wiktor-Jedrzejczak, W. and Gordon, S., (1996) Cytokine regulation of the macrophage (M phi) system studied using the colony stimulating factor-1-deficient op/op mouse. Physiol Rev. 76(4): p. 927-47.

130. Nandi, S., Gokhan, S., Dai, X.M., Wei, S., Enikolopov, G., Lin, H., Mehler, M.F., and Stanley, E.R., (2012) The CSF-1 receptor ligands IL-34 and CSF-1 exhibit distinct developmental brain expression patterns and regulate neural progenitor cell maintenance and maturation. Dev Biol. 367(2): p. 100-13.

131. Nandi, S., Cioce, M., Yeung, Y.G., Nieves, E., Tesfa, L., Lin, H., Hsu, A.W., Halenbeck, R., Cheng, H.Y., Gokhan, S., et al., (2013) Receptor-type protein-tyrosine phosphatase zeta is a functional receptor for interleukin-34. J Biol Chem. 288(30): p. 21972-86.

132. Ulbricht, U., Eckerich, C., Fillbrandt, R., Westphal, M., and Lamszus, K., (2006) RNA interference targeting protein tyrosine phosphatase zeta/receptor-type protein tyrosine phosphatase beta suppresses glioblastoma growth in vitro and in vivo. J Neurochem. 98(5): p. 1497-506.

133. Wang, Y., Szretter, K.J., Vermi, W., Gilfillan, S., Rossini, C., Cella, M., Barrow, A.D., Diamond, M.S., and Colonna, M., (2012) IL-34 is a tissue-restricted ligand of CSF1R required for the development of Langerhans cells and microglia. Nat Immunol. 13(8): p. 753-60.

134. Chitu V, S.E., (2006) Colony stimulating factor 1 in immunity and inflammation Curr Opin Immunol. 18: p. 39 - 48.

135. Teitelbaum SL, R.F., (2003) Genetic regulation of osteoclast development and function. Nat Rev Genet. 4: p. 638 - 649.

136. Burns C, W.A., (2011) c-FMS inhibitors: a patent review. Expert Opin Ther Patents. 21(2): p. 147 - 165.

137. Dai XM, R.G., Hapel AJ et al., (2002) Targeted disruption of the mouse colony stimulating factor 1 receptor gene results in osteopetrosis, mononuclear

phagocyte deficiency, increased primitive progenitor cell frequencies, and reproductive effects Blood. 99: p. 111 - 120.

138. Danks L, S.A., Gundle R, et al., (2002) Synovial macrophage-osteoclast differentiation in inflammatory arthritis. Ann Rheum Dis. 61: p. 916 - 921.

139. ME, R., (1992) Macrophage colony stimulating factor mRNA and protein in atherosclerotic lesions of rabitts and humans Am J Pathol. 140: p. 291 - 300.

140. Chen X, L.H., Focia PJ et al., (2008) Structure of macrophage colony stimulating factor bound to FMS: diverse signaling assemblies of class III receptor tyrosine kinases. Proc Natl Acad Sci USA. 105(47): p. 18267 - 72.

141. Lamprecht B, W.K., Kreher S, et al., (2010) Derepression of an endogenous long terminal repeat activates the CSF1R proto-oncogene in human lymphoma. Nat Med. 16(571 - 579).

142. Paietta E, R.J., Stanley ER, et al., (1990) Expression of the macrophage growth factor, CSF1 and its receptor c-fms by a Hadgkin's disease-derived cell line and its variants. Cancer Research. 50: p. 2049 - 2055.

143. Sapi E, S.B., (1999) The role of CSF1 in normal and neoplastic breast physiology. Proc Soc Exp Biol Med. 220: p. 1 - 8.

144. BM, K., (1997) CSF1 and its receptor in breast carcinomas and neoplasms of the female reproductive tract. Mol Reprod Dev. 46: p. 71 - 74.

145. Toy EP, A.M., Folk NL, et al., (2009) Enhanced ovarian cancer tumorigenesis and metastasis by the macrophage colonu-stimulating factor. Neoplasia. 11(2): p. 136 - 144.

146. Toy EP, C.J., Kacinski BM, et al., (2001) The activated macrophage colony stimulating factor (CSF-1) receptor as a predictor of poor outcome in advanced epithelial ovarian carcinoma. Gynecol Oncol. 80: p. 194 - 200.

147. Yee LD, L.L., (2000) The constitutive production of colony stimulating factor 1 by invasive human breast cancer cells. Anticancer Res. 20: p. 4379 - 4383.

148. Steidl Ch, D.A., Lee T, Gacoyne R, (2012) Gene expression profiling of microdissected Hodgkin Reed-Sternberg cells correlates with treatment outcome in classical Hodgkin Lymphoma. Blood. 120(17): p. 3530 - 3540.

149. Eshhar Z, W.T., Gross G, et al., (1993) Specific activation and targeting of cytotoxic lymphocytes through chimeric single chains consisting of antibody-binding domains and the gamma or zeta subunits of the immunoglobulin and T-cell receptors. Proc Natl Acad Sci USA. 90(2): p. 720 - 724.

150. Gross, G., Waks, T., and Eshhar, Z., (1989) Expression of immunoglobulin-T-cell receptor chimeric molecules as functional receptors with antibody-type specificity. Proc Natl Acad Sci U S A. 86(24): p. 10024-8.

151. Rappl, G., Riet, T., Awerkiew, S., Schmidt, A., Hombach, A.A., Pfister, H., and Abken, H., (2012) The CD3-zeta chimeric antigen receptor overcomes TCR Hypo-responsiveness of human terminal late-stage T cells. PLoS One. 7(1): p. e30713.

152. Muniappan A, B.B., Lebkowski J, et al., (2000) Ligand-mediated cytolysis of tumor cells: use of heregulin-zeta chimeras to redirect cytotoxic T lymphocites. Cancer Gene Ther. 7(128 - 134).

153. Shaffer, D.R., Savoldo, B., Yi, Z., Chow, K.K., Kakarla, S., Spencer, D.M., Dotti, G., Wu, M.F., Liu, H., Kenney, S., et al., (2011) T cells redirected against CD70 for the immunotherapy of CD70-positive malignancies. Blood. 117(16): p. 4304-14.

154. Kahlon, K.S., Brown, C., Cooper, L.J., Raubitschek, A., Forman, S.J., and Jensen, M.C., (2004) Specific recognition and killing of glioblastoma multiforme by interleukin 13-zetakine redirected cytolytic T cells. Cancer Res. 64(24): p. 9160-6.

155. Song, D.G., Ye, Q., Santoro, S., Fang, C., Best, A., and Powell, D.J., Jr., (2013) Chimeric NKG2D CAR-expressing T cell-mediated attack of human ovarian cancer is enhanced by histone deacetylase inhibition. Hum Gene Ther. 24(3): p. 295-305.

156. Davies DM, P.A., Chiapero-Stanke L, et al., (2012) Flexible targeting of ErbB dimers that drive tumirgenesis using genetically egineered T cells. Mol Med. 18(565 - 576).

157. Urbanska, K., Lanitis, E., Poussin, M., Lynn, R.C., Gavin, B.P., Kelderman, S., Yu, J., Scholler, N., and Powell, D.J., Jr., (2012) A universal strategy for adoptive immunotherapy of cancer through use of a novel T-cell antigen receptor. Cancer Res. 72(7): p. 1844-52.

158. Tamada, K., Geng, D., Sakoda, Y., Bansal, N., Srivastava, R., Li, Z., and Davila, E., (2012) Redirecting gene-modified T cells toward various cancer types using tagged antibodies. Clin Cancer Res. 18(23): p. 6436-45.

159. Kudo, K., Imai, C., Lorenzini, P., Kamiya, T., Kono, K., Davidoff, A.M., Chng, W.J., and Campana, D., (2014) T lymphocytes expressing a CD16 signaling receptor exert antibody-dependent cancer cell killing. Cancer Res. 74(1): p. 93-103.

160. Sadelain, M., (2009) T-cell engineering for cancer immunotherapy. Cancer J. 15(6): p. 451 - 455.

161. Guest, R.D., Hawkins, R.E., Kirillova, N., Cheadle, E.J., Arnold, J., O'Neill, A., Irlam, J., Chester, K.A., Kemshead, J.T., Shaw, D.M., et al., (2005) The role of extracellular spacer regions in the optimal design of chimeric immune receptors: evaluation of four different scFvs and antigens. J Immunother. 28(3): p. 203-11.

162. Wilkie S, P.G., Foster J et al., (2008) Retargeting of human T cells to tumor-associated MUC1: the evolution of a chimeric antigen receptor. J Immunol. 180(7): p. 4901 - 9.

163. Hombach, A., Hombach, A.A., and Abken, H., (2010) Adoptive immunotherapy with genetically engineered T cells: modification of the IgG1 Fc 'spacer' domain in the extracellular moiety of chimeric antigen receptors avoids 'off-target' activation and unintended initiation of an innate immune response. Gene Ther. 17(10): p. 1206-13.

164. Hudecek, M., Sommermeyer, D., Kosasih, P.L., Silva-Benedict, A., Liu, L., Rader, C., Jensen, M.C., and Riddell, S.R., (2015) The nonsignaling extracellular spacer domain of chimeric antigen receptors is decisive for in vivo antitumor activity. Cancer Immunol Res. 3(2): p. 125-35.

165. Hombach A, S.R., Heuser C, et al., (1998) Chimeric anti-TAG72 receptors with immunoglobulin constant Fc domains and gamma or zeta signaling chains. Int J Mol Med. 2(1): p. 99 - 103.

166. Gong, M.C., Latouche, J.B., Krause, A., Heston, W.D., Bander, N.H., and Sadelain, M., (1999) Cancer patient T cells genetically targeted to prostate-specific membrane antigen specifically lyse prostate cancer cells and release cytokines in response to prostate-specific membrane antigen. Neoplasia. 1(2): p. 123-7.

167. Bridgeman, J.S., Hawkins, R.E., Bagley, S., Blaylock, M., Holland, M., and Gilham, D.E., (2010) The optimal antigen response of chimeric antigen receptors harboring the CD3zeta transmembrane domain is dependent upon incorporation of the receptor into the endogenous TCR/CD3 complex. J Immunol. 184(12): p. 6938-49.

168. Irving BA, W.A., (1991) The cytoplasmic domain of the T cell receptor zeta chain is sufficient to couple to receptor-associated signal transduction pathways. Cell. 64: p. 891 - 901.

169. Kershaw MH, W.J., Parker LL, et al., (2006) A phase I study on adoptive immunotherapy using gene-modified T cells for ovarian cancer. Clin Cancer Res. 12: p. 6106 - 6115.

170. Park JR, D.D., Slovak M, et al., (2007) Adoptive transfer of chimeric antigen receptor re-directed cytolytic T lymphocyte clones in patients with neuroblastoma. Mol Ther. 15(825 - 833).

171. Till BG, J.M., Wang J, et al., (2008) Adoptive immunotherapy for indolent non-Hodgkin lymphoma and mantle cell lymphoma using genetically modified autologous CD20-specific T cells. Blood. 112: p. 2261 - 2271.

172. Pule, M.A., Savoldo, B., Myers, G.D., Rossig, C., Russell, H.V., Dotti, G., Huls, M.H., Liu, E., Gee, A.P., Mei, Z., et al., (2008) Virus-specific T cells engineered to coexpress tumor-specific receptors: persistence and antitumor activity in individuals with neuroblastoma. Nat Med. 14(11): p. 1264-70.

173. Finney HM, L.A., Bebbington CR, et al., (1998) Chimeric receptors providing both primary and costimulatory signaling in T cells from a single gene product. J Immunol. 161: p. 2791 - 2797.

174. Maher, J., Brentjens, R.J., Gunset, G., Riviere, I., and Sadelain, M., (2002) Human T-lymphocyte cytotoxicity and proliferation directed by a single chimeric TCRzeta /CD28 receptor. Nat Biotechnol. 20(1): p. 70-5.

175. Imai C, M.K., Andreansky M, et al., (2004) Chimeric receptors with 4-1BB signaling capacity provoke potent cytotoxicity against acute lymphoblastic leukemia. Leukemia. 18: p. 676 - 684.

176. Finney, H.M., Akbar, A.N., and Lawson, A.D., (2004) Activation of resting human primary T cells with chimeric receptors: costimulation from CD28, inducible costimulator, CD134, and CD137 in series with signals from the TCR zeta chain. J Immunol. 172(1): p. 104-13.

177. Pule MA, S.K., Dotti G, et al. , (2005) A chimeric T cell antigen receptor that augments cytokine release and supports clonal expansion of primary human T cells. Mol Ther. 12: p. 933 - 941.

178. Guedan, S., Chen, X., Madar, A., Carpenito, C., McGettigan, S.E., Frigault, M.J., Lee, J., Posey, A.D., Jr., Scholler, J., Scholler, N., et al., (2014) ICOS-based chimeric antigen receptors program bipolar TH17/TH1 cells. Blood. 124(7): p. 1070-80.

179. Song, D.G., Ye, Q., Poussin, M., Harms, G.M., Figini, M., and Powell, D.J., Jr., (2012) CD27 costimulation augments the survival and antitumor activity of redirected human T cells in vivo. Blood. 119(3): p. 696-706.

180. Brentjens, R.J., Santos, E., Nikhamin, Y., Yeh, R., Matsushita, M., La Perle, K., Quintas-Cardama, A., Larson, S.M., and Sadelain, M., (2007) Genetically

targeted T cells eradicate systemic acute lymphoblastic leukemia xenografts. Clin Cancer Res. 13(18 Pt 1): p. 5426-35.

181. Altvater, B., Landmeier, S., Pscherer, S., Temme, J., Juergens, H., Pule, M., and Rossig, C., (2009) 2B4 (CD244) signaling via chimeric receptors costimulates tumor-antigen specific proliferation and in vitro expansion of human T cells. Cancer Immunol Immunother. 58(12): p. 1991-2001.

182. Loskog, A., Giandomenico, V., Rossig, C., Pule, M., Dotti, G., and Brenner, M.K., (2006) Addition of the CD28 signaling domain to chimeric T-cell receptors enhances chimeric T-cell resistance to T regulatory cells. Leukemia. 20(10): p. 1819-28.

183. Kofler DM, C.M., Rappl G et al., (2011) CD28 costimulation Impairs the efficacy of a redirected t-cell antitumor attack in the presence of regulatory t cells which can be overcome by preventing Lck activation. Mol Ther. 19(4): p. 760 - 7.

184. Carpenito, C., Milone, M.C., Hassan, R., Simonet, J.C., Lakhal, M., Suhoski, M.M., Varela-Rohena, A., Haines, K.M., Heitjan, D.F., Albelda, S.M., et al., (2009) Control of large, established tumor xenografts with genetically retargeted human T cells containing CD28 and CD137 domains. Proc Natl Acad Sci U S A. 106(9): p. 3360-5.

185. Milone, M.C., Fish, J.D., Carpenito, C., Carroll, R.G., Binder, G.K., Teachey, D., Samanta, M., Lakhal, M., Gloss, B., Danet-Desnoyers, G., et al., (2009) Chimeric receptors containing CD137 signal transduction domains mediate enhanced survival of T cells and increased antileukemic efficacy in vivo. Mol Ther. 17(8): p. 1453-64.

186. Geiger, T.L., Nguyen, P., Leitenberg, D., and Flavell, R.A., (2001) Integrated src kinase and costimulatory activity enhances signal transduction through single-chain chimeric receptors in T lymphocytes. Blood. 98(8): p. 2364-71.

187. Hombach AA, H.J., Foppe M et al., (2012) OX40 costimulation by a chimeric antigen receptor abrogates CD28 and IL-2 induced IL-10 secretion by redirected CD4(+) T cells. Oncoimmunology. 1(4): p. 458 - 66.

188. Zhong XS, M.M., Plotkin J et al., (2010) Chimeric antigen receptors combining 4-1BB and CD28 signaling domains augment PI3kinase/AKT/Bcl-XL activation and CD8+ T cell-mediated tumor eradication. Mol Ther. 18(2): p. 413 - 20.

189. Wang J, J.M., Lin Y et al., (2007) Optimizing adoptive polyclonal T cell immunotherapy of lymphomas, using a chimeric T cell receptor possessing CD28 and CD137 costimulatory domains. Hum Gene Ther. 18(8): p. 712 - 25.

190. Cairo, M.S. and Bishop, M., (2004) Tumour lysis syndrome: new therapeutic strategies and classification. Br J Haematol. 127(1): p. 3-11.

191. Cairo, M.S., Coiffier, B., Reiter, A., and Younes, A., (2010) Recommendations for the evaluation of risk and prophylaxis of tumour lysis syndrome (TLS) in adults and children with malignant diseases: an expert TLS panel consensus. Br J Haematol. 149(4): p. 578-86.

192. Panelli, M.C., White, R., Foster, M., Martin, B., Wang, E., Smith, K., and Marincola, F.M., (2004) Forecasting the cytokine storm following systemic interleukin (IL)-2 administration. J Transl Med. 2(1): p. 17.

193. Suntharalingam, G., Perry, M.R., Ward, S., Brett, S.J., Castello-Cortes, A., Brunner, M.D., and Panoskaltsis, N., (2006) Cytokine storm in a phase 1 trial of the anti-CD28 monoclonal antibody TGN1412. N Engl J Med. 355(10): p. 1018-28.

194. Bugelski, P.J., Achuthanandam, R., Capocasale, R.J., Treacy, G., and Bouman-Thio, E., (2009) Monoclonal antibody-induced cytokine-release syndrome. Expert Rev Clin Immunol. 5(5): p. 499-521.

195. Morgan, R.A., Yang, J.C., Kitano, M., Dudley, M.E., Laurencot, C.M., and Rosenberg, S.A., (2010) Case report of a serious adverse event following the administration of T cells transduced with a chimeric antigen receptor recognizing ERBB2. Mol Ther. 18(4): p. 843-51.

196. Porter, D.L., Levine, B.L., Kalos, M., Bagg, A., and June, C.H., (2011) Chimeric antigen receptor-modified T cells in chronic lymphoid leukemia. N Engl J Med. 365(8): p. 725-33.

197. Brentjens RJ, D.M., Riviere I et al., (2013) CD19-targeted T cells rapidly induce molecular remissions in adults with chemotherapy-refractory acute lymphoblastic leukemia Sci Transl Med. 5(177): p. 177ar38.

198. Grupp SA, K.M., Barrett D et al., (2013) Chimeric antigen receptor-modified T cells for acute lymphoid leukemia. N Engl J Med. 386 (16): p. 1509 - 18.

199. Xu, X.J. and Tang, Y.M., (2014) Cytokine release syndrome in cancer immunotherapy with chimeric antigen receptor engineered T cells. Cancer Lett. 343(2): p. 172-8.

200. Davila, M.L., Riviere, I., Wang, X., Bartido, S., Park, J., Curran, K., Chung, S.S., Stefanski, J., Borquez-Ojeda, O., Olszewska, M., et al., (2014) Efficacy and toxicity management of 19-28z CAR T cell therapy in B cell acute lymphoblastic leukemia. Sci Transl Med. 6(224): p. 224ra25.

201. Lee, D.W., Kochenderfer, J.N., Stetler-Stevenson, M., Cui, Y.K., Delbrook, C., Feldman, S.A., Fry, T.J., Orentas, R., Sabatino, M., Shah, N.N., et al., (2015) T cells expressing CD19 chimeric antigen receptors for acute lymphoblastic leukaemia in children and young adults: a phase 1 dose-escalation trial. Lancet. 385(9967): p. 517-28.

202. Maude, S.L., Frey, N., Shaw, P.A., Aplenc, R., Barrett, D.M., Bunin, N.J., Chew, A., Gonzalez, V.E., Zheng, Z., Lacey, S.F., et al., (2014) Chimeric antigen receptor T cells for sustained remissions in leukemia. N Engl J Med. 371(16): p. 1507-17.

203. Buie, L.W., Pecoraro, J.J., Horvat, T.Z., and Daley, R.J., (2015) Blinatumomab: A First-in-Class Bispecific T-Cell Engager for Precursor B-Cell Acute Lymphoblastic Leukemia. Ann Pharmacother. 49(9): p. 1057-67.

204. Topp, M.S., Gokbuget, N., Stein, A.S., Zugmaier, G., O'Brien, S., Bargou, R.C., Dombret, H., Fielding, A.K., Heffner, L., Larson, R.A., et al., (2015) Safety and activity of blinatumomab for adult patients with relapsed or refractory B-precursor acute lymphoblastic leukaemia: a multicentre, single-arm, phase 2 study. Lancet Oncol. 16(1): p. 57-66.

205. Maus, M.V., Haas, A.R., Beatty, G.L., Albelda, S.M., Levine, B.L., Liu, X., Zhao, Y., Kalos, M., and June, C.H., (2013) T cells expressing chimeric antigen receptors can cause anaphylaxis in humans. Cancer Immunol Res. 1: p. 26-31.

206. Lamers, C.H., Sleijfer, S., van Steenbergen, S., van Elzakker, P., van Krimpen, B., Groot, C., Vulto, A., den Bakker, M., Oosterwijk, E., Debets, R., et al., (2013) Treatment of metastatic renal cell carcinoma with CAIX CAR-engineered T cells: clinical evaluation and management of on-target toxicity. Mol Ther. 21(4): p. 904-12.

207. Lamers, C.H., Sleijfer, S., Vulto, A.G., Kruit, W.H., Kliffen, M., Debets, R., Gratama, J.W., Stoter, G., and Oosterwijk, E., (2006) Treatment of metastatic renal cell carcinoma with autologous T-lymphocytes genetically retargeted against carbonic anhydrase IX: first clinical experience. J Clin Oncol. 24(13): p. e20-2.

208. Lamers, C.H., Willemsen, R., van Elzakker, P., van Steenbergen-Langeveld, S., Broertjes, M., Oosterwijk-Wakka, J., Oosterwijk, E., Sleijfer, S., Debets, R., and Gratama, J.W., (2011) Immune responses to transgene and retroviral vector in patients treated with ex vivo-engineered T cells. Blood. 117(1): p. 72-82.

209. Heslop, H.E., (2010) Safer CARS. Mol Ther. 18(4): p. 661-2.

210. Grupp, S.A., Kalos, M., Barrett, D., Aplenc, R., Porter, D.L., Rheingold, S.R., Teachey, D.T., Chew, A., Hauck, B., Wright, J.F., et al., (2013) Chimeric antigen receptor-modified T cells for acute lymphoid leukemia. N Engl J Med. 368(16): p. 1509-18.

211. Warren, R.S., Bergsland, E.K., Pennathur-Das, R., Nemunaitis, J., Venook, A.P., and Hege, K.M., (1998) Clinical studies of regional and systemic gene therapy with autologous CC49-z modified T cells in colorectal cancer metastatic to the liver. (Abstract, 7th International Conference on Gene Therapy of Cancer). . Cancer Gene Therapy. 5(S1–S2).

212. Ma, Q., Gonzalo-Daganzo, R.M., and Junghans, R.P., (2002) Genetically engineered T cells as adoptive immunotherapy of cancer. Cancer Chemother Biol Response Modif. 20: p. 315-41.

213. Louis, C.U., Savoldo, B., Dotti, G., Pule, M., Yvon, E., Myers, G.D., Rossig, C., Russell, H.V., Diouf, O., Liu, E., et al., (2011) Antitumor activity and long-term fate of chimeric antigen receptor-positive T cells in patients with neuroblastoma. Blood. 118(23): p. 6050-6.

214. Ahmed, N., Brawley, V.S., Hegde, M., Robertson, C., Ghazi, A., Gerken, C., Liu, E., Dakhova, O., Ashoori, A., Corder, A., et al., (2015) Human Epidermal Growth Factor Receptor 2 (HER2) -Specific Chimeric Antigen Receptor-Modified T Cells for the Immunotherapy of HER2-Positive Sarcoma. J Clin Oncol. 33(15): p. 1688-96.

215. Beatty, G.L., Haas, A.R., Maus, M.V., Torigian, D.A., Soulen, M.C., Plesa, G., Chew, A., Zhao, Y., Levine, B.L., Albelda, S.M., et al., (2014) Mesothelin-specific chimeric antigen receptor mRNA-engineered T cells induce anti-tumor activity in solid malignancies. Cancer Immunol Res. 2(2): p. 112-20.

216. Katz, S.C., Burga, R.A., McCormack, E., Wang, L.J., Mooring, W., Point, G.R., Khare, P.D., Thorn, M., Ma, Q., Stainken, B.F., et al., (2015) Phase I Hepatic Immunotherapy for Metastases Study of Intra-Arterial Chimeric Antigen Receptor-Modified T-cell Therapy for CEA+ Liver Metastases. Clin Cancer Res. 21(14): p. 3149-59.

217. Saied, A., Licata, L., Burga, R.A., Thorn, M., McCormack, E., Stainken, B.F., Assanah, E.O., Khare, P.D., Davies, R., Espat, N.J., et al., (2014) Neutrophil:lymphocyte ratios and serum cytokine changes after hepatic artery chimeric antigen receptor-modified T-cell infusions for liver metastases. Cancer Gene Ther. 21(11): p. 457-62.

218. Brown, C.E., Badie, B., Barish, M.E., Weng, L., Ostberg, J.R., Chang, W.C., Naranjo, A., Starr, R., Wagner, J., Wright, C., et al., (2015) Bioactivity and

Safety of IL13Ralpha2-Redirected Chimeric Antigen Receptor CD8+ T Cells in Patients with Recurrent Glioblastoma. Clin Cancer Res. 21(18): p. 4062-72.

219. Kochenderfer, J.N., Wilson, W.H., Janik, J.E., Dudley, M.E., Stetler-Stevenson, M., Feldman, S.A., Maric, I., Raffeld, M., Nathan, D.A., Lanier, B.J., et al., (2010) Eradication of B-lineage cells and regression of lymphoma in a patient treated with autologous T cells genetically engineered to recognize CD19. Blood. 116(20): p. 4099-102.

220. Kochenderfer JN, D.M., Feldman SA et al., (2012) B-cell depletion and remissions of malignancy along with cytokineassociated toxicity in a clinical trial of anti-CD19 chimeric-antigen-receptor-transduced T cells. Blood. 119: p. 2709 - 20.

221. Jensen, M.C., Popplewell, L., Cooper, L.J., DiGiusto, D., Kalos, M., Ostberg, J.R., and Forman, S.J., (2010) Antitransgene rejection responses contribute to attenuated persistence of adoptively transferred CD20/CD19-specific chimeric antigen receptor redirected T cells in humans. Biol Blood Marrow Transplant. 16(9): p. 1245-56.

222. Savoldo B, R.C., Liu E et al., (2011) CD28 costimulation improves expansion and persistence of chimeric antigen receptor-modified T cells in lymphoma patients. J Clin Invest. 121(5): p. 1822 - 6.

223. Kalos M, L.B., Porter DL, et al., (2011) T cells with chimeric antigen receptors have potent antitumor effects and can establish memory in patients with advanced leukemia Sci Transl Med. 3: p. 95ra73.

224. Brentjens RJ, R.I., Park JH et al., (2011) Safety and persistence of adoptively transferred autologous CD19-targeted T cells in patients with relapsed or chemotherapy refractory B-cell leukemias. Blood. 118(4817 - 28).

225. Kochenderfer, J.N., Dudley, M.E., Carpenter, R.O., Kassim, S.H., Rose, J.J., Telford, W.G., Hakim, F.T., Halverson, D.C., Fowler, D.H., Hardy, N.M., et al., (2013) Donor-derived CD19-targeted T cells cause regression of malignancy

persisting after allogeneic hematopoietic stem cell transplantation. Blood. 122(25): p. 4129-39.

226. Cruz, C.R., Micklethwaite, K.P., Savoldo, B., Ramos, C.A., Lam, S., Ku, S., Diouf, O., Liu, E., Barrett, A.J., Ito, S., et al., (2013) Infusion of donor-derived CD19-redirected virus-specific T cells for B-cell malignancies relapsed after allogeneic stem cell transplant: a phase 1 study. Blood. 122(17): p. 2965-73.

227. Kochenderfer, J.N., Dudley, M.E., Kassim, S.H., Somerville, R.P., Carpenter, R.O., Stetler-Stevenson, M., Yang, J.C., Phan, G.Q., Hughes, M.S., Sherry, R.M., et al., (2015) Chemotherapy-refractory diffuse large B-cell lymphoma and indolent B-cell malignancies can be effectively treated with autologous T cells expressing an anti-CD19 chimeric antigen receptor. J Clin Oncol. 33(6): p. 540-9.

228. Brudno, J.N., Somerville, R.P., Shi, V., Rose, J.J., Halverson, D.C., Fowler, D.H., Gea-Banacloche, J.C., Pavletic, S.Z., Hickstein, D.D., Lu, T.L., et al., (2016) Allogeneic T Cells That Express an Anti-CD19 Chimeric Antigen Receptor Induce Remissions of B-Cell Malignancies That Progress After Allogeneic Hematopoietic Stem-Cell Transplantation Without Causing Graft-Versus-Host Disease. J Clin Oncol.

229. Till BG, J.M., Wang J et al., (2008) Adoptive immunotherapy for indolent non-Hodgkin lymphoma and mantle cell lymphoma using genetically modified autologous CD20-specific T cells. Blood. 112(2261 - 71).

230. Till BG, J.M., Wang J et al., (2012) CD20-specific adoptive immunotherapy for lymphoma using a chimeric antigen receptor with both CD28 and 4-1BB domains: pilot clinical trial results. Blood. 119(17): p. 3940 - 50.

231. Wang, Y., Zhang, W.Y., Han, Q.W., Liu, Y., Dai, H.R., Guo, Y.L., Bo, J., Fan, H., Zhang, Y., Zhang, Y.J., et al., (2014) Effective response and delayed toxicities of refractory advanced diffuse large B-cell lymphoma treated by CD20-directed chimeric antigen receptor-modified T cells. Clin Immunol. 155(2): p. 160-75.

232. Ritchie DS, N.P., Khot A et al., (2013) Persistence and Efficacy of Second Generation CAR T Cell Against the LeY Antigen in Acute Myeloid Leukemia. Mol Ther. Epub ahead of print.

233. Wang, Q.S., Wang, Y., Lv, H.Y., Han, Q.W., Fan, H., Guo, B., Wang, L.L., and Han, W.D., (2015) Treatment of CD33-directed chimeric antigen receptor-modified T cells in one patient with relapsed and refractory acute myeloid leukemia. Mol Ther. 23(1): p. 184-91.

234. Parente-Pereira, A.C., Burnet, J., Ellison, D., Foster, J., Davies, D.M., van der Stegen, S., Burbridge, S., Chiapero-Stanke, L., Wilkie, S., Mather, S., et al., (2011) Trafficking of CAR-engineered human T cells following regional or systemic adoptive transfer in SCID beige mice. J Clin Immunol. 31(4): p. 710-8.

235. Parente-Pereira, A.C., Whilding, L.M., Brewig, N., van der Stegen, S.J., Davies, D.M., Wilkie, S., van Schalkwyk, M.C., Ghaem-Maghami, S., and Maher, J., (2013) Synergistic Chemoimmunotherapy of Epithelial Ovarian Cancer Using ErbB-Retargeted T Cells Combined with Carboplatin. J Immunol. 191(5): p. 2437-45.

236. Kalbasi, A., June, C.H., Haas, N., and Vapiwala, N., (2013) Radiation and immunotherapy: a synergistic combination. J Clin Invest. 123(7): p. 2756-63.

237. John, L.B., Devaud, C., Duong, C.P., Yong, C.S., Beavis, P.A., Haynes, N.M., Chow, M.T., Smyth, M.J., Kershaw, M.H., and Darcy, P.K., (2013) Anti-PD-1 antibody therapy potently enhances the eradication of established tumors by gene-modified T cells. Clin Cancer Res. 19(20): p. 5636-46.

238. Adusumilli, P.S., Cherkassky, L., Villena-Vargas, J., Colovos, C., Servais, E., Plotkin, J., Jones, D.R., and Sadelain, M., (2014) Regional delivery of mesothelin-targeted CAR T cell therapy generates potent and long-lasting CD4-dependent tumor immunity. Sci Transl Med. 6(261): p. 261ra151.

239. van Schalkwyk, M.C., Papa, S.E., Jeannon, J.P., Guerrero Urbano, T., Spicer, J.F., and Maher, J., (2013) Design of a phase I clinical trial to evaluate intratumoral delivery of ErbB-targeted chimeric antigen receptor T-cells in

locally advanced or recurrent head and neck cancer. Hum Gene Ther Clin Dev. 24(3): p. 134-42.

240. van der Stegen, S.J., Davies, D.M., Wilkie, S., Foster, J., Sosabowski, J.K., Burnet, J., Whilding, L.M., Petrovic, R.M., Ghaem-Maghami, S., Mather, S., et al., (2013) Preclinical in vivo modeling of cytokine release syndrome induced by ErbB-retargeted human T cells: identifying a window of therapeutic opportunity? J Immunol. 191(9): p. 4589-98.

241. Stephan, S.B., Taber, A.M., Jileaeva, I., Pegues, E.P., Sentman, C.L., and Stephan, M.T., (2015) Biopolymer implants enhance the efficacy of adoptive T-cell therapy. Nat Biotechnol. 33(1): p. 97-101.

242. Maher, J., (2014) Clinical immunotherapy of B-cell malignancy using CD19-targeted CAR T-cells. Curr Gene Ther. 14(1): p. 35-43.

243. Tedder, T.F., Zhou, L.J., and Engel, P., (1994) The CD19/CD21 signal transduction complex of B lymphocytes. Immunol Today. 15(9): p. 437-42.

244. Gill, S. and June, C.H., (2015) Going viral: chimeric antigen receptor T-cell therapy for hematological malignancies. Immunol Rev. 263(1): p. 68-89.

245. Imai C, I.S., Campana D et al., (2005) Genetic modification of primary natural killer cells overcomes inhibitory signals and induces specific killing of leukemic cells. Blood. 106: p. 376 - 383.

246. Wilkie, S., Burbridge, S.E., Chiapero-Stanke, L., Pereira, A.C., Cleary, S., van der Stegen, S.J., Spicer, J.F., Davies, D.M., and Maher, J., (2010) Selective expansion of chimeric antigen receptor-targeted T-cells with potent effector function using interleukin-4. J Biol Chem. 285(33): p. 25538-44.

247. Donnelly, M.L., Hughes, L.E., Luke, G., Mendoza, H., ten Dam, E., Gani, D., and Ryan, M.D., (2001) The 'cleavage' activities of foot-and-mouth disease virus 2A site-directed mutants and naturally occurring '2A-like' sequences. J Gen Virol. 82(Pt 5): p. 1027-41.

248. Donnelly, M.L., Luke, G., Mehrotra, A., Li, X., Hughes, L.E., Gani, D., and Ryan, M.D., (2001) Analysis of the aphthovirus 2A/2B polyprotein 'cleavage'

mechanism indicates not a proteolytic reaction, but a novel translational effect: a putative ribosomal 'skip'. J Gen Virol. 82(Pt 5): p. 1013-25.

249. Klock, H.E., Koesema, E.J., Knuth, M.W., and Lesley, S.A., (2008) Combining the polymerase incomplete primer extension method for cloning and mutagenesis with microscreening to accelerate structural genomics efforts. Proteins. 71(2): p. 982-94.

250. Hartley, J.L., Temple, G.F., and Brasch, M.A., (2000) DNA cloning using in vitro site-specific recombination. Genome Res. 10(11): p. 1788-95.

251. Olsen, D.B. and Eckstein, F., (1989) Incomplete primer extension during in vitro DNA amplification catalyzed by Taq polymerase; exploitation for DNA sequencing. Nucleic Acids Res. 17(23): p. 9613-20.

252. Birnboim, H.C. and Doly, J., (1979) A rapid alkaline extraction procedure for screening recombinant plasmid DNA. Nucleic Acids Res. 7(6): p. 1513-23.

253. Kamesaki, H., Fukuhara, S., Tatsumi, E., Uchino, H., Yamabe, H., Miwa, H., Shirakawa, S., Hatanaka, M., and Honjo, T., (1986) Cytochemical, immunologic, chromosomal, and molecular genetic analysis of a novel cell line derived from Hodgkin's disease. Blood. 68(1): p. 285-92.

254. Fischer, P., Nacheva, E., Mason, D.Y., Sherrington, P.D., Hoyle, C., Hayhoe, F.G., and Karpas, A., (1988) A Ki-1 (CD30)-positive human cell line (Karpas 299) established from a high-grade non-Hodgkin's lymphoma, showing a 2;5 translocation and rearrangement of the T-cell receptor beta-chain gene. Blood. 72(1): p. 234-40.

255. Barbey, S., Gogusev, J., Mouly, H., Le Pelletier, O., Smith, W., Richard, S., Soulie, J., and Nezelof, C., (1990) DEL cell line: a "malignant histiocytosis" CD30+ t(5;6)(q35;p21) cell line. Int J Cancer. 45(3): p. 546-53.

256. del Mistro, A., Leszl, A., Bertorelle, R., Calabro, M.L., Panozzo, M., Menin, C., D'Andrea, E., and Chieco-Bianchi, L., (1994) A CD30-positive T cell line established from an aggressive anaplastic large cell lymphoma, originally diagnosed as Hodgkin's disease. Leukemia. 8(7): p. 1214-9.

257. Kadin, M.E., Cavaille-Coll, M.W., Sioutos, N., Fletcher, J.A., Morton, C.C., Pastuszak, W., Rezuke, W., and Altman, A.J., (1990) Childhood Ki-1+ anaplastic large cell lymphoma: establishment and characterization of a new tumor cell line transplantable to SCID mice. Blood. 76: p. 354a.

258. Diehl, V., Kirchner, H.H., Schaadt, M., Fonatsch, C., Stein, H., Gerdes, J., and Boie, C., (1981) Hodgkin's disease: establishment and characterization of four in vitro cell lies. J Cancer Res Clin Oncol. 101(1): p. 111-24.

259. Keydar, I., Chen, L., Karby, S., Weiss, F.R., Delarea, J., Radu, M., Chaitcik, S., and Brenner, H.J., (1979) Establishment and characterization of a cell line of human breast carcinoma origin. Eur J Cancer. 15(5): p. 659-70.

260. Vogt, V., (1997) Retroviral Virions and Genomes In: Coffin JM, Hughes SH, Varmus HE, editors. Retroviruses. . Cold Spring Harbor (NY): Cold Spring Harbor Laboratory Press. Available from: http://www.ncbi.nlm.nih.gov/books/NBK19454/.

261. Rigg, R.J., Chen, J., Dando, J.S., Forestell, S.P., Plavec, I., and Bohnlein, E., (1996) A novel human amphotropic packaging cell line: high titer, complement resistance, and improved safety. Virology. 218(1): p. 290-5.

262. Soneoka, Y., Cannon, P.M., Ramsdale, E.E., Griffiths, J.C., Romano, G., Kingsman, S.M., and Kingsman, A.J., (1995) A transient three-plasmid expression system for the production of high titer retroviral vectors. Nucleic Acids Res. 23(4): p. 628-33.

263. Bender, M.A., Palmer, T.D., Gelinas, R.E., and Miller, A.D., (1987) Evidence that the packaging signal of Moloney murine leukemia virus extends into the gag region. J Virol. 61(5): p. 1639-46.

264. Ory, D.S., Neugeboren, B.A., and Mulligan, R.C., (1996) A stable human-derived packaging cell line for production of high titer retrovirus/vesicular stomatitis virus G pseudotypes. Proc Natl Acad Sci U S A. 93(21): p. 11400-6.

265. Graham, F.L., Smiley, J., Russell, W.C., and Nairn, R., (1977) Characteristics of a human cell line transformed by DNA from human adenovirus type 5. J Gen Virol. 36(1): p. 59-74.

266. Miller, A.D., Garcia, J.V., von Suhr, N., Lynch, C.M., Wilson, C., and Eiden, M.V., (1991) Construction and properties of retrovirus packaging cells based on gibbon ape leukemia virus. J Virol. 65(5): p. 2220-4.

267. Ghani, K., Cottin, S., de Campos-Lima, P.O., Caron, M.C., and Caruso, M., (2009) Characterization of an alternative packaging system derived from the cat RD114 retrovirus for gene delivery. J Gene Med. 11(8): p. 664-9.

268. Riviere, I., Brose, K., and Mulligan, R.C., (1995) Effects of retroviral vector design on expression of human adenosine deaminase in murine bone marrow transplant recipients engrafted with genetically modified cells. Proc Natl Acad Sci U S A. 92(15): p. 6733-7.

269. Swanstrom R, W.J., (1997) Synthesis, Assembly, and Processing of Viral Proteins. In: Coffin JM, Hughes SH, Varmus HE, editors, Retroviruses. Cold Spring Harbor (NY): Cold Spring Harbor Laboratory Press. Available from: http://www.ncbi.nlm.nih.gov/books/NBK19456/.

270. Coffin JM, H.S., Varmus HE, (1997) Retroviruses. Cold Spring Harbor (NY): Cold Spring Harbor Laboratory Press. Principles of Retroviral Vector Design.(Available from: http://www.ncbi.nlm.nih.gov/books/NBK19423/).

271. Pollok, K.E., Hanenberg, H., Noblitt, T.W., Schroeder, W.L., Kato, I., Emanuel, D., and Williams, D.A., (1998) High-efficiency gene transfer into normal and adenosine deaminase-deficient T lymphocytes is mediated by transduction on recombinant fibronectin fragments. J Virol. 72(6): p. 4882-92.

272. Hanenberg, H., Xiao, X.L., Dilloo, D., Hashino, K., Kato, I., and Williams, D.A., (1996) Colocalization of retrovirus and target cells on specific fibronectin fragments increases genetic transduction of mammalian cells. Nat Med. 2(8): p. 876-82.

273. Green, L.M., Reade, J.L., and Ware, C.F., (1984) Rapid colorimetric assay for cell viability: application to the quantitation of cytotoxic and growth inhibitory lymphokines. J Immunol Methods. 70(2): p. 257-68.

274. Nakatsu, T., Ichiyama, S., Hiratake, J., Saldanha, A., Kobashi, N., Sakata, K., and Kato, H., (2006) Structural basis for the spectral difference in luciferase bioluminescence. Nature. 440(7082): p. 372-6.

275. O'Neill, K., Lyons, S.K., Gallagher, W.M., Curran, K.M., and Byrne, A.T., (2010) Bioluminescent imaging: a critical tool in pre-clinical oncology research. J Pathol. 220(3): p. 317-27.

276. Inouye, S., (2010) Firefly luciferase: an adenylate-forming enzyme for multicatalytic functions. Cell Mol Life Sci. 67(3): p. 387-404.

277. Josephy, P.D., Eling, T., and Mason, R.P., (1982) The horseradish peroxidase-catalyzed oxidation of 3,5,3',5'-tetramethylbenzidine. Free radical and charge-transfer complex intermediates. J Biol Chem. 257(7): p. 3669-75.

278. Laemmli, U.K., (1970) Cleavage of structural proteins during the assembly of the head of bacteriophage T4. Nature. 227(5259): p. 680-5.

279. Rohrschneider, L.R., Rothwell, V.M., and Nicola, N.A., (1989) Transformation of murine fibroblasts by a retrovirus encoding the murine c-fms proto-oncogene. Oncogene. 4(8): p. 1015-22.

280. Kacinski, B.M., (1997) CSF-1 and its receptor in breast carcinomas and neoplasms of the female reproductive tract. Mol Reprod Dev. 46(1): p. 71-4.

281. Tang, R., Beuvon, F., Ojeda, M., Mosseri, V., Pouillart, P., and Scholl, S., (1992) M-CSF (monocyte colony stimulating factor) and M-CSF receptor expression by breast tumour cells: M-CSF mediated recruitment of tumour infiltrating monocytes? J Cell Biochem. 50(4): p. 350-6.

282. Kirma, N., Hammes, L.S., Liu, Y.G., Nair, H.B., Valente, P.T., Kumar, S., Flowers, L.C., and Tekmal, R.R., (2007) Elevated expression of the oncogene c-fms and its ligand, the macrophage colony-stimulating factor-1, in cervical

cancer and the role of transforming growth factor-beta1 in inducing c-fms expression. Cancer Res. 67(5): p. 1918-26.

283. Skrzypski, M., Dziadziuszko, R., Jassem, E., Szymanowska-Narloch, A., Gulida, G., Rzepko, R., Biernat, W., Taron, M., Jelitto-Gorska, M., Marjanski, T., et al., (2013) Main histologic types of non-small-cell lung cancer differ in expression of prognosis-related genes. Clin Lung Cancer. 14(6): p. 666-673.e2.

284. Tamimi, R.M., Brugge, J.S., Freedman, M.L., Miron, A., Iglehart, J.D., Colditz, G.A., and Hankinson, S.E., (2008) Circulating colony stimulating factor-1 and breast cancer risk. Cancer Res. 68(1): p. 18-21.

285. Aharinejad, S., Salama, M., Paulus, P., Zins, K., Berger, A., and Singer, C.F., (2013) Elevated CSF1 serum concentration predicts poor overall survival in women with early breast cancer. Endocr Relat Cancer. 20(6): p. 777-83.

286. Suzuki, M., Kobayashi, H., Ohwada, M., Terao, T., and Sato, I., (1998) Macrophage colony-stimulating factor as a marker for malignant germ cell tumors of the ovary. Gynecol Oncol. 68(1): p. 35-7.

287. Suzuki, M., Tamura, N., Kobayashi, H., Ohwada, M., Terao, T., and Sato, I., (2000) Clinical significance of combined use of macrophage colony-stimulating factor and squamous cell carcinoma antigen as a selective diagnostic marker for squamous cell carcinoma arising in mature cystic teratoma of the ovary. Gynecol Oncol. 77(3): p. 405-9.

288. Mroczko, B., Szmitkowski, M., and Okulczyk, B., (2002) Granulocyte-colony stimulating factor (G-CSF) and macrophagecolony stimulating factor (M-CSF) in colorectal cancer patients. Clin Chem Lab Med. 40(4): p. 351-5.

289. Mroczko, B., Groblewska, M., Wereszczynska-Siemiatkowska, U., Okulczyk, B., Kedra, B., Laszewicz, W., Dabrowski, A., and Szmitkowski, M., (2007) Serum macrophage-colony stimulating factor levels in colorectal cancer patients correlate with lymph node metastasis and poor prognosis. Clin Chim Acta. 380(1-2): p. 208-12.

290. Groblewska, M., Mroczko, B., Wereszczynska-Siemiatkowska, U., Mysliwiec, P., Kedra, B., and Szmitkowski, M., (2007) Serum levels of granulocyte colony-stimulating factor (G-CSF) and macrophage colony-stimulating factor (M-CSF) in pancreatic cancer patients. Clin Chem Lab Med. 45(1): p. 30-4.

291. Moreau, A., Praloran, V., Berrada, L., Coupey, L., and Gaillard, F., (1992) Immunohistochemical detection of cells positive for colony-stimulating factor 1 in lymph nodes from reactive lymphadenitis, and Hodgkin's disease. Leukemia. 6(2): p. 126-30.

292. Kowalska, M., Tajer, J., Chechlinska, M., Fuksiewicz, M., Kotowicz, B., Kaminska, J., and Walewski, J., (2012) Serum macrophage colony-stimulating factor (M-CSF) in patients with Hodgkin lymphoma. Med Oncol. 29(3): p. 2143-7.

293. Kowalska, M., Tajer, J., Chechlinska, M., Fuksiewicz, M., Kotowicz, B., Syczewska, M., Walewski, J., and Kaminska, J., (2012) Discriminant analysis involving serum cytokine levels and prediction of the response to therapy of patients with Hodgkin lymphoma. Tumour Biol. 33(5): p. 1733-8.

294. Sapi, E., (2004) The role of CSF-1 in normal physiology of mammary gland and breast cancer: an update. Exp Biol Med (Maywood). 229(1): p. 1-11.

295. Kacinski, B.M., Scata, K.A., Carter, D., Yee, L.D., Sapi, E., King, B.L., Chambers, S.K., Jones, M.A., Pirro, M.H., Stanley, E.R., et al., (1991) FMS (CSF-1 receptor) and CSF-1 transcripts and protein are expressed by human breast carcinomas in vivo and in vitro. Oncogene. 6(6): p. 941-52.

296. Scholl, S.M., Pallud, C., Beuvon, F., Hacene, K., Stanley, E.R., Rohrschneider, L., Tang, R., Pouillart, P., and Lidereau, R., (1994) Anti-colony-stimulating factor-1 antibody staining in primary breast adenocarcinomas correlates with marked inflammatory cell infiltrates and prognosis. J Natl Cancer Inst. 86(2): p. 120-6.

297. Scholl, S.M., Mosseri, V., Tang, R., Beuvon, F., Palud, C., Lidereau, R., and Pouillart, P., (1993) Expression of colony-stimulating factor-1 and its receptor

(the protein product of c-fms) in invasive breast tumor cells. Induction of urokinase production via this pathway? Ann N Y Acad Sci. 698: p. 131-5.

298. Kluger, H.M., Dolled-Filhart, M., Rodov, S., Kacinski, B.M., Camp, R.L., and Rimm, D.L., (2004) Macrophage colony-stimulating factor-1 receptor expression is associated with poor outcome in breast cancer by large cohort tissue microarray analysis. Clin Cancer Res. 10(1 Pt 1): p. 173-7.

299. Lin, E.Y., Nguyen, A.V., Russell, R.G., and Pollard, J.W., (2001) Colony-stimulating factor 1 promotes progression of mammary tumors to malignancy. J Exp Med. 193(6): p. 727-40.

300. Maher, M.G., Sapi, E., Turner, B., Gumbs, A., Perrotta, P.L., Carter, D., Kacinski, B.M., and Haffty, B.G., (1998) Prognostic significance of colony-stimulating factor receptor expression in ipsilateral breast cancer recurrence. Clin Cancer Res. 4(8): p. 1851-6.

301. Aharinejad, S., Paulus, P., Sioud, M., Hofmann, M., Zins, K., Schafer, R., Stanley, E.R., and Abraham, D., (2004) Colony-stimulating factor-1 blockade by antisense oligonucleotides and small interfering RNAs suppresses growth of human mammary tumor xenografts in mice. Cancer Res. 64(15): p. 5378-84.

302. Lin, E.Y., Li, J.F., Gnatovskiy, L., Deng, Y., Zhu, L., Grzesik, D.A., Qian, H., Xue, X.N., and Pollard, J.W., (2006) Macrophages regulate the angiogenic switch in a mouse model of breast cancer. Cancer Res. 66(23): p. 11238-46.

303. Lee, P.S., Wang, Y., Dominguez, M.G., Yeung, Y.G., Murphy, M.A., Bowtell, D.D., and Stanley, E.R., (1999) The Cbl protooncoprotein stimulates CSF-1 receptor multiubiquitination and endocytosis, and attenuates macrophage proliferation. Embo j. 18(13): p. 3616-28.

304. Lewis, C.E. and Pollard, J.W., (2006) Distinct role of macrophages in different tumor microenvironments. Cancer Res. 66(2): p. 605-12.

305. Paulus, P., Stanley, E.R., Schafer, R., Abraham, D., and Aharinejad, S., (2006) Colony-stimulating factor-1 antibody reverses chemoresistance in human MCF-7 breast cancer xenografts. Cancer Res. 66(8): p. 4349-56.

306. Sorrentino, A., Liu, C.G., Addario, A., Peschle, C., Scambia, G., and Ferlini, C., (2008) Role of microRNAs in drug-resistant ovarian cancer cells. Gynecol Oncol. 111(3): p. 478-86.

307. Chambers, S.K., Kacinski, B.M., Ivins, C.M., and Carcangiu, M.L., (1997) Overexpression of epithelial macrophage colony-stimulating factor (CSF-1) and CSF-1 receptor: a poor prognostic factor in epithelial ovarian cancer, contrasted with a protective effect of stromal CSF-1. Clin Cancer Res. 3(6): p. 999-1007.

308. Scholl, S.M., Bascou, C.H., Mosseri, V., Olivares, R., Magdelenat, H., Dorval, T., Palangie, T., Validire, P., Pouillart, P., and Stanley, E.R., (1994) Circulating levels of colony-stimulating factor 1 as a prognostic indicator in 82 patients with epithelial ovarian cancer. Br J Cancer. 69(2): p. 342-6.

309. Price, F.V., Chambers, S.K., Chambers, J.T., Carcangiu, M.L., Schwartz, P.E., Kohorn, E.I., Stanley, E.R., and Kacinski, B.M., (1993) Colony-stimulating factor-1 in primary ascites of ovarian cancer is a significant predictor of survival. Am J Obstet Gynecol. 168(2): p. 520-7.

310. Skates, S.J., Horick, N., Yu, Y., Xu, F.J., Berchuck, A., Havrilesky, L.J., de Bruijn, H.W., van der Zee, A.G., Woolas, R.P., Jacobs, I.J., et al., (2004) Preoperative sensitivity and specificity for early-stage ovarian cancer when combining cancer antigen CA-125II, CA 15-3, CA 72-4, and macrophage colony-stimulating factor using mixtures of multivariate normal distributions. J Clin Oncol. 22(20): p. 4059-66.

311. Toy, E.P., Azodi, M., Folk, N.L., Zito, C.M., Zeiss, C.J., and Chambers, S.K., (2009) Enhanced ovarian cancer tumorigenesis and metastasis by the macrophage colony-stimulating factor. Neoplasia. 11(2): p. 136-44.

312. Chambers, S.K., Wang, Y., Gertz, R.E., and Kacinski, B.M., (1995) Macrophage colony-stimulating factor mediates invasion of ovarian cancer cells through urokinase. Cancer Res. 55(7): p. 1578-85.

313. Chambers, S.K., Ivins, C.M., and Carcangiu, M.L., (1998) Plasminogen activator inhibitor-1 is an independent poor prognostic factor for survival in

advanced stage epithelial ovarian cancer patients. Int J Cancer. 79(5): p. 449-54.

314. Kuhn, W., Schmalfeldt, B., Reuning, U., Pache, L., Berger, U., Ulm, K., Harbeck, N., Spathe, K., Dettmar, P., Hofler, H., et al., (1999) Prognostic significance of urokinase (uPA) and its inhibitor PAI-1 for survival in advanced ovarian carcinoma stage FIGO IIIc. Br J Cancer. 79(11-12): p. 1746-51.

315. Wilhelm, O., Schmitt, M., Hohl, S., Senekowitsch, R., and Graeff, H., (1995) Antisense inhibition of urokinase reduces spread of human ovarian cancer in mice. Clin Exp Metastasis. 13(4): p. 296-302.

316. Baiocchi, G., Kavanagh, J.J., Talpaz, M., Wharton, J.T., Gutterman, J.U., and Kurzrock, R., (1991) Expression of the macrophage colony-stimulating factor and its receptor in gynecologic malignancies. Cancer. 67(4): p. 990-6.

317. Steidl C, L.T., Shah SP, et al., (2010) Tumor-associated macrophages and survival in classic Hodgkin's lymphoma. N Engl J Med. 362(10): p. 875 - 885.

318. Janowska-Wieczorek, A., Belch, A.R., Jacobs, A., Bowen, D., Padua, R.A., Paietta, E., and Stanley, E.R., (1991) Increased circulating colony-stimulating factor-1 in patients with preleukemia, leukemia, and lymphoid malignancies. Blood. 77(8): p. 1796-803.

319. Ide, H., Seligson, D.B., Memarzadeh, S., Xin, L., Horvath, S., Dubey, P., Flick, M.B., Kacinski, B.M., Palotie, A., and Witte, O.N., (2002) Expression of colony-stimulating factor 1 receptor during prostate development and prostate cancer progression. Proc Natl Acad Sci U S A. 99(22): p. 14404-9.

320. Patsialou, A., Wang, Y., Pignatelli, J., Chen, X., Entenberg, D., Oktay, M., and Condeelis, J.S., (2015) Autocrine CSF1R signaling mediates switching between invasion and proliferation downstream of TGFbeta in claudin-low breast tumor cells. Oncogene. 34(21): p. 2721-31.

321. Chambers, S.K., Wang, Y., Gilmore-Hebert, M., and Kacinski, B.M., (1994) Post-transcriptional regulation of c-fms proto-oncogene expression by

dexamethasone and of CSF-1 in human breast carcinomas in vitro. Steroids. 59(9): p. 514-22.

322. Flick, M.B., Sapi, E., and Kacinski, B.M., (2002) Hormonal regulation of the c-fms proto-oncogene in breast cancer cells is mediated by a composite glucocorticoid response element. J Cell Biochem. 85(1): p. 10-23.

323. Sapi, E., Flick, M.B., Gilmore-Hebert, M., Rodov, S., and Kacinski, B.M., (1995) Transcriptional regulation of the c-fms (CSF-1R) proto-oncogene in human breast carcinoma cells by glucocorticoids. Oncogene. 10(3): p. 529-42.

324. Verreck, F.A., de Boer, T., Langenberg, D.M., Hoeve, M.A., Kramer, M., Vaisberg, E., Kastelein, R., Kolk, A., de Waal-Malefyt, R., and Ottenhoff, T.H., (2004) Human IL-23-producing type 1 macrophages promote but IL-10-producing type 2 macrophages subvert immunity to (myco)bacteria. Proc Natl Acad Sci U S A. 101(13): p. 4560-5.

325. Fleetwood, A.J., Dinh, H., Cook, A.D., Hertzog, P.J., and Hamilton, J.A., (2009) GM-CSF- and M-CSF-dependent macrophage phenotypes display differential dependence on type I interferon signaling. J Leukoc Biol. 86(2): p. 411-21.

326. Hsu, S.M., Waldron, J., Xie, S.S., and Hsu, P.L., (1995) Hodgkin's Disease and Anaplastic Large Cell Lymphoma Revisited. 1. unique cytokine and cytokine receptor profile distinguished from that of non-hodgkin's lymphomas. J Biomed Sci. 2(4): p. 302-313.

327. Barbetti, V., Morandi, A., Tusa, I., Digiacomo, G., Riverso, M., Marzi, I., Cipolleschi, M.G., Bessi, S., Giannini, A., Di Leo, A., et al., (2014) Chromatin-associated CSF-1R binds to the promoter of proliferation-related genes in breast cancer cells. Oncogene. 33(34): p. 4359-64.

328. Brameier, M., Krings, A., and MacCallum, R.M., (2007) NucPred--predicting nuclear localization of proteins. Bioinformatics. 23(9): p. 1159-60.

329. Muller, S., Kunkel, P., Lamszus, K., Ulbricht, U., Lorente, G.A., Nelson, A.M., von Schack, D., Chin, D.J., Lohr, S.C., Westphal, M., et al., (2003) A role for

receptor tyrosine phosphatase zeta in glioma cell migration. Oncogene. 22(43): p. 6661-8.

330. Ulbricht, U., Brockmann, M.A., Aigner, A., Eckerich, C., Muller, S., Fillbrandt, R., Westphal, M., and Lamszus, K., (2003) Expression and function of the receptor protein tyrosine phosphatase zeta and its ligand pleiotrophin in human astrocytomas. J Neuropathol Exp Neurol. 62(12): p. 1265-75.

331. Foehr, E.D., Lorente, G., Kuo, J., Ram, R., Nikolich, K., and Urfer, R., (2006) Targeting of the receptor protein tyrosine phosphatase beta with a monoclonal antibody delays tumor growth in a glioblastoma model. Cancer Res. 66(4): p. 2271-8.

332. Maeda, N., Nishiwaki, T., Shintani, T., Hamanaka, H., and Noda, M., (1996) 6B4 proteoglycan/phosphacan, an extracellular variant of receptor-like protein-tyrosine phosphatase zeta/RPTPbeta, binds pleiotrophin/heparin-binding growth-associated molecule (HB-GAM). J Biol Chem. 271(35): p. 21446-52.

333. Grzelinski, M., Bader, N., Czubayko, F., and Aigner, A., (2005) Ribozyme-targeting reveals the rate-limiting role of pleiotrophin in glioblastoma. Int J Cancer. 117(6): p. 942-51.

334. Rettenmier, C.W., Roussel, M.F., Ashmun, R.A., Ralph, P., Price, K., and Sherr, C.J., (1987) Synthesis of membrane-bound colony-stimulating factor 1 (CSF-1) and downmodulation of CSF-1 receptors in NIH 3T3 cells transformed by cotransfection of the human CSF-1 and c-fms (CSF-1 receptor) genes. Mol Cell Biol. 7(7): p. 2378-87.

335. Sherr, C.J., (1990) Colony-stimulating factor-1 receptor. Blood. 75(1): p. 1-12.

336. Wells, A., Welsh, J.B., Lazar, C.S., Wiley, H.S., Gill, G.N., and Rosenfeld, M.G., (1990) Ligand-induced transformation by a noninternalizing epidermal growth factor receptor. Science. 247(4945): p. 962-4.

337. Mori, S., Tanaka, K., Omura, S., and Saito, Y., (1995) Degradation process of ligand-stimulated platelet-derived growth factor beta-receptor involves ubiquitin-proteasome proteolytic pathway. J Biol Chem. 270(49): p. 29447-52.

338. Jeffers, M., Taylor, G.A., Weidner, K.M., Omura, S., and Vande Woude, G.F., (1997) Degradation of the Met tyrosine kinase receptor by the ubiquitin-proteasome pathway. Mol Cell Biol. 17(2): p. 799-808.

339. Levkowitz, G., Waterman, H., Zamir, E., Kam, Z., Oved, S., Langdon, W.Y., Beguinot, L., Geiger, B., and Yarden, Y., (1998) c-Cbl/Sli-1 regulates endocytic sorting and ubiquitination of the epidermal growth factor receptor. Genes Dev. 12(23): p. 3663-74.

340. Manger, R., Najita, L., Nichols, E.J., Hakomori, S., and Rohrschneider, L., (1984) Cell surface expression of the McDonough strain of feline sarcoma virus fms gene product (gp 140fms). Cell. 39(2 Pt 1): p. 327-37.

341. Palma, L., Amatori, S., Cruz Chamorro, I., Fanelli, M., and Magnani, M., (2014) Promoter-specific relevance of histone modifications induced by dexamethasone during the regulation of pro-inflammatory mediators. Biochim Biophys Acta. 1839(7): p. 571-8.

342. Barnes, P.J., (1998) Anti-inflammatory actions of glucocorticoids: molecular mechanisms. Clin Sci (Lond). 94(6): p. 557-72.

343. Roberts, W.M., Shapiro, L.H., Ashmun, R.A., and Look, A.T., (1992) Transcription of the human colony-stimulating factor-1 receptor gene is regulated by separate tissue-specific promoters. Blood. 79(3): p. 586-93.

344. Chambers, S.K., Ivins, C.M., Kacinski, B.M., and Hochberg, R.B., (2004) An unexpected effect of glucocorticoids on stimulation of c-fms proto-oncogene expression in choriocarcinoma cells that express little glucocorticoid receptor. Am J Obstet Gynecol. 190(4): p. 974-85.

345. Sapi, E., Flick, M.B., Rodov, S., Gilmore-Hebert, M., Kelley, M., Rockwell, S., and Kacinski, B.M., (1996) Independent regulation of invasion and anchorage-independent growth by different autophosphorylation sites of the macrophage colony-stimulating factor 1 receptor. Cancer Res. 56(24): p. 5704-12.

346. Liu, Y., Cousin, J.M., Hughes, J., Van Damme, J., Seckl, J.R., Haslett, C., Dransfield, I., Savill, J., and Rossi, A.G., (1999) Glucocorticoids promote

nonphlogistic phagocytosis of apoptotic leukocytes. J Immunol. 162(6): p. 3639-46.

347. Wilkie, S., van Schalkwyk, M.C., Hobbs, S., Davies, D.M., van der Stegen, S.J., Pereira, A.C., Burbridge, S.E., Box, C., Eccles, S.A., and Maher, J., (2012) Dual targeting of ErbB2 and MUC1 in breast cancer using chimeric antigen receptors engineered to provide complementary signaling. J Clin Immunol. 32(5): p. 1059-70.

348. Kloss CC, C.M., Cartellieri M et al., (2013) Combinatorial antigen recognition with balanced signaling promotes selective tumor eradication by engineered T cells. Nat Biotechnol. 31(1): p. 71 - 5.

349. Grada, Z., Hegde, M., Byrd, T., Shaffer, D.R., Ghazi, A., Brawley, V.S., Corder, A., Schonfeld, K., Koch, J., Dotti, G., et al., (2013) TanCAR: A Novel Bispecific Chimeric Antigen Receptor for Cancer Immunotherapy. Mol Ther Nucleic Acids. 2: p. e105.

350. Stephan, M.T., Ponomarev, V., Brentjens, R.J., Chang, A.H., Dobrenkov, K.V., Heller, G., and Sadelain, M., (2007) T cell-encoded CD80 and 4-1BBL induce auto- and transcostimulation, resulting in potent tumor rejection. Nat Med. 13(12): p. 1440-9.

351. Traversari, C., Marktel, S., Magnani, Z., Mangia, P., Russo, V., Ciceri, F., Bonini, C., and Bordignon, C., (2007) The potential immunogenicity of the TK suicide gene does not prevent full clinical benefit associated with the use of TK-transduced donor lymphocytes in HSCT for hematologic malignancies. Blood. 109(11): p. 4708-15.

352. Zhou, X., Di Stasi, A., Tey, S.K., Krance, R.A., Martinez, C., Leung, K.S., Durett, A.G., Wu, M.F., Liu, H., Leen, A.M., et al., (2014) Long-term outcome after haploidentical stem cell transplant and infusion of T cells expressing the inducible caspase 9 safety transgene. Blood. 123(25): p. 3895-905.

353. Di Stasi, A., Tey, S.K., Dotti, G., Fujita, Y., Kennedy-Nasser, A., Martinez, C., Straathof, K., Liu, E., Durett, A.G., Grilley, B., et al., (2011) Inducible apoptosis as a safety switch for adoptive cell therapy. N Engl J Med. 365(18): p. 1673-83.

354. Philip, B., Kokalaki, E., Mekkaoui, L., Thomas, S., Straathof, K., Flutter, B., Marin, V., Marafioti, T., Chakraverty, R., Linch, D., et al., (2014) A highly compact epitope-based marker/suicide gene for easier and safer T-cell therapy. Blood. 124(8): p. 1277-87.

355. Wang, X., Chang, W.C., Wong, C.W., Colcher, D., Sherman, M., Ostberg, J.R., Forman, S.J., Riddell, S.R., and Jensen, M.C., (2011) A transgene-encoded cell surface polypeptide for selection, in vivo tracking, and ablation of engineered cells. Blood. 118(5): p. 1255-63.

356. Fedorov, V.D., Themeli, M., and Sadelain, M., (2013) PD-1- and CTLA-4-based inhibitory chimeric antigen receptors (iCARs) divert off-target immunotherapy responses. Sci Transl Med. 5(215): p. 215ra172.

357. Chmielewski, M., Kopecky, C., Hombach, A.A., and Abken, H., (2011) IL-12 release by engineered T cells expressing chimeric antigen receptors can effectively Muster an antigen-independent macrophage response on tumor cells that have shut down tumor antigen expression. Cancer Res. 71(17): p. 5697-706.

358. Zhang, L., Kerkar, S.P., Yu, Z., Zheng, Z., Yang, S., Restifo, N.P., Rosenberg, S.A., and Morgan, R.A., (2011) Improving adoptive T cell therapy by targeting and controlling IL-12 expression to the tumor environment. Mol Ther. 19(4): p. 751-9.

359. Tugues, S., Burkhard, S.H., Ohs, I., Vrohlings, M., Nussbaum, K., Vom Berg, J., Kulig, P., and Becher, B., (2015) New insights into IL-12-mediated tumor suppression. Cell Death Differ. 22(2): p. 237-46.

360. Chmielewski, M., Hombach, A.A., and Abken, H., (2014) Of CARs and TRUCKs: chimeric antigen receptor (CAR) T cells engineered with an inducible cytokine to modulate the tumor stroma. Immunol Rev. 257(1): p. 83-90.

361. Pegram, H.J., Lee, J.C., Hayman, E.G., Imperato, G.H., Tedder, T.F., Sadelain, M., and Brentjens, R.J., (2012) Tumor-targeted T cells modified to secrete IL-12 eradicate systemic tumors without need for prior conditioning. Blood. 119(18): p. 4133-41.

362. Markley, J.C. and Sadelain, M., (2010) IL-7 and IL-21 are superior to IL-2 and IL-15 in promoting human T cell-mediated rejection of systemic lymphoma in immunodeficient mice. Blood. 115(17): p. 3508-19.

363. Quintarelli, C., Vera, J.F., Savoldo, B., Giordano Attianese, G.M., Pule, M., Foster, A.E., Heslop, H.E., Rooney, C.M., Brenner, M.K., and Dotti, G., (2007) Co-expression of cytokine and suicide genes to enhance the activity and safety of tumor-specific cytotoxic T lymphocytes. Blood. 110(8): p. 2793-802.

364. Vera, J.F., Hoyos, V., Savoldo, B., Quintarelli, C., Giordano Attianese, G.M., Leen, A.M., Liu, H., Foster, A.E., Heslop, H.E., Rooney, C.M., et al., (2009) Genetic manipulation of tumor-specific cytotoxic T lymphocytes to restore responsiveness to IL-7. Mol Ther. 17(5): p. 880-8.

365. Wilkie S, B.S., Chiapero-Stanke L, et al., (2010) Selective expansion of chimeric antigen receptor-targeted T-cells with potent effector function using interleukin-4. J Biol Chem. 285(33): p. 25538 - 25544.

366. Lo, A.S., Taylor, J.R., Farzaneh, F., Kemeny, D.M., Dibb, N.J., and Maher, J., (2008) Harnessing the tumour-derived cytokine, CSF-1, to co-stimulate T-cell growth and activation. Mol Immunol. 45(5): p. 1276-87.

367. Kershaw, M.H., Wang, G., Westwood, J.A., Pachynski, R.K., Tiffany, H.L., Marincola, F.M., Wang, E., Young, H.A., Murphy, P.M., and Hwu, P., (2002) Redirecting migration of T cells to chemokine secreted from tumors by genetic modification with CXCR2. Hum Gene Ther. 13(16): p. 1971-80.

368. Peng, W., Ye, Y., Rabinovich, B.A., Liu, C., Lou, Y., Zhang, M., Whittington, M., Yang, Y., Overwijk, W.W., Lizee, G., et al., (2010) Transduction of tumor-specific T cells with CXCR2 chemokine receptor improves migration to tumor and antitumor immune responses. Clin Cancer Res. 16(22): p. 5458-68.

369. Craddock, J.A., Lu, A., Bear, A., Pule, M., Brenner, M.K., Rooney, C.M., and Foster, A.E., (2010) Enhanced tumor trafficking of GD2 chimeric antigen receptor T cells by expression of the chemokine receptor CCR2b. J Immunother. 33(8): p. 780-8.

370. Moon, E.K., Carpenito, C., Sun, J., Wang, L.C., Kapoor, V., Predina, J., Powell, D.J., Jr., Riley, J.L., June, C.H., and Albelda, S.M., (2011) Expression of a functional CCR2 receptor enhances tumor localization and tumor eradication by retargeted human T cells expressing a mesothelin-specific chimeric antibody receptor. Clin Cancer Res. 17(14): p. 4719-30.

371. Di Stasi, A., De Angelis, B., Rooney, C.M., Zhang, L., Mahendravada, A., Foster, A.E., Heslop, H.E., Brenner, M.K., Dotti, G., and Savoldo, B., (2009) T lymphocytes coexpressing CCR4 and a chimeric antigen receptor targeting CD30 have improved homing and antitumor activity in a Hodgkin tumor model. Blood. 113(25): p. 6392-402.

372. Lo AS, T.J., Farzaneh F et al., (2008) Harnessing the tumour-derived cytokine, CSF-1, to co-stimulate T-cell growth and activation. Mol Immunol. 45(5): p. 1276 - 87.

373. Wang, X., Naranjo, A., Brown, C.E., Bautista, C., Wong, C.W., Chang, W.C., Aguilar, B., Ostberg, J.R., Riddell, S.R., Forman, S.J., et al., (2012) Phenotypic and functional attributes of lentivirus-modified CD19-specific human CD8+ central memory T cells manufactured at clinical scale. J Immunother. 35(9): p. 689-701.

374. Restifo, N.P. and Gattinoni, L., (2013) Lineage relationship of effector and memory T cells. Curr Opin Immunol. 25(5): p. 556-63.

375. Gattinoni, L., Klebanoff, C.A., and Restifo, N.P., (2012) Paths to stemness: building the ultimate antitumour T cell. Nat Rev Cancer. 12(10): p. 671-84.

376. Cieri, N., Camisa, B., Cocchiarella, F., Forcato, M., Oliveira, G., Provasi, E., Bondanza, A., Bordignon, C., Peccatori, J., Ciceri, F., et al., (2013) IL-7 and IL-

15 instruct the generation of human memory stem T cells from naive precursors. Blood. 121(4): p. 573-84.

377. Gattinoni, L. and Restifo, N.P., (2013) Moving T memory stem cells to the clinic. Blood. 121(4): p. 567-8.

378. Wilkie S, B.S., Chiapero-Stanke L et al., (2010) Selective expansion of chimeric antigen receptor-targeted T-cells with potent effector function using interleukin-4. J Biol Chem. 285(33): p. 25538 - 44.

379. Lichtenfels, R., Biddison, W.E., Schulz, H., Vogt, A.B., and Martin, R., (1994) CARE-LASS (calcein-release-assay), an improved fluorescence-based test system to measure cytotoxic T lymphocyte activity. J Immunol Methods. 172(2): p. 227-39.

380. Weston, S.A. and Parish, C.R., (1990) New fluorescent dyes for lymphocyte migration studies. Analysis by flow cytometry and fluorescence microscopy. J Immunol Methods. 133(1): p. 87-97.

381. Skinnider BF, M.T., (2002) The role of cytokines in classical Hodgkin lymphoma. Blood. 99(12): p. 4283 - 97.

382. Willers J, D.R., Kempf W et al., (2003) Proliferation of CD30+ T-helper 2 lymphoma cells can be inhibited by CD30 receptor cross-linking with recombinant CD30 ligand. Clin Cancer Res. 9(7): p. 2744 - 54.

383. Kurre, P., Morris, J., Miller, A.D., and Kiem, H.P., (2001) Envelope fusion protein binding studies in an inducible model of retrovirus receptor expression and in CD34(+) cells emphasize limited transduction at low receptor levels. Gene Ther. 8(8): p. 593-9.

384. Green, B.J., Lee, C.S., and Rasko, J.E., (2004) Biodistribution of the RD114/mammalian type D retrovirus receptor, RDR. J Gene Med. 6(3): p. 249-59.

385. Valitutti, S., Muller, S., Cella, M., Padovan, E., and Lanzavecchia, A., (1995) Serial triggering of many T-cell receptors by a few peptide-MHC complexes. Nature. 375(6527): p. 148-51.

386. Alam, S.M., Travers, P.J., Wung, J.L., Nasholds, W., Redpath, S., Jameson, S.C., and Gascoigne, N.R., (1996) T-cell-receptor affinity and thymocyte positive selection. Nature. 381(6583): p. 616-20.

387. al-Ramadi, B.K., Jelonek, M.T., Boyd, L.F., Margulies, D.H., and Bothwell, A.L., (1995) Lack of strict correlation of functional sensitization with the apparent affinity of MHC/peptide complexes for the TCR. J Immunol. 155(2): p. 662-73.

388. Sykulev, Y., Vugmeyster, Y., Brunmark, A., Ploegh, H.L., and Eisen, H.N., (1998) Peptide antagonism and T cell receptor interactions with peptide-MHC complexes. Immunity. 9(4): p. 475-83.

389. Baker, B.M., Gagnon, S.J., Biddison, W.E., and Wiley, D.C., (2000) Conversion of a T cell antagonist into an agonist by repairing a defect in the TCR/peptide/MHC interface: implications for TCR signaling. Immunity. 13(4): p. 475-84.

390. Kalergis, A.M., Boucheron, N., Doucey, M.A., Palmieri, E., Goyarts, E.C., Vegh, Z., Luescher, I.F., and Nathenson, S.G., (2001) Efficient T cell activation requires an optimal dwell-time of interaction between the TCR and the pMHC complex. Nat Immunol. 2(3): p. 229-34.

391. Zhao, Z., Condomines, M., van der Stegen, S.J., Perna, F., Kloss, C.C., Gunset, G., Plotkin, J., and Sadelain, M., (2015) Structural Design of Engineered Costimulation Determines Tumor Rejection Kinetics and Persistence of CAR T Cells. Cancer Cell. 28(4): p. 415-28.

392. Refaeli, Y., Van Parijs, L., Alexander, S.I., and Abbas, A.K., (2002) Interferon gamma is required for activation-induced death of T lymphocytes. J Exp Med. 196(7): p. 999-1005.

393. Badovinac, V.P., Tvinnereim, A.R., and Harty, J.T., (2000) Regulation of antigen-specific CD8+ T cell homeostasis by perforin and interferon-gamma. Science. 290(5495): p. 1354-8.

394. Rathmell, J.C. and Thompson, C.B., (2002) Pathways of apoptosis in lymphocyte development, homeostasis, and disease. Cell. 109 Suppl: p. S97-107.

395. Sasmono, R.T., Oceandy, D., Pollard, J.W., Tong, W., Pavli, P., Wainwright, B.J., Ostrowski, M.C., Himes, S.R., and Hume, D.A., (2003) A macrophage colony-stimulating factor receptor-green fluorescent protein transgene is expressed throughout the mononuclear phagocyte system of the mouse. Blood. 101(3): p. 1155-63.

396. MacDonald KP, P.J., Cronau S et al., (2010) An antibody against the colony-stimulating factor 1 receptor depletes the resident subset of monocytes and tissue- and tumor-associated macrophages but does not inhibit inflammation. Blood. 116(19): p. 3955 - 63.

397. Kitagawa D, G.M., Kirii Y, et al., (2012) Characterization of kinase inhibitors using different phosphorylation states of colony stimulating factor 1 receptor tyrosine kinase. J Biochem. 151(1): p. 47 - 55.

398. Patel, S. and Player, M.R., (2009) Colony-stimulating factor-1 receptor inhibitors for the treatment of cancer and inflammatory disease. Curr Top Med Chem. 9(7): p. 599-610.

399. Karaman, M.W., Herrgard, S., Treiber, D.K., Gallant, P., Atteridge, C.E., Campbell, B.T., Chan, K.W., Ciceri, P., Davis, M.I., Edeen, P.T., et al., (2008) A quantitative analysis of kinase inhibitor selectivity. Nat Biotechnol. 26(1): p. 127-32.

400. Brownlow, N., Vaid, M., and Dibb, N.J., (2008) Tandutinib inhibits FMS receptor signalling, and macrophage and osteoclast formation in vitro. Leukemia. 22(7): p. 1452-3.

401. Conway, J.G., McDonald, B., Parham, J., Keith, B., Rusnak, D.W., Shaw, E., Jansen, M., Lin, P., Payne, A., Crosby, R.M., et al., (2005) Inhibition of colony-stimulating-factor-1 signaling in vivo with the orally bioavailable cFMS kinase inhibitor GW2580. Proc Natl Acad Sci U S A. 102(44): p. 16078-83.

402. Ohno, H., Kubo, K., Murooka, H., Kobayashi, Y., Nishitoba, T., Shibuya, M., Yoneda, T., and Isoe, T., (2006) A c-fms tyrosine kinase inhibitor, Ki20227, suppresses osteoclast differentiation and osteolytic bone destruction in a bone metastasis model. Mol Cancer Ther. 5(11): p. 2634-43.

403. Blay, J.Y., El Sayadi, H., Thiesse, P., Garret, J., and Ray-Coquard, I., (2008) Complete response to imatinib in relapsing pigmented villonodular synovitis/tenosynovial giant cell tumor (PVNS/TGCT). Ann Oncol. 19(4): p. 821-2.

404. Dewar, A.L., Cambareri, A.C., Zannettino, A.C., Miller, B.L., Doherty, K.V., Hughes, T.P., and Lyons, A.B., (2005) Macrophage colony-stimulating factor receptor c-fms is a novel target of imatinib. Blood. 105(8): p. 3127-32.

405. Cassier, P.A., Gelderblom, H., Stacchiotti, S., Thomas, D., Maki, R.G., Kroep, J.R., van der Graaf, W.T., Italiano, A., Seddon, B., Domont, J., et al., (2012) Efficacy of imatinib mesylate for the treatment of locally advanced and/or metastatic tenosynovial giant cell tumor/pigmented villonodular synovitis. Cancer. 118(6): p. 1649-55.

406. Gelderblom, H., Pérol, D., Chevreau, C., Tattersall, M., Stacchiotti, S., Casali, P., Cropet, C., Piperno-Neumann, S., Le Cesne, A., Italiano, A., et al., (2013) An open-label international multicentric phase II study of nilotinib in progressive pigmented villo-nodular synovitis (PVNS) not amenable to a conservative surgical treatment. Proc Am Soc Clon Oncol. 31(suppl): p. abstr 10516.

407. Stacchiotti, S., Crippa, F., Messina, A., Pilotti, S., Gronchi, A., Blay, J.Y., and Casali, P.G., (2013) Response to imatinib in villonodular pigmented synovitis (PVNS) resistant to nilotinib. Clin Sarcoma Res. 3(1): p. 8.

408. Ries, C.H., Cannarile, M.A., Hoves, S., Benz, J., Wartha, K., Runza, V., Rey-Giraud, F., Pradel, L.P., Feuerhake, F., Klaman, I., et al., (2014) Targeting tumor-associated macrophages with anti-CSF-1R antibody reveals a strategy for cancer therapy. Cancer Cell. 25(6): p. 846-59.

409. Gomez-Roca, C.A., Cassier, P.A., Italiano, A., Cannarile, M., Ries, C., Brillouet, A., Mueller, C., Jegg, A., Meneses-Lorente, G., Baehner, M., et al., (2015) Phase I study of RG7155, a novel anti-CSF1R antibody, in patients with advanced/metastatic solid tumors. J Clin Oncol. 33(suppl): p. abstr 3005.

410. Schaerli, P. and Moser, B., (2005) Chemokines: control of primary and memory T-cell traffic. Immunol Res. 31(1): p. 57-74.

411. Marelli-Berg, F.M., Fu, H., Vianello, F., Tokoyoda, K., and Hamann, A., (2010) Memory T-cell trafficking: new directions for busy commuters. Immunology. 130(2): p. 158-65.

412. Gattinoni, L., Lugli, E., Ji, Y., Pos, Z., Paulos, C.M., Quigley, M.F., Almeida, J.R., Gostick, E., Yu, Z., Carpenito, C., et al., (2011) A human memory T cell subset with stem cell-like properties. Nat Med. 17(10): p. 1290-7.

413. Liu, S., Riley, J., Rosenberg, S., and Parkhurst, M., (2006) Comparison of common gamma-chain cytokines, interleukin-2, interleukin-7, and interleukin-15 for the in vitro generation of human tumor-reactive T lymphocytes for adoptive cell transfer therapy. J Immunother. 29(3): p. 284-93.

414. Kaneko, S., Mastaglio, S., Bondanza, A., Ponzoni, M., Sanvito, F., Aldrighetti, L., Radrizzani, M., La Seta-Catamancio, S., Provasi, E., Mondino, A., et al., (2009) IL-7 and IL-15 allow the generation of suicide gene-modified alloreactive self-renewing central memory human T lymphocytes. Blood. 113(5): p. 1006-15.

415. Riker, A., Cormier, J., Panelli, M., Kammula, U., Wang, E., Abati, A., Fetsch, P., Lee, K.H., Steinberg, S., Rosenberg, S., et al., (1999) Immune selection after antigen-specific immunotherapy of melanoma. Surgery. 126(2): p. 112-20.

416. Klein, L., Trautman, L., Psarras, S., Schnell, S., Siermann, A., Liblau, R., von Boehmer, H., and Khazaie, K., (2003) Visualizing the course of antigen-specific CD8 and CD4 T cell responses to a growing tumor. Eur J Immunol. 33(3): p. 806-14.

417. Ju, S.T., Panka, D.J., Cui, H., Ettinger, R., el-Khatib, M., Sherr, D.H., Stanger, B.Z., and Marshak-Rothstein, A., (1995) Fas(CD95)/FasL interactions required for programmed cell death after T-cell activation. Nature. 373(6513): p. 444-8.

418. Robbins, P.F., Dudley, M.E., Wunderlich, J., El-Gamil, M., Li, Y.F., Zhou, J., Huang, J., Powell, D.J., Jr., and Rosenberg, S.A., (2004) Cutting edge: persistence of transferred lymphocyte clonotypes correlates with cancer regression in patients receiving cell transfer therapy. J Immunol. 173(12): p. 7125-30.

419. Ito, M., Hiramatsu, H., Kobayashi, K., Suzue, K., Kawahata, M., Hioki, K., Ueyama, Y., Koyanagi, Y., Sugamura, K., Tsuji, K., et al., (2002) NOD/SCID/gamma(c)(null) mouse: an excellent recipient mouse model for engraftment of human cells. Blood. 100(9): p. 3175-82.

420. Ishikawa, F., Yasukawa, M., Lyons, B., Yoshida, S., Miyamoto, T., Yoshimoto, G., Watanabe, T., Akashi, K., Shultz, L.D., and Harada, M., (2005) Development of functional human blood and immune systems in NOD/SCID/IL2 receptor {gamma} chain(null) mice. Blood. 106(5): p. 1565-73.

421. Shultz, L.D., Lyons, B.L., Burzenski, L.M., Gott, B., Chen, X., Chaleff, S., Kotb, M., Gillies, S.D., King, M., Mangada, J., et al., (2005) Human lymphoid and myeloid cell development in NOD/LtSz-scid IL2R gamma null mice engrafted with mobilized human hemopoietic stem cells. J Immunol. 174(10): p. 6477-89.

422. Kurtz, D.M., Tschetter, L.K., Allred, J.B., Geyer, S.M., Kurtin, P.J., Putnam, W.D., Rowland, K.M., Jr., Wiesenfeld, M., Soori, G.S., Tenglin, R.C., et al., (2007) Subcutaneous interleukin-4 (IL-4) for relapsed and resistant non-Hodgkin lymphoma: a phase II trial in the North Central Cancer Treatment Group, NCCTG 91-78-51. Leuk Lymphoma. 48(7): p. 1290-8.

423. Majhail, N.S., Hussein, M., Olencki, T.E., Budd, G.T., Wood, L., Elson, P., and Bukowski, R.M., (2004) Phase I trial of continuous infusion recombinant human interleukin-4 in patients with cancer. Invest New Drugs. 22(4): p. 421-6.

424. Chen, L. and Flies, D.B., (2013) Molecular mechanisms of T cell co-stimulation and co-inhibition. Nat Rev Immunol. 13(4): p. 227-42.

425. Oren, R., Hod-Marco, M., Haus-Cohen, M., Thomas, S., Blat, D., Duvshani, N., Denkberg, G., Elbaz, Y., Benchetrit, F., Eshhar, Z., et al., (2014) Functional comparison of engineered T cells carrying a native TCR versus TCR-like antibody-based chimeric antigen receptors indicates affinity/avidity thresholds. J Immunol. 193(11): p. 5733-43.

426. Wei, S., Nandi, S., Chitu, V., Yeung, Y.G., Yu, W., Huang, M., Williams, L.T., Lin, H., and Stanley, E.R., (2010) Functional overlap but differential expression of CSF-1 and IL-34 in their CSF-1 receptor-mediated regulation of myeloid cells. J Leukoc Biol. 88(3): p. 495-505.

427. Elegheert, J., Desfosses, A., Shkumatov, A.V., Wu, X., Bracke, N., Verstraete, K., Van Craenenbroeck, K., Brooks, B.R., Svergun, D.I., Vergauwen, B., et al., (2011) Extracellular complexes of the hematopoietic human and mouse CSF-1 receptor are driven by common assembly principles. Structure. 19(12): p. 1762-72.

428. Chihara, T., Suzu, S., Hassan, R., Chutiwitoonchai, N., Hiyoshi, M., Motoyoshi, K., Kimura, F., and Okada, S., (2010) IL-34 and M-CSF share the receptor Fms but are not identical in biological activity and signal activation. Cell Death Differ. 17(12): p. 1917-27.

Appendix

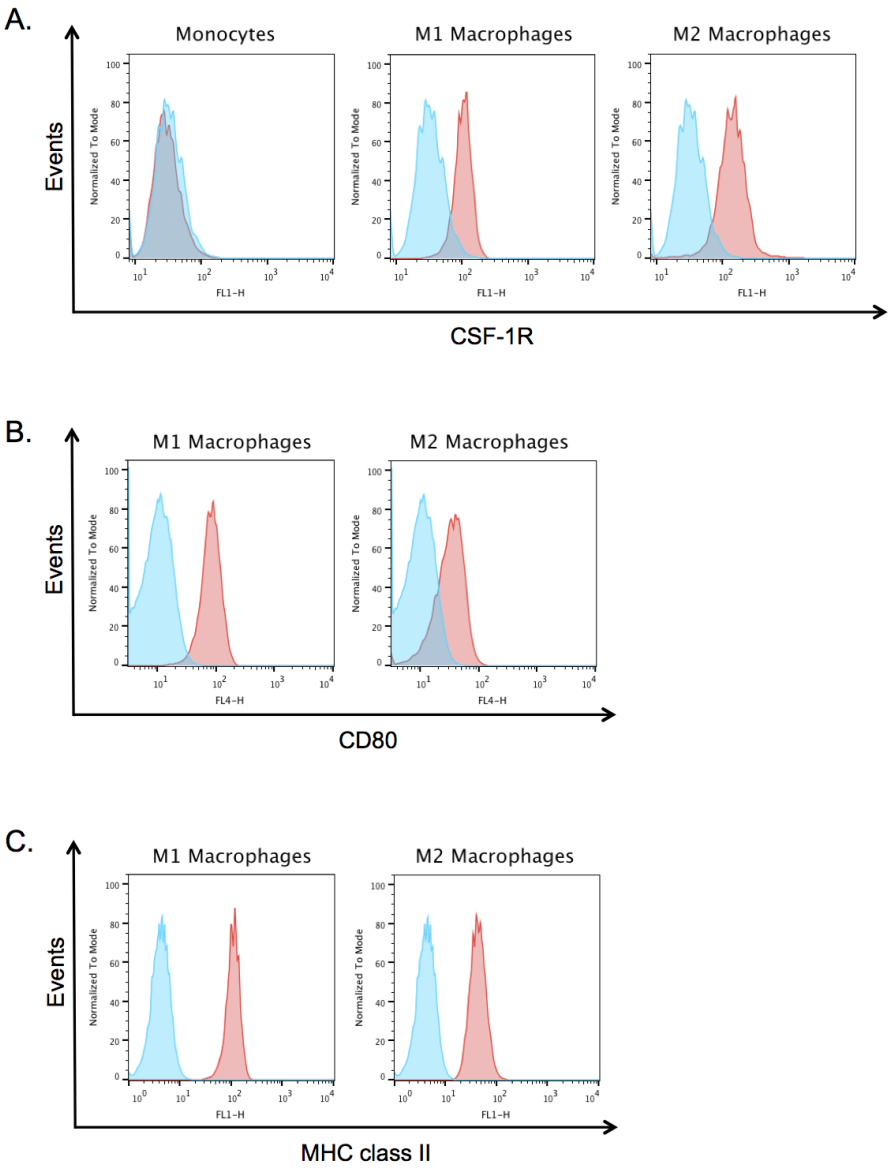

Supplementary Figure S1 Phenotyping of human monocyte-derived macrophages for M1/M2 polarisation. MACS-separated CD14^{+} human monocytes were differentiated into M1 or M2 macrophages by cultivation for 7 days in GM-CSF or CSF-1 respectively. **(A)** Macrophages were probed for the cell surface expression of CSF-1R using a monoclonal rat anti-human CSF-1R antibody followed by a goat anti-rat FITC secondary antibody (red histograms). Cells were also stained using the secondary antibody only (blue histograms) to show the specificity of staining. **(B and C)** Macrophages were stained for expression of CD80 (pink histogram, B.) and MHC class II (pink histogram, C.) using a monoclonal anti-human CD80-APC and monoclonal anti-human HLA-DR-FITC respectively. Blue histograms represent staining with matched isotype controls.

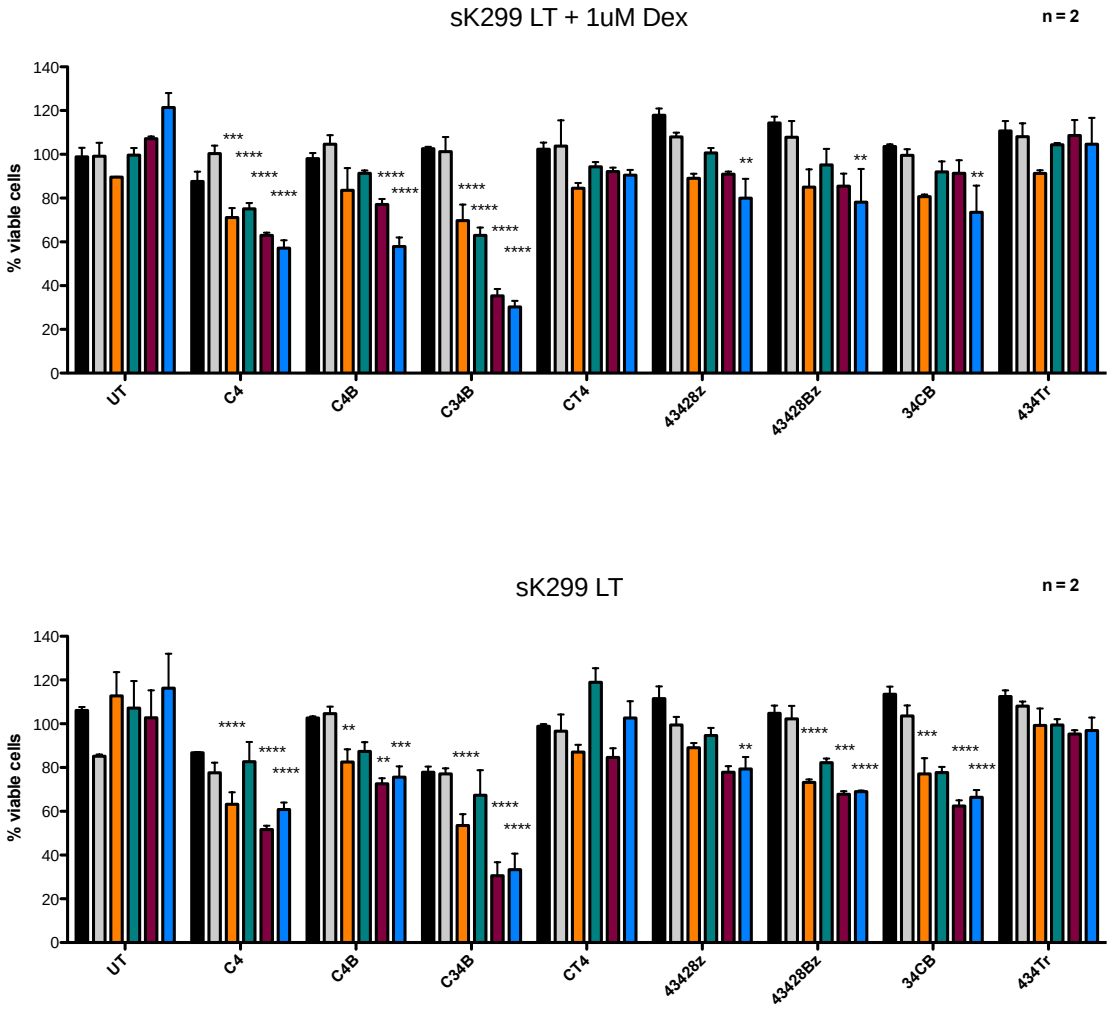

Supplementary Figure S2 Cytotoxicity of CSF-1R-retargeted T-cells against the K299 cell line *in vitro* in the presence or absence of 1uM dexamethasone. The ALCL cell line K299 was pre-treated with 1uM dexamethasone or medium alone for 48h, then washed and co-cultured with a panel of CAR-grafted T-cells at a 1:1 ratio for the indicated period of time. The level of target cell viability co-culture was monitored using a luciferase assay. The data was normalised against the maximal luminescence, as shown by tumour cells grown in the absence of T-cells. Normalisation was achieved using the following equation: Tumour cell viability = (Sample luminescence value / Average No T-cell luminescence value)*100

Data are presented as mean ± SD from two independent experiments. **** = p<0.0001; *** = p<0.001; ** = p<0.01; * = p<0.05 relative to UT T-cells at any given time point.

A.

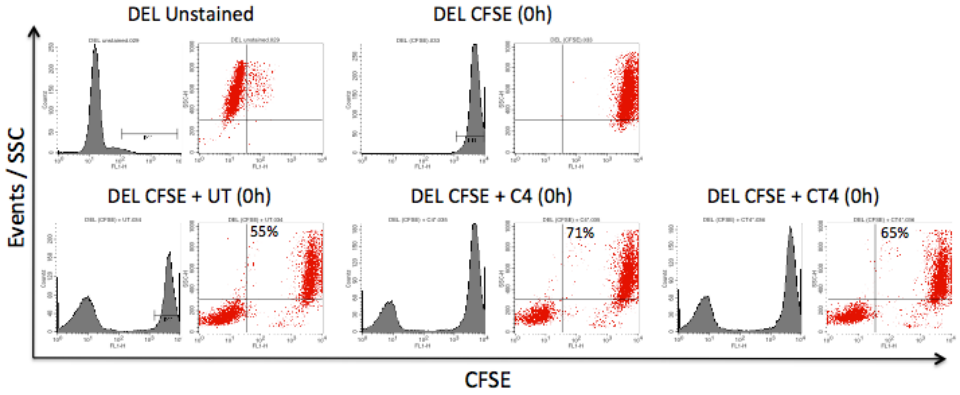

B.

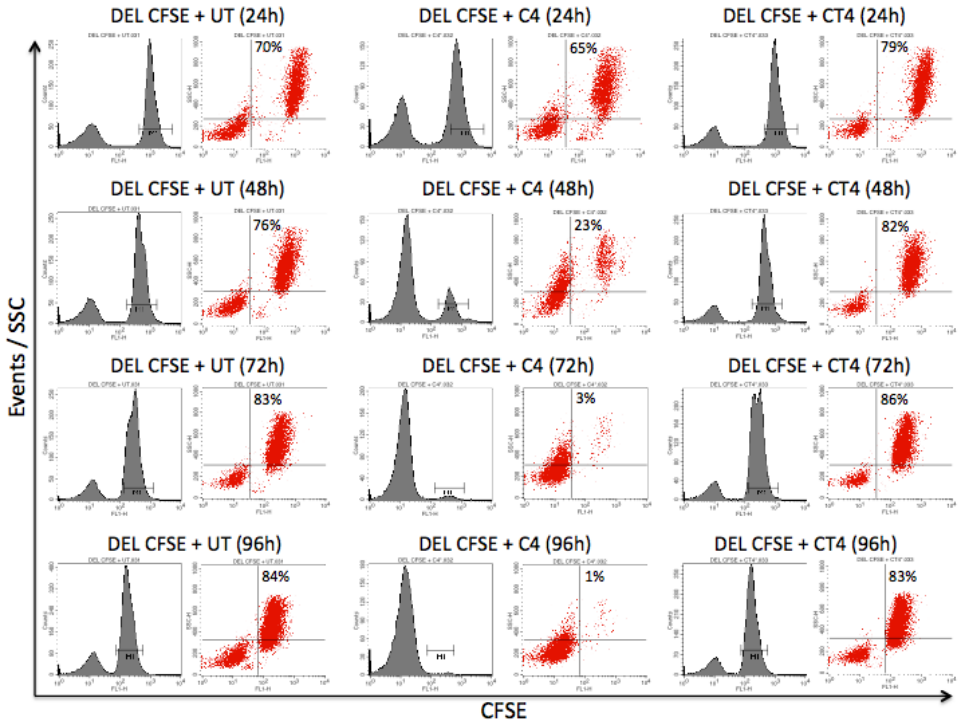

Supplementary Figure S3 DEL cell line destruction upon co-culture with C4⁺ T-cells.

The lymphoma cell line DEL was CFSE-labelled and co-cultured in 1:1 ratio with UT, C4⁺ and CT4⁺ T-cells. Cancer cell destruction was assessed by clearance of CFSE-labelled cells as determined by flow cytometry. Co-cultures were probed at 0h (A.), 24h, 48h, 72h and 96h (B.). Data are representative of 2 separate experiments.

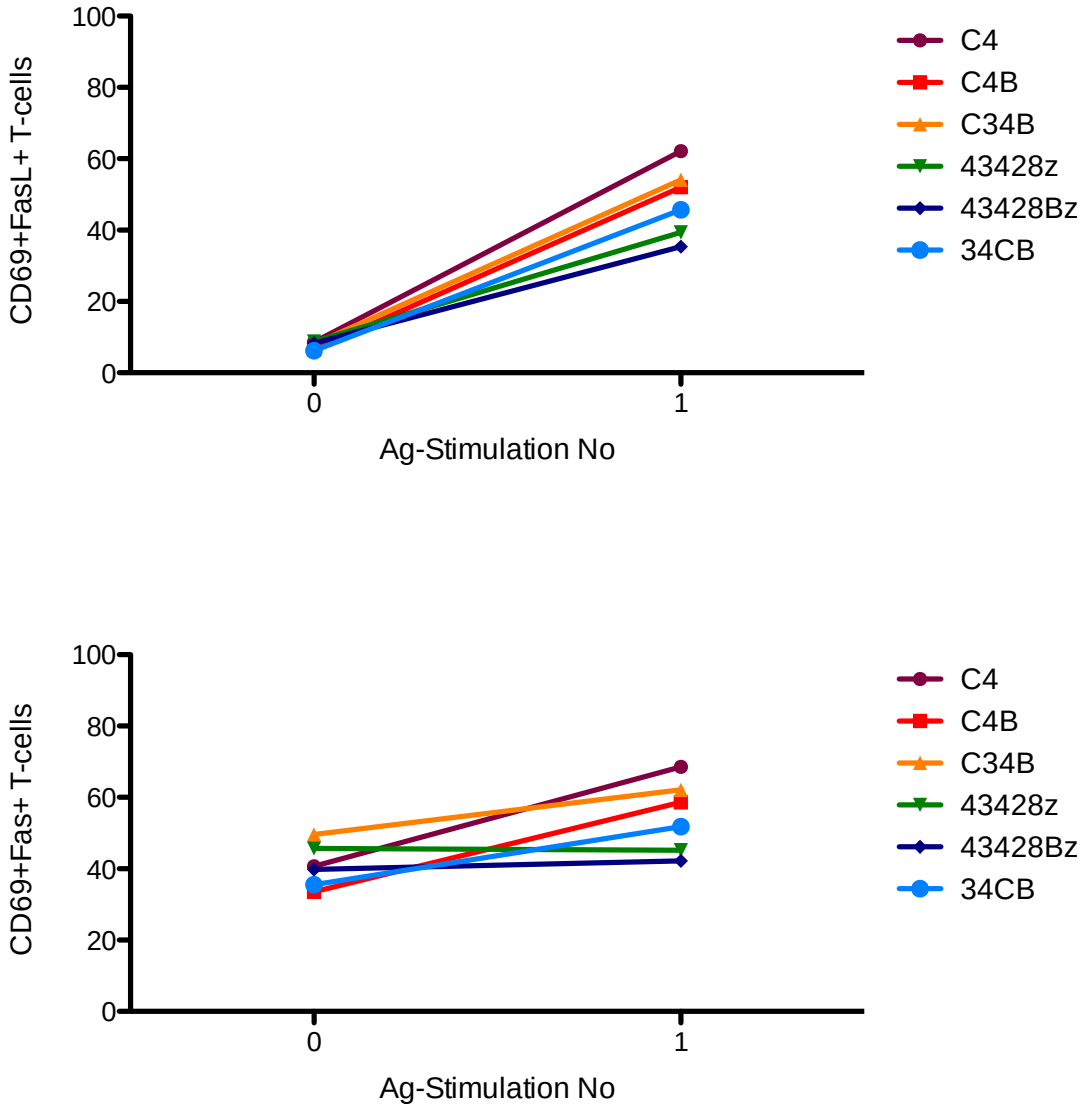

Supplementary Figure S4 Fas and FasL expression on CAR+ T-cells before and after antigen stimulation. CAR^+ T-cells were probed for the cell surface expression of Fas and FasL prior and post antigen stimulation on T47D FMS monolayers using anti-human CD95-PerCP-Cy5.5, CD95L-PE and CD69-APC-Cy7.

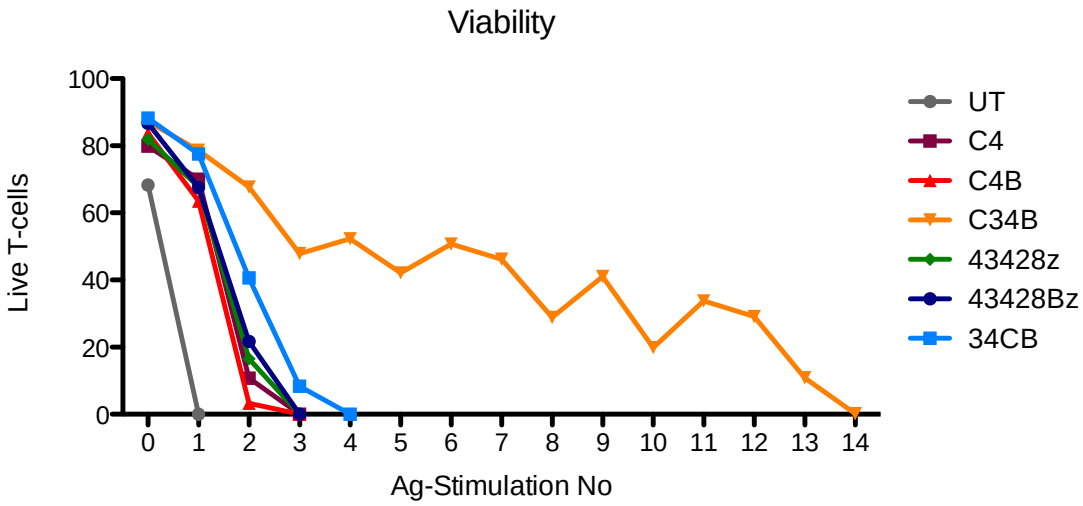

Supplementary Figure S5 T-cell viability after successive rounds of antigen-stimulation

CAR^{+} T-cells were subjected to successive rounds of antigen stimulation by co-culturing on T47D FMS monolayers at 1:1 ratio. T-cells were assessed for cell viability after each round of antigen stimulation by staining with DAPI. Data presented are from a single experiment.

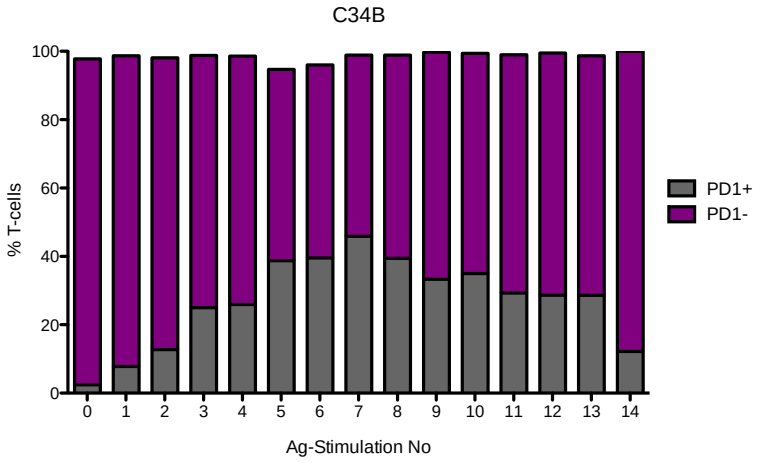

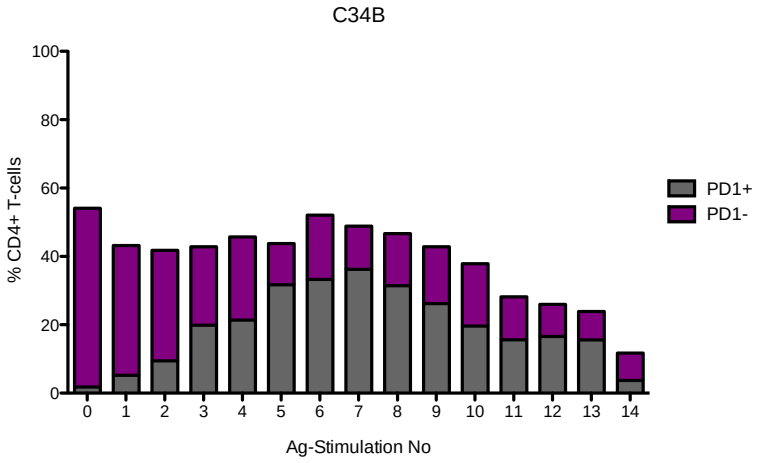

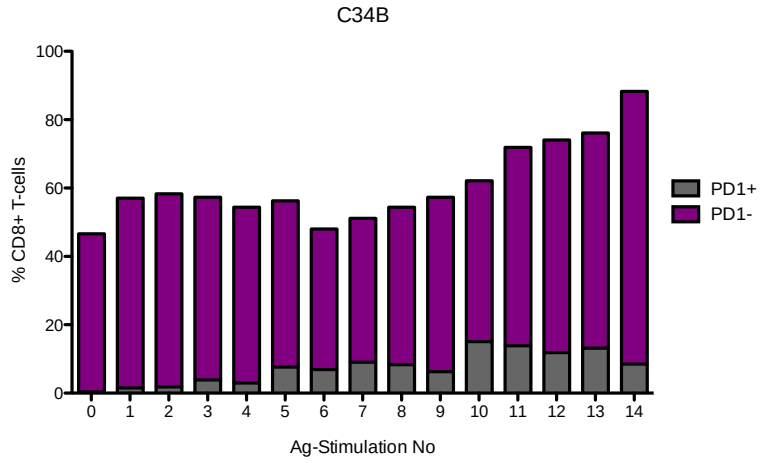

Supplementary Figure S6 PD1 expression on C34B+ T-cells after successive rounds of antigen-stimulation. C34B^{+} T-cells were subjected to successive rounds of antigen stimulation by co-culturing on T47D FMS monolayers at 1:1 ratio. T-cells were stained for the cell surface expression of PD1, CD4 and CD8 using anti-human PD1-APC-Cy7, CD8-PE-Cy7 and CD4-PE.

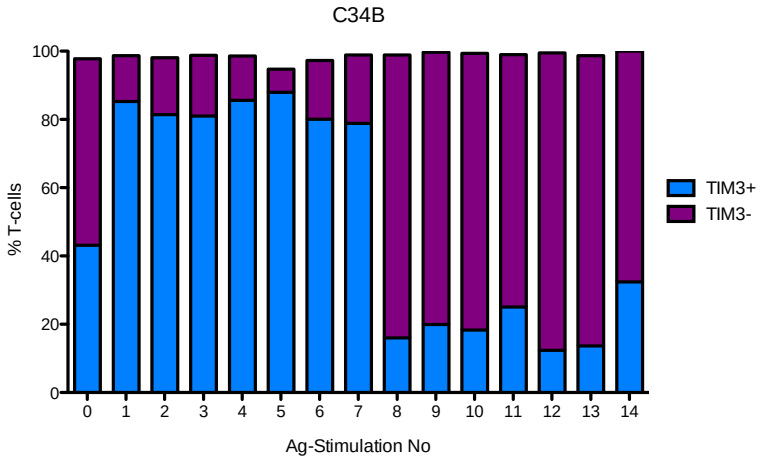

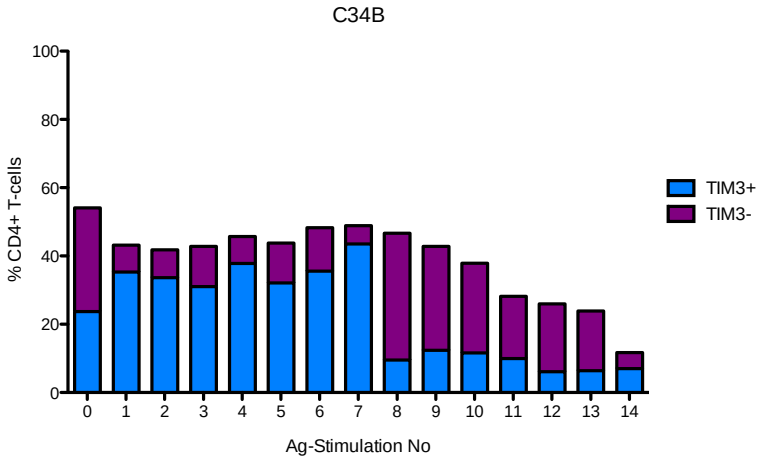

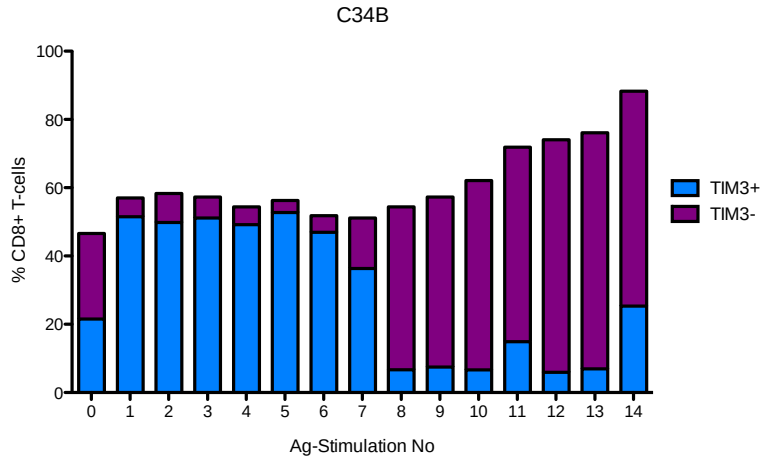

Supplementary Figure S7 TIM3 expression on C34B+ T-cells after successive rounds of antigen-stimulation C34B^{+} T-cells were subjected to successive rounds of antigen stimulation by co-culturing on T47D FMS monolayers at 1:1 ratio. T-cells were probed for the cell surface expression of TIM3, CD4 and CD8 using anti-human TIM3-PerCP-Cy5.5, CD8-PE-Cy7 and CD4-PE.

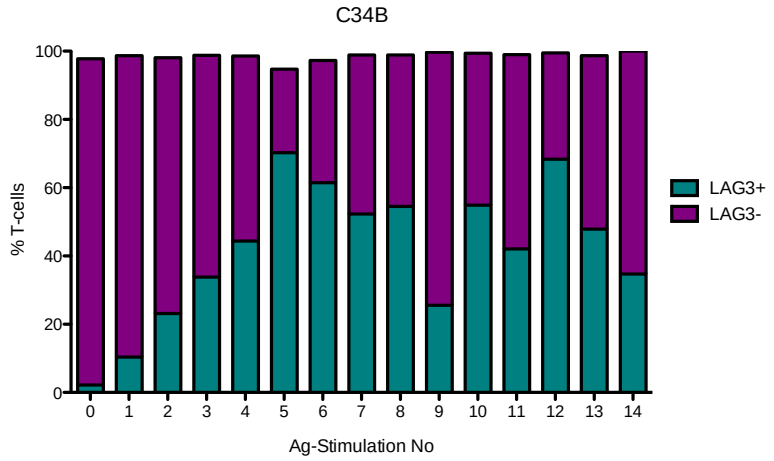

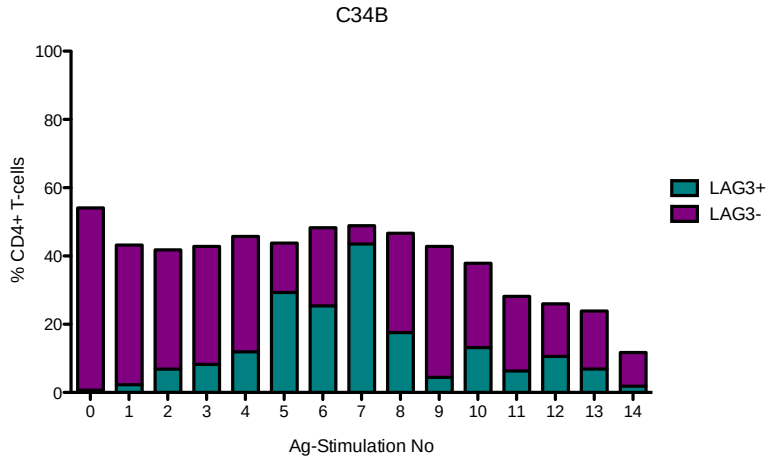

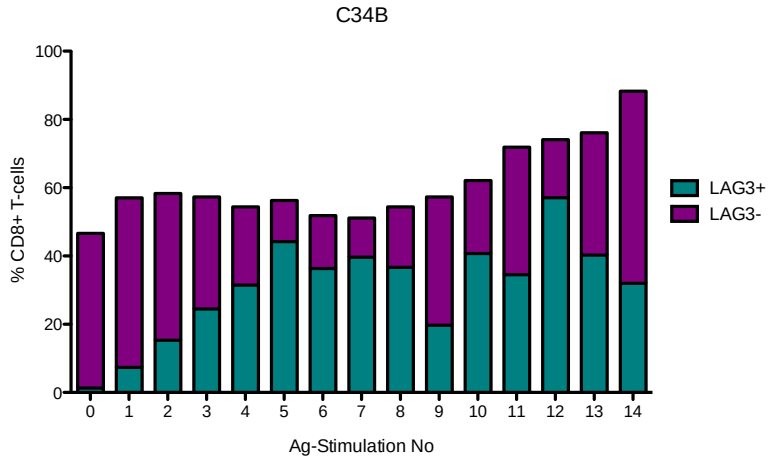

Supplementary Figure S8 LAG3 expression on C34B+ T-cells after successive rounds of antigen-stimulation C34B^{+} T-cells were subjected to successive rounds of antigen stimulation by co-culturing on T47D FMS monolayers at 1:1 ratio. T-cells were probed for the cell surface expression of LAG3, CD4 and CD8 using anti-human LAG3-APC, CD8-PE-Cy7 and CD4-PE.

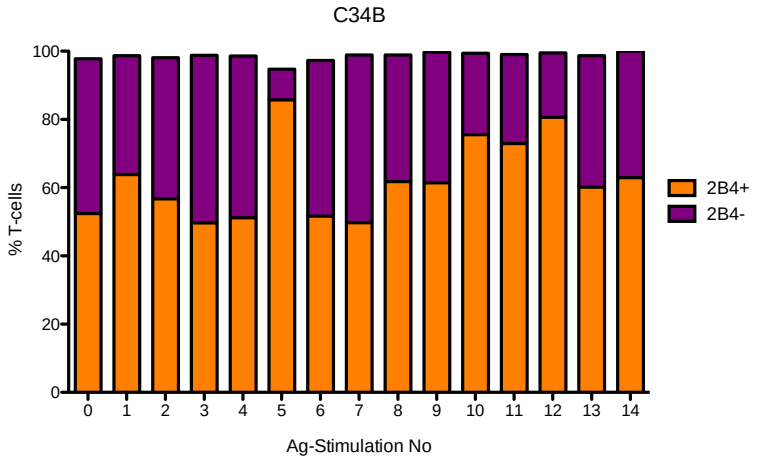

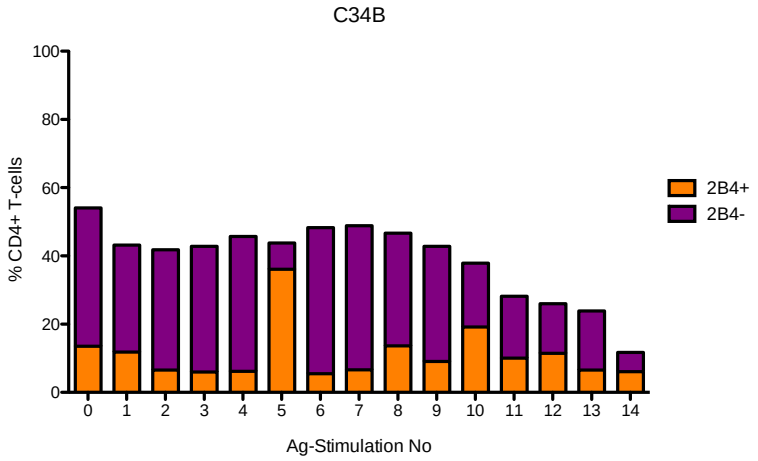

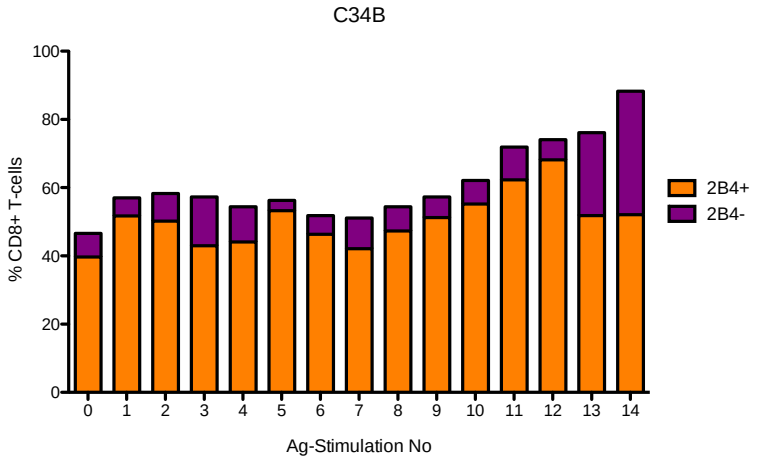

Supplementary Figure S9 2B4 expression on C34B+ T-cells after successive rounds of antigen-stimulation C34B^{+} T-cells were subjected to successive rounds of antigen stimulation by co-culturing on T47D FMS monolayers at 1:1 ratio. T-cells were probed for the cell surface expression of 2B4, CD4 and CD8 using anti-human 2B4-FITC, CD8-PE-Cy7 and CD4-PE.

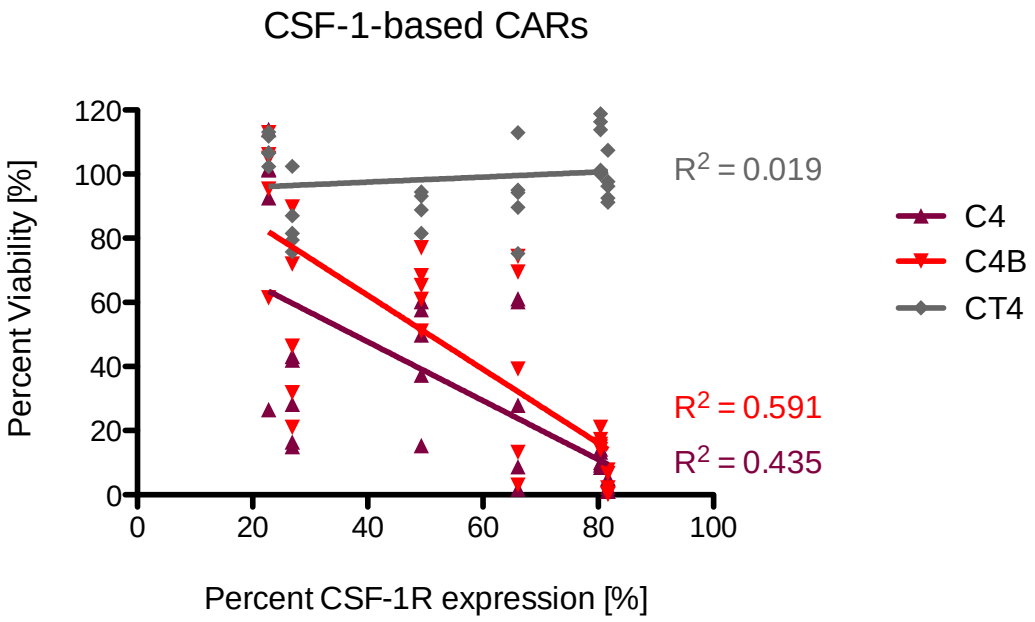
CSF-1-based CARs
Percent Viability [%]
120
100
80
60
40
20
0
0
20
40
60
80
100
Percent CSF-1R expression [%]
R2 = 0.019
R2 = 0.591
R2 = 0.435
C4
C4B
CT4

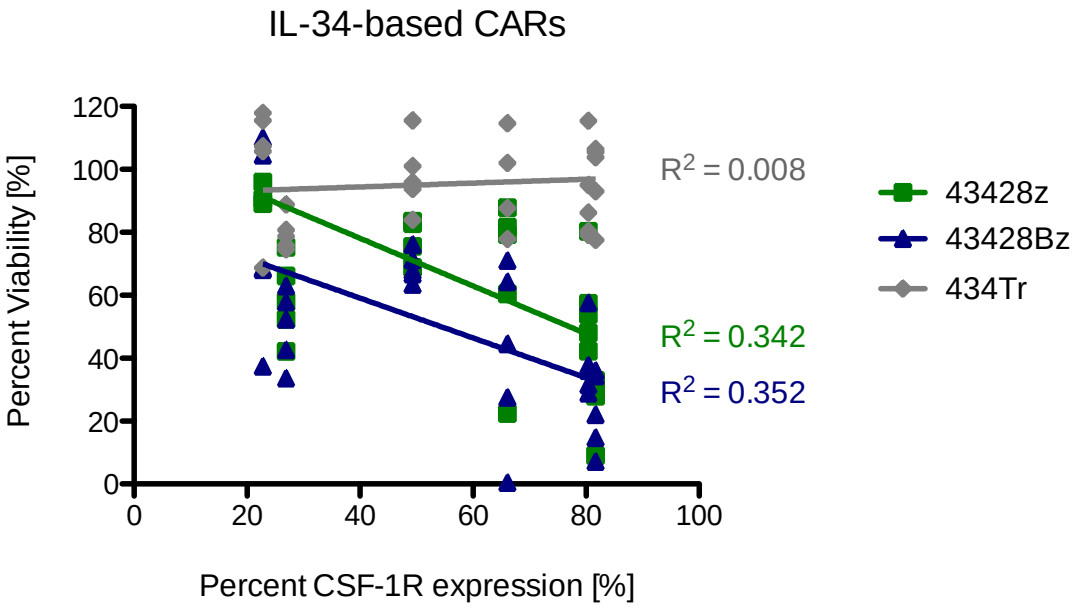
IL-34-based CARs
Percent Viability [%]
120
100
80
60
40
20
0
0
20
40
60
80
100
Percent CSF-1R expression [%]
R2 = 0.008
R2 = 0.342
R2 = 0.352
43428z
43428Bz
434Tr

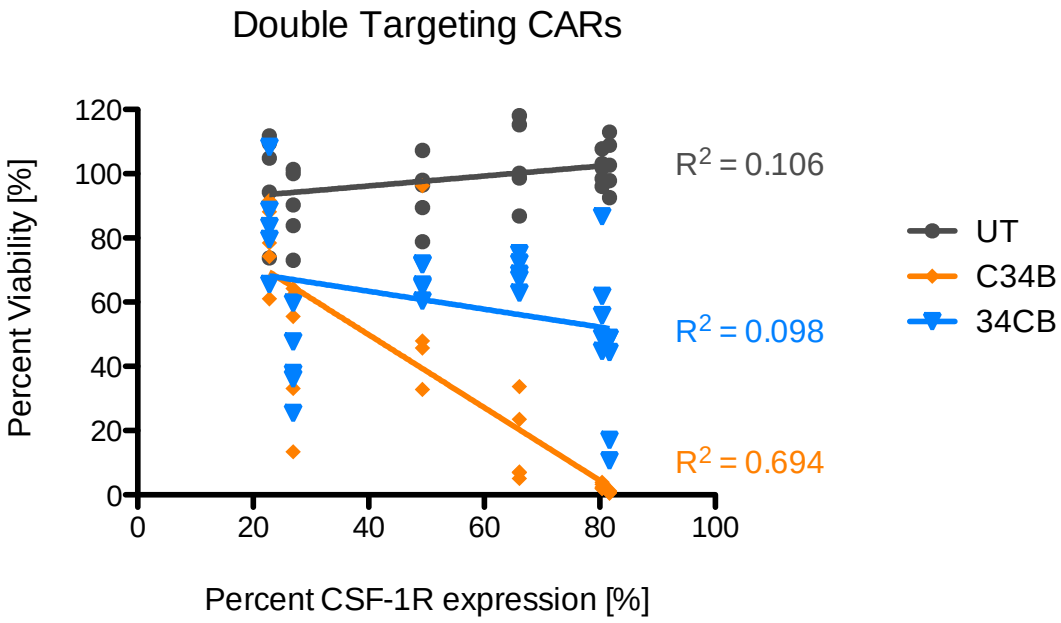

Supplementary Figure S10 CAR+ T-cells were co-cultured with the panel of lymphoma cell lines for 72 hours, before cancer cell viability was quantified using a luciferase assay. This was subsequently plotted against the percent CSF-1R expression on each lymphoma cell line, which had been measured using flow cytometry. The data presented has been gained from a minimum of five independent experiments and each dot represents an individual sample measured for lymphoma cell viability.

Supplementary Table S1 – statistical significance of cancer cell viability post treatment with different CAR^+ T-cell populations as determined by two-way ANOVA, followed by a Bonferroni post-hoc test.

A. $C4^+$ vs. $43428\zeta^+$ T-cells

	KM-H2	K299	DEL	FE-PD	JB6	L540
24h	ns	ns	****	ns	ns	ns
48h	ns	ns	****	****	ns	ns
72h	ns	**	*	****	ns	ns
96h	**	ns	ns	****	*	ns
120h	*	ns	ns	**	ns	ns
144h	*	ns	ns	****	ns	ns

B. $C4B^+$ vs. $43428B\zeta^+$ T-cells

	KM-H2	K299	DEL	FE-PD	JB6	L540
24h	ns	ns	ns	ns	ns	ns
48h	ns	ns	ns	ns	ns	ns
72h	ns	ns	ns	ns	ns	ns
96h	ns	ns	*	ns	ns	ns
120h	ns	ns	ns	ns	ns	ns
144h	ns	ns	ns	ns	ns	ns

C. C34B^{+} vs. 34CB^{+} T-cells

	KM-H2	K299	DEL	FE-PD	JB6	L540
24h	ns	ns	****	****	ns	ns
48h	ns	ns	****	****	ns	ns
72h	ns	ns	****	****	**	ns
96h	ns	ns	ns	****	**	**
120h	ns	ns	ns	****	ns	**
144h	ns	ns	ns	****	ns	***

D. C4^{+} vs. C4B^{+} T-cells

	KM-H2	K299	DEL	FE-PD	JB6	L540
24h	ns	ns	ns	ns	ns	ns
48h	ns	ns	ns	ns	ns	ns
72h	ns	ns	ns	ns	ns	ns
96h	ns	ns	ns	ns	ns	ns
120h	ns	ns	ns	ns	ns	ns
144h	ns	ns	ns	ns	ns	ns

E. 43428ζ^{+} vs. 43428Bζ^{+} T-cells

	KM-H2	K299	DEL	FE-PD	JB6	L540
24h	ns	ns	ns	ns	ns	ns
48h	ns	ns	ns	ns	ns	ns
72h	ns	ns	ns	ns	ns	ns
96h	ns	ns	ns	ns	ns	ns
120h	ns	ns	ns	ns	ns	ns
144h	ns	ns	ns	ns	ns	ns

F. C4B^{+} vs. C34B^{+} T-cells

	KM-H2	K299	DEL	FE-PD	JB6	L540
24h	ns	ns	ns	ns	ns	ns
48h	ns	ns	ns	ns	ns	ns
72h	ns	ns	ns	ns	ns	ns
96h	ns	ns	ns	ns	**	*
120h	ns	ns	ns	ns	ns	*
144h	ns	ns	ns	ns	ns	ns

G. 43428Bζ^{+} vs. C34B^{+} T-cells

	KM-H2	K299	DEL	FE-PD	JB6	L540
24h	ns	ns	*	**	ns	ns
48h	ns	ns	ns	****	ns	ns
72h	ns	ns	ns	***	ns	ns
96h	ns	ns	**	****	*	ns
120h	ns	ns	*	ns	ns	ns
144h	ns	ns	ns	*	ns	ns

H. C4B^{+} vs. 34CB^{+} T-cells

	KM-H2	K299	DEL	FE-PD	JB6	L540
24h	ns	ns	****	**	ns	ns
48h	ns	ns	****	****	ns	ns
72h	ns	ns	***	****	ns	ns
96h	ns	ns	ns	****	ns	ns
120h	ns	ns	ns	**	ns	ns
144h	ns	ns	ns	***	ns	ns

I. 43428Bζ^{+} vs. 34CB^{+} T-cells

	KM-H2	K299	DEL	FE-PD	JB6	L540
24h	ns	ns	ns	ns	ns	ns
48h	ns	ns	ns	ns	ns	ns
72h	ns	ns	ns	ns	ns	ns
96h	ns	ns	ns	ns	ns	ns
120h	ns	ns	ns	ns	ns	ns
144h	ns	ns	ns	ns	ns	ns

Supplementary Table S2 – statistical significance of cytokine release by different CAR$^+$ T-cell populations upon co-culture with the panel of lymphoma cell lines as determined by two-way ANOVA, followed by a Bonferroni post-hoc test.

A. IFN-γ release

	KM-H2	K299	DEL	FE-PD	JB6	L540
C4 vs. 43428ζ	ns	ns	ns	ns	ns	ns
C4B vs. 43428Bζ	ns	ns	ns	ns	ns	ns
C34B vs. 34CB	ns	ns	*	ns	ns	ns
C4 vs. C4B	ns	ns	ns	ns	ns	ns
43428ζ vs. 43428Bζ	ns	ns	ns	ns	ns	ns
C4B vs. C34B	ns	ns	ns	ns	ns	ns
43428Bζ vs. C34B	ns	ns	*	ns	ns	ns
C4B vs. 34CB	ns	ns	ns	ns	ns	ns
43428Bζ vs. 34CB	ns	ns	ns	ns	ns	ns

B. IL-2 release

	KM-H2	K299	DEL	FE-PD	JB6	L540
C4 vs. 43428ζ	ns	ns	ns	ns	ns	ns
C4B vs. 43428Bζ	ns	ns	ns	ns	ns	ns
C34B vs. 34CB	ns	ns	ns	ns	ns	ns
C4 vs. C4B	ns	ns	ns	ns	ns	ns
43428ζ vs. 43428Bζ	ns	ns	ns	ns	ns	ns
C4B vs. C34B	ns	ns	ns	ns	ns	ns
43428Bζ vs. C34B	ns	ns	ns	ns	ns	ns
C4B vs. 34CB	ns	ns	ns	ns	ns	ns
43428Bζ vs. 34CB	ns	ns	ns	ns	ns	ns

Sequences

C4

CCATGGGCTGGCTGTGTTCCGGCCTGCTGTTTCCTGTGTCCTGTCTGGTGCTGCT

GCAGGTGGCCAGCTCCGGGAACATGAAAGTGCTGCAGGAGCCCACATGTGTGTC

CGACTACATGTCCATCTCTACATGTGAGTGGAAGATGAACGGCCCCACAAACTGC

TCTACCGAGCTGCGGCTGCTGTACCAGCTGGTGTTTCTGCTGAGCGAGGCCCAC

ACCTGTATCCCAGAAAATAATGGCGGGGCCGGGTGTGTGTGCCACCTGCTGATG

GATGACGTGGTGTCTGCCGACAATTACACCCTGGACCTGTGGGCCGGACAGCAG

CTGCTGTGGAAGGGGTCCTTCAAACCCTCTGAGCACGTGAAGCCAAGGGCCCCC

GGCAACCTGACAGTGCACACCAACGTGTCTGATACACTGCTGCTGACATGGAGCA

ATCCATACCCTCCTGACAACTACCTGTACAACCACCTGACCTACGCCGTGAATATC

TGGAGCGAAAATGATCCTGCCGACTTTCGGATTTACAATGTGACCTATCTGGAGC

CCTCCCTGAGAATTGCCGCCTCTACCCTGAAATCTGGAATCTCCTACCGCGCCAG

GGTGCGGGCCTGGGCCCAGTGTTACAACACCACCTGGTCTGAGTGGAGCCCAAG

CACCAAGTGGCACAATTCTTATCGGGAGCCTTTTGAGCAGCACCTGATCCCCTGG

CTGGGACACCTGCTGGTGGGGCTGTCTGGCGCCTTTGGCTTCATCATTCTGGTGT

ACCTGCTGATCAACTGTAGGAATACAGGCCCTTGGCTGAAGAAGGTGCTGAAGTG

TAACACCCCCGACCCCTCTAAGTTCTTCAGCCAGCTGTCCTCTGAACACGGGGGA

GATGTGCAGAAGTGGCTGTCCAGCCCTTTCCCATCCAGCTCCTTTAGCCCCGGG

GGCCTGGCCCCTGAGATCTCTCCACTGGAAGTGCTGGAGCGGGACAAGGTGACC

CAGCTGCTGCTGCAGCAGGACAAGGTGCCAGAACCCGCCTCCCTGAGCTCCAAC

CACAGCCTGACATCTTGCTTTACAAATCAGGGATACTTCTTCTTCCACCTGCCCGA

TGCCCTGGAGATCGAGGCCTGCCAGGTGTACTTCACCTACGATCCCTACTCTGAG

GAAGACCCAGATGAGGGCGTGGCCGGGGCCCCAACCGGGTCCAGCCCACAGCC

ACTGCAGCCACTGTCCGGCGAAGATGACGCCTACTGCACATTCCCTTCCAGGGAT

GACCTGCTGCTGTTCAGCCCATCTCTGCTGGGCGGACCCTCTCCTCCAAGCACA

GCCCCAGGGGGATCCGGCGCCGGGGAAGAGAGGATGCCCCCTAGCCTGCAGGA

GCGCGTGCCCAGAGACTGGGACCCCCAGCCCCTGGGCCCTCCAACCCCTGGGG

TGCCCGACCTGGTGGACTTCCAGCCTCCACCCGAGCTGGTGCTGAGGGAGGCC

GGCGAAGAGGTGCCCGACGCCGGCCCCCGGGAGGGCGTGTCCTTCCCTTGGTC

CAGACCTCCAGGACAGGGCGAGTTCCGCGCCCTGAACGCCAGGCTGCCTCTGAA

CACCGATGCCTACCTGTCTCTGCAGGAACTGCAGGGCCAGGACCCAACCCACCT

GGTGCGGAGAAAGCGCAGCGGCTCCGGCGAGGGCCGGGGCAGCCTGCTGACCT

GCGGCGACGTGGAAGAGAACCCCGGACCCATGGCTCTCCCAGTGACTGCCCTAC

TGCTTCCCCTAGCGCTTCTCCTGCATGCAGAGGAGGTGTCGGAGTACTGTAGCCA

CATGATTGGGAGTGGACACCTGCAGTCTCTGCAGCGGCTGATTGACAGTCAGATG

GAGACCTCGTGCCAAATTACATTTGAGTTTGTAGACCAGGAACAGTTGAAAGATCC

AGTGTGCTACCTTAAGAAGGCATTTCTCCTGGTACAATACATAATGGAGGACACCA

TGCGCTTCAGAGATAACACCCCCAATGCCATCGCCATTGTGCAGCTGCAGGAACT

CTCTTTGAGGCTGAAGAGCTGCTTCACCAAGGATTATGAAGAGCATGACAAGGCC

TGCGTCCGAACTTTCTATGAGACACCTCTCCAGTTGCTGGAGAAGGTCAAGAATG

TCTTTAATGAAACAAAGAATCTCCTTGACAAGGACTGGAATATTTTCAGCAAGAAC

TGCAACAACAGCTTTGCTGAATGCTCCAGCCAAGGCCATGAGAGGCAGTCCGAG

GGAGCGGCCGCAATTGAAGTTATGTATCCTCCTCCTTACCTAGACAATGAGAAGA

GCAATGGAACCATTATCCATGTGAAAGGGAAACACCTTTGTCCAAGTCCCCTATTT

CCCGGACCTTCTAAGCCCTTTTGGGTGCTGGTGGTGGTTGGTGGAGTCCTGGCTT

GCTATAGCTTGCTAGTAACAGTGGCCTTTATTATTTTCTGGGTGAGGAGTAAGAGG

AGCAGGCTCCTGCACAGTGACTACATGAACATGACTCCCCGCCGCCCCGGGCCC

ACCCGCAAGCATTACCAGCCCTATGCCCCACCACGCGACTTCGCAGCCTATCGCT

CCAGAGTGAAGTTCAGCAGGAGCGCAGAGCCCCCCGCGTACCAGCAGGGCCAG

AACCAGCTCTATAACGAGCTCAATCTAGGACGAAGAGAGGAGTACGATGTTTTGG

ACAAGAGACGTGGCCGGGACCCTGAGATGGGGGGAAAGCCGAGAAGGAAGAAC

CCTCAGGAAGGCCTGTACAATGAACTGCAGAAAGATAAGATGGCGGAGGCCTAC

AGTGAGATTGGGATGAAAGGCGAGCGCCGGAGGGGCAAGGGGCACGATGGCCT

TTACCAGGGTCTCAGTACAGCCACCAAGGACACCTACGACGCCCTTCACATGCAG

GCCCTGCCCCCTCGCTAACAGCCACTCGAG

C4B

CCATGGGCTGGCTGTGTTCCGGCCTGCTGTTTCCTGTGTCCTGTCTGGTGCTGCT

GCAGGTGGCCAGCTCCGGGAACATGAAAGTGCTGCAGGAGCCCACATGTGTGTC

CGACTACATGTCCATCTCTACATGTGAGTGGAAGATGAACGGCCCCACAAACTGC

TCTACCGAGCTGCGGCTGCTGTACCAGCTGGTGTTTCTGCTGAGCGAGGCCCAC

ACCTGTATCCCAGAAAATAATGGCGGGGCCGGGTGTGTGTGCCACCTGCTGATG

GATGACGTGGTGTCTGCCGACAATTACACCCTGGACCTGTGGGCCGGACAGCAG

CTGCTGTGGAAGGGGTCCTTCAAACCCTCTGAGCACGTGAAGCCAAGGGCCCCC

GGCAACCTGACAGTGCACACCAACGTGTCTGATACACTGCTGCTGACATGGAGCA

ATCCATACCCTCCTGACAACTACCTGTACAACCACCTGACCTACGCCGTGAATATC

TGGAGCGAAAATGATCCTGCCGACTTTCGGATTTACAATGTGACCTATCTGGAGC

CCTCCCTGAGAATTGCCGCCTCTACCCTGAAATCTGGAATCTCCTACCGCGCCAG

GGTGCGGGCCTGGGCCCAGTGTTACAACACCACCTGGTCTGAGTGGAGCCCAAG

CACCAAGTGGCACAATTCTTATCGGGAGCCTTTTGAGCAGCACCTGATCCCCTGG

CTGGGACACCTGCTGGTGGGGCTGTCTGGCGCCTTTGGCTTCATCATTCTGGTGT

ACCTGCTGATCAACTGTAGGAATACAGGCCCTTGGCTGAAGAAGGTGCTGAAGTG

TAACACCCCCGACCCCTCTAAGTTCTTCAGCCAGCTGTCCTCTGAACACGGGGGA

GATGTGCAGAAGTGGCTGTCCAGCCCTTTCCCATCCAGCTCCTTTAGCCCCGGG

GGCCTGGCCCCTGAGATCTCTCCACTGGAAGTGCTGGAGCGGGACAAGGTGACC

CAGCTGCTGCTGCAGCAGGACAAGGTGCCAGAACCCGCCTCCCTGAGCTCCAAC

CACAGCCTGACATCTTGCTTTACAAATCAGGGATACTTCTTCTTCCACCTGCCCGA

TGCCCTGGAGATCGAGGCCTGCCAGGTGTACTTCACCTACGATCCCTACTCTGAG

GAAGACCCAGATGAGGGCGTGGCCGGGGCCCCAACCGGGTCCAGCCCACAGCC

ACTGCAGCCACTGTCCGGCGAAGATGACGCCTACTGCACATTCCCTTCCAGGGAT

GACCTGCTGCTGTTCAGCCCATCTCTGCTGGGCGGACCCTCTCCTCCAAGCACA

GCCCCAGGGGGATCCGGCGCCGGGGAAGAGAGGATGCCCCCTAGCCTGCAGGA

GCGCGTGCCCAGAGACTGGGACCCCCAGCCCCTGGGCCCTCCAACCCCTGGGG

TGCCCGACCTGGTGGACTTCCAGCCTCCACCCGAGCTGGTGCTGAGGGAGGCC

GGCGAAGAGGTGCCCGACGCCGGCCCCCGGGAGGGCGTGTCCTTCCCTTGGTC

CAGACCTCCAGGACAGGGCGAGTTCCGCGCCCTGAACGCCAGGCTGCCTCTGAA

CACCGATGCCTACCTGTCTCTGCAGGAACTGCAGGGCCAGGACCCAACCCACCT

GGTGCGGAGAAAGCGCAGCGGCTCCGGCGAGGGCCGGGGCAGCCTGCTGACCT

GCGGCGACGTGGAAGAGAACCCCGGACCCATGGCTCTCCCAGTGACTGCCCTAC

TGCTTCCCCTAGCGCTTCTCCTGCATGCAGAGGAGGTGTCGGAGTACTGTAGCCA

CATGATTGGGAGTGGACACCTGCAGTCTCTGCAGCGGCTGATTGACAGTCAGATG

GAGACCTCGTGCCAAATTACATTTGAGTTTGTAGACCAGGAACAGTTGAAAGATCC

AGTGTGCTACCTTAAGAAGGCATTTCTCCTGGTACAATACATAATGGAGGACACCA

TGCGCTTCAGAGATAACACCCCCAATGCCATCGCCATTGTGCAGCTGCAGGAACT

CTCTTTGAGGCTGAAGAGCTGCTTCACCAAGGATTATGAAGAGCATGACAAGGCC

TGCGTCCGAACTTTCTATGAGACACCTCTCCAGTTGCTGGAGAAGGTCAAGAATG

TCTTTAATGAAACAAAGAATCTCCTTGACAAGGACTGGAATATTTTCAGCAAGAAC

TGCAACAACAGCTTTGCTGAATGCTCCAGCCAAGGCCATGAGAGGCAGTCCGAG

GGAGCGGCCGCAATTGAAGTTATGTATCCTCCTCCTTACCTAGACAATGAGAAGA

GCAATGGAACCATTATCCATGTGAAAGGGAAACACCTTTGTCCAAGTCCCCTATTT

CCCGGACCTTCTAAGCCCTTTTGGGTGCTGGTGGTGGTTGGTGGAGTCCTGGCTT

GCTATAGCTTGCTAGTAACAGTGGCCTTTATTATTTTCTGGGTGAGGAGTAAGAGG

AGCAGGCTCCTGCACAGTGACTACATGAACATGACTCCCCGCCGCCCCGGGCCC

ACCCGCAAGCATTACCAGCCCTATGCCCCACCACGCGACTTCGCAGCCTATCGCT

CCAAGCGGGGCCGGAAGAAGCTGCTGTACATCTTCAAGCAGCCCTTCATGCGGC

CCGTGCAGACCACCCAGGAGGAGGACGGCTGCAGCTGCCGGTTTCCCGAGGAG

GAGGAGGGCGGCTGCGAGCTGAGAGTGAAGTTCAGCAGGAGCGCAGAGCCCCC

CGCGTACCAGCAGGGCCAGAACCAGCTCTATAACGAGCTCAATCTAGGACGAAG

AGAGGAGTACGATGTTTTGGACAAGAGACGTGGCCGGGACCCTGAGATGGGGGG

AAAGCCGAGAAGGAAGAACCCTCAGGAAGGCCTGTACAATGAACTGCAGAAAGAT

AAGATGGCGGAGGCCTACAGTGAGATTGGGATGAAAGGCGAGCGCCGGAGGGG

CAAGGGGCACGATGGCCTTTACCAGGGTCTCAGTACAGCCACCAAGGACACCTA

CGACGCCCTTCACATGCAGGCCCTGCCCCCTCGCTAATAACAGCCACTCGAG

C34B

CCATGGGCTGGCTGTGTTCCGGCCTGCTGTTTCCTGTGTCCTGTCTGGTGCTGCT

GCAGGTGGCCAGCTCCGGGAACATGAAAGTGCTGCAGGAGCCCACATGTGTGTC

CGACTACATGTCCATCTCTACATGTGAGTGGAAGATGAACGGCCCCACAAACTGC

TCTACCGAGCTGCGGCTGCTGTACCAGCTGGTGTTTCTGCTGAGCGAGGCCCAC

ACCTGTATCCCAGAAAATAATGGCGGGGCCGGGTGTGTGTGCCACCTGCTGATG

GATGACGTGGTGTCTGCCGACAATTACACCCTGGACCTGTGGGCCGGACAGCAG

CTGCTGTGGAAGGGGTCCTTCAAACCCTCTGAGCACGTGAAGCCAAGGGCCCCC

GGCAACCTGACAGTGCACACCAACGTGTCTGATACACTGCTGCTGACATGGAGCA

ATCCATACCCTCCTGACAACTACCTGTACAACCACCTGACCTACGCCGTGAATATC

TGGAGCGAAAATGATCCTGCCGACTTTCGGATTTACAATGTGACCTATCTGGAGC

CCTCCCTGAGAATTGCCGCCTCTACCCTGAAATCTGGAATCTCCTACCGCGCCAG

GGTGCGGGCCTGGGCCCAGTGTTACAACACCACCTGGTCTGAGTGGAGCCCAAG

CACCAAGTGGCACAATTCTTATCGGGAGCCTTTTGAGCAGCACCTGATCCCCTGG

CTGGGACACCTGCTGGTGGGGCTGTCTGGCGCCTTTGGCTTCATCATTCTGGTGT

ACCTGCTGATCAACTGTAGGAATACAGGCCCTTGGCTGAAGAAGGTGCTGAAGTG

TAACACCCCCGACCCCTCTAAGTTCTTCAGCCAGCTGTCCTCTGAACACGGGGGA

GATGTGCAGAAGTGGCTGTCCAGCCCTTTCCCATCCAGCTCCTTTAGCCCCGGG

GGCCTGGCCCCTGAGATCTCTCCACTGGAAGTGCTGGAGCGGGACAAGGTGACC

CAGCTGCTGCTGCAGCAGGACAAGGTGCCAGAACCCGCCTCCCTGAGCTCCAAC

CACAGCCTGACATCTTGCTTTACAAATCAGGGATACTTCTTCTTCCACCTGCCCGA

TGCCCTGGAGATCGAGGCCTGCCAGGTGTACTTCACCTACGATCCCTACTCTGAG

GAAGACCCAGATGAGGGCGTGGCCGGGGCCCCAACCGGGTCCAGCCCACAGCC

ACTGCAGCCACTGTCCGGCGAAGATGACGCCTACTGCACATTCCCTTCCAGGGAT

GACCTGCTGCTGTTCAGCCCATCTCTGCTGGGCGGACCCTCTCCTCCAAGCACA

GCCCCAGGGGGATCCGGCGCCGGGGAAGAGAGGATGCCCCCTAGCCTGCAGGA

GCGCGTGCCCAGAGACTGGGACCCCCAGCCCCTGGGCCCTCCAACCCCTGGGG

TGCCCGACCTGGTGGACTTCCAGCCTCCACCCGAGCTGGTGCTGAGGGAGGCC

GGCGAAGAGGTGCCCGACGCCGGCCCCCGGGAGGGCGTGTCCTTCCCTTGGTC

CAGACCTCCAGGACAGGGCGAGTTCCGCGCCCTGAACGCCAGGCTGCCTCTGAA

CACCGATGCCTACCTGTCTCTGCAGGAACTGCAGGGCCAGGACCCAACCCACCT

GGTGCGGAGAAAGCGCAGCGGCTCCGGCGAGGGCCGGGGCAGCCTGCTGACCT

GCGGCGACGTGGAAGAGAACCCCGGACCCATGGCTCTCCCAGTGACTGCCCTAC

TGCTTCCCCTAGCGCTTCTCCTGCATGCAGAGGAGGTGTCGGAGTACTGTAGCCA

CATGATTGGGAGTGGACACCTGCAGTCTCTGCAGCGGCTGATTGACAGTCAGATG

GAGACCTCGTGCCAAATTACATTTGAGTTTGTAGACCAGGAACAGTTGAAAGATCC

AGTGTGCTACCTTAAGAAGGCATTTCTCCTGGTACAATACATAATGGAGGACACCA

TGCGCTTCAGAGATAACACCCCCAATGCCATCGCCATTGTGCAGCTGCAGGAACT

CTCTTTGAGGCTGAAGAGCTGCTTCACCAAGGATTATGAAGAGCATGACAAGGCC

TGCGTCCGAACTTTCTATGAGACACCTCTCCAGTTGCTGGAGAAGGTCAAGAATG

TCTTTAATGAAACAAAGAATCTCCTTGACAAGGACTGGAATATTTTCAGCAAGAAC

TGCAACAACAGCTTTGCTGAATGCTCCAGCCAAGGCCATGAGAGGCAGTCCGAG

GGAGCGGCCGCAATTGAAGTTATGTATCCTCCTCCTTACCTAGACAATGAGAAGA

GCAATGGAACCATTATCCATGTGAAAGGGAAACACCTTTGTCCAAGTCCCCTATTT

CCCGGACCTTCTAAGCCCTTTTGGGTGCTGGTGGTGGTTGGTGGAGTCCTGGCTT

GCTATAGCTTGCTAGTAACAGTGGCCTTTATTATTTTCTGGGTGAGGAGTAAGAGG

AGCAGGCTCCTGCACAGTGACTACATGAACATGACTCCCCGCCGCCCCGGGCCC

ACCCGCAAGCATTACCAGCCCTATGCCCCACCACGCGACTTCGCAGCCTATCGCT

CCAGAGTGAAGTTCAGCAGGAGCGCAGAGCCCCCCGCGTACCAGCAGGGCCAG

AACCAGCTCTATAACGAGCTCAATCTAGGACGAAGAGAGGAGTACGATGTTTTGG

ACAAGAGACGTGGCCGGGACCCTGAGATGGGGGGAAAGCCGAGAAGGAAGAAC

CCTCAGGAAGGCCTGTACAATGAACTGCAGAAAGATAAGATGGCGGAGGCCTAC

AGTGAGATTGGGATGAAAGGCGAGCGCCGGAGGGGCAAGGGGCACGATGGCCT

TTACCAGGGTCTCAGTACAGCCACCAAGGACACCTACGACGCCCTTCACATGCAG

GCCCTGCCCCCTCGCAGGAGGAAGAGAAGTGGATCCGGGGAGGGCAGGGGCTC

TCTCCTGACATGTGGAGATGTGGAAGAGAACCCCGGGCCCATGCCTAGAGGCTT

CACATGGCTGAGGTATCTGGGCATCTTCCTGGGCGTGGCTCTGGGAAACGAACC

TCTGGAAATGTGGCCACTGACACAGAATGAAGAGTGCACCGTTACAGGCTTCCTG

CGGGACAAGCTGCAGTACAGGTCTAGGTTGCAGTACATGAAACACTATTTCCCTA

TTAACTACAAGATCTCCGTGCCTTACGAGGGAGTGTTCAGGATCGCCAACGTGAC

ACGGCTGCAGAGGGCTCAGGTCAGCGAGCGGGAGCTGCGGTATCTGTGGGTGC

TGGTGAGCCTGAGCGCCACCGAGAGCGTGCAAGACGTCCTGCTGGAAGGCCATC

CTAGCTGGAAGTACCTGCAGGAGGTGGAGACCCTGCTGCTGAACGTGCAGCAAG

GCTTGACCGACGTCGAGGTGAGCCCAAAGGTGGAGAGCGTGCTCAGCCTGCTGA

ACGCTCCTGGACCAAACCTGAAGCTGGTGAGGCCTAAGGCCCTGCTGGACAACT

GCTTCAGAGTGATGGAGCTGCTGTACTGCAGCTGCTGTAAGCAGAGCAGCGTGC

TGAACTGGCAAGACTGCGAAGTGCCTAGTCCTCAGAGCTGCAGCCCTGAGCCCA

GCCTGCAGTACGCTGCAACCCAGCTGTACCCTCCTCCACCTTGGAGCCCTAGCA

GCCCTCCTCACAGCACCGGAAGCGTGAGGCCTGTGAGAGCCCAAGGCGAGGGA

CTGCTGCCTGCGGCCGCACCCACCACGACGCCAGCGCCGCGACCACCAACCCC

GGCGCCCACGATCGCGTCGCAGCCCCTGTCCCTGCGCCCAGAGGCGTGCCGGC

CAGCGGCGGGGGGCGCAGTGCACACGAGGGGGCTGGACTTCGCCTGTGATATC

TACATCTGGGCGCCCTTGGCCGGGACTTGTGGGGTCCTTCTCCTGTCACTGGTTA

TCACCAAGCGGGGCCGGAAGAAGCTGCTGTACATCTTCAAGCAGCCCTTCATGC

GGCCCGTGCAGACCACCCAGGAGGAGGACGGCTGCAGCTGCCGGTTTCCCGAG

GAGGAGGAGGGCGGCTGCGAGCTGTAATAACAGCCACTCGAG

CT4

CCATGGGCTGGCTGTGTTCCGGCCTGCTGTTTCCTGTGTCCTGTCTGGTGCTGCT

GCAGGTGGCCAGCTCCGGGAACATGAAAGTGCTGCAGGAGCCCACATGTGTGTC

CGACTACATGTCCATCTCTACATGTGAGTGGAAGATGAACGGCCCCACAAACTGC

TCTACCGAGCTGCGGCTGCTGTACCAGCTGGTGTTTCTGCTGAGCGAGGCCCAC

ACCTGTATCCCAGAAAATAATGGCGGGGCCGGGTGTGTGTGCCACCTGCTGATG

GATGACGTGGTGTCTGCCGACAATTACACCCTGGACCTGTGGGCCGGACAGCAG

CTGCTGTGGAAGGGGTCCTTCAAACCCTCTGAGCACGTGAAGCCAAGGGCCCCC

GGCAACCTGACAGTGCACACCAACGTGTCTGATACACTGCTGCTGACATGGAGCA

ATCCATACCCTCCTGACAACTACCTGTACAACCACCTGACCTACGCCGTGAATATC

TGGAGCGAAAATGATCCTGCCGACTTTCGGATTTACAATGTGACCTATCTGGAGC

CCTCCCTGAGAATTGCCGCCTCTACCCTGAAATCTGGAATCTCCTACCGCGCCAG

GGTGCGGGCCTGGGCCCAGTGTTACAACACCACCTGGTCTGAGTGGAGCCCAAG

CACCAAGTGGCACAATTCTTATCGGGAGCCTTTTGAGCAGCACCTGATCCCCTGG

CTGGGACACCTGCTGGTGGGGCTGTCTGGCGCCTTTGGCTTCATCATTCTGGTGT

ACCTGCTGATCAACTGTAGGAATACAGGCCCTTGGCTGAAGAAGGTGCTGAAGTG

TAACACCCCCGACCCCTCTAAGTTCTTCAGCCAGCTGTCCTCTGAACACGGGGGA

GATGTGCAGAAGTGGCTGTCCAGCCCTTTCCCATCCAGCTCCTTTAGCCCCGGG

GGCCTGGCCCCTGAGATCTCTCCACTGGAAGTGCTGGAGCGGGACAAGGTGACC

CAGCTGCTGCTGCAGCAGGACAAGGTGCCAGAACCCGCCTCCCTGAGCTCCAAC

CACAGCCTGACATCTTGCTTTACAAATCAGGGATACTTCTTCTTCCACCTGCCCGA

TGCCCTGGAGATCGAGGCCTGCCAGGTGTACTTCACCTACGATCCCTACTCTGAG

GAAGACCCAGATGAGGGCGTGGCCGGGGCCCCAACCGGGTCCAGCCCACAGCC

ACTGCAGCCACTGTCCGGCGAAGATGACGCCTACTGCACATTCCCTTCCAGGGAT

GACCTGCTGCTGTTCAGCCCATCTCTGCTGGGCGGACCCTCTCCTCCAAGCACA

GCCCCAGGGGGATCCGGCGCCGGGGAAGAGAGGATGCCCCCTAGCCTGCAGGA

GCGCGTGCCCAGAGACTGGGACCCCCAGCCCCTGGGCCCTCCAACCCCTGGGG

TGCCCGACCTGGTGGACTTCCAGCCTCCACCCGAGCTGGTGCTGAGGGAGGCC

GGCGAAGAGGTGCCCGACGCCGGCCCCCGGGAGGGCGTGTCCTTCCCTTGGTC

CAGACCTCCAGGACAGGGCGAGTTCCGCGCCCTGAACGCCAGGCTGCCTCTGAA

CACCGATGCCTACCTGTCTCTGCAGGAACTGCAGGGCCAGGACCCAACCCACCT

GGTGCGGAGAAAGCGCAGCGGCTCCGGCGAGGGCCGGGGCAGCCTGCTGACCT

GCGGCGACGTGGAAGAGAACCCCGGACCCATGGCTCTCCCAGTGACTGCCCTAC

TGCTTCCCCTAGCGCTTCTCCTGCATGCAGAGGAGGTGTCGGAGTACTGTAGCCA

CATGATTGGGAGTGGACACCTGCAGTCTCTGCAGCGGCTGATTGACAGTCAGATG

GAGACCTCGTGCCAAATTACATTTGAGTTTGTAGACCAGGAACAGTTGAAAGATCC

AGTGTGCTACCTTAAGAAGGCATTTCTCCTGGTACAATACATAATGGAGGACACCA

TGCGCTTCAGAGATAACACCCCCAATGCCATCGCCATTGTGCAGCTGCAGGAACT

CTCTTTGAGGCTGAAGAGCTGCTTCACCAAGGATTATGAAGAGCATGACAAGGCC

TGCGTCCGAACTTTCTATGAGACACCTCTCCAGTTGCTGGAGAAGGTCAAGAATG

TCTTTAATGAAACAAAGAATCTCCTTGACAAGGACTGGAATATTTTCAGCAAGAAC

TGCAACAACAGCTTTGCTGAATGCTCCAGCCAAGGCCATGAGAGGCAGTCCGAG

GGAGCGGCCGCAATTGAAGTTATGTATCCTCCTCCTTACCTAGACAATGAGAAGA

GCAATGGAACCATTATCCATGTGAAAGGGAAACACCTTTGTCCAAGTCCCCTATTT

CCCGGACCTTCTAAGCCCTTTTGGGTGCTGGTGGTGGTTGGTGGAGTCCTGGCTT

GCTATAGCTTGCTAGTAACAGTGGCCTTTATTATTTTCTGGGTGAGGAGTAA

43428ζ

CCATGGGCTGGCTGTGTTCCGGCCTGCTGTTTCCTGTGTCCTGTCTGGTGCTGCT

GCAGGTGGCCAGCTCCGGGAACATGAAAGTGCTGCAGGAGCCCACATGTGTGTC

CGACTACATGTCCATCTCTACATGTGAGTGGAAGATGAACGGCCCCACAAACTGC

TCTACCGAGCTGCGGCTGCTGTACCAGCTGGTGTTTCTGCTGAGCGAGGCCCAC

ACCTGTATCCCAGAAAATAATGGCGGGGCCGGGTGTGTGTGCCACCTGCTGATG

GATGACGTGGTGTCTGCCGACAATTACACCCTGGACCTGTGGGCCGGACAGCAG

CTGCTGTGGAAGGGGTCCTTCAAACCCTCTGAGCACGTGAAGCCAAGGGCCCCC

GGCAACCTGACAGTGCACACCAACGTGTCTGATACACTGCTGCTGACATGGAGCA

ATCCATACCCTCCTGACAACTACCTGTACAACCACCTGACCTACGCCGTGAATATC

TGGAGCGAAAATGATCCTGCCGACTTTCGGATTTACAATGTGACCTATCTGGAGC

CCTCCCTGAGAATTGCCGCCTCTACCCTGAAATCTGGAATCTCCTACCGCGCCAG

GGTGCGGGCCTGGGCCCAGTGTTACAACACCACCTGGTCTGAGTGGAGCCCAAG

CACCAAGTGGCACAATTCTTATCGGGAGCCTTTTGAGCAGCACCTGATCCCCTGG

CTGGGACACCTGCTGGTGGGGCTGTCTGGCGCCTTTGGCTTCATCATTCTGGTGT

ACCTGCTGATCAACTGTAGGAATACAGGCCCTTGGCTGAAGAAGGTGCTGAAGTG

TAACACCCCCGACCCCTCTAAGTTCTTCAGCCAGCTGTCCTCTGAACACGGGGGA

GATGTGCAGAAGTGGCTGTCCAGCCCTTTCCCATCCAGCTCCTTTAGCCCCGGG

GGCCTGGCCCCTGAGATCTCTCCACTGGAAGTGCTGGAGCGGGACAAGGTGACC

CAGCTGCTGCTGCAGCAGGACAAGGTGCCAGAACCCGCCTCCCTGAGCTCCAAC

CACAGCCTGACATCTTGCTTTACAAATCAGGGATACTTCTTCTTCCACCTGCCCGA

TGCCCTGGAGATCGAGGCCTGCCAGGTGTACTTCACCTACGATCCCTACTCTGAG

GAAGACCCAGATGAGGGCGTGGCCGGGGCCCCAACCGGGTCCAGCCCACAGCC

ACTGCAGCCACTGTCCGGCGAAGATGACGCCTACTGCACATTCCCTTCCAGGGAT

GACCTGCTGCTGTTCAGCCCATCTCTGCTGGGCGGACCCTCTCCTCCAAGCACA

GCCCCAGGGGGATCCGGCGCCGGGGAAGAGAGGATGCCCCCTAGCCTGCAGGA

GCGCGTGCCCAGAGACTGGGACCCCCAGCCCCTGGGCCCTCCAACCCCTGGGG

TGCCCGACCTGGTGGACTTCCAGCCTCCACCCGAGCTGGTGCTGAGGGAGGCC

GGCGAAGAGGTGCCCGACGCCGGCCCCCGGGAGGGCGTGTCCTTCCCTTGGTC

CAGACCTCCAGGACAGGGCGAGTTCCGCGCCCTGAACGCCAGGCTGCCTCTGAA

CACCGATGCCTACCTGTCTCTGCAGGAACTGCAGGGCCAGGACCCAACCCACCT

GGTGCGGAGAAAGCGCAGCGGCTCCGGCGAGGGCCGGGGCAGCCTGCTGACCT

GCGGCGACGTGGAAGAGAACCCCGGACCCATGCCTAGAGGCTTCACATGGCTGA

GGTATCTGGGCATCTTCCTGGGCGTGGCTCTGGGAAACGAACCTCTGGAAATGT

GGCCACTGACACAGAATGAAGAGTGCACCGTTACAGGCTTCCTGCGGGACAAGC

TGCAGTACAGGTCTAGGTTGCAGTACATGAAACACTATTTCCCTATTAACTACAAG

ATCTCCGTGCCTTACGAGGGAGTGTTCAGGATCGCCAACGTGACACGGCTGCAG

AGGGCTCAGGTCAGCGAGCGGGAGCTGCGGTATCTGTGGGTGCTGGTGAGCCT

GAGCGCCACCGAGAGCGTGCAAGACGTCCTGCTGGAAGGCCATCCTAGCTGGAA

GTACCTGCAGGAGGTGGAGACCCTGCTGCTGAACGTGCAGCAAGGCTTGACCGA

CGTCGAGGTGAGCCCAAAGGTGGAGAGCGTGCTCAGCCTGCTGAACGCTCCTGG

ACCAAACCTGAAGCTGGTGAGGCCTAAGGCCCTGCTGGACAACTGCTTCAGAGT

GATGGAGCTGCTGTACTGCAGCTGCTGTAAGCAGAGCAGCGTGCTGAACTGGCA

AGACTGCGAAGTGCCTAGTCCTCAGAGCTGCAGCCCTGAGCCCAGCCTGCAGTA

CGCTGCAACCCAGCTGTACCCTCCTCCACCTTGGAGCCCTAGCAGCCCTCCTCAC

AGCACCGGAAGCGTGAGGCCTGTGAGAGCCCAAGGCGAGGGACTGCTGCCTGC

GGCCGCAATTGAAGTTATGTATCCTCCTCCTTACCTAGACAATGAGAAGAGCAATG

GAACCATTATCCATGTGAAAGGGAAACACCTTTGTCCAAGTCCCCTATTTCCCGGA

CCTTCTAAGCCCTTTTGGGTGCTGGTGGTGGTTGGTGGAGTCCTGGCTTGCTATA

GCTTGCTAGTAACAGTGGCCTTTATTATTTTCTGGGTGAGGAGTAAGAGGAGCAG

GCTCCTGCACAGTGACTACATGAACATGACTCCCCGCCGCCCCGGGCCCACCCG

CAAGCATTACCAGCCCTATGCCCCACCACGCGACTTCGCAGCCTATCGCTCCAGA

GTGAAGTTCAGCAGGAGCGCAGAGCCCCCCGCGTACCAGCAGGGCCAGAACCA

GCTCTATAACGAGCTCAATCTAGGACGAAGAGAGGAGTACGATGTTTTGGACAAG

AGACGTGGCCGGGACCCTGAGATGGGGGGAAAGCCGAGAAGGAAGAACCCTCA

GGAAGGCCTGTACAATGAACTGCAGAAAGATAAGATGGCGGAGGCCTACAGTGA

GATTGGGATGAAAGGCGAGCGCCGGAGGGGCAAGGGGCACGATGGCCTTTACC

AGGGTCTCAGTACAGCCACCAAGGACACCTACGACGCCCTTCACATGCAGGCCC

TGCCCCCTCGCTAACAGCCACTCGAG

43428Bζ

CCATGGGCTGGCTGTGTTCCGGCCTGCTGTTTCCTGTGTCCTGTCTGGTGCTGCT

GCAGGTGGCCAGCTCCGGGAACATGAAAGTGCTGCAGGAGCCCACATGTGTGTC

CGACTACATGTCCATCTCTACATGTGAGTGGAAGATGAACGGCCCCACAAACTGC

TCTACCGAGCTGCGGCTGCTGTACCAGCTGGTGTTTCTGCTGAGCGAGGCCCAC

ACCTGTATCCCAGAAAATAATGGCGGGGCCGGGTGTGTGTGCCACCTGCTGATG

GATGACGTGGTGTCTGCCGACAATTACACCCTGGACCTGTGGGCCGGACAGCAG

CTGCTGTGGAAGGGGTCCTTCAAACCCTCTGAGCACGTGAAGCCAAGGGCCCCC

GGCAACCTGACAGTGCACACCAACGTGTCTGATACACTGCTGCTGACATGGAGCA

ATCCATACCCTCCTGACAACTACCTGTACAACCACCTGACCTACGCCGTGAATATC

TGGAGCGAAAATGATCCTGCCGACTTTCGGATTTACAATGTGACCTATCTGGAGC

CCTCCCTGAGAATTGCCGCCTCTACCCTGAAATCTGGAATCTCCTACCGCGCCAG

GGTGCGGGCCTGGGCCCAGTGTTACAACACCACCTGGTCTGAGTGGAGCCCAAG

CACCAAGTGGCACAATTCTTATCGGGAGCCTTTTGAGCAGCACCTGATCCCCTGG

CTGGGACACCTGCTGGTGGGGCTGTCTGGCGCCTTTGGCTTCATCATTCTGGTGT

ACCTGCTGATCAACTGTAGGAATACAGGCCCTTGGCTGAAGAAGGTGCTGAAGTG

TAACACCCCCGACCCCTCTAAGTTCTTCAGCCAGCTGTCCTCTGAACACGGGGGA

GATGTGCAGAAGTGGCTGTCCAGCCCTTTCCCATCCAGCTCCTTTAGCCCCGGG

GGCCTGGCCCCTGAGATCTCTCCACTGGAAGTGCTGGAGCGGGACAAGGTGACC

CAGCTGCTGCTGCAGCAGGACAAGGTGCCAGAACCCGCCTCCCTGAGCTCCAAC

CACAGCCTGACATCTTGCTTTACAAATCAGGGATACTTCTTCTTCCACCTGCCCGA

TGCCCTGGAGATCGAGGCCTGCCAGGTGTACTTCACCTACGATCCCTACTCTGAG

GAAGACCCAGATGAGGGCGTGGCCGGGGCCCCAACCGGGTCCAGCCCACAGCC

ACTGCAGCCACTGTCCGGCGAAGATGACGCCTACTGCACATTCCCTTCCAGGGAT

GACCTGCTGCTGTTCAGCCCATCTCTGCTGGGCGGACCCTCTCCTCCAAGCACA

GCCCCAGGGGGATCCGGCGCCGGGGAAGAGAGGATGCCCCCTAGCCTGCAGGA

GCGCGTGCCCAGAGACTGGGACCCCCAGCCCCTGGGCCCTCCAACCCCTGGGG

TGCCCGACCTGGTGGACTTCCAGCCTCCACCCGAGCTGGTGCTGAGGGAGGCC

GGCGAAGAGGTGCCCGACGCCGGCCCCCGGGAGGGCGTGTCCTTCCCTTGGTC

CAGACCTCCAGGACAGGGCGAGTTCCGCGCCCTGAACGCCAGGCTGCCTCTGAA

CACCGATGCCTACCTGTCTCTGCAGGAACTGCAGGGCCAGGACCCAACCCACCT

GGTGCGGAGAAAGCGCAGCGGCTCCGGCGAGGGCCGGGGCAGCCTGCTGACCT

GCGGCGACGTGGAAGAGAACCCCGGACCCATGCCTAGAGGCTTCACATGGCTGA

GGTATCTGGGCATCTTCCTGGGCGTGGCTCTGGGAAACGAACCTCTGGAAATGT

GGCCACTGACACAGAATGAAGAGTGCACCGTTACAGGCTTCCTGCGGGACAAGC

TGCAGTACAGGTCTAGGTTGCAGTACATGAAACACTATTTCCCTATTAACTACAAG

ATCTCCGTGCCTTACGAGGGAGTGTTCAGGATCGCCAACGTGACACGGCTGCAG

AGGGCTCAGGTCAGCGAGCGGGAGCTGCGGTATCTGTGGGTGCTGGTGAGCCT

GAGCGCCACCGAGAGCGTGCAAGACGTCCTGCTGGAAGGCCATCCTAGCTGGAA

GTACCTGCAGGAGGTGGAGACCCTGCTGCTGAACGTGCAGCAAGGCTTGACCGA

CGTCGAGGTGAGCCCAAAGGTGGAGAGCGTGCTCAGCCTGCTGAACGCTCCTGG

ACCAAACCTGAAGCTGGTGAGGCCTAAGGCCCTGCTGGACAACTGCTTCAGAGT

GATGGAGCTGCTGTACTGCAGCTGCTGTAAGCAGAGCAGCGTGCTGAACTGGCA

AGACTGCGAAGTGCCTAGTCCTCAGAGCTGCAGCCCTGAGCCCAGCCTGCAGTA

CGCTGCAACCCAGCTGTACCCTCCTCCACCTTGGAGCCCTAGCAGCCCTCCTCAC

AGCACCGGAAGCGTGAGGCCTGTGAGAGCCCAAGGCGAGGGACTGCTGCCTGC

GGCCGCAATCGAGGTGGAGCAGAAGCTGATCAGCGAGGAGGACCTGCTGGACA

ACGAGAAGAGCAACGGCACCATCATCCACGTGAAGGGCAAGCACCTGTGCCCTT

CTCCCCTGTTCCCCGGCCCTAGCAAGCCCTTCTGGGTGCTGGTTGTGGTGGGCG

GAGTGCTGGCTTGCTACAGCCTGCTGGTGACCGTGGCCTTCATCATCTTCTGGGT

GCGGAGCAAGCGGAGCCGGCTGCTGCACAGCGACTACATGAACATGACCCCTCG

GAGGCCCGGCCCCACCCGGAAGCACTACCAGCCCTACGCCCCTCCCCGGGACT

TCGCCGCTTACCGGAGCAAGCGGGGCAGGAAGAAGCTGCTGTACATCTTCAAGC

AGCCTTTCATGCGGCCTGTGCAGACCACCCAGGAGGAGGACGGCTGCAGCTGCC

GGTTCCCTGAGGAGGAAGAGGGCGGGTGCGAGCTGAGAGTGAAGTTCAGCAGG

AGCGCAGAGCCCCCCGCGTACCAGCAGGGCCAGAACCAGCTCTATAACGAGCTC

AATCTAGGACGAAGAGAGGAGTACGATGTTTTGGACAAGAGACGTGGCCGGGAC

CCTGAGATGGGGGGAAAGCCGAGAAGGAAGAACCCTCAGGAAGGCCTGTACAAT

GAACTGCAGAAAGATAAGATGGCGGAGGCCTACAGTGAGATTGGGATGAAAGGC

GAGCGCCGGAGGGGCAAGGGGCACGATGGCCTTTACCAGGGTCTCAGTACAGC

CACCAAGGACACCTACGACGCCCTTCACATGCAGGCCCTGCCCCCTCGCTAATAA

34CB

CCATGGGCTGGCTGTGTTCCGGCCTGCTGTTTCCTGTGTCCTGTCTGGTGCTGCT

GCAGGTGGCCAGCTCCGGGAACATGAAAGTGCTGCAGGAGCCCACATGTGTGTC

CGACTACATGTCCATCTCTACATGTGAGTGGAAGATGAACGGCCCCACAAACTGC

TCTACCGAGCTGCGGCTGCTGTACCAGCTGGTGTTTCTGCTGAGCGAGGCCCAC

ACCTGTATCCCAGAAAATAATGGCGGGGCCGGGTGTGTGTGCCACCTGCTGATG

GATGACGTGGTGTCTGCCGACAATTACACCCTGGACCTGTGGGCCGGACAGCAG

CTGCTGTGGAAGGGGTCCTTCAAACCCTCTGAGCACGTGAAGCCAAGGGCCCCC

GGCAACCTGACAGTGCACACCAACGTGTCTGATACACTGCTGCTGACATGGAGCA

ATCCATACCCTCCTGACAACTACCTGTACAACCACCTGACCTACGCCGTGAATATC

TGGAGCGAAAATGATCCTGCCGACTTTCGGATTTACAATGTGACCTATCTGGAGC

CCTCCCTGAGAATTGCCGCCTCTACCCTGAAATCTGGAATCTCCTACCGCGCCAG

GGTGCGGGCCTGGGCCCAGTGTTACAACACCACCTGGTCTGAGTGGAGCCCAAG

CACCAAGTGGCACAATTCTTATCGGGAGCCTTTTGAGCAGCACCTGATCCCCTGG

CTGGGACACCTGCTGGTGGGGCTGTCTGGCGCCTTTGGCTTCATCATTCTGGTGT

ACCTGCTGATCAACTGTAGGAATACAGGCCCTTGGCTGAAGAAGGTGCTGAAGTG

TAACACCCCCGACCCCTCTAAGTTCTTCAGCCAGCTGTCCTCTGAACACGGGGGA

GATGTGCAGAAGTGGCTGTCCAGCCCTTTCCCATCCAGCTCCTTTAGCCCCGGG

GGCCTGGCCCCTGAGATCTCTCCACTGGAAGTGCTGGAGCGGGACAAGGTGACC

CAGCTGCTGCTGCAGCAGGACAAGGTGCCAGAACCCGCCTCCCTGAGCTCCAAC

CACAGCCTGACATCTTGCTTTACAAATCAGGGATACTTCTTCTTCCACCTGCCCGA

TGCCCTGGAGATCGAGGCCTGCCAGGTGTACTTCACCTACGATCCCTACTCTGAG

GAAGACCCAGATGAGGGCGTGGCCGGGGCCCCAACCGGGTCCAGCCCACAGCC

ACTGCAGCCACTGTCCGGCGAAGATGACGCCTACTGCACATTCCCTTCCAGGGAT

GACCTGCTGCTGTTCAGCCCATCTCTGCTGGGCGGACCCTCTCCTCCAAGCACA

GCCCCAGGGGGATCCGGCGCCGGGGAAGAGAGGATGCCCCCTAGCCTGCAGGA

GCGCGTGCCCAGAGACTGGGACCCCCAGCCCCTGGGCCCTCCAACCCCTGGGG

TGCCCGACCTGGTGGACTTCCAGCCTCCACCCGAGCTGGTGCTGAGGGAGGCC

GGCGAAGAGGTGCCCGACGCCGGCCCCCGGGAGGGCGTGTCCTTCCCTTGGTC

CAGACCTCCAGGACAGGGCGAGTTCCGCGCCCTGAACGCCAGGCTGCCTCTGAA

CACCGATGCCTACCTGTCTCTGCAGGAACTGCAGGGCCAGGACCCAACCCACCT

GGTGCGGAGAAAGCGCAGCGGCTCCGGCGAGGGCCGGGGCAGCCTGCTGACCT

GCGGCGACGTGGAAGAGAACCCCGGACCCATGCCTAGAGGCTTCACATGGCTGA

GGTATCTGGGCATCTTCCTGGGCGTGGCTCTGGGAAACGAACCTCTGGAAATGT

GGCCACTGACACAGAATGAAGAGTGCACCGTTACAGGCTTCCTGCGGGACAAGC

TGCAGTACAGGTCTAGGTTGCAGTACATGAAACACTATTTCCCTATTAACTACAAG

ATCTCCGTGCCTTACGAGGGAGTGTTCAGGATCGCCAACGTGACACGGCTGCAG

AGGGCTCAGGTCAGCGAGCGGGAGCTGCGGTATCTGTGGGTGCTGGTGAGCCT

GAGCGCCACCGAGAGCGTGCAAGACGTCCTGCTGGAAGGCCATCCTAGCTGGAA

GTACCTGCAGGAGGTGGAGACCCTGCTGCTGAACGTGCAGCAAGGCTTGACCGA

CGTCGAGGTGAGCCCAAAGGTGGAGAGCGTGCTCAGCCTGCTGAACGCTCCTGG

ACCAAACCTGAAGCTGGTGAGGCCTAAGGCCCTGCTGGACAACTGCTTCAGAGT

GATGGAGCTGCTGTACTGCAGCTGCTGTAAGCAGAGCAGCGTGCTGAACTGGCA

AGACTGCGAAGTGCCTAGTCCTCAGAGCTGCAGCCCTGAGCCCAGCCTGCAGTA

CGCTGCAACCCAGCTGTACCCTCCTCCACCTTGGAGCCCTAGCAGCCCTCCTCAC

AGCACCGGAAGCGTGAGGCCTGTGAGAGCCCAAGGCGAGGGACTGCTGCCTGC

GGCCGCAATTGAAGTTATGTATCCTCCTCCTTACCTAGACAATGAGAAGAGCAATG

GAACCATTATCCATGTGAAAGGGAAACACCTTTGTCCAAGTCCCCTATTTCCCGGA

CCTTCTAAGCCCTTTTGGGTGCTGGTGGTGGTTGGTGGAGTCCTGGCTTGCTATA

GCTTGCTAGTAACAGTGGCCTTTATTATTTTCTGGGTGAGGAGTAAGAGGAGCAG

GCTCCTGCACAGTGACTACATGAACATGACTCCCCGCCGCCCCGGGCCCACCCG

CAAGCATTACCAGCCCTATGCCCCACCACGCGACTTCGCAGCCTATCGCTCCAGA

GTGAAGTTCAGCAGGAGCGCAGAGCCCCCCGCGTACCAGCAGGGCCAGAACCA

GCTCTATAACGAGCTCAATCTAGGACGAAGAGAGGAGTACGATGTTTTGGACAAG

AGACGTGGCCGGGACCCTGAGATGGGGGGAAAGCCGAGAAGGAAGAACCCTCA

GGAAGGCCTGTACAATGAACTGCAGAAAGATAAGATGGCGGAGGCCTACAGTGA

GATTGGGATGAAAGGCGAGCGCCGGAGGGGCAAGGGGCACGATGGCCTTTACC

AGGGTCTCAGTACAGCCACCAAGGACACCTACGACGCCCTTCACATGCAGGCCC

TGCCCCCTCGCAGGAGGAAGAGAAGTGGATCCGGGGAGGGCAGGGGCTCTCTC

CTGACATGTGGAGATGTGGAAGAGAACCCCGGGCCCATGGCTCTCCCAGTGACT

GCCCTACTGCTTCCCCTAGCGCTTCTCCTGCATGCAGAGGAGGTGTCGGAGTACT

GTAGCCACATGATTGGGAGTGGACACCTGCAGTCTCTGCAGCGGCTGATTGACA

GTCAGATGGAGACCTCGTGCCAAATTACATTTGAGTTTGTAGACCAGGAACAGTT

GAAAGATCCAGTGTGCTACCTTAAGAAGGCATTTCTCCTGGTACAATACATAATGG

AGGACACCATGCGCTTCAGAGATAACACCCCCAATGCCATCGCCATTGTGCAGCT

GCAGGAACTCTCTTTGAGGCTGAAGAGCTGCTTCACCAAGGATTATGAAGAGCAT

GACAAGGCCTGCGTCCGAACTTTCTATGAGACACCTCTCCAGTTGCTGGAGAAGG

TCAAGAATGTCTTTAATGAAACAAAGAATCTCCTTGACAAGGACTGGAATATTTTCA

GCAAGAACTGCAACAACAGCTTTGCTGAATGCTCCAGCCAAGGCCATGAGAGGCA

GTCCGAGGGAGCGGCCGCACCCACCACGACGCCAGCGCCGCGACCACCAACCC

CGGCGCCCACGATCGCGTCGCAGCCCCTGTCCCTGCGCCCAGAGGCGTGCCGG

CCAGCGGCGGGGGGCGCAGTGCACACGAGGGGGCTGGACTTCGCCTGTGATAT

CTACATCTGGGCGCCCTTGGCCGGGACTTGTGGGGTCCTTCTCCTGTCACTGGTT

ATCACCAAGCGGGGCCGGAAGAAGCTGCTGTACATCTTCAAGCAGCCCTTCATGC

GGCCCGTGCAGACCACCCAGGAGGAGGACGGCTGCAGCTGCCGGTTTCCCGAG

GAGGAGGAGGGCGGCTGCGAGCTGTAATAACAGCCACTCGAG

434Tr

CCATGGGCTGGCTGTGTTCCGGCCTGCTGTTTCCTGTGTCCTGTCTGGTGCTGCT

GCAGGTGGCCAGCTCCGGGAACATGAAAGTGCTGCAGGAGCCCACATGTGTGTC

CGACTACATGTCCATCTCTACATGTGAGTGGAAGATGAACGGCCCCACAAACTGC

TCTACCGAGCTGCGGCTGCTGTACCAGCTGGTGTTTCTGCTGAGCGAGGCCCAC

ACCTGTATCCCAGAAAATAATGGCGGGGCCGGGTGTGTGTGCCACCTGCTGATG

GATGACGTGGTGTCTGCCGACAATTACACCCTGGACCTGTGGGCCGGACAGCAG

CTGCTGTGGAAGGGGTCCTTCAAACCCTCTGAGCACGTGAAGCCAAGGGCCCCC

GGCAACCTGACAGTGCACACCAACGTGTCTGATACACTGCTGCTGACATGGAGCA

ATCCATACCCTCCTGACAACTACCTGTACAACCACCTGACCTACGCCGTGAATATC

TGGAGCGAAAATGATCCTGCCGACTTTCGGATTTACAATGTGACCTATCTGGAGC

CCTCCCTGAGAATTGCCGCCTCTACCCTGAAATCTGGAATCTCCTACCGCGCCAG

GGTGCGGGCCTGGGCCCAGTGTTACAACACCACCTGGTCTGAGTGGAGCCCAAG

CACCAAGTGGCACAATTCTTATCGGGAGCCTTTTGAGCAGCACCTGATCCCCTGG

CTGGGACACCTGCTGGTGGGGCTGTCTGGCGCCTTTGGCTTCATCATTCTGGTGT

ACCTGCTGATCAACTGTAGGAATACAGGCCCTTGGCTGAAGAAGGTGCTGAAGTG

TAACACCCCCGACCCCTCTAAGTTCTTCAGCCAGCTGTCCTCTGAACACGGGGGA

GATGTGCAGAAGTGGCTGTCCAGCCCTTTCCCATCCAGCTCCTTTAGCCCCGGG

GGCCTGGCCCCTGAGATCTCTCCACTGGAAGTGCTGGAGCGGGACAAGGTGACC

CAGCTGCTGCTGCAGCAGGACAAGGTGCCAGAACCCGCCTCCCTGAGCTCCAAC

CACAGCCTGACATCTTGCTTTACAAATCAGGGATACTTCTTCTTCCACCTGCCCGA

TGCCCTGGAGATCGAGGCCTGCCAGGTGTACTTCACCTACGATCCCTACTCTGAG

GAAGACCCAGATGAGGGCGTGGCCGGGGCCCCAACCGGGTCCAGCCCACAGCC

ACTGCAGCCACTGTCCGGCGAAGATGACGCCTACTGCACATTCCCTTCCAGGGAT

GACCTGCTGCTGTTCAGCCCATCTCTGCTGGGCGGACCCTCTCCTCCAAGCACA

GCCCCAGGGGGATCCGGCGCCGGGGAAGAGAGGATGCCCCCTAGCCTGCAGGA

GCGCGTGCCCAGAGACTGGGACCCCCAGCCCCTGGGCCCTCCAACCCCTGGGG

TGCCCGACCTGGTGGACTTCCAGCCTCCACCCGAGCTGGTGCTGAGGGAGGCC

GGCGAAGAGGTGCCCGACGCCGGCCCCCGGGAGGGCGTGTCCTTCCCTTGGTC

CAGACCTCCAGGACAGGGCGAGTTCCGCGCCCTGAACGCCAGGCTGCCTCTGAA

CACCGATGCCTACCTGTCTCTGCAGGAACTGCAGGGCCAGGACCCAACCCACCT

GGTGCGGAGAAAGCGCAGCGGCTCCGGCGAGGGCCGGGGCAGCCTGCTGACCT

GCGGCGACGTGGAAGAGAACCCCGGACCCATGCCTAGAGGCTTCACATGGCTGA

GGTATCTGGGCATCTTCCTGGGCGTGGCTCTGGGAAACGAACCTCTGGAAATGT

GGCCACTGACACAGAATGAAGAGTGCACCGTTACAGGCTTCCTGCGGGACAAGC

TGCAGTACAGGTCTAGGTTGCAGTACATGAAACACTATTTCCCTATTAACTACAAG

ATCTCCGTGCCTTACGAGGGAGTGTTCAGGATCGCCAACGTGACACGGCTGCAG

AGGGCTCAGGTCAGCGAGCGGGAGCTGCGGTATCTGTGGGTGCTGGTGAGCCT

GAGCGCCACCGAGAGCGTGCAAGACGTCCTGCTGGAAGGCCATCCTAGCTGGAA

GTACCTGCAGGAGGTGGAGACCCTGCTGCTGAACGTGCAGCAAGGCTTGACCGA

CGTCGAGGTGAGCCCAAAGGTGGAGAGCGTGCTCAGCCTGCTGAACGCTCCTGG

ACCAAACCTGAAGCTGGTGAGGCCTAAGGCCCTGCTGGACAACTGCTTCAGAGT

GATGGAGCTGCTGTACTGCAGCTGCTGTAAGCAGAGCAGCGTGCTGAACTGGCA

AGACTGCGAAGTGCCTAGTCCTCAGAGCTGCAGCCCTGAGCCCAGCCTGCAGTA

CGCTGCAACCCAGCTGTACCCTCCTCCACCTTGGAGCCCTAGCAGCCCTCCTCAC

AGCACCGGAAGCGTGAGGCCTGTGAGAGCCCAAGGCGAGGGACTGCTGCCTGC

GGCCGCAATTGAAGTTATGTATCCTCCTCCTTACCTAGACAATGAGAAGAGCAATG

GAACCATTATCCATGTGAAAGGGAAACACCTTTGTCCAAGTCCCCTATTTCCCGGA

CCTTCTAAGCCCTTTTGGGTGCTGGTGGTGGTTGGTGGAGTCCTGGCTTGCTATA

GCTTGCTAGTAACAGTGGCCTTTATTATTTTCTGGGTGAGGAGTAA